PERFORMANCE ANALYSIS OF DIVERSITY COMBINING FOR FREQUENCY-HOP COMMUNICATIONS UNDER PARTIAL-BAND AND MULTITONE INTERFERENCE

by

GANG LI

B.Sc., University of Science and Technology of China, Hefei, 1982

M.Sc., Northwest Telecommunication Engineering Institute, Xi'an, 1984

A Dissertation Submitted in Partial Fulfillment of the
Requirements for the Degree of

DOCTOR OF PHILOSOPHY

in the Department of Electrical and Computer Engineering

We accept this dissertation as conforming to the required standard

Dr. Qiang Wang, Supervisor (Department of ECE)

Dr. Vijay K. Bhargava, Co-Supervisor (Department of ECE)

Dr. Nikitas J. Dimopoulos, Departmental Member (Department of ECE)

Dr. Micaela Serra, Outside Member (Department of CS)

Dr. James A. Ritcey, External Member (University of Washington)

PERFORMANCE ANALYSIS OF DIVERSITY COMBINING FOR FREQUENCY-HOP COMMUNICATIONS UNDER PARTIAL-BAND AND MULTITONE INTERFERENCE

by

Gang Li

Supervisors: **Professor Qiang Wang** and **Professor Vijay K. Bhargava**

ABSTRACT

This dissertation is concerned with performance analysis of diversity combining schemes in frequency-hop spread spectrum communications under the worst case partial-band noise and multitone jamming.

Performance of a ratio-threshold diversity combining scheme in fast frequency hop spread spectrum systems with M-ary frequency shift keying modulation (FFH/MFSK) under partial-band noise (PBN) and band multitone jamming without and with the additive white Gaussian noise (AWGN) is analyzed. The analysis is based on exact bit error probabilities, instead of bounds on the bit error probabilities. A method to compute the bit error probability for ratio-threshold combining on jamming channel is developed. Relationship between the system performance and the system parameters, such as ratio-threshold, diversity order, and thermal noise level, is illustrated. The performances under band multitone jamming and under partial-band noise jamming are compared. For binary FSK modulation, the performance under the two types of jamming is almost the same, but for 8-ary FSK modulation, tone jamming is more effective against communications. The structure of the combiner is very simple and easy to implement. Another merit of this combiner is that its output can be directly fed to a soft-decision FEC decoder.

Maximum-likelihood diversity combining for an FFH/MFSK spread spectrum system on a PBN interference channel is investigated. The structure of maximum-

likelihood diversity reception on a PBN channel with AWGN is derived. It is shown that signal-to-noise ratio and the noise variance at each hop have to be known to implement this optimum diversity combining. Several sub-optimum diversity combining schemes, which require the information on noise variance of each hop to operate, are also considered. The performance of the maximum-likelihood combining can be used as a standard in judging the performance of other sub-optimum, but more practical diversity combining schemes. The performance of the optimum combining scheme is evaluated by simulations. It is shown that the Adaptive Gain Control (AGC) diversity combining actually achieves the optimum performance when interference is not very weak. But the performance difference between some of the known diversity combining schemes, which do not require channel information to operate, and the optimum scheme is not small when the diversity order is low.

An error-correction scheme is proposed for an M-ary symmetric channel characterized by a large error probability p_e. Performance of the scheme is analyzed. The value of p_e can be close to, but smaller than, $1 - 1/M$ for which the channel capacity is zero. Such a large p_e may occur, for example, in a jamming environment. The coding scheme considered consists of an outer convolutional code and an inner repetition code of length m which is used for each convolutional code symbol. At the receiving end, the m inner code symbols are used to form a soft-decision metric, which is subsequently passed to a soft-decision decoder for the convolutional code. Emphasis is placed on using a binary convolutional code due to the consideration that there exist commercial codecs for such a code. New methods to generate binary metrics from M-ary ($M > 2$) inner code symbols are developed. For the binary symmetric channel, it is shown that the overall code rate is larger than $0.6R_0$, where R_0 is the cutoff rate of the channel. New union bounds on the bit error probability for systems with a binary convolutional code on 4-ary and 8-ary orthogonal channels are presented. Owing to the variable m which has no effect on the decoding procedure, this scheme has a clear opera-

tional advantage over some other schemes. For a BSC and a large m, a method is presented for BER approximation based on the central limit theorem.

Examiners:

Dr. Qiang Wang, Supervisor (Department of ECE)

Dr. Vijay K. Bhargava, Co-Supervisor (Department of ECE)

Dr. Nikitas J. Dimopoulos, Departmental Member (Department of ECE)

Dr. Micaela Serra, Outside Member (Department of CS)

Dr. James A. Ritcey, External Member (University of Washington)

Contents

List of Tables

List of Figures

Acknowledgements

I would like to thank my supervisors, Professor Qiang Wang and Professor Vijay K. Bhargava for their guidance, inspiration and encouragement throughout my graduate education at the University of Victoria. I am grateful to Communications Canada for their financial support through a research contract granted to Professor Vijay K. Bhargava and Professor Qiang Wang. I am also grateful to the University of Victoria for the support in the form of an University of Victoria Fellowship.

I would also like to thank Professor Micaela Serra and Professor Nikitas J Dimopoulos for serving on my supervisory committee, and Professor James A. Ritcey for serving as the external examiner in my Ph.D. oral examination. I owe many thanks to Mr. Ron Kerr for proofreading parts of the dissertation.

Finally, my special thanks to my wife, Pam Xiaoping Li, for her support and consideration throughout this work.

To
MY PARENTS
and
PAM

Chapter 1

Introduction

In many communication systems, in addition to background thermal noise, there are some other forms of disturbance to the transmitted signals. The disturbance is called interference to the communications. One type of interference is intentional, and this type of interference is called jamming. In order to provide adequate performance of the communication link in an environment with interference or jamming, communication systems have to be designed with the capability of working properly in such a severe environment. Spread spectrum is a technique which can be used to increase the anti-jam capability of communication systems. One of two major classes of spread spectrum techniques is frequency hopping. This dissertation is concerned with the anti-jam capability of frequency-hop spread spectrum communications.

1.1 Frequency-Hop Communications

A diagram of frequency hopped frequency shift keying spread spectrum (FH/FSK SS) communication system is depicted in Figure 1.1. The FH/FSK SS system is basically an ordinary FSK system with the carrier frequency hopping over the spread spectrum communication bandwidth, denoted as W_{ss}, under the control of a psuedonoise (PN) code. The FSK modulated signal is called data symbol, or for short, symbol. The bandwidth of the FSK modulated signal is much smaller

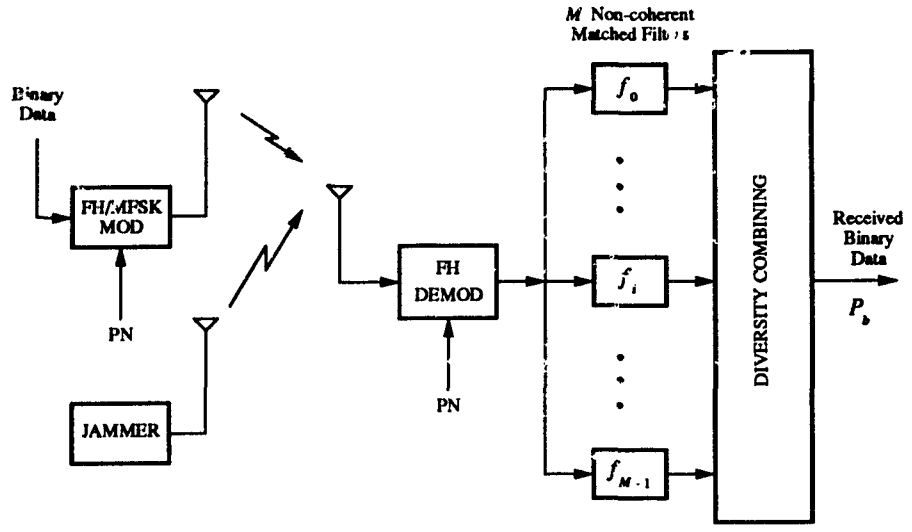

Figure 1.1: The FH noncoherent FSK spread spectrum system

than W_{ss}. But by averaging over many hops, the spectrum of FH/FSK signal has a bandwidth of W_{ss}. The carrier frequency changing rate is called hop rate. For a FH system, if the hop rate is greater than symbol rate, the FH system is called a fast frequency hopping (FFH) system. Otherwise, it is called a slow frequency hopping (SFH) system. In a FFH system, one symbol is transmitted over more than one hop. In this case, one hop is also called one chip. Let the duration of one symbol be T_s, and the duration of one hop, or chip, T_c. Suppose one symbol is transmitted over m ($m > 1$) hops, then $T_s = mT_c$. Since one symbol is transmitted over different time intervals, the transmission is a time diversity transmission. The transmission is also a frequency diversity transmission since one symbol is transmitted over different frequency by carrier frequency hopping. The parameter m is called diversity order. The unit of m is chips/symbol. When the energy of a symbol is fixed, there is usually an optimum diversity order, in the sense that there is a value of m which requires the least signal-to-noise ratio to achieve a given final bit error probability, P_b.

1.2 Intelligent Jamming

An intelligent jammer is a jammer which can adjust its jamming power distribution over the entire spread spectrum signal bandwidth W_{ss} to maximize its jamming effect based on the certain amount of information about the structure of the communication system to be jammed. In other words, the jammer can find and use the best strategy to maximize its jamming effect. From the communicator's point of view, this kind of jamming is the worst case jamming. In this dissertation, we are concerned with the performance of FH communication systems under worst case jamming. We assume that the jammer knows everything about the system except the PN code which controls the carrier frequency hopping sequence. We also assume that the total jamming power of the jammer is finite and fixed.

Two types of intelligent jamming are considered, partial-band noise (PBN) and multitone jamming. Partial-band noise jamming concentrates the total jamming power in a fraction of the spread spectrum signal bandwidth, and injects jamming power into a receiver in the form of additive Gaussian noise. Multitone jamming injects the total jamming power into a finite number of tones, which coincide with some of the FSK signal tones used by the communicator. According to the distribution of the jamming tones, multitone jamming can be divided into two classes: band multitone jamming and independent multitone jamming. It is known that the worst case multitone jamming usually occurs when there is only one tone in a jammed frequency hop slot (or a M-ary FSK symbol bandwidth) [1, 2].

1.3 Diversity Reception in FH Communications under Jamming

Since the jamming power distribution in the spread spectrum bandwidth is nonuniform, time variant, and unknown to the receiver, then after FH demodulation, the channel is stationary only in every hop interval T_c, and the channel is nonsta-

tionary for the symbol duration T_s. Several diversity receiver structures for this kind of channel have been proposed [3, 4, 5, 6] in last decade.

The information on the channel condition for a hop, whether jamming is present or not, is called side information. Some diversity combining schemes require side information, or some other channel information. Soft decision linear energy combining (or soft decision square-law envelope combining) needs side information to work well in strong jamming. If no side information is available, the performance is very poor [7]. Clipped-linear combining needs information on the signal amplitude [5]. Adaptive Gain Control (AGC) combining requires the noise variance of each hop [8]. Providing side information or other information increases the system complexity, and the imperfection of the information may cause some performance loss. Therefore, diversity combining schemes which do not require side information or information other than outputs of M non-coherent matched filters are more attractive.

In most of the previous works on analysis of diversity receivers, the influence of the background thermal noise is ignored. This approximation is accurate when the jamming is so strong that the worst case jamming is simply full band jamming (distributing jamming power uniformly over the full spread spectrum bandwidth W_{ss}). But when the jamming is not very strong, this approximation is no longer valid, due to the noncoherent combining loss in background noise, which is modeled as additive white Gaussian noise (AWGN), and lower signal-to-noise ratio at the chip level. The influence of these two factors increases as the diversity order increases. Another reason to consider background noise is that it is the existence of background noise that makes the extraction of accurate side information difficult. Thus, performance of diversity combining schemes without the requirement of side information should be analyzed in an environment where the influence of the background noise is not small. Therefore, in a complete analysis for strong, moderate, and weak jamming or interference, background thermal noise should be considered.

1.3.1 Diversity Combining Using Ratio-Threshold Test Technique

Viterbi [9] first proposed to use ratio-threshold test technique to combat jamming in FH/FSK spread spectrum communication systems. By using a ratio-threshold test, an estimation of channel condition can be obtained. This estimation can then be used to form a soft decision decoding metric. Viterbi analyzed the performance of this technique in a FH/FSK system with coding but without diversity under multitone and PBN jamming, using the computational cutoff rate technique [9, 10]. The results indicated that certain performance improvement is possible.

Since then, there have been further works in this direction. Chang analyzed the ratio-threshold (R-T) anti-jam technique from the information theory point of view and used game theory approach in the analysis [11]. She showed the performance improvement by R-T technique over a hard decision receiver. Clifford and Schonhoff analyzed the performance of R-T anti-jam technique in multitone jamming channel with background noise [12]. Their analysis is also based on cutoff rate. The above analyses concentrated on systems without diversity. There are several ways to use the R-T technique in diversity combining [13, 14]. The scheme proposed in [14] is further studied in this dissertation.

Since the R-T diversity combining scheme has a very simple structure, it is quite easy to implement. This type of diversity combining does not require side information but with an adjustable parameter. The purpose of our research is to investigate the performance of ratio-threshold test technique when used in diversity combining and the influence of the parameter of threshold to the system performance. This dissertation analyzed the performance of the R-T diversity combining scheme under partial-band noise jamming and multitone jamming with the influence of background thermal noise taken into account. The analysis is based on the exact bit error probability instead of bounds on bit error probability or cutoff rate. Thus more accurate and direct results on system performance are obtained

in this dissertation. The performance comparison of the various diversity combining schemes is more accurate when it is based on the exact bit error probabilities rather than bounds.

1.3.2 Optimum Diversity Reception in PBN with AWGN

According to signal detection theory, the optimum diversity receiver structure can be derived given the properties of the transmission channel. Although many profound works have been done in design and analysis of diversity receivers in jammed channels, the optimum structures of diversity receiver on partial-band noise and multitone jamming channel with background thermal noise are unknown. Keller considered optimum diversity reception on PBN channel with perfect side information and no background thermal noise [13]. In this case, the optimum diversity reception in PBN can be treated as the problem of the optimum diversity reception in additive white Gaussian noise. The optimum diversity reception on PBN channel with thermal noise is investigated in this dissertation. Although the optimum structure may require even more channel information, and thus is impractical, the performance of optimum diversity reception can provide a upper bound on the performance of a non-optimum diversity receiver on PBN channel. And the upper bound can be used to judge non-optimum but practical diversity receivers. The impractical structure may provide guidance when designing practical diversity receiver.

1.4 Concatenated Coding for High-Error-Rate Channels

From a channel coding theory point of view, since one symbol is independently transmitted several times in a fast frequency hop system, there is repetition coding inherently in the system. If the transmitted data are encoded with an error correction code, then the entire system is equivalent to a concatenated coding

cheme with a repetition code as the inner code.

The inner most transmission channel, i.e., the channel in which the data with repetition coding are transmitted, can be quite different depending on, such as, the modulation, the presence or absence of interference, and the types of interference. For different inner channel models, different analysis methods have to be used to analyze the system performance.

If the channel is modeled as a soft decision non-coherent MFSK channel, then decoding of repetition code is a form of diversity combining. However, if the inner most transmission channel is modeled as hard decision non-coherent MFSK channel, or M-ary orthogonal channel, then the channel belongs to the M-ary symmetrical channel (MSC). The case where the error rate of the communication channel is very high (as high as in the order of 0.1) is considered. This high error rate may be due to strong interference and/or a relatively low signal-to-jamming ratio at the chip level (i.e., chip energy-to-jamming power spectral density ratio). Since the jamming is assumed to be very strong, the worst case jamming is full-band jamming. Thus, the channel is assumed to be stationary. Low rate coding has to be employed in a channel with such high error rate. Concatenated coding with a repetition code as the inner code provides a way to implement low rate coding. As we mentioned before, this coding structure is inherent in coded FFH/MFSK systems. On M-ary symmetric channel, the maximum-likelihood decoding (MLD) of repetition code is by a simple majority vote [15, page 60]. But in order to implement soft decision decoding of the concatenated code, a method must be found for the decoder of inner repetition code to generate soft decision metrics for the soft decision decoder of outer code. Furthermore, the outer code and the inner code are not necessarily in the same domain. For example, the outer code may be a binary code, and the inner code may be an M-ary repetition code. Thus, it is interesting to investigate the performance of a code with decoding metrics generated from a different domain. A convolutional code concatenated with repetition code as the inner code is called repeated convolutional code. In

this dissertation, a new coding scheme with a binary convolutional code as the outer code and an M-ary repetition code as the inner code is proposed. Methods of generating the decoding metrics for this coding scheme are developed, and new generating functions of a binary convolutional code are found. The performance of the new scheme is analyzed in various conditions.

1.5 Dissertation Outline

In Chapter 2 and 3, the performance of a FFH/MFSK system with R-T diversity combining scheme is analyzed under partial-band noise jamming and band multitone jamming, respectively. By using an average computation model developed in Chapter 2, the exact bit error probability of the FFH/MFSK system under worst case PBN and multitone jamming including thermal noise influence is computed. Effects on the system performance of different system parameters, such as diversity order, ratio-threshold, and signal-to-thermal-noise ratio, and jamming parameters are also analyzed.

Chapter 4 discusses maximum-likelihood diversity combining on a PBN channel. The structure of maximum-likelihood diversity combining in PBN, and some sub-optimum combining schemes are investigated. The optimum performance is obtained by Monte Carlo simulation. The results show that the AGC diversity combining scheme is actually optimum with regard to the system performance under worst case jamming when the PBN jamming is not too weak.

In Chapter 5, a repeated convolutional code for an M-ary symmetric channel (MSC) characterized by a large error probability p_e is considered. Emphasis is placed on using a binary convolutional code. The effect of finite quantization and methods to generate binary metrics for $M > 2$ are investigated. New union bounds on the bit error probability for systems with a binary convolutional code on 4-ary and 8-ary orthogonal channels are presented.

Conclusions and suggestions for future research are given in Chapter 6.

Chapter 2

Performance of Ratio-Threshold Diversity Combining Scheme in FFH/FSK Systems under Partial-Band Noise Jamming

2.1 Introduction

The Ratio-threshold technique, proposed by Viterbi [9], can be used in fast frequency hop M-ary frequency shift keying (FFH/MFSK) spread spectrum communication systems to combat jamming. Viterbi analyzed the performance of this scheme in coded FFH/MFSK systems under multitone and partial-band noise jamming using the computational cutoff rate technique [9] [10]. His results indicated that certain performance improvement is possible.

When diversity is used in a frequency hop system, with or without an outer error correction code, the ratio-threshold technique can be used in diversity combining. This, in fact, is equivalent to implementing soft decision decoding of a repetition code. Laufer and Reichman [14] discussed this scheme, and analyzed the performance of the scheme in worst case partial-band noise (PBN) jamming. However, their emphasis is on the effects of non-ideal interleaving.

In this chapter, we first give a brief description of the ratio-threshold (R-T) di-

versity combining scheme. Then a method for computation of the bit error probability of a FFH/MFSK system with ratio-threshold diversity combining under jamming is introduced. Next the bit error probabilities of the FFH/MFSK system with ratio-threshold diversity combining under worst case partial band noise are computed. Some results are compared with the performance of the FFH/MFSK systems with diversity utilizing the soft decision metric with side information. Effects on the system performance of different system parameters, such as diversity order, ratio-threshold, and signal-to-thermal-noise ratio, and jamming parameters are also analyzed.

2.2 Ratio-Threshold Diversity Combining

The structure of ratio-threshold diversity combining scheme is quite simple and is described as follows.

The ratio-threshold test is made on every matched filter output at each hop, and a hard decision is made with a quality bit. The hard decision of each M-ary symbol is mapped back to $k = \log_2 M$ bit binary symbols. The outputs of all hops (in the form of binary symbols) are accumulated with good quality bits and with poor quality bits, respectively. If there is at least one hop decision with a good quality bit and there is a majority decision without a tie, then the output of the combiner is the majority decision with a good output quality bit attached. If there is a tie between 0 and 1 (or "space" and "mark") with good quality bits, or there is no hop decision with a good quality bit, a decision is made based on hop decisions with poor quality bits (if there is a tie, flip a coin), and this output of the combiner is attached with a poor output quality bit.

If there is no outer error correction code, the outputs of diversity combiner are also the output of the receiver, and the output quality bit has no use and can be discarded. However, if there is an outer error correction code, the soft decision decoding can be carried out based on the outputs of the diversity combiner.

2.3 Average Computation Model for Bit Error Probability

Consider a FFH/MFSK spread spectrum system (Figure 1.1) with a R-T diversity combiner. Assume that the diversity order, the number of chips or hops per data symbol, is m. Let the output of the non-coherent matched filter for the ith symbol at the kth hop be X_{ik}, where $i = 0, 1, \cdots, M$, and $k = 1, 2, \cdots, m$. Let the ratio threshold be θ, which is a parameter chosen by the communicator. At first we assume that there is only system thermal noise, but no jamming.

First we consider a binary FFH/FSK system. The hop decision is made based on which non-coherent matched filter output is larger, and the quality bit q is set according to

$$q(k) = \begin{cases} 0 \quad \text{(good)} & \text{if } \frac{X_{max}(k)}{X_{min}(k)} \geq \theta, \\ 1 \quad \text{(poor)} & \text{otherwise,} \end{cases}$$

where

$$X_{max}(k) = \max\{X_{0k}, X_{1k}\},$$

$$X_{min}(k) = \min\{X_{0k}, X_{1k}\}.$$

and $k = 1, 2, \cdots, m$. This results in a channel with binary inputs and quaternary outputs, as shown in Figure 2.1. The transition probabilities of the channel are known to be [10]:

$$\begin{aligned} P_C &= F_C(\theta), \\ P_{CX} &= F_C(1) - F_C(\theta), \\ P_{EX} &= F_E(1) - F_E(\theta), \\ P_E &= F_E(\theta), \end{aligned}$$

where

$$\begin{aligned} F_C(\theta) &= \Pr\{X_{0k} \geq \theta X_{1k} | \text{ “0” sent}\}, \\ F_E(\theta) &= \Pr\{X_{1k} \geq \theta X_{0k} | \text{ “0” sent}\}. \end{aligned}$$

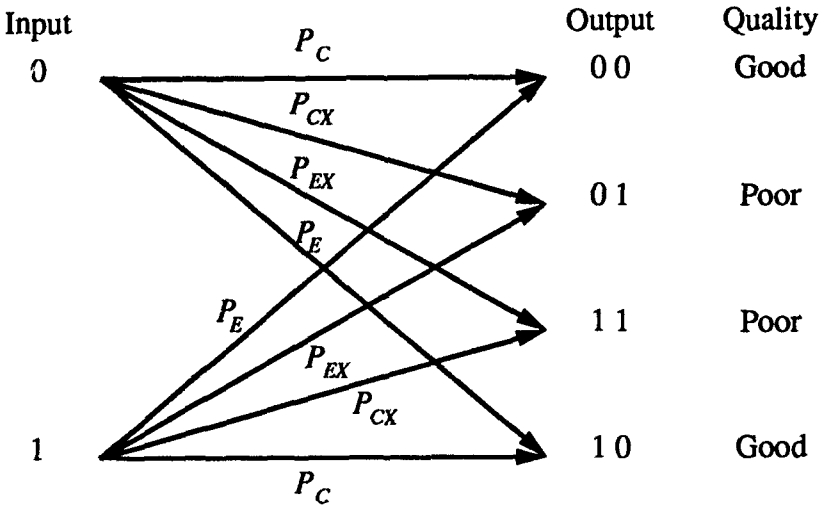

Figure 2.1: The Channel Model

$F_C(\theta)$ and $F_E(\theta)$ can be derived from the distribution of the two matched filter outputs, X_{0k} and X_{1k}. The bit error probability at the output of R-T combiner can be derived from P_C, P_{CX}, P_{EX} and P_E accordingly.

Let l be the output of the diversity combiner before flipping the two-sided coin. There are five possible values for l:

$$l = \begin{cases} 00 & \text{decision is 0, good quality,} \\ 01 & \text{decision is 0, poor quality,} \\ x & \text{tie} \\ 11 & \text{decision is 1, poor quality,} \\ 10 & \text{decision is 1, good quality.} \end{cases}$$

The conditional distribution of l given that "0" is sent is

$$\Pr(l = 00|0 \text{ sent}) = \sum_{S_K, k_1 > k_2} C_m^{k_1,k_2,k_3,k_4} P_C^{k_1} P_E^{k_2} P_{CX}^{k_3} P_{EX}^{k_4} \tag{2.1}$$

$$\Pr(l = 01|0 \text{ sent}) = \sum_{S_K, k_2 = k_1, k_3 > k_4} C_m^{k_1,k_2,k_3,k_4} P_C^{k_1} P_E^{k_2} P_{CX}^{k_3} P_{EX}^{k_4} \tag{2.2}$$

$$\Pr(l = 11|0 \text{ sent}) = \sum_{S_K, k_2 = k_1, k_3 < k_4} C_m^{k_1,k_2,k_3,k_4} P_C^{k_1} P_E^{k_2} P_{CX}^{k_3} P_{EX}^{k_4} \tag{2.3}$$

$$\Pr(l = 10|0 \text{ sent}) = \sum_{S_K, k_1 < k_2} C_m^{k_1,k_2,k_3,k_4} P_C^{k_1} P_E^{k_2} P_{CX}^{k_3} P_{EX}^{k_4} \tag{2.4}$$

$$\Pr(l = x|0 \text{ sent}) = \sum_{S_K, k_2 = k_1, k_3 = k_4} C_m^{k_1,k_2,k_3,k_4} P_C^{k_1} P_E^{k_2} P_{CX}^{k_3} P_{EX}^{k_4} \tag{2.5}$$

where

$$S_K = \{k_1, k_2, k_3, k_4 | 0 \le k_1, k_2, k_3, k_4 \le m, k_1 + k_2 + k_3 + k_4 = m\}$$

and $C_m^{k_1,k_2,k_3,k_4}$ is multinomial number, which is given by

$$C_m^{k_1,k_2,k_3,k_4} = \frac{m!}{k_1!k_2!k_3!k_4!}.$$

Suppose that the two symbols are equiprobable, then the bit error probability at the diversity combiner output is

$$P_b = \Pr(l = 11|0 \text{ sent}) + \Pr(l = 10|0 \text{ sent}) + \frac{1}{2}\Pr(l = x|0 \text{ sent}). \tag{2.6}$$

For M-ary FFH/FSK systems, the hop decision is made by choosing the largest output of M matched filters. Suppose that, for the kth hop,

$$X_{jk} = \max_{0 \le i \le M-1} X_{ik}$$

then the quality bit can be assigned as:

$$q(k) = \begin{cases} 0 & \text{good} \quad \text{if } \frac{X_{jk}}{X_{ik}} \ge \theta \text{ for all } i \ne j, \\ 1 & \text{poor} \quad \text{otherwise.} \end{cases}$$

Assume that the $K = \log_2 M$ binary information bits associated with each transmitted M-ary symbol are ideally interleaved. Then the channel model is the same as the binary case shown in Figure 2.1. But the transition probabilities are changed into [10]:

$$P_C = F_C(\theta) + \left(\frac{M}{2} - 1\right) F_E(\theta), \tag{2.7}$$

$$P_{CX} = [F_C(1) - F_C(\theta)] + \left(\frac{M}{2} - 1\right)[F_E(1) - F_E(\theta)], \tag{2.8}$$

$$P_{EX} = \frac{M}{2}[F_E(1) - F_E(\theta)], \tag{2.9}$$

$$P_E = \frac{M}{2}F_E(\theta), \tag{2.10}$$

where

$$F_C(\theta) = \Pr\{X_{jk} \geq \theta X_{ik} \text{ for all } i \neq j | j \text{ sent}\},$$

$$F_E(\theta) = \Pr\{X_{nk} \geq \theta X_{ik} \text{ for a specific } n \neq j \text{ and all } i \neq n | j \text{ sent }\}.$$

Similar to the binary case, $F_C(\theta)$ and $F_E(\theta)$ can be derived from the distributions of M matched filter outputs $X_{0k}, X_{1k}, \cdots, X_{(M-1)k}$. Then bit error probability at the output of the combiner can be computed by using (2.6).

Note that the above results are for channels without jamming. The statistics of these channels are stationary. A channel with jamming present, however, is nonstationary. For one hop, the signal is either jammed or not jammed. Therefore the channel has two states. One is that a hop is being jammed; and the other one is that a hop is free of jamming.

Let Q_C, Q_E, Q_{CX}, and Q_{EC} be the transition probabilities of the channel state without jamming. They can be computed by

$$Q_C = F_{C0}(\theta) + \left(\frac{M}{2} - 1\right)F_{E0}(\theta),$$

$$Q_{CX} = [F_{C0}(1) - F_{C0}(\theta)] + \left(\frac{M}{2} - 1\right)[F_{E0}(1) - F_{E0}(\theta)],$$

$$Q_{EX} = \frac{M}{2}[F_{E0}(1) - F_{E0}(\theta)],$$

$$Q_E = \frac{M}{2}F_{E0}(\theta),$$

where

$$F_{C0}(\theta) = \Pr\{X_{jk} \geq \theta X_{ik} \text{ for all } i \neq j | j \text{ sent, without jamming}\},$$

$$F_{E0}(\theta) = \Pr\{X_{nk} \geq \theta X_{ik} \text{ for a specific } n \neq j \text{ and all } i \neq n | j \text{ sent, without jamming}\}.$$

Similarly, let R_C, R_E, R_{CX}, and R_{EX} be the transition probabilities of the channel state with jamming. And they can be computed in the similar way as Q_C, etc. by using

$$F_{C1}(\theta) = \Pr\{X_{jk} \geq \theta X_{ik} \text{ for all } i \neq j | j \text{ sent, with jamming}\},$$

$$F_{E1}(\theta) = \Pr\{X_{nk} \geq \theta X_{ik} \text{ for a specific } n \neq j \text{ and all } i \neq n | j \text{ sent, with jamming}\}.$$

Assume the probability of a hop being jammed is ρ, then the conditional probability distribution of l given that "0" is sent is

$$\Pr(l = 00|0 \text{ sent}) = \sum_{S_K, k_1 > k_2} f_2(k_1, k_2, k_3, k_4, Q_C, Q_E, Q_{CX}, Q_{EX}, R_C, R_E, R_{CX}, R_{EX}, \rho) \tag{2.11}$$

$$\Pr(l = 01|0 \text{ sent}) = \sum_{S_K, k_1 = k_2, k_3 > k_4} f_2(k_1, k_2, k_3, k_4, Q_C, Q_E, Q_{CX}, Q_{EX}, R_C, R_E, R_{CX}, R_{EX}, \rho) \tag{2.12}$$

$$\Pr(l = 11|0 \text{ sent}) = \sum_{S_K, k_1 = k_2, k_3 < k_4} f_2(k_1, k_2, k_3, k_4, Q_C, Q_E, Q_{CX}, Q_{EX}, R_C, R_E, R_{CX}, R_{EX}, \rho) \tag{2.13}$$

$$\Pr(l = 10|0 \text{ sent}) = \sum_{S_K, k_1 < k_2} f_2(k_1, k_2, k_3, k_4, Q_C, Q_E, Q_{CX}, Q_{EX}, R_C, R_E, R_{CX}, R_{EX}, \rho) \tag{2.14}$$

$$\Pr(l = x|0 \text{ sent}) = \sum_{S_K, k_1 = k_2, k3 = k4} f_2(k_1, k_2, k_3, k_4, Q_C, Q_E, Q_{CX}, Q_{EX}, R_C, R_E, R_{CX}, R_{EX}, \rho) \tag{2.15}$$

where

$$f_2(k_1, k_2, k_3, k_4, q_1, q_2, q_3, q_4, r_1, r_2, r_3, r_4, \rho)$$

$$= \sum_{l_1=0}^{k_1}\sum_{l_2=0}^{k_2}\sum_{l_3=0}^{k_3}\sum_{l_4=0}^{k_4} C_m^{l_1,l_2,l_3,l_4,k_1-l_1,k_2-l_2,k_3-l_3,k_4-l_4}$$

$$\times(1-\rho)^{l_1+l_2+l_3+l_4}\rho^{m-l_1-l_2-l_3-l_4}q_1^{l_1}q_2^{l_2}q_3^{l_3}q_4^{l_4}r_1^{k_1-l_1}r_2^{k_2-l_2}r_3^{k_3-l_3}r_4^{k_4-l_4}.$$

In order to simplify the computation, it can be shown that equations (2.11) - (2.15) can be computed with (2.1) - (2.5) by substituting P_C,P_E,P_{CX}, and P_{EX} with the average transition probabilities (see Section 2.7 for detail) :

$$\bar{P}_C = (1-\rho)Q_C + \rho R_C \tag{2.16}$$

$$\bar{P}_E = (1-\rho)Q_E + \rho R_E \tag{2.17}$$

$$\bar{P}_{CX} = (1-\rho)Q_{CX} + \rho R_{CX} \tag{2.18}$$

$$\bar{P}_{EX} = (1-\rho)Q_{EX} + \rho R_{EX} \tag{2.19}$$

Further, the average transition probabilities $\bar{P}_C$, etc. can be computed with (2.7) - (2.10) by substituting $F_C(\theta)$ and $F_E(\theta)$ with averaged version of $\bar{F}_C(\theta)$ and $\bar{F}_E(\theta)$ which are given by:

$$\bar{F}_C(\theta) = (1-\rho)F_{C0}(\theta) + \rho F_{C1}(\theta) \tag{2.20}$$

$$\bar{F}_E(\theta) = (1-\rho)F_{E0}(\theta) + \rho F_{E1}(\theta) \tag{2.21}$$

Thus, even the jamming channel considered here is a two state channel, the bit error probability can be computed by using an equivalent single state channel which is characterized by one average of statistical properties of the two channel states. To simplify the notations, $\bar{F}_C$ and $\bar{F}_E$ will be just written as F_C and F_E respectively in the following part of this chapter and the next chapter.

2.4 Performance in Additive White Gaussian Noise

We first analyze the performance of the R-T diversity combiner in additive white Gaussian noise (AWGN) only. This is the simplest case, and it also represents the

asymptotic situation when jamming is very weak.

Let E_b be the energy per information bit, N_0 the power spectral density of AWGN. Then the energy per hop to noise spectral density ratio is KE_b/mN_0. $F_C(\theta)$ and $F_E(\theta)$ are:

$$F_C(\theta) = \int_0^\infty p_{s+n}(x)\left[\int_0^{x/\theta} p_n(y)dy\right]^{M-1} dx,$$

$$F_E(\theta) = \int_0^\infty p_n(x)\left[\int_0^{x/\theta} p_{s+n}(y)dy\right]\left[\int_0^{x/\theta} p_n(z)dz\right]^{M-2} dx,$$

where

$$p_{s+n}(x) = x\exp\left(-\frac{x^2+2\frac{KE_b}{mN_0}}{2}\right) I_0\left(x\sqrt{\frac{2KE_b}{mN_0}}\right),$$

$$p_n(x) = x\exp\left(-\frac{x^2}{2}\right),$$

and $I_0(x)$ is the modified zeroth order Bessel function. Carrying out the integrals, we can obtain

$$F_C(\theta) = 1 + \sum_{k=1}^{M-1}(-1)^k \binom{M-1}{k} \frac{\theta^2}{k+\theta^2}\exp\left(-\frac{k}{k+\theta^2}\frac{KE_b}{mN_0}\right), \tag{2.22}$$

and

$$F_E(\theta) = \frac{1}{M-1}\sum_{k=1}^{M-1}(-1)^{k+1}\binom{M-1}{k}\frac{\theta^2}{k+\theta^2}\frac{k}{k+\theta^2-1} \times \exp\left(-\frac{k+\theta^2-1}{k+\theta^2}\frac{KE_b}{mN_0}\right). \tag{2.23}$$

Eqs. (2.22) and (2.23) can also be obtained from equations (3.9) and (3.10) in [10] by substituting $\rho = 1$ and changing E_s into E_b/m, and N_J into N_0, respectively.

Figure 2.2, Figure 2.3 and Figure 2.4 show the bit error rates of the binary systems with m = 4,5, and 9, respectively. Bit error rates of the binary systems

without diversity are also plotted in these figures for reference (it is known that time diversity can not generate any gains in AWGN, and in contrast, there are some diversity combining losses). It can be seen that $\theta = 2$ is roughly optimum in all three cases. The performance of a system with very large θ ($\theta > 10$) is almost the same as the performance of a system with hard decision only ($\theta = 1$). To see the performance dependence on θ, the E_b/N_0 required to achieve BER = 10^{-5} versus reciprocal of θ is plotted in Figure 2.5. For a fixed m, it can be seen that the left end ($\theta \rightarrow \infty$) and right end ($\theta = 1$) of the curve have the same height. This means that the performance of a system with sufficiently large θ is the same as that of a system with $\theta = 1$. This is because large θ causes the decision output for a hop to be almost always with bad quality bit, forming a two quantization level, instead of four. Thus it is equivalent to hard decision system. It also can be seen that the optimum θ which requires the least E_b/N_0 to achieve BER=10^{-5} is less than 2 and the exact optimum θ depends on diversity order m. For $m = 2$ with optimum θ, the minimum E_b/N_0 required to have a BER of 10^{-5} is about 1.5 dB more than that for the system without diversity.

The bit error rate of 8-ary system with m=4,5, and 9 are plotted in Figure 2.6 to Figure 2.8. The required E_b/N_0 to achieve BER=10^{-5} versus the reciprocal of θ for 4-ary, 8-ary and 16-ary systems are plotted in Figure 2.9, Figure 2.10, and Figure 2.11, respectively. Similarly, the performance of a M-ary system ($M \geq 4$) with large enough θ is almost the same as the performance of the system with hard decision in each hop ($\theta = 1$). When m is small, $\theta = 1$ and very large θ gives worse performance. But when m is large, the performance is quite sensitive to θ. The optimum θ is also less than 2, and the specific optimum point depends on m.

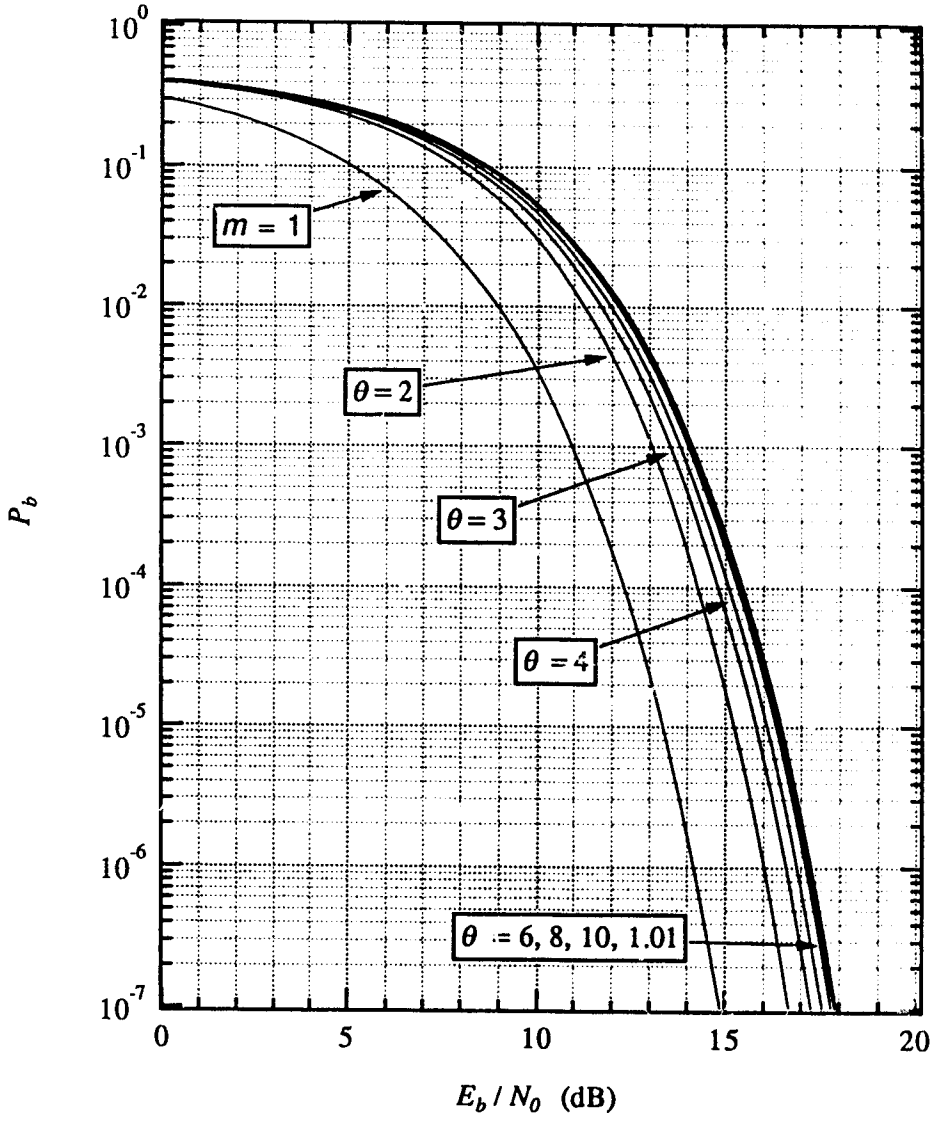

Figure 2.2: Performance of FH/BFSK with diversity $m = 4$ chips/bit and R-T diversity combiner with threshold θ in additive white Gaussian noise.

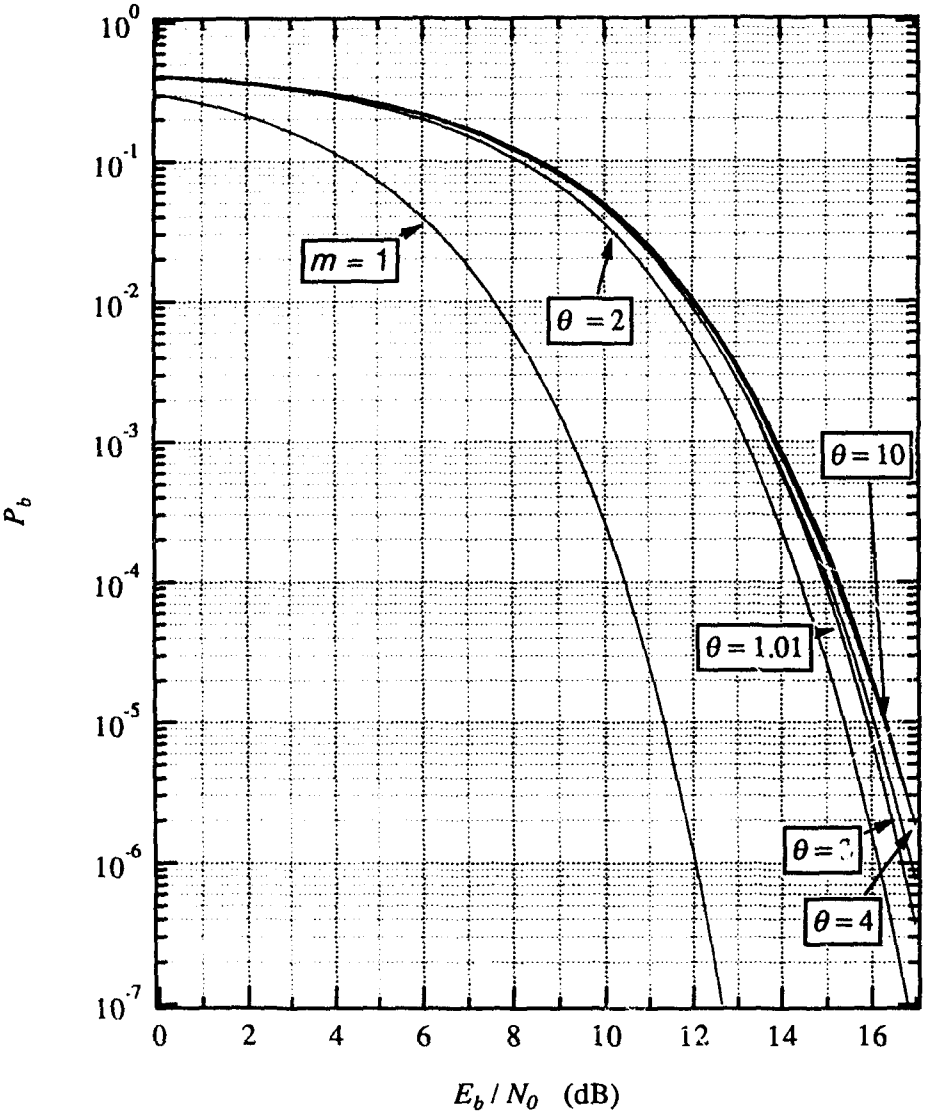

Figure 2.3: Performance of FH/BFSK with diversity $m = 5$ chips/bit and R-T diversity combiner with threshold θ in additive white Gaussian noise.

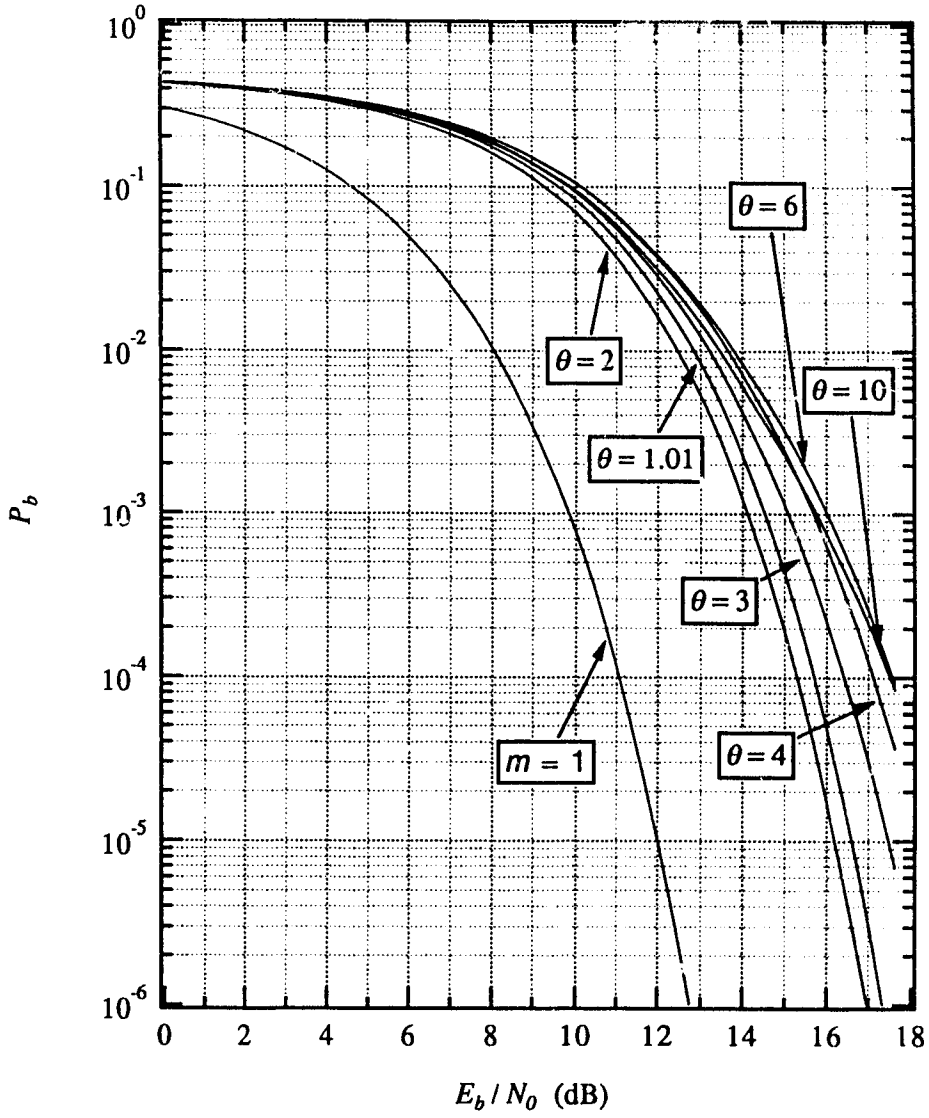

Figure 2.4: Performance of FH/BFSK with diversity $m = 9$ chips/bit and R-T diversity combiner with threshold θ in additive white Gaussian noise.

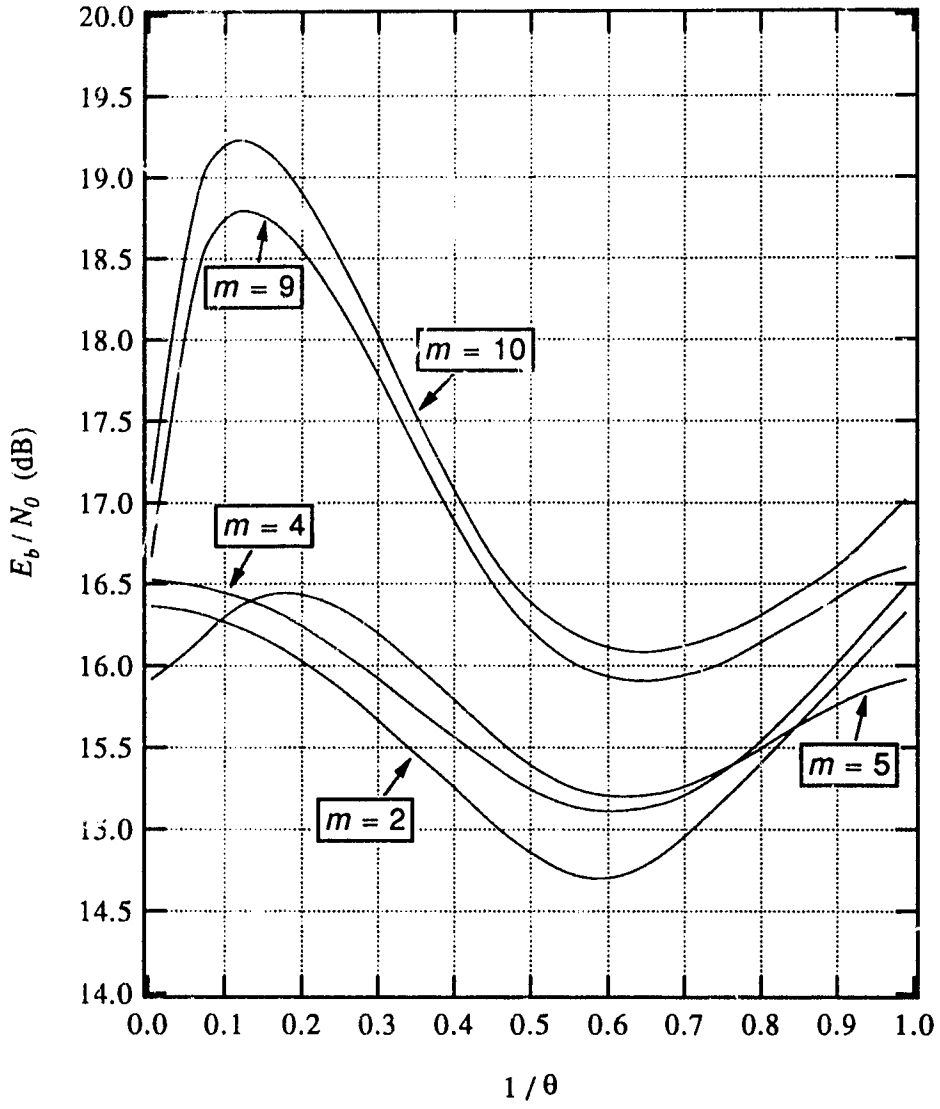

Figure 2.5: E_b/N_0 required to achieve BER=10^{-5} versus $1/\theta$ for FH/BFSK systems with diversity m in additive white Gaussian noise. $E_b/N_0 = 13.35$ dB for $m = 1$.

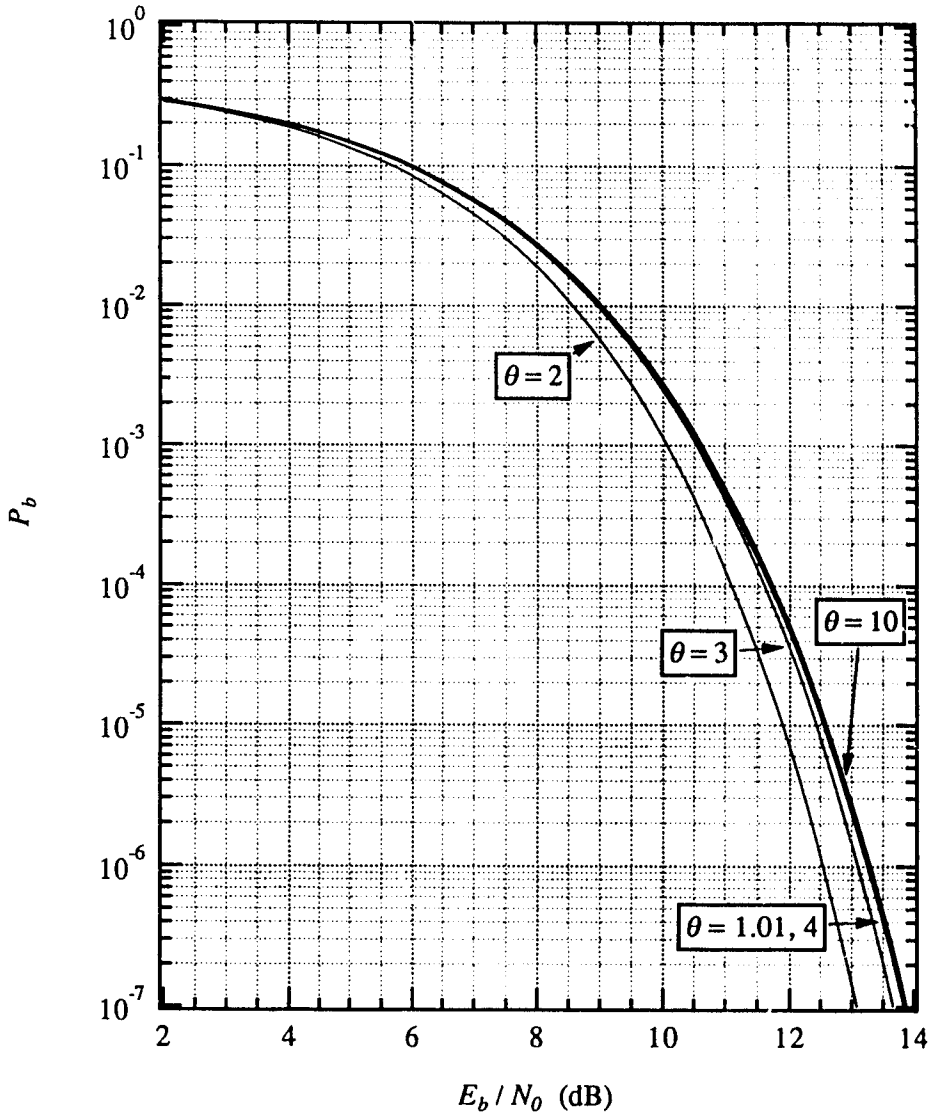

Figure 2.6: Performance of FH/8FSK with diversity $m = 4$ chips/bit and R-T diversity combiner with threshold θ in additive white Gaussian noise.

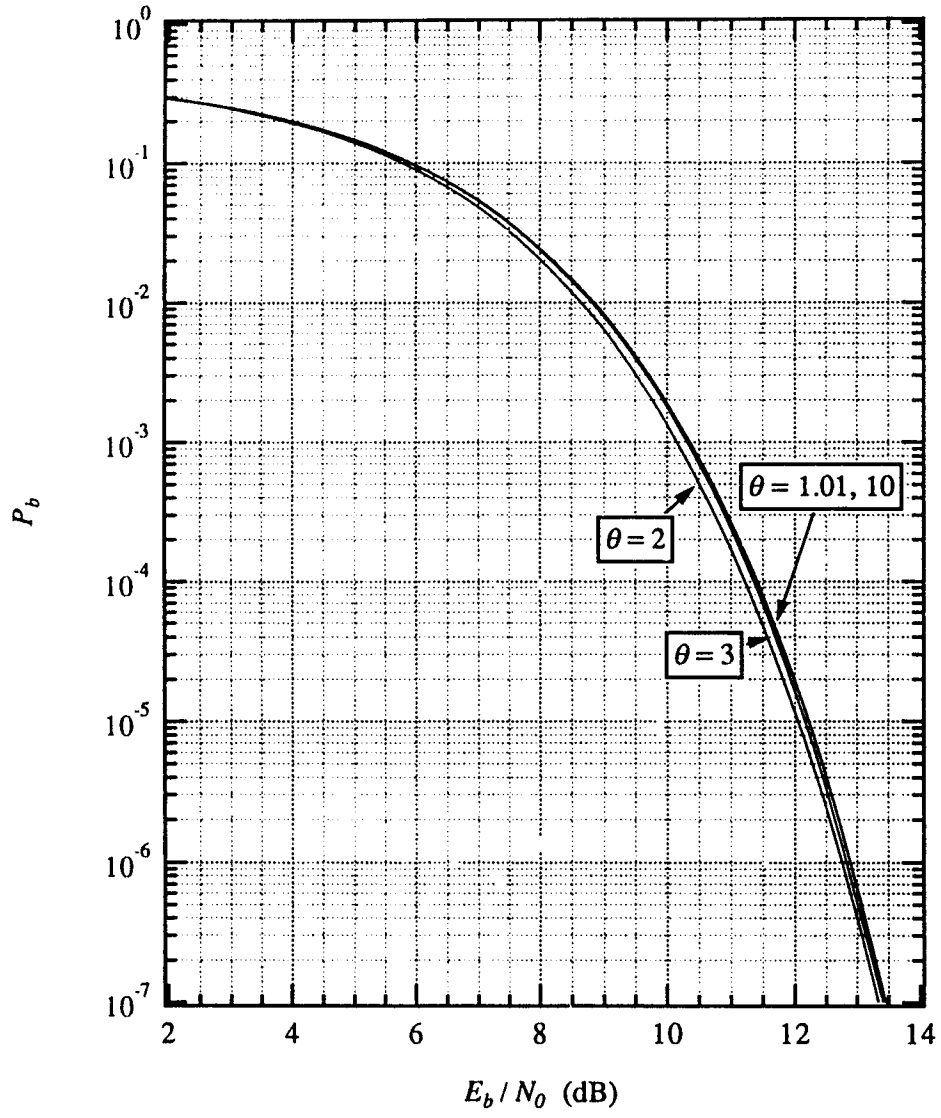

Figure 2.7: Performance of FH/8FSK with diversity $m = 5$ chips/bit and R-T diversity combiner with threshold θ in additive white Gaussian noise.

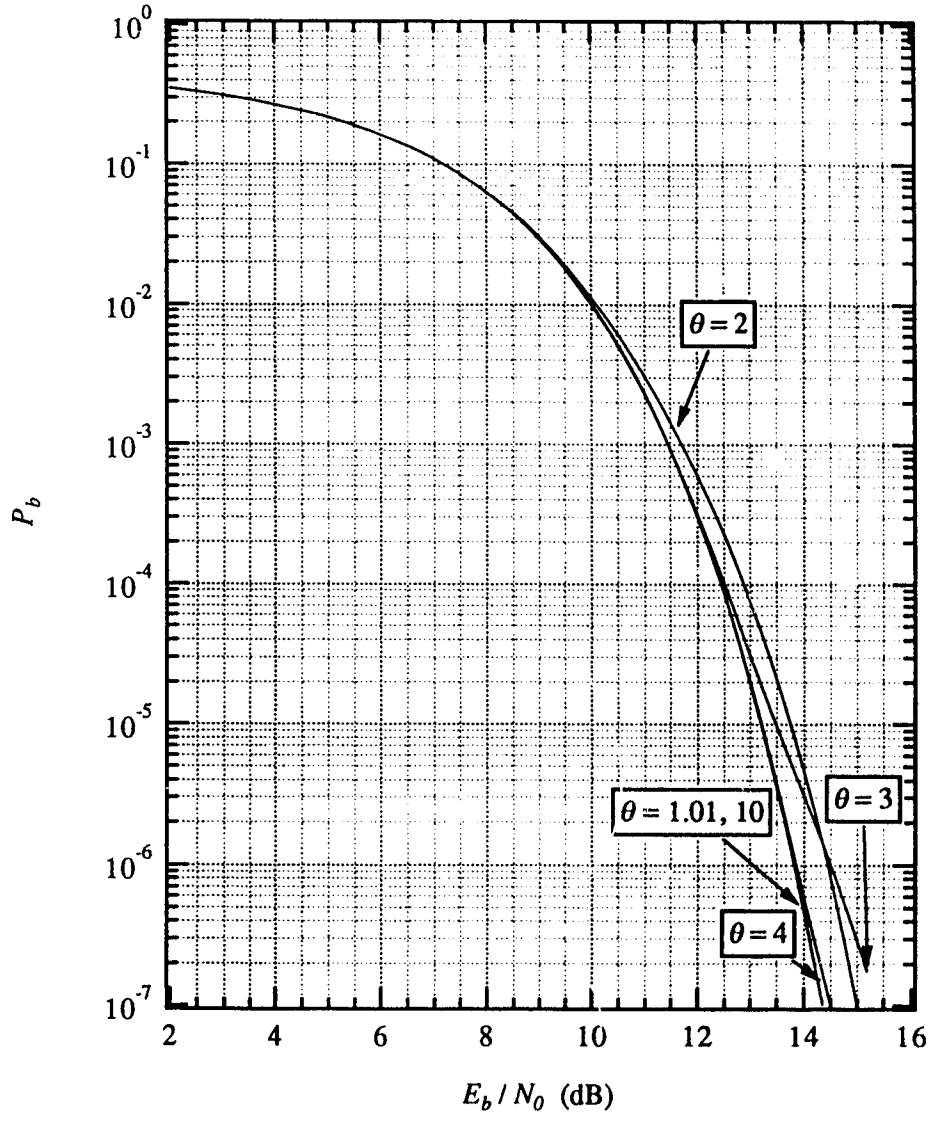

Figure 2.8: Performance of FH/8FSK with diversity $m = 9$ chips/bit and R-T diversity combiner with threshold θ in additive white Gaussian noise.

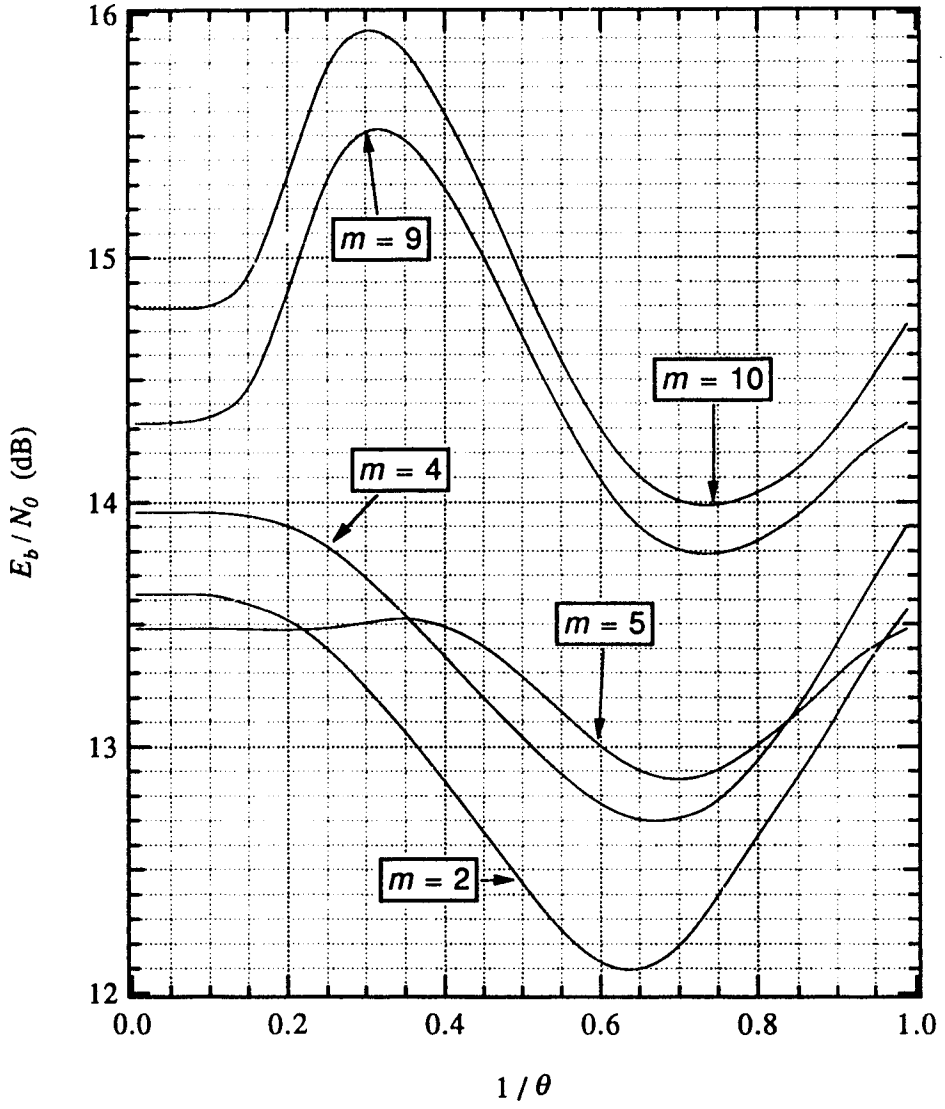

Figure 2.9: E_b/N_0 required to achieve BER=10^{-5} versus $1/\theta$ for FH/4FSK systems with diversity m in additive white Gaussian noise. $E_b/N_0 = 10.61$ dB for $m = 1$.

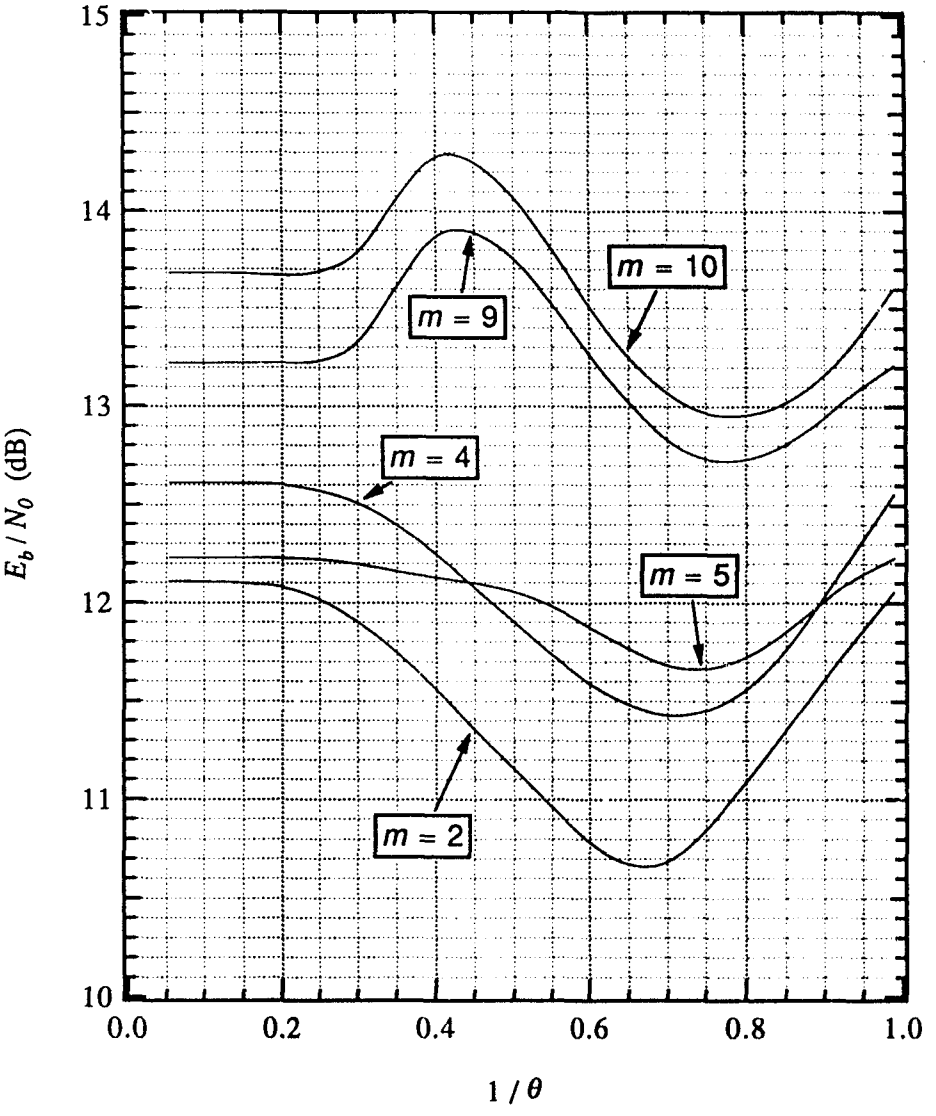

Figure 2.10: E_b/N_0 required to achieve BER=10^{-5} versus $1/\theta$ for FH/8FSK systems with diversity m in additive white Gaussian noise. E_b/N_0 = 9.10 dB for m = 1.

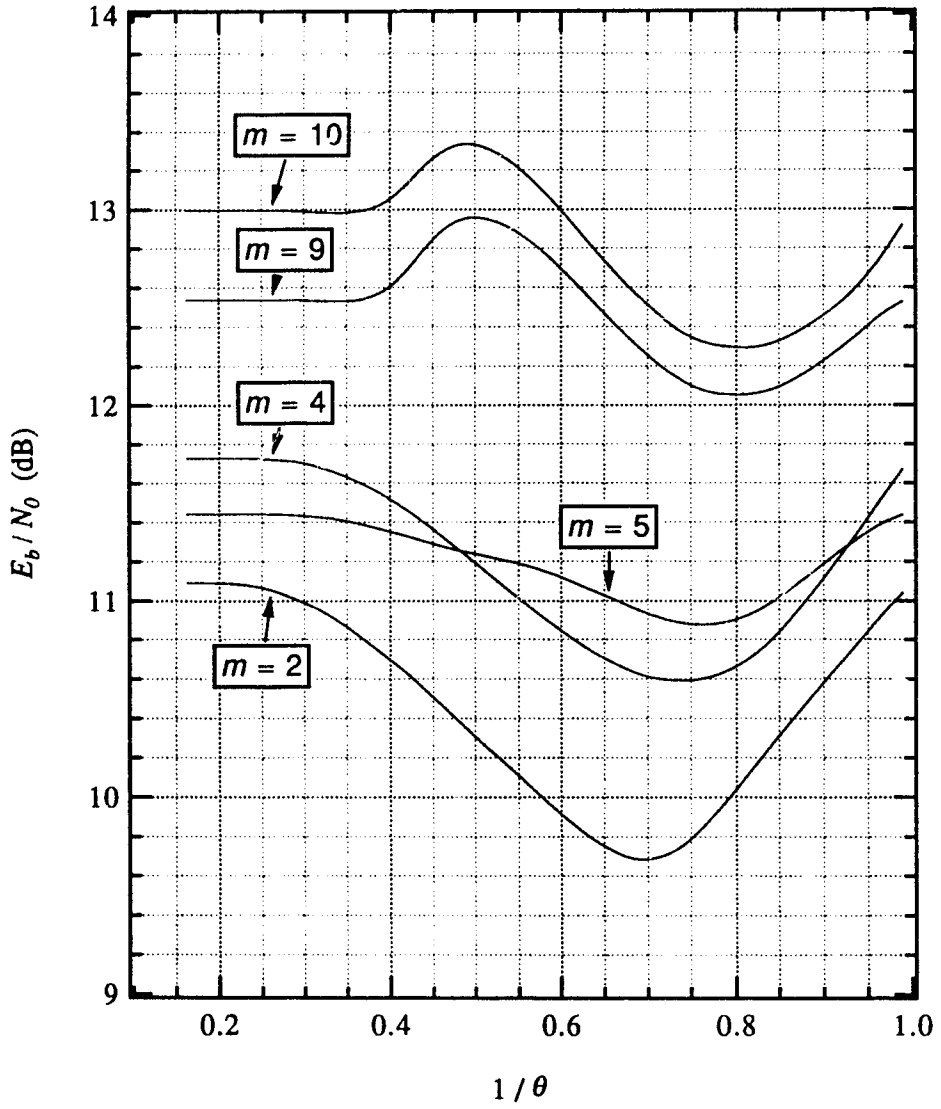

Figure 2.11: E_b/N_0 required to achieve BER=10^{-5} versus $1/\theta$ for FH/16FSK systems with diversity m in additive white Gaussian noise. E_b/N_0 = 7.07 dB for m = 1.

2.5 Performance under Partial-Band Noise Jamming

When a partial-band noise jammer jams a fraction ρ of the transmission band with noise power density N_J/ρ, $F_C(\theta)$ and $F_E(\theta)$ cab be computed according to (2.20) and (2.21):

$$F_C(\theta) = (1-\rho)F_{C0}(\theta) + \rho F_{C1}(\theta)$$

$$F_E(\theta) = (1-\rho)F_{E0}(\theta) + \rho F_{E1}(\theta)$$

and

$$\begin{aligned}
F_{C0}(\theta) &= \int_0^\infty p_{s+n}(x)\left[\int_0^{x/\theta} p_n(y)dy\right]^{M-1} dx \\
&= \int_0^\infty x\exp\left(-\frac{x^2+2\frac{KE_b}{mN_0}}{2}\right) I_0\left(x\sqrt{\frac{2KE_b}{mN_0}}\right) \\
&\quad \times\left[\int_0^{x/\theta} y\exp(-y^2/2)dy\right]^{M-1} dx \\
&= \sum_{k=0}^{M-1}(-1)^k\binom{M-1}{k}\frac{\theta^2}{\theta^2+k}\exp\left(-\frac{k}{\theta^2+k}\frac{KE_b}{mN_0}\right), \\
F_{C1}(\theta) &= \int_0^\infty p_{s+j+n}(x)\left[\int_0^{x/\theta} p_{j+n}(y)dy\right]^{M-1} dx \\
&= \int_0^\infty x\exp\left(-\frac{x^2+2KE_b/[m(N_0+N_J/\rho)]}{2}\right) \\
&\quad \times I_0\left(x\sqrt{\frac{2KE_b}{m(N_0+N_J/\rho)}}\right)\left[\int_0^{x/\theta}\exp(-y^2/2)dy\right]^{M-1} dx \\
&= \sum_{k=0}^{M-1}(-1)^k\binom{M-1}{k}\frac{\theta^2}{\theta^2+k}\exp\left(-\frac{k}{\theta^2+k}\frac{KE_b}{m(N_0+N_J/\rho)}\right), \\
F_{E0}(\theta) &= \int_0^\infty p_n(x)\left[\int_0^{x/\theta} p_{s+n}(y)dy\right]\left[\int_0^{x/\theta} p_n(z)dz\right]^{M-2} dx
\end{aligned}$$

$$= \int_0^\infty x\exp(-x^2/2)\left[\int_0^{x/\theta} y\exp\left(-\frac{y^2+2\frac{KE_b}{mN_0}}{2}\right) I_0\left(y\sqrt{\frac{2KE_b}{mN_0}}\right)dy\right]$$

$$\times\left[\int_0^{x/c} z\exp(-z^2/2)dz\right]^{M-2} dx$$

$$= \sum_{k=0}^{M-2}(-1)^k\binom{M-2}{k}\frac{\theta^2}{\theta^2+k}\frac{1}{\theta^2+k+1}\exp\left(-\frac{\theta^2+k}{\theta^2+k+1}\frac{KE_b}{mN_0}\right),$$

$$F_{E1}(\theta) = \int_0^\infty p_{j+n}(x)\left[\int_0^{x/\theta} p_{s+j+n}(y)dy\right]\left[\int_0^{x/\theta} p_{j+n}(z)dz\right]^{M-2} dx$$

$$= \int_0^\infty x\exp(-x^2/2)\left[\int_0^{x/\theta} y\exp\left(-\frac{y^2+2KE_b/[m(N_0+N_J/\rho)]}{2}\right)\right.$$

$$\left.\times I_0\left(y\sqrt{\frac{2KE_b}{m(N_0+N_J/\rho)}}\right)dy\right]\left[\int_0^{x/\theta} z\exp(-z^2/2)dz\right]^{M-2} dx$$

$$= \sum_{k=0}^{M-2}(-1)^k\binom{M-2}{k}\frac{\theta^2}{\theta^2+k}\frac{1}{\theta^2+k+1}$$

$$\times\exp\left(-\frac{\theta^2+k}{\theta^2+k+1}\frac{KE_b}{m(N_0+N_J/\rho)}\right).$$

So

$$F_C(\theta) = \sum_{k=0}^{M-1}(-1)^k\binom{M-1}{k}\frac{\theta^2}{\theta^2+k}\left[(1-\rho)\exp\left(-\frac{k}{\theta^2+k}\frac{KE_b}{mN_0}\right)\right.$$

$$\left.+\rho\exp\left(-\frac{k}{\theta^2+k}\frac{KE_b}{m(N_0+N_J/\rho)}\right)\right],$$

$$F_E(\theta) = \sum_{k=0}^{M-2}(-1)^k\binom{M-2}{k}\frac{\theta^2}{\theta^2+k}\frac{1}{\theta^2+k+1}$$

$$\times\left[(1-\rho)\exp\left(-\frac{\theta^2+k}{\theta^2+k+1}\frac{KE_b}{mN_0}\right)\right.$$

$$\left.+\rho\exp\left(-\frac{\theta^2+k}{\theta^2+k+1}\frac{KE_b}{m(N_0+N_J/\rho)}\right)\right].$$

The worst ρ, denoted as ρ_{wc}, and the corresponding worst case performance, can be easily computed numerically using the above equation. The bit error rate (BER) of the binary system under PBN jamming with the worst ρ verses E_b/N_J with θ as parameter and $E_b/N_0 = 17$ dB for $m = 4$,5 and 9 are plotted in upper figures of Figure 2.12, Figure 2.13, and Figure 2.14, respectively. The worst ρ verses E_b/N_J for $m = 4$,5, and 9 are depicted in lower figures of Figure 2.12, Figure 2.13, and Figure 2 14, respectively.

From these figures, it can be seen that $\theta = 2$ is the best. However, when E_b/N_J is small, i.e., jamming is dominant, the differences in BER for different θ are not large. At the high end of E_b/N_J, where AWGN becomes dominant, noise floors form in BER curves. The height of the floor is determined by θ. The results in last section can be used here to determine the floor level from θ.

The worst jamming parameter ρ_{wc} is almost a linear inverse function of E_b/N_J, when E_b/N_J exceeds a certain threshold. For E_b/N_J less than the threshold, $\rho_{wc} = 1$. For $m = 4$ and 5, ρ_{wc} for different θ are almost the same. But for $m = 9$, ρ_{wc} is different for different θ.

The worst case BER of 4-ary, 8-ary and 16-ary systems and the corresponding ρ_{wc} are plotted in Figure 2.15 to Figure 2.23. $\theta = 2$ is the best in E_b/N_J region of interest for $m = 4$. The behavior of BER and ρ_{wc} are similar to those for the binary case. However as M increases, the differences in BER for different θ become small.

To see the influence of θ and m on the system performance clearly, E_b/N_J required to achieve a fixed BER $= 10^{-5}$ versus $\frac{1}{\theta}$ with m as parameter are plotted in Figure 2.24, Figure 2.25 and Figure 2.26 for binary, 4-ary and 8-ary system, respectively. First, it can be seen that all curves have a property: the values of left end ($\theta \to \infty$) and right end ($\theta = 1$) are identical. This means that the performances for $\theta = 1$ and very large θ are the same. The reason, as discussed in last section, is that sufficiently large θ will cause almost all decisions to be of

bad quality and in fact form two level outputs instead of four levels. Secondly, the optimum θ which requires the least E_b/N_J to achieve certain BER, are located in the range of $1 < \theta < 3$. The maximum points are located either $3 < \theta < \infty$ (if there is a peak in the curves), or at $\theta = 1$ or $\theta \to \infty$. Finally, some curves are relatively flat, which indicate that the choice of θ is not very critical to the performance. Others have a deep valley and high peak shape, meaning that the performance differences among different θ are quite large. Thus, the performance is very sensitive to θ for some diversity order m, but not for others. Therefore, the proper choice of diversity order m should be the one which makes the system sustain certain BER with the minimum E_b/N_J while not being very sensitive to θ.

In the binary FSK system, Figure 2.24, the curve for $m = 2$ is the most flat one. But the minimum point is quite high. It requires more than 40 dB in E_b/N_J to have BER=10^{-5}. Curves for $m = 5, 9$, and 10 have much lower minimum points (about 23 dB). But $m = 9$ and 10 have very high peaks. Therefore, there may be a trade-off between the sensitivity to θ and the minimum E_b/N_J required.

In 4-ary and 8-ary systems, $m = 5$ requires lower E_b/N_J to achieve BER= 10^{-5}, and is also insensitive to θ.

In order to evaluate the performance of R-T diversity combiner, the worst case BER of soft linear diversity combiner with perfect side information (SLC with PSI) and without AWGN for m=4 is also plotted in Figure 2.12, Figure 2.15, Figure 2.18 and Figure 2.21. The worst case BER for the soft linear diversity combiner with perfect side information for large E_b/N_J is given by [1]:

$$P_b = \beta \left(\frac{mN_J}{KE_b} \right)^m \quad \text{when } E_b/N_J \geq \gamma \tag{2.24}$$

where $K = 1$ in the binary case, and $K = \log_2 M$ for M-ary modulation; β and γ are constants given in Table 2.4 in [1]. In the region of $E_b/N_J < \gamma$, simulation results are plotted. The BER performance of the soft diversity combiner with perfect side information without AWGN can be viewed as the best possible performance

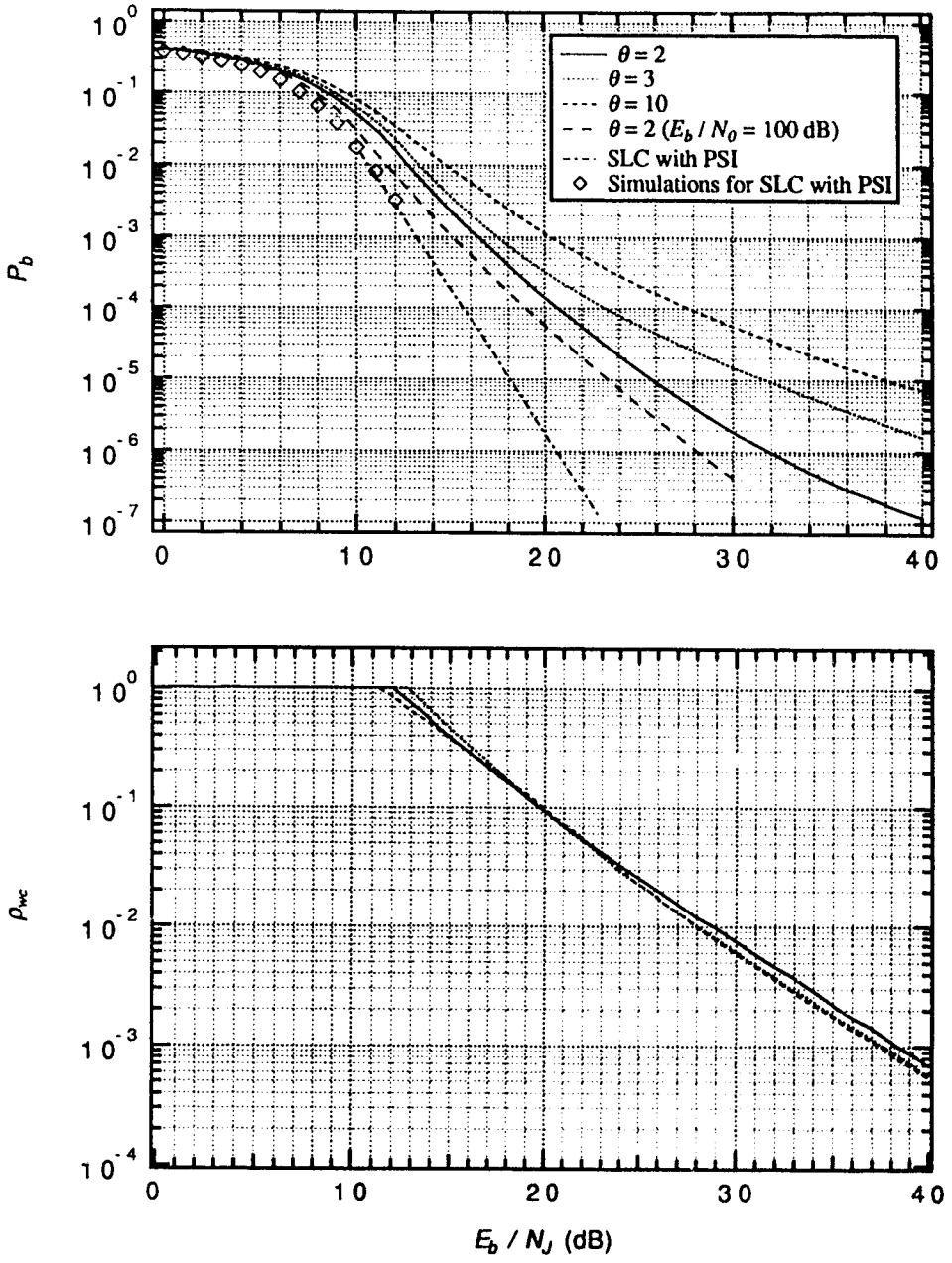

Figure 2.12: Performance of FH/BFSK with diversity $m = 4$ chips/bit and R-T diversity combiner with threshold θ in worst case partial-band noise jamming. $E_b/N_0 = 17$ dB. Upper: BER. Lower: the worst jamming parameter ρ_{wc}.

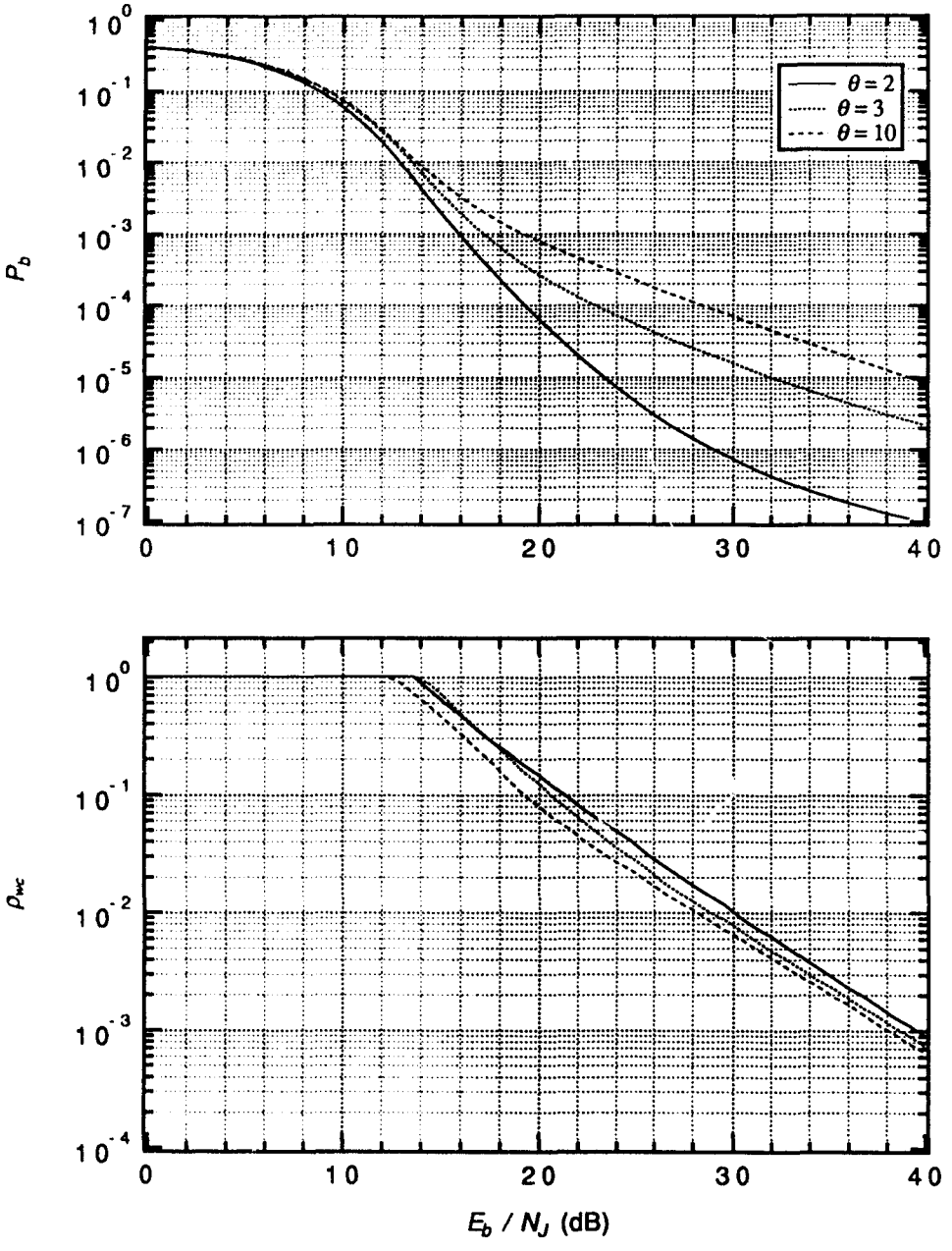

Figure 2.13: Performance of FH/BFSK with diversity $m = 5$ chips/bit and R-T diversity combiner with threshold θ in worst case partial-band noise jamming. $E_b/N_0 = 17$ dB. Upper: BER. Lower: the worst jamming parameter ρ_{wc}.

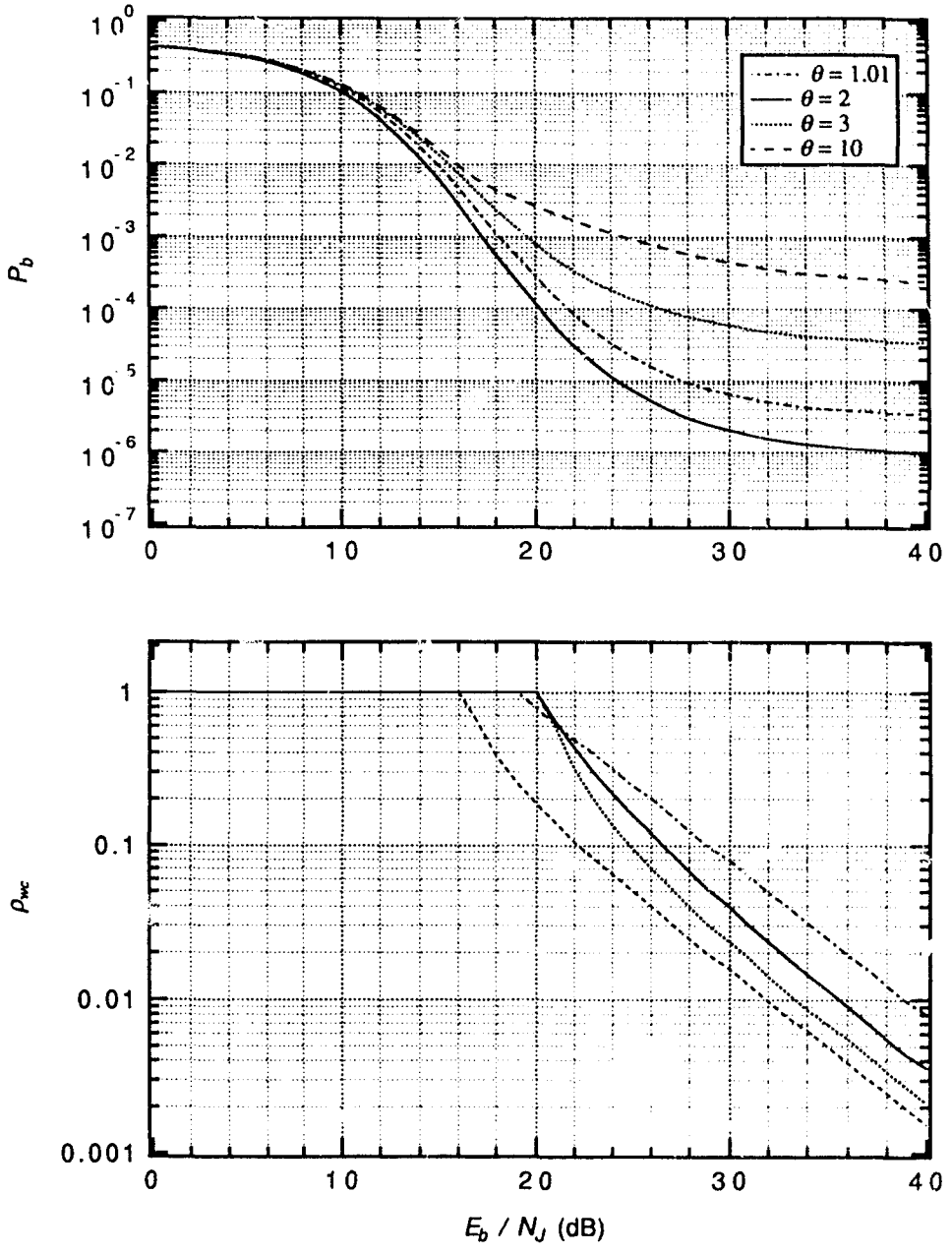

Figure 2.14: Performance of FH/BFSK with diversity $m = 9$ chips/bit and R-T diversity combiner with threshold θ in worst case partial-band noise jamming. $E_b/N_0 = 17$ dB. Upper: BER. Lower: the worst jamming parameter ρ_{wc}.

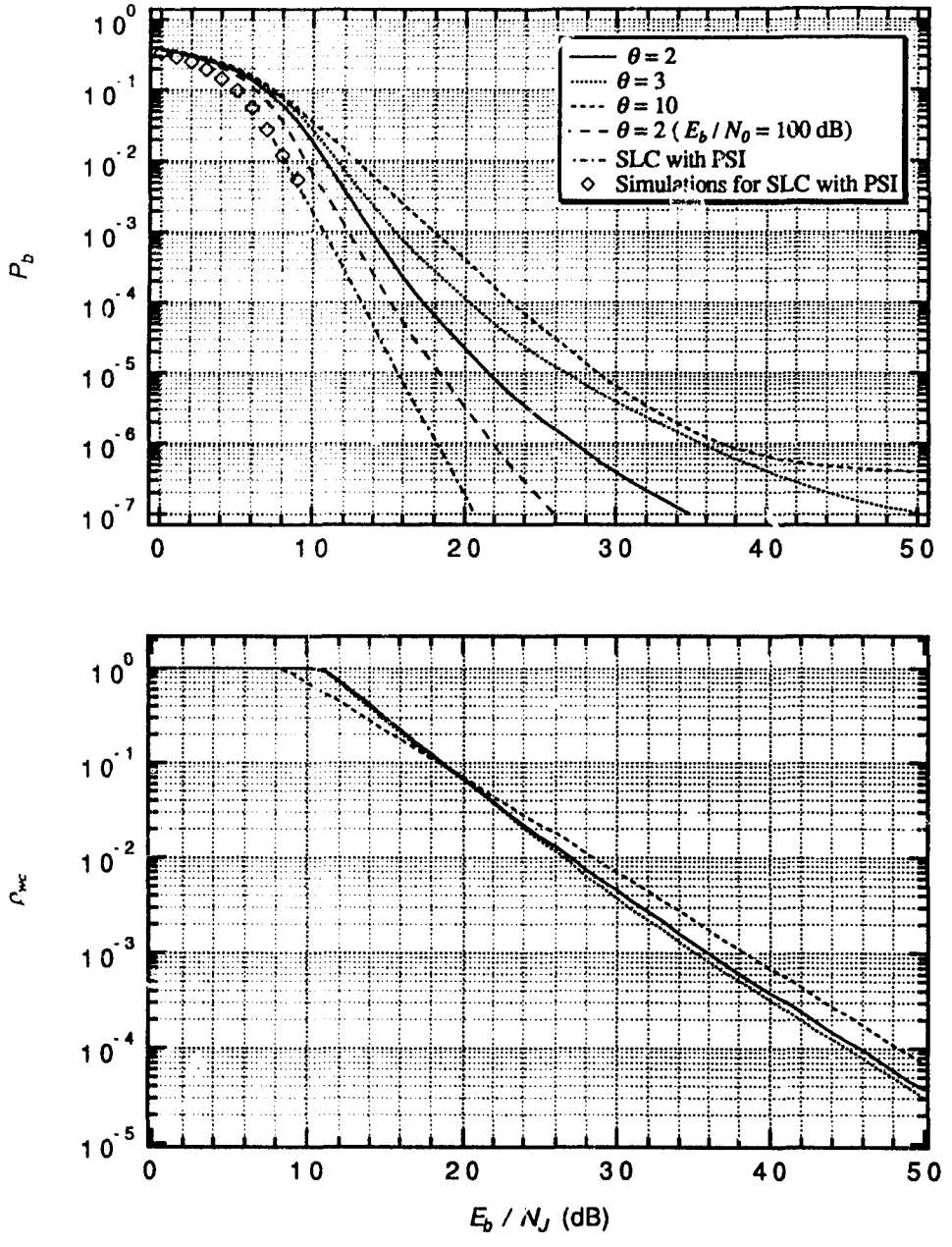

Figure 2.15: Performance of FH/4FSK with diversity $m = 4$ chips/bit and R-T diversity combiner with threshold θ in worst case partial-band noise jamming. $E_b/N_0 = 15$ dB. Upper: BER. Lower: the worst jamming parameter ρ_{wc}.

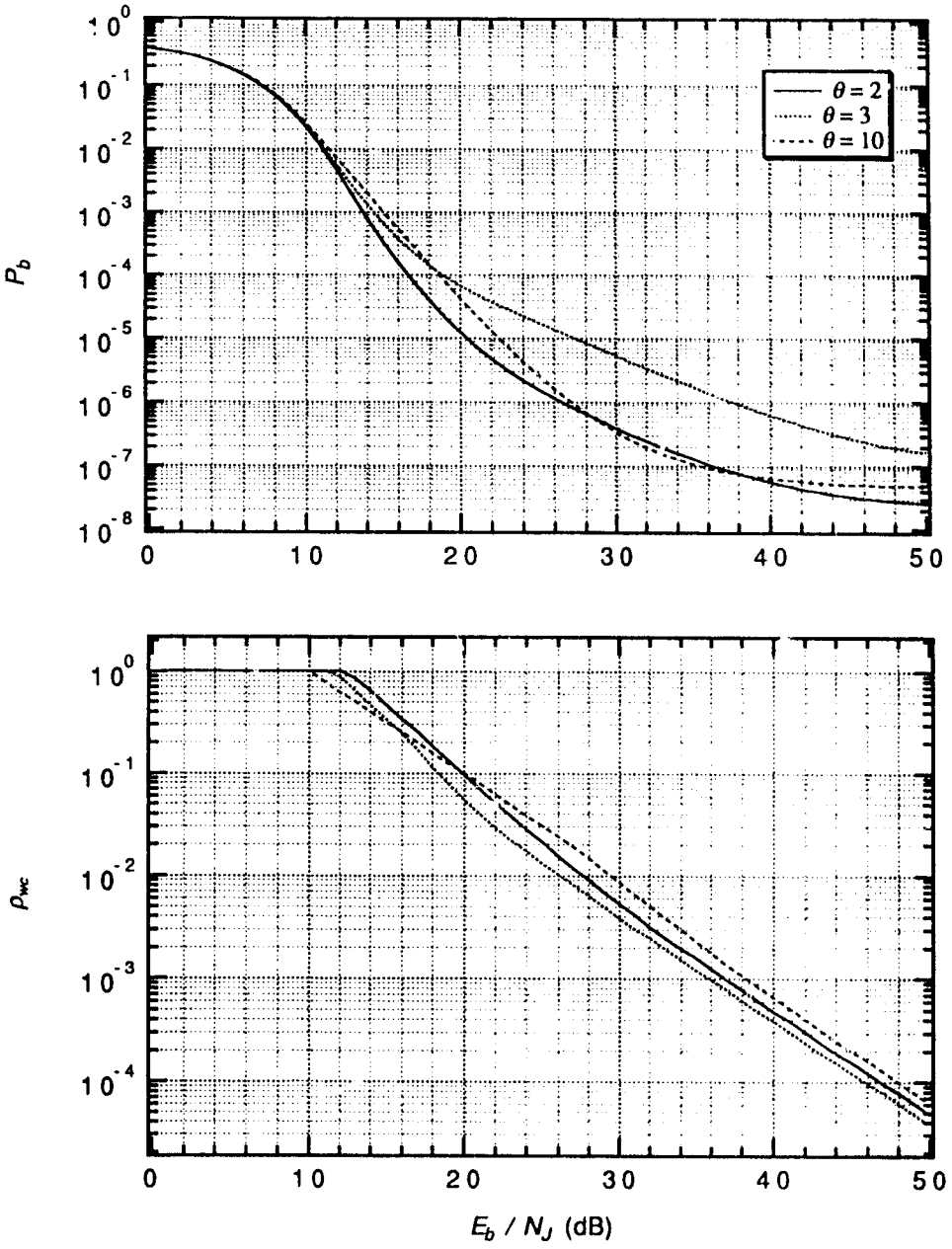

Figure 2.16: Performance of FH/4FSK with diversity $m = 5$ chips/bit and R-T diversity combiner with threshold θ in worst case partial-band noise jamming. $E_b/N_0 = 15$ dB. Upper: BER. Lower: the worst jamming parameter ρ_{wc}.

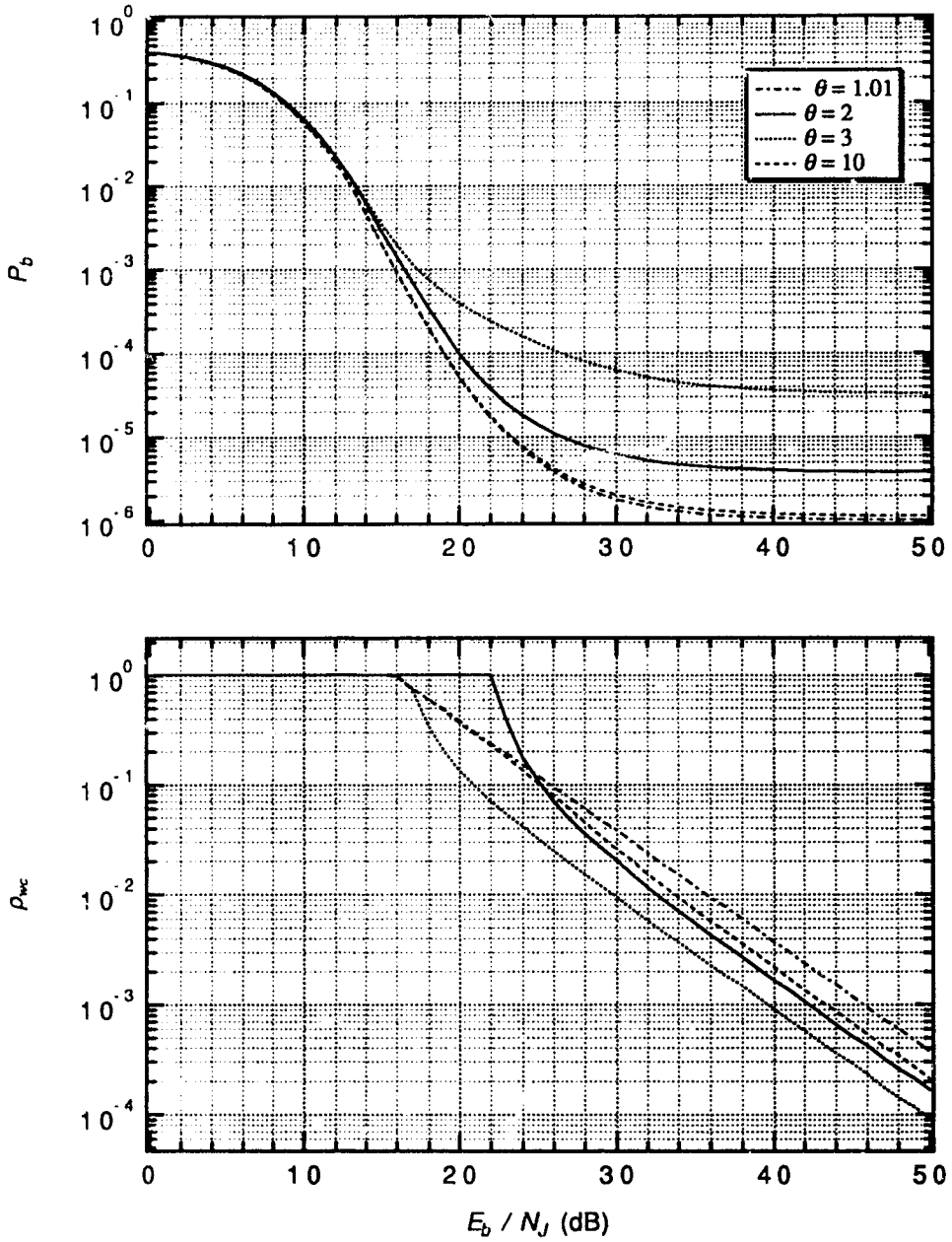

Figure 2.17: Performance of FH/4FSK with diversity $m = 9$ chips/bit and R-T diversity combiner with threshold θ in worst case partial-band noise jamming. $E_b/N_0 = 15$ dB. Upper: BER. Lower: the worst jamming parameter ρ_{wc}.

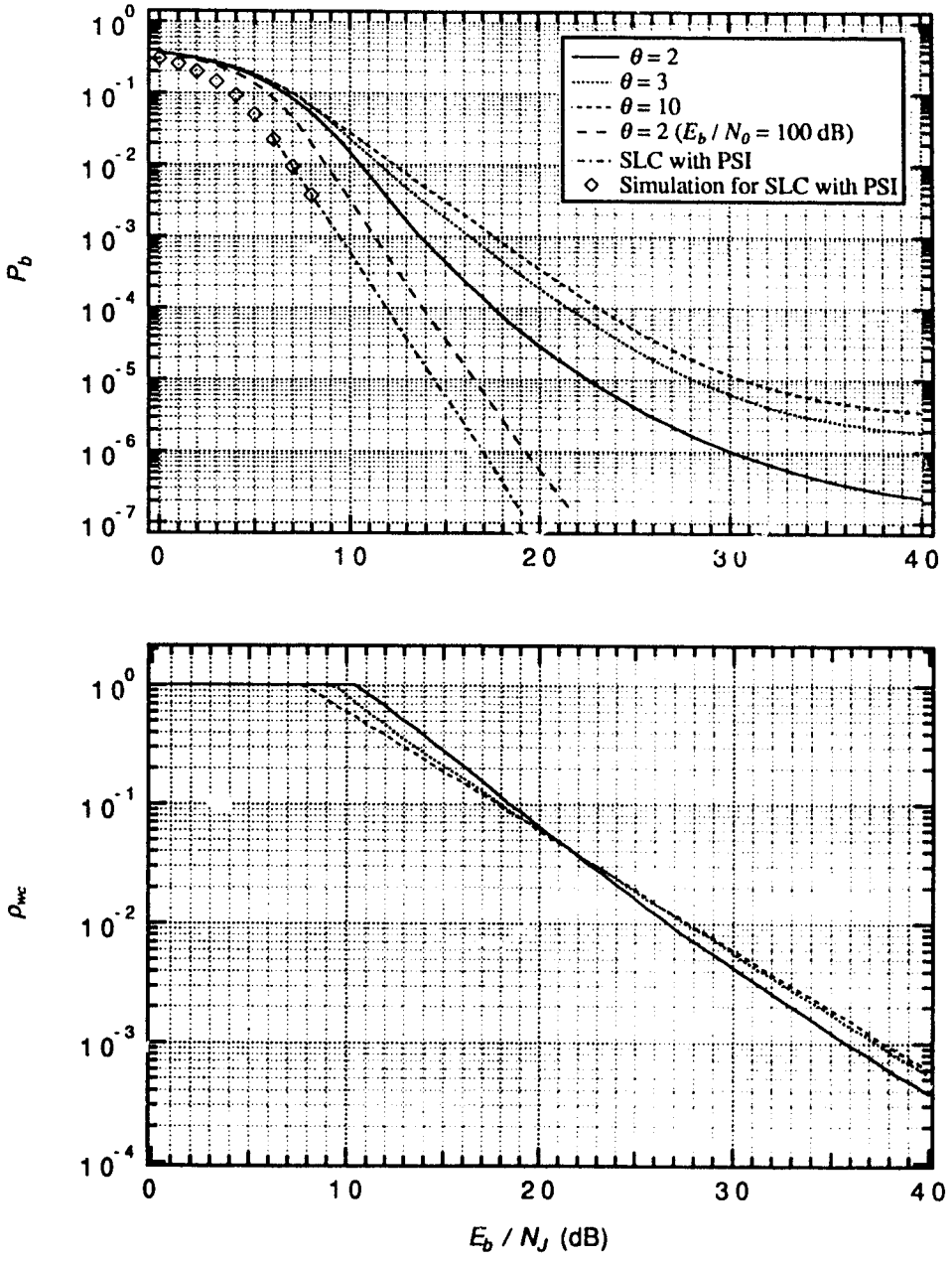

Figure 2.18: Performance of FH/8FSK with diversity $m = 4$ chips/bit and R-T diversity combiner with threshold θ in worst case partial-band noise jamming. $E_b/N_0 = 13$ dB. Upper: BER. Lower: the worst jamming parameter ρ_{wc}.

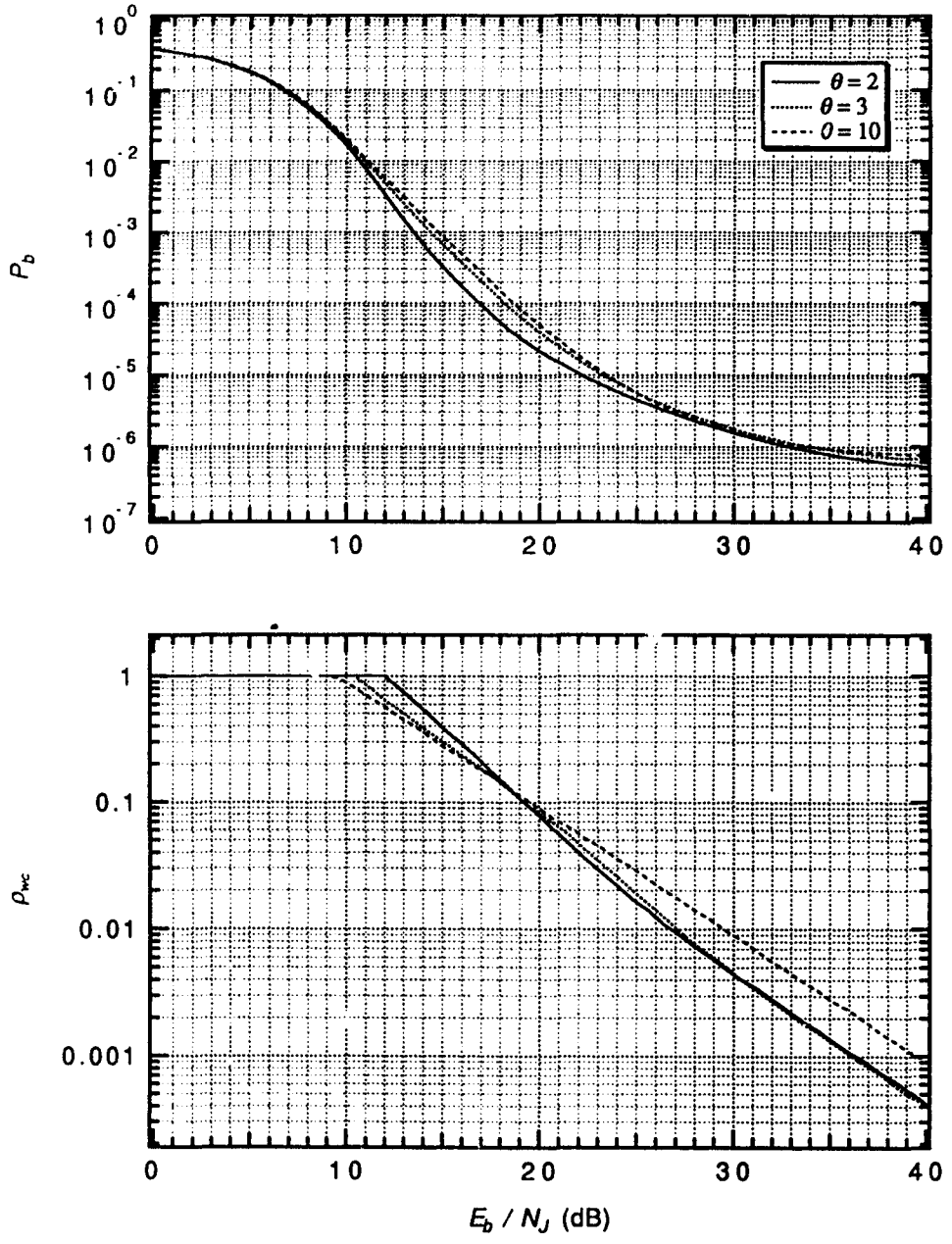

Figure 2.19: Performance of FH/8FSK with diversity $m = 5$ chips/bit and R-T diversity combiner with threshold θ in worst case partial-band noise jamming. $E_b/N_0 = 13$ dB. Upper: BER. Lower: the worst jamming parameter ρ_{wc}.

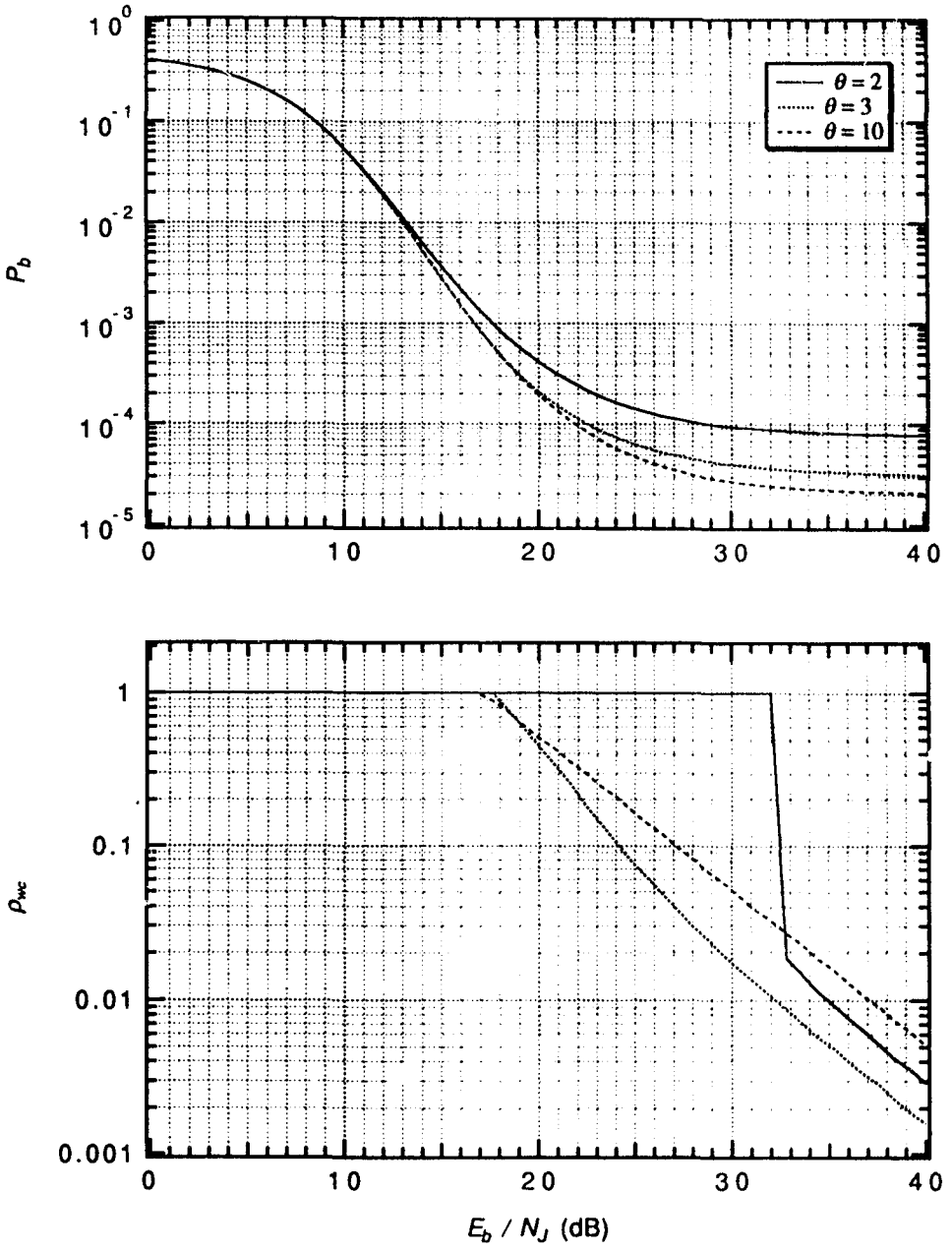

Figure 2.20: Performance of FH/8FSK with diversity $m = 9$ chips/bit and R-T diversity combiner with threshold θ in worst case partial-band noise jamming. $E_b/N_0 = 13$ dB. Upper: BER. Lower: the worst jamming parameter ρ_{wc}.

for a diversity combiner without side information. The BER of R-T combining scheme without AWGN (or with a very large E_b/N_0, e.g., 100 dB) for $m = 4$ and $\theta = 2$ is also plotted in Figure 2.12, Figure 2.15, Figure 2.18 and Figure 2.21. It can be seen that the difference in E_b/N_J at BER = 10^{-5} between R-T combiner with $\theta = 2$ and soft linear combiner with perfect side information is about 2 dB for 4-ary, 8-ary and 16-ary systems (excluding the effect of AWGN). But in binary systems, the difference is as large as 5 dB.

2.6 Conclusion

The performance of FFH/FSK spread spectrum system with ratio-threshold diversity combining has been analyzed. The exact bit error probabilities in worst case partial-band noise jamming and additive white Gaussian noise are computed.

In partial-band noise jamming, for a given M, the optimum BER performance with an optimum ratio-threshold θ is almost the same for diversity order m = 4 - 10. However, only when m is around 5, the system performance is not very sensitive to the choice of θ. For large m (m=9, or 10), the performance can be very poor for some θ which may not be far away from the optimum θ. It is also observed that for m around 5, higher the M for MFSK modulation, less sensitive to θ is the system performance. The difference in required E_b/N_J to achieve BER = 10^{-5} between the ratio-threshold combining with $m = 4$ and optimum θ and soft linear combining with perfect side information is about 2 dB in 4-ary, 8-ary, 16-ary systems, and 5 dB in binary systems (without AWGN).

2.7 Proof of Equivalence between Two States Model and the Average Single State Model

We only need to show that the summation terms in (2.1) - (2.5) using average transition probabilities $\bar{P}_C$, $\bar{P}_E$,$\bar{P_{CX}}$, $\bar{P_{EX}}$ and those in (2.11) - (2.15) are equal.

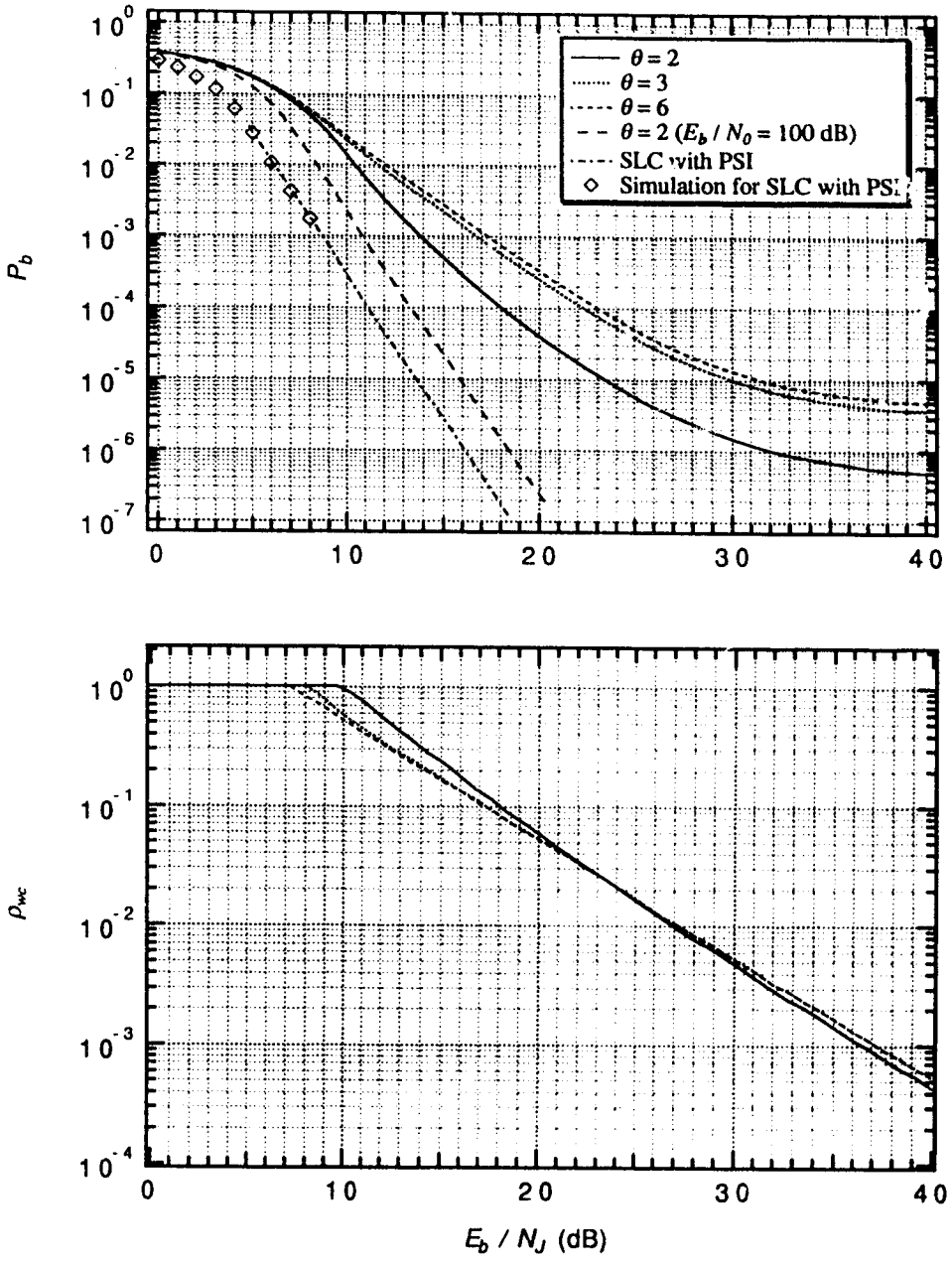

Figure 2.21: Performance of FH/16FSK with diversity $m = 4$ chips/bit and R-T diversity combiner with threshold θ in worst case partial-band noise jamming. $E_b/N_0 = 12$ dB. Upper: BER. Lower: the worst jamming parameter ρ_{wc}.

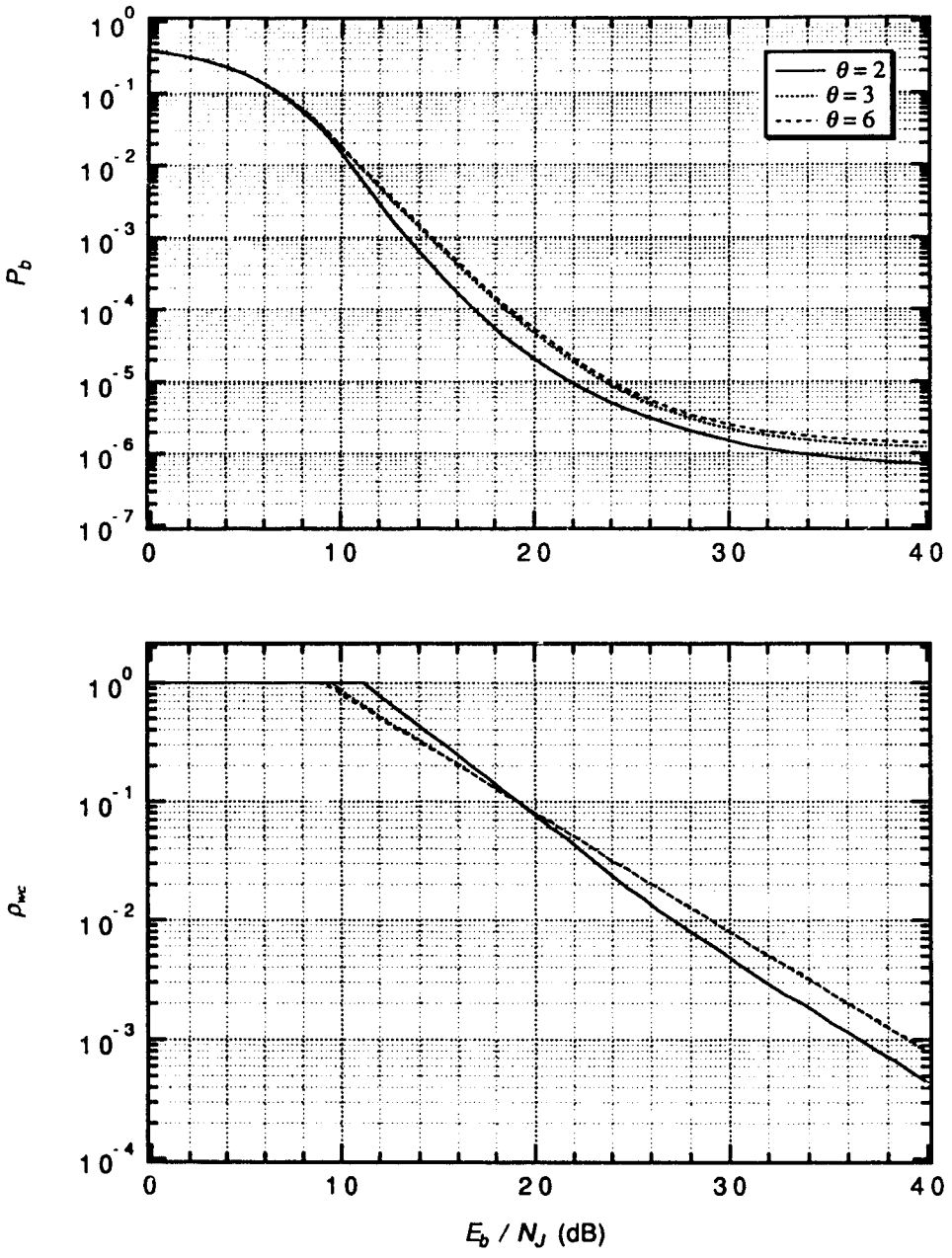

Figure 2.22: Performance of FH/16FSK with diversity $m = 5$ chips/bit and R-T diversity combiner with threshold θ in worst case partial-band noise jamming. $E_b/N_0 = 12$ dB. Upper: BER. Lower: the worst jamming parameter ρ_{wc}.

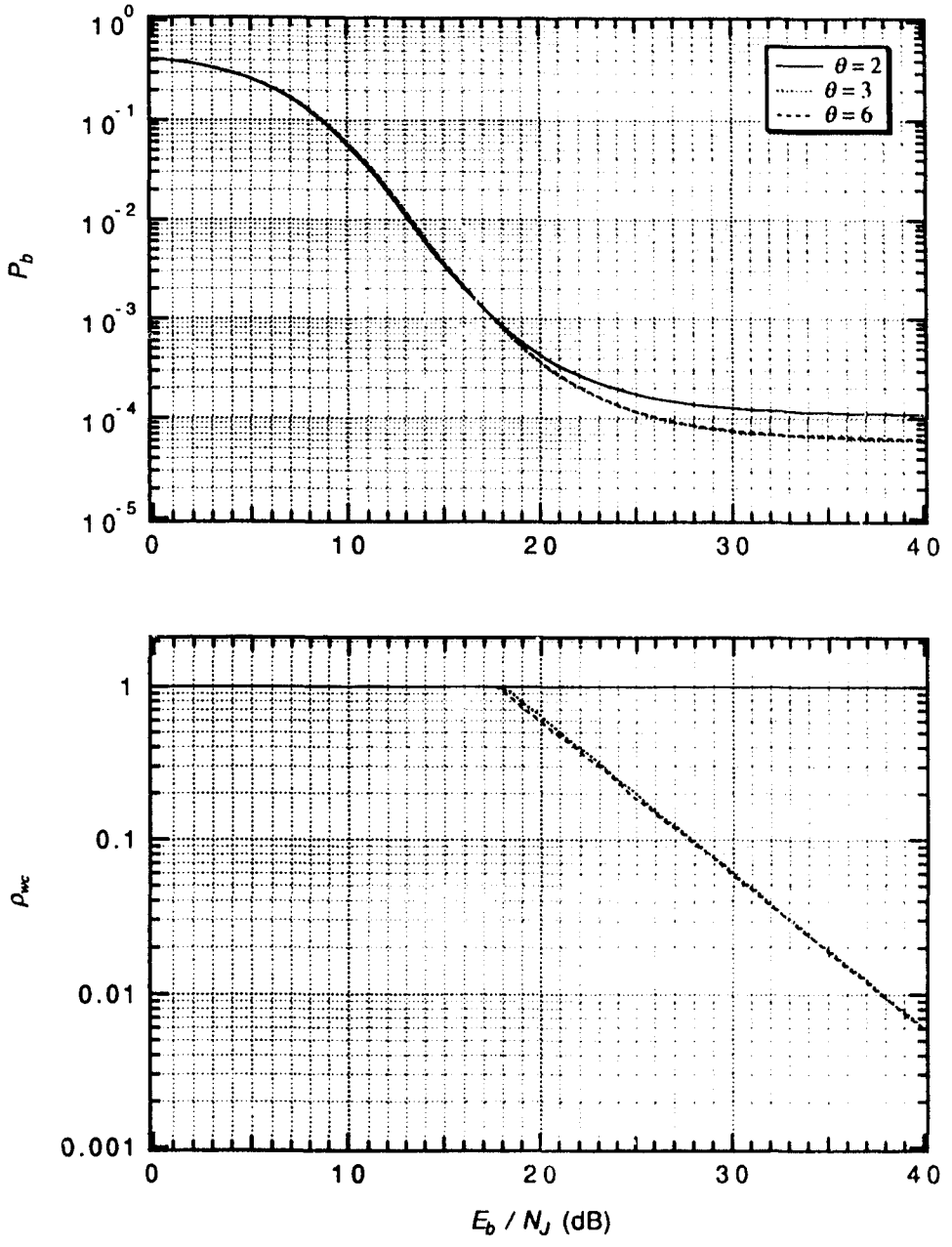

Figure 2.23: Performance of FH/16FSK with diversity $m = 9$ chips/bit and R-T diversity combiner with threshold θ in worst case partial-band noise jamming. $E_b/N_0 = 12$ dB. Upper: BER. Lower: the worst jamming parameter ρ_{wc}.

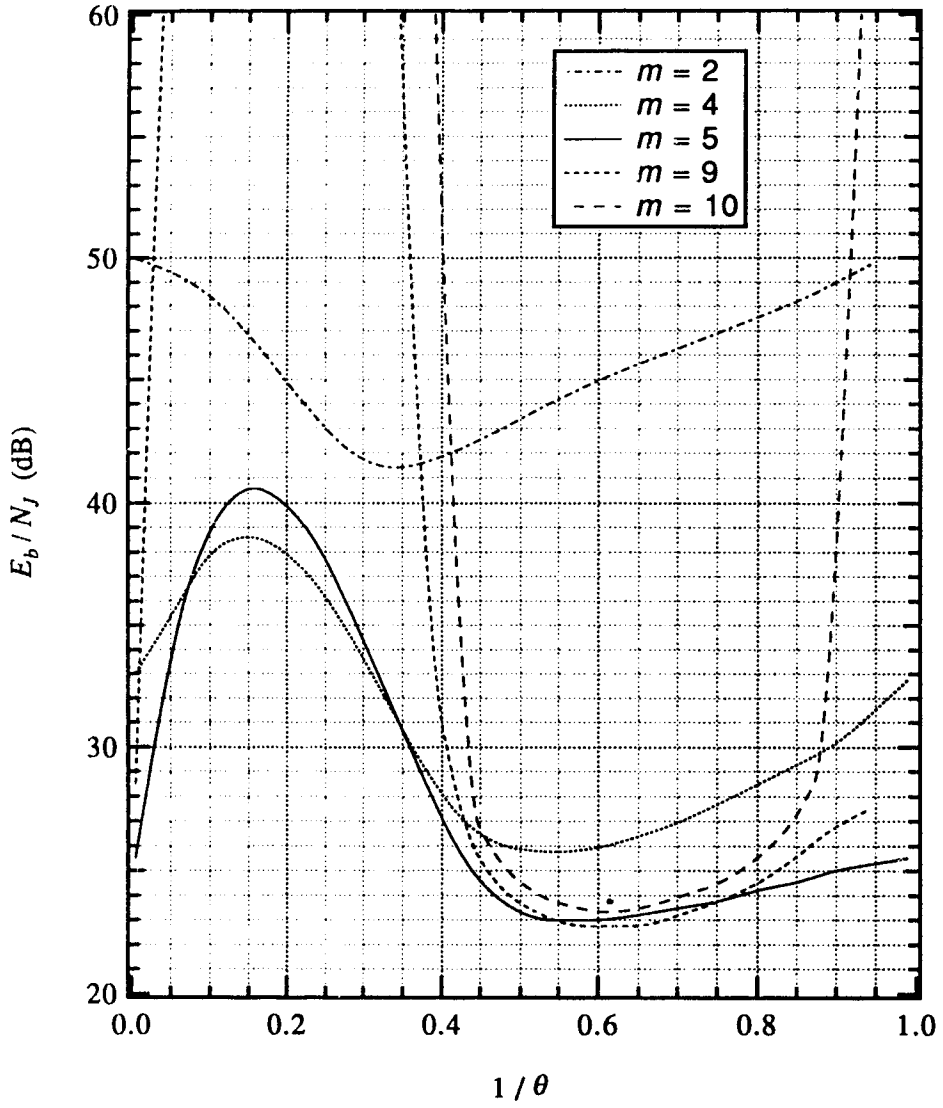

Figure 2.24: E_b/N_J required to achieve BER = 10^{-5} versus $1/\theta$ for the binary system in worst case partial-band noise jamming. $E_b/N_0 = 17$ dB.

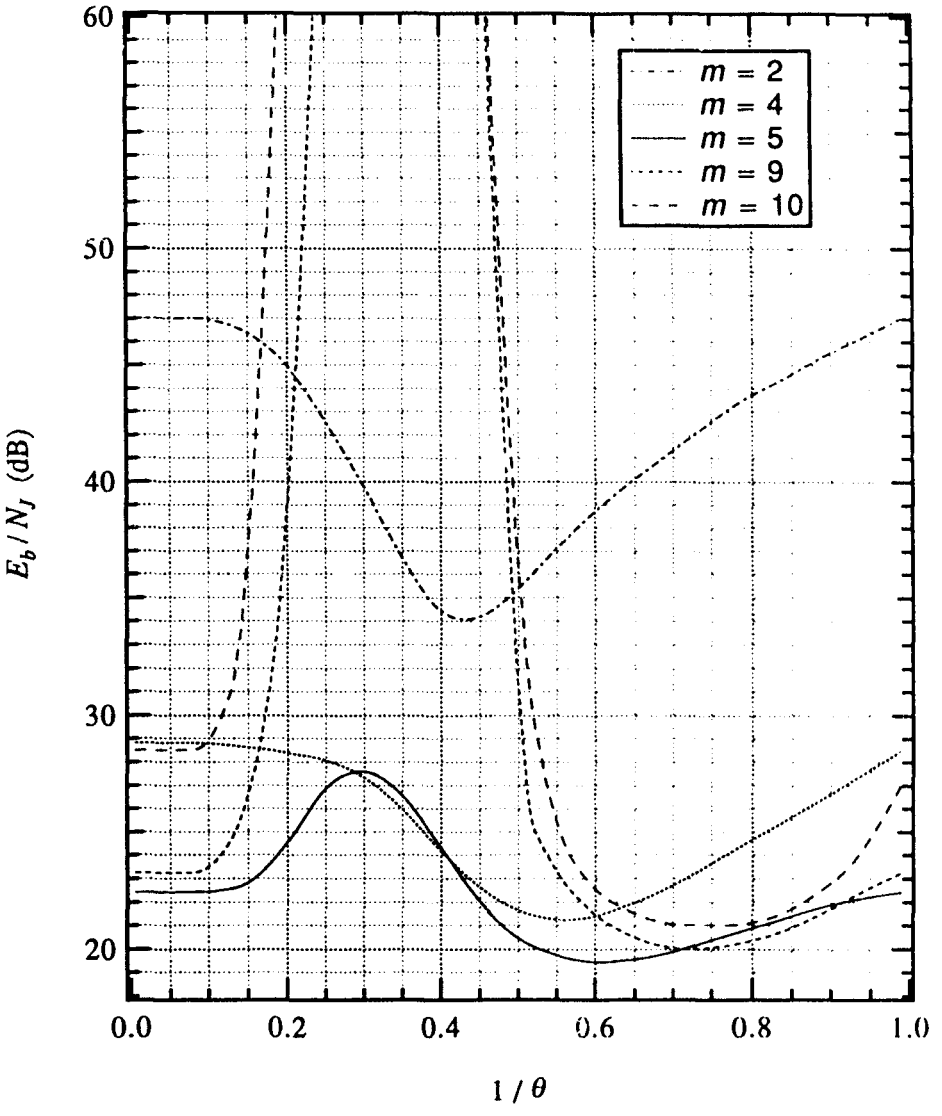

Figure 2.25: E_b/N_J required to achieve BER $= 10^{-5}$ versus $1/\theta$ for the 4-ary system in worst case partial-band noise jamming. $E_b/N_0 = 15$ dB.

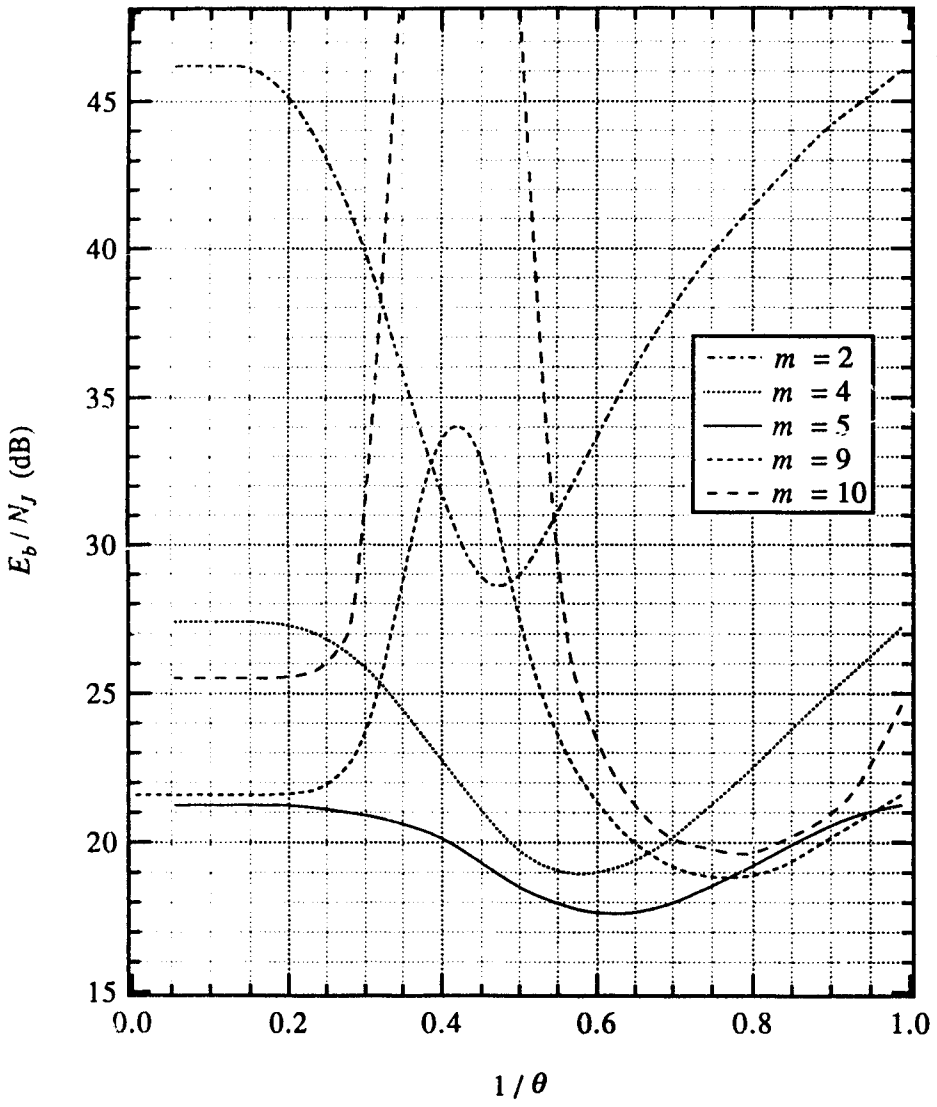

Figure 2.26: E_b/N_J required to achieve BER = 10^{-5} versus $1/\theta$ for the 8-ary system in worst case partial-band noise jamming. $E_b/N_0 = 14$ dB.

For $k_1, k_2, k_3, k_4 \in S_K$, there are

$$
\begin{aligned}
& C_m^{k_1,k_2,k_3,k_4} \bar{P_C}^{k_1} \bar{P_E}^{k_2} \bar{P_{CX}}^{k_3} \bar{P_{EX}}^{k_4} \\
= \; & C_m^{k_1,k_2,k_3,k_4} [(1-\rho)Q_C + \rho R_C]^{k_1} [(1-\rho)Q_E + \rho R_E]^{k_2} [(1-\rho)Q_{CX} + \rho R_{CX}]^{k_3} \\
& \times [(1-\rho)Q_{EX} + \rho R_{EX}]^{k_4} \\
= \; & C_m^{k_1,k_2,k_3,k_4} \sum_{l_1=0}^{k_1} C_{k_1}^{l_1} (1-\rho)^{l_1} \rho^{k_1-l_1} Q_C^{l_1} R_C^{k_1-l_1} \sum_{l_2=0}^{k_2} C_{k_2}^{l_2} (1-\rho)^{l_2} \rho^{k_2-l_2} Q_E^{l_2} R_E^{k_2-l_2} \\
& \times \sum_{l_3=0}^{k_3} C_{k_3}^{l_3} (1-\rho)^{l_3} \rho^{k_3-l_3} Q_{CX}^{l_3} R_{CX}^{k_3-l_3} \sum_{l_4=0}^{k_4} C_{k_4}^{l_4} (1-\rho)^{l_4} \rho^{k_4-l_4} Q_{EX}^{l_4} R_{EX}^{k_4-l_4} \\
= \; & \sum_{l_1=0}^{k_1} \sum_{l_2=0}^{k_2} \sum_{l_3=0}^{k_3} \sum_{l_4=0}^{k_4} C_m^{k_1,k_2,k_3,k_4} C_{k_1}^{l_1} C_{k_2}^{l_2} C_{k_3}^{l_3} C_{k_4}^{l_4} (1-\rho)^{l_1+l_2+l_3+l_4} \\
& \times \rho^{k_1+k_2+k_3+k_4-l_1-l_2-l_3-l_4} Q_C^{l_1} Q_E^{l_2} Q_{CX}^{l_3} Q_{EX}^{l_4} R_C^{k_1-l_1} R_E^{k_2-l_2} R_{CX}^{k_3-l_3} R_{EX}^{k_4-l_4} \\
= \; & f_2(k_1, k_2, k_3, k_4, Q_C, Q_E, Q_{CX}, Q_{EX}, R_C, R_E, R_{CX}, R_{EX}, \rho).
\end{aligned}
$$

Here we have used the following relations:

$$
\begin{aligned}
& C_m^{k_1,k_2,k_3,k_4} C_{k_1}^{l_1} C_{k_2}^{l_2} C_{k_3}^{l_3} C_{k_4}^{l_4} \\
= \; & \frac{m!}{k_1!k_2!k_3!k_4!} \frac{k_1!}{l_1!(k_1-l_1)!} \frac{k_2!}{l_2!(k_2-l_2)!} \frac{k_3!}{l_3!(k_3-l_3)!} \frac{k_4!}{l_4!(k_4-l_4)!} \\
= \; & \frac{r!}{l_1!l_2!l_3!l_4!(k_1-l_1)!(k_2-l_2)!(k_3-l_3)!(k_4-l_4)!} \\
= \; & C_m^{l_1,l_2,l_3,l_4,k_1-l_1,k_2-l_2,k_3-l_3,k_4-l_4}
\end{aligned}
$$

and

$$
k_1 + k_2 + k_3 + k_4 = m \qquad \text{for } k_1, k_2, k_3, k_4 \in S_K.
$$

Chapter 3

Performance of Ratio-Threshold Diversity Combining Scheme in FFH/FSK Systems under Multitone Jamming

3.1 Introduction

In this chapter, the bit error probabilities of the FFH/MFSK system with ratio-threshold diversity combining under worst case multitone jamming with and without background thermal noise are computed by using the average computation model developed in the previous chapter. Results are compared with the performance of the FFH/MFSK systems with diversity utilizing the soft decision metric with perfect side information. The effect on the system performance of different system parameters, such as diversity order, ratio-threshold, and signal-to-thermal-noise ratio, and jamming parameters are also analyzed. Finally, the performance of the system with ratio-threshold diversity combining under partial-band noise and band tone jamming are compared.

3.2 Performance under Band Multitone Jamming without Thermal Noise

We consider band multitone jamming with the number of jamming tones in each M-ary FSK band $n = 1$. We illustrate the performance of R-T diversity combiner under band tone jamming without thermal noise at first. Some interesting behavior of the worst jamming parameter α has been found. In next section, we analyze the performance of R-T diversity combiner under band tone jamming with thermal background noise which is modeled by AWGN.

The analysis for $n = 1$ band multitone jamming is relatively simple, because the random jamming phase has no effect on the system performance in this case. This type of band multitone jamming seems to be the most effective in almost all cases [1].

3.2.1 Binary Case

It can be shown that $F_C(\theta)$ and $F_E(\theta)$ are (see Section 3.6 for detail derivation):

$$F_C(\theta) = \begin{cases} 1 & \text{if } \alpha > \theta^2; \\ 1 - \frac{\mu}{2} & \text{otherwise.} \end{cases}$$

$$F_E(\theta) = \begin{cases} \frac{\mu}{2} & \text{if } 0 < \alpha < \frac{1}{\theta^2}; \\ 0 & \text{otherwise.} \end{cases}$$

Here α is the power ratio of signal to one jamming tone, and can be optimized by the jammer on the range $0 < \alpha < +\infty$. μ is the probability of one binary band being jammed, and in our case is given by [1]:

$$\mu = \frac{2m\alpha}{E_b/N_J}. \tag{3.1}$$

Then P_C, P_{CX}, P_{EX}, and P_E are given by:

$$P_C(\theta) = \begin{cases} 1 & \text{if } \alpha > \theta^2; \\ 1 - \frac{\mu}{2} & \text{otherwise.} \end{cases}$$

$$P_{CX}(\theta) = \begin{cases} \frac{\mu}{2} & \text{if } 1 < \alpha < \theta^2; \\ 0 & \text{otherwise.} \end{cases}$$

$$P_{EX}(\theta) = \begin{cases} \frac{\mu}{2} & \text{if } \frac{1}{\theta^2} < \alpha < 1; \\ 0 & \text{otherwise.} \end{cases}$$

$$P_E(\theta) = \begin{cases} \frac{\mu}{2} & \text{if } 0 < \alpha < \frac{1}{\theta^2}; \\ 0 & \text{otherwise.} \end{cases}$$

We can see that when $\alpha > 1$, P_E and P_{EX} are always zero, and therefore, there are no errors in transmission, i.e., $P_b = 0$.

When $\frac{1}{\theta^2} < \alpha < 1$, $P_E = 0$, $P_{EX} = \frac{\mu}{2}$, $P_{CX} = 0$, and $P_C = 1 - \frac{\mu}{2}$. According to the combining rule, the hop decisions with good quality have priority. So an incorrect decision can be made only when all m hop decisions are bad. Hence,

$$P_b = P_{EX}^m = \left(\frac{\mu}{2}\right)^m.$$

When $\alpha < \frac{1}{\theta^2}$, both P_{CX} and P_{EX} are zero. So the final decision is based on those hop decisions with good quality bits. Therefore,

$$\begin{aligned} P_b &= \sum_{k=\lceil \frac{m}{2} \rceil}^{m} \left[1 - 0.5\delta(k - \frac{m}{2})\right] \binom{m}{k} P_E^k P_C^{m-k} \\ &= \sum_{k=\lceil \frac{m}{2} \rceil}^{m} \left[1 - 0.5\delta(k - \frac{m}{2})\right] \binom{m}{k} \left(\frac{\mu}{2}\right)^k \left(1 - \frac{\mu}{2}\right)^{m-k}, \end{aligned}$$

where

$$\delta(x) = \begin{cases} 1 & \text{if } x = 0; \\ 0 & \text{otherwise.} \end{cases}$$

Thus the bit error rate under band tone jamming with $n = 1$ is:

$$P_b = \begin{cases} 0 & \text{if } \alpha > 1; \\ \left(\frac{\mu}{2}\right)^m & \text{if } \frac{1}{\theta^2} < \alpha < 1; \\ \sum_{k=\lceil \frac{m}{2} \rceil}^{m} \left[1 - 0.5\delta(k - \frac{m}{2})\right] \binom{m}{k} & \\ \times \left(\frac{\mu}{2}\right)^k \left(1 - \frac{\mu}{2}\right)^{m-k} & \text{if } \alpha < \frac{1}{\theta^2}. \end{cases} \tag{3.2}$$

We can now analyze the worst case, in which the jammer optimizes α to cause the worst transmission performance. First we note that P_b given in (3.2) is a piecewise monotonically increasing function of μ when $\mu \leq 1$. And from (3.1) we know that μ is a monotonically increasing function of α. When $\mu = 1$, it means that there is one jamming tone in every binary FSK band. Thus, α cannot be further increased to provide more jamming tones under the assumption that there is at most one jamming tone per binary FSK band. Therefore,

$$\alpha \leq \alpha_{max} = \frac{E_b/N_J}{2m}$$

When $\alpha_{max} < \frac{1}{\theta^2}$, or $\frac{E_b}{N_J} < \frac{2m}{\theta^2}$, because P_b is a monotonically increasing function of α, the only choice for α is

$$\alpha_{wc} = \alpha_{max} = \frac{E_b/N_J}{2m}.$$

This α causes P_b to be 0.5.

When $\frac{1}{\theta^2} < \alpha_{max} < 1$, or $\frac{2m}{\theta^2} < \frac{E_b}{N_J} < 2m$, α has two possible choices:

$$\alpha = \alpha_{max} = \frac{E_b/N_J}{2m}$$

and the corresponding

$$P_b^{(1)} = 0.5^m;$$

or

$$\alpha = \left(\frac{1}{\theta^2}\right)^-$$

where $(A)^- = \lim_{x<A, x\to A} x$, and the corresponding

$$P_b^{(2)} = \sum_{k=\lceil \frac{m}{2} \rceil}^{m} \left[1 - 0.5\delta(k - \frac{m}{2})\right] \binom{m}{k} \left(\frac{\mu}{2}\right)^k \left(1 - \frac{\mu}{2}\right)^{m-k}.$$

The worst α should be the one which gives larger P_b.

When $\alpha_{max} > 1$, α also has two possible choices:

$$\alpha = 1^-$$

and the corresponding

$$P_b^{(1)} = \left(\frac{m}{E_b/N_J}\right)^m;$$

or

$$\alpha = \left(\frac{1}{\theta^2}\right)^-$$

and the corresponding

$$P_b^{(2)} = \sum_{k=\lceil \frac{m}{2} \rceil}^{m} \left[1 - 0.5\delta(k - \frac{m}{2})\right] \left(\begin{array}{c} m \\ k \end{array} \right) \left(\frac{\mu}{2}\right)^k \left(1 - \frac{\mu}{2}\right)^{m-k}.$$

And the worst α should be the one which gives larger P_b.

In order to determine what the worst α is, we have to know the behavior of the following two functions

$$\begin{aligned} h_1(x) &= \left(\frac{x}{2}\right)^m, \\ h_2(x,\theta) &= \sum_{k=\lceil \frac{m}{2} \rceil}^{m} C(m,k) \left(\frac{x}{2\theta^2}\right)^k \left(1 - \frac{x}{2\theta^2}\right)^{m-k}, \end{aligned}$$

where

$$C(m,k) = \left[1 - 0.5\delta\left(k - \frac{m}{2}\right)\right] \left(\begin{array}{c} m \\ k \end{array} \right).$$

We are only interested in the regions $0 \leq x \leq 1$ for $h_1(x)$ and $0 \leq x \leq \theta^2$ with $\theta \geq 1$ for $h_2(x,\theta)$.

First, we note that $h_1(x)$ equals 0.5^m at $x = 1$, and that $h_1(x)$ decreases as x decreases. When $x = 0$, $h_1(x) = 0$. Secondly, it can be seen that $h_2(x,\theta)$ equals

m	$1/\mu_0$
1	1.000
2	2.000
3	2.262
4	3.284
5	3.144
6	4.039
7	3.762
8	4.541
9	4.216
10	4.902

Table 3.1: The cross point of $h_2(x,1)$ with 0.5^m, μ_0.

0.5 at $x = 1$ and $\theta = 1$, and that $h_2(x,\theta)$ decreases as x decreases with a fixed θ or as θ increases with a fixed x. Also there is $h_2(0,\theta) = h_2(x,\infty) = 0$.

Now we compare $h_2(x,1)$ with 0.5^m. Because $h_2(1,1) = 0.5$, $h_2(0,1) = 0$, and $h_2(x,1)$ is a monotonic function of x, there is one, and only one point of x such that $h_2(x,1) = 0.5^m$. We call this point as μ_0. And μ_0 is solution of the following equation:

$$\sum_{k=\lceil \frac{m}{2} \rceil}^{m} C(m,k) \left(\frac{x}{2}\right)^k \left(1 - \frac{x}{2}\right)^{m-k} = 0.5^m. \tag{3.3}$$

It can be seen later that $1/\mu_0$ is a very useful parameter. $1/\mu_0$ for m =1 to 10 are given in Table 3.1.

$h_1(x)$ and $h_2(x,\theta)$ versus $1/x$ with θ as parameter for $m = 4$ are plotted in Figure 3.1. Because when $\theta = 1$, $h_1(x)$ is one term in the summation of $h_2(x,\theta)$, and all terms in the summation of $h_2(x,\theta)$ are nonnegative, $h_2(x,1)$ is always greater than or equal to $h_1(x)$. Now we focus on the region for $0 \leq x \leq 1$. The figure shows that as θ increases, the curve of $h_2(x,\theta)$ moves lower. There is a θ_0 so that when $\theta < \theta_0$, $h_2(x,\theta)$ is always greater than $h_1(x)$, and there is no cross point between them. And when $\theta > \theta_0$, we can show that there is one and only one cross

point between $h_1(x)$ and $h_2(x,\theta)$. At the left side of cross point, $h_1(x) > h_2(x,\theta)$. While at the right side of cross point $h_2(x,\theta) > h_1(x)$.

θ_0 is such that $h_1(x)$ equals $h_2(x,\theta)$ at $x = 1$. θ_0 always exists. Because when $x = 1$, $h_1(1) = 0.5^m$, and $h_2(1,1) = 0.5$, $h_2(1,\infty) = 0$, and $h_2(1,\theta)$ is a monotonic function of θ, there must be one and only one θ such that

$$h_2(1,\theta) = h_1(1).$$

θ_0 can be determined by solving the following equation:

$$\sum_{k=\lceil \frac{m}{2} \rceil}^{m} C(m,k) \left(\frac{1}{2\theta_0^2}\right)^k \left(1 - \frac{1}{2\theta_0^2}\right)^{m-k} = 0.5^m$$

Comparing with Eq. (3.3), it is easy to find that

$$\theta_0^2 = \frac{1}{\mu_0}$$

Consider $\frac{h_2(x,\theta)}{h_1(x)}$ in the region of $0 < x \leq 1$.

$$\begin{aligned}
\frac{h_2(x,\theta)}{h_1(x)} &= \sum_{k=\lceil \frac{m}{2} \rceil}^{m} C(m,k) \frac{\left(\frac{x}{2\theta^2}\right)^k \left(1 - \frac{x}{2\theta^2}\right)^{m-k}}{\left(\frac{x}{2}\right)^m} \\
&= \sum_{k=\lceil \frac{m}{2} \rceil}^{m} \frac{C(m,k)}{\theta^{2m}} \left(\frac{1 - \frac{x}{2\theta^2}}{\frac{x}{2\theta^2}}\right)^{m-k} \\
&= \sum_{k=\lceil \frac{m}{2} \rceil}^{m} \frac{C(m,k)}{\theta^{2m}} \left(\frac{2\theta^2}{x} - 1\right)^{m-k}.
\end{aligned}$$

It is easy to see that every term in the summation is positive and increases with x decreasing. Thus $\frac{h_2}{h_1}$ is a monotonic function of x in the specified region. Also note that $\frac{h_2}{h_1} > 1$ when x is small enough. Furthermore, when $\theta > \theta_0$, $h_1(1) > h_2(1,\theta)$,

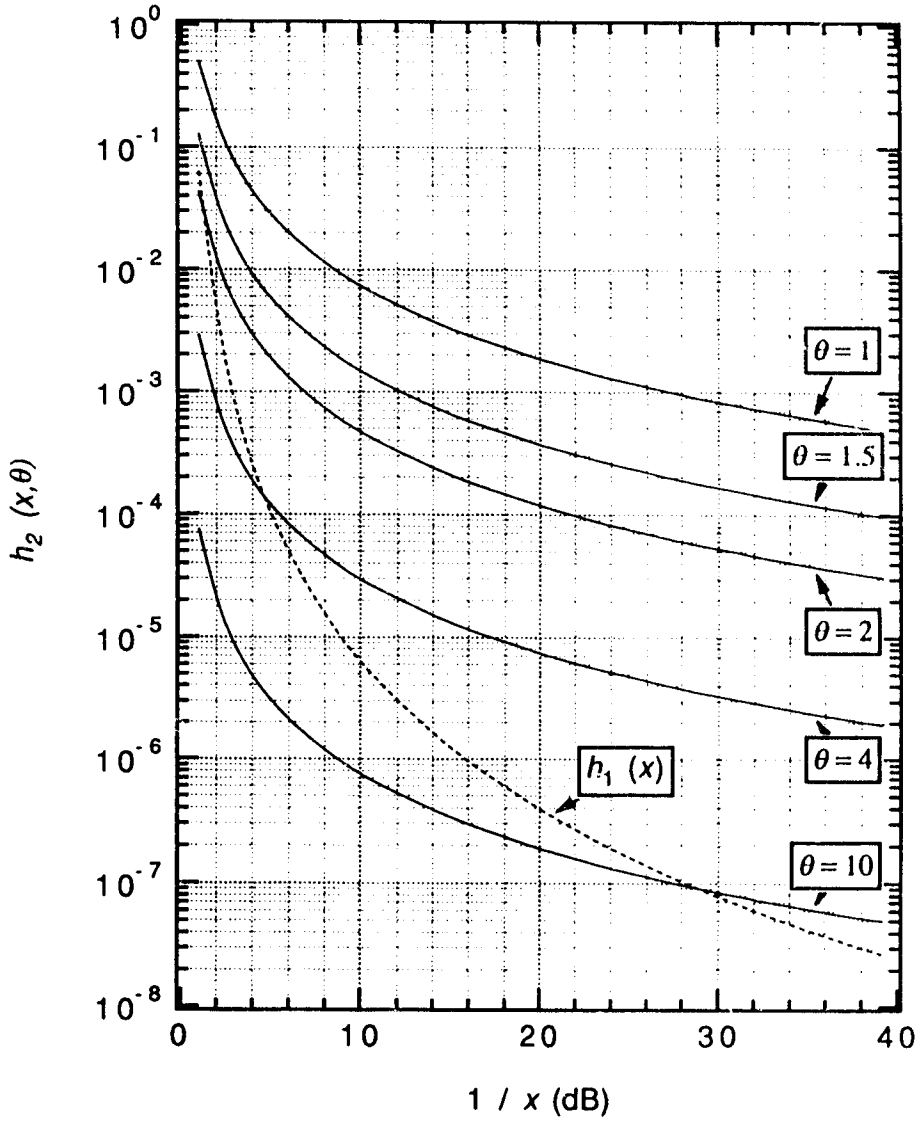

Figure 3.1: $h_1(x)$ and $h_2(x,\theta)$ with θ as parameter versus $1/x$. $m = 4$; $\theta = 1, 1.5, 2, 4$, and 10.

i.e., $\frac{h_2}{h_1} < 1$ at $x = 1$. Therefore, there is one and only one cross point between $h_1(x)$ and $h_2(x,\theta)$ when $\theta > \theta_0$.

With the knowledge of $h_1(x)$ and $h_2(x,\theta)$, now we can continue the work to determine the worst α.

When $\frac{1}{\theta^2} < \alpha_{max} < 1$, or $\frac{2m}{\theta^2} < \frac{E_b}{N_J} < 2m$,

$$P_b^{(2)} = h_2\left(\frac{2m}{E_b/N_J}, \theta\right) = h_2\left(1, \sqrt{\frac{E_b/N_J}{2m}}\theta\right).$$

According to the analysis of $h_1(x)$ and $h_2(x,\theta)$, we can see that if $\sqrt{\frac{E_b/N_J}{2m}}\theta > \theta_0$, or $\frac{E_b}{N_J} > \frac{2m}{\theta^2\mu_0} = \left(\frac{E_b}{N_J}\right)_{T1}$, $P_b^{(2)} < P_b^{(1)} = 0.5^m$. So $\alpha_{wc} = \alpha_{max}$, and the corresponding $P_b = P_b^{(1)}$. On the other hand, if $\frac{E_b}{N_J} < \left(\frac{E_b}{N_J}\right)_{T1}$, $P_b^{(2)} > P_b^{(1)}$. So $\alpha_{wc} = \left(\frac{1}{\theta}\right)^-$, and the corresponding $P_b = P_b^{(2)}$. In summary, the worst α is

$$\alpha_{wc} = \begin{cases} \left(\frac{1}{\theta^2}\right)^- & \text{if } \frac{E_b}{N_J} < \left(\frac{E_b}{N_J}\right)_{T1}; \\ \alpha_{max} & \text{otherwise.} \end{cases} \tag{3.4}$$

The corresponding P_b is

$$P_b = \begin{cases} \sum_{k=\lceil \frac{m}{2} \rceil}^{m} C(m,k)\left(\frac{m}{\theta^2 E_b/N_J}\right)^k \left(1 - \frac{m}{\theta^2 E_b/N_J}\right)^{m-k} & \text{if } \frac{E_b}{N_J} < \left(\frac{E_b}{N_J}\right)_{T1}; \\ 0.5^m & \text{otherwise.} \end{cases} \tag{3.5}$$

When $\alpha_{max} > 1$, or $E_b/N_J > 2m$, there are

$$P_b^{(1)} = h_1\left(\frac{2m}{E_b/N_J}\right);$$

$$P_b^{(2)} = h_2\left(\frac{2m}{E_b/N_J}, \theta\right).$$

If $\theta^2 < \theta_0^2 = \frac{1}{\mu_0}$, $P_b^{(2)}$ is always no less than $P_b^{(1)}$. When $\theta^2 > \theta_0^2$, there is a cross point between $P_b^{(1)}$ and $P_b^{(2)}$. Define the cross point as $\left(\frac{E_b}{N_J}\right)_{T2}$. Then for

$\frac{E_b}{N_J} < \left(\frac{E_b}{N_J}\right)_{T2}$, $P_b^{(1)} > P_b^{(2)}$; and for $\frac{E_b}{N_J} > \left(\frac{E_b}{N_J}\right)_{T2}$, $P_b^{(2)} > P_b^{(1)}$. Therefore, the worst α is

$$\alpha_{wc} = \begin{cases} \left(\frac{1}{\theta^2}\right)^- & \text{if } \theta^2 < \frac{1}{\mu_0}; \\ 1^- & \text{if } \theta^2 > \frac{1}{\mu_0} \text{ and } \frac{E_b}{N_J} < \left(\frac{E_b}{N_J}\right)_{T2}; \\ \left(\frac{1}{\theta^2}\right)^- & \text{if } \theta^2 > \frac{1}{\mu_0} \text{ and } \frac{E_b}{N_J} > \left(\frac{E_b}{N_J}\right)_{T2}; \end{cases} \tag{3.6}$$

where the crossing point $\left(\frac{E_b}{N_J}\right)_{T2}$ is the solution of the following equation:

$$\left(\frac{m}{E_b/N_J}\right)^m = \sum_{k=\lceil \frac{m}{2} \rceil}^{m} \left[1 - 0.5\delta(k - \frac{m}{2})\right] \binom{m}{k} \left(\frac{m}{\theta^2 E_b/N_J}\right)^k \times \left(1 - \frac{m}{\theta^2 E_b/N_J}\right)^{m-k}.$$

The corresponding P_b is

$$P_b = \begin{cases} \sum_{k=\lceil \frac{m}{2} \rceil}^{m} C(m,k) \left(\frac{m}{\theta^2 E_b/N_J}\right)^k & \\ \times \left(1 - \frac{m}{\theta^2 E_b/N_J}\right)^{m-k} & \text{if } \theta^2 < \frac{1}{\mu_0}; \\ \left(\frac{m}{E_b/N_J}\right)^m & \text{if } \theta^2 > \frac{1}{\mu_0} \text{ and } \frac{E_b}{N_J} < \left(\frac{E_b}{N_J}\right)_{T2}; \\ \sum_{k=\lceil \frac{m}{2} \rceil}^{m} C(m,k) \left(\frac{m}{\theta^2 E_b/N_J}\right)^k & \\ \times \left(1 - \frac{m}{\theta^2 E_b/N_J}\right)^{m-k} & \text{if } \theta^2 > \frac{1}{\mu_0} \text{ and } \frac{E_b}{N_J} > \left(\frac{E_b}{N_J}\right)_{T2}. \end{cases} \tag{3.7}$$

The bit error rate of a R-T combiner under band multitone jamming with $n = 1$ for $m = 2, 4$, and 9 in worst case are plotted in upper figures of Figs. 3.2, 3.3, and 3.4, respectively. The worst case performances are obtained by using (3.2) with a numerical search for the worst α. The numerical results verify our analytical results in (3.4), (3.5), (3.6), and (3.7).

These figures show that unlike the PBN case, choice of the parameter θ is very important. Larger θ gives much better performance. The lowest curve in the family of curves is the bit error probability of the R-T combiner with the largest θ and this is the best performance. This curve also forms the lower envelope of the

family of curves. In fact, the lower envelope of the BER curves with sufficiently large θ is the BER of a soft linear diversity combiner with perfect side information under the worst case band multitone jamming with $n = 1$, given by [1, Eq. (2.76)]. So, when θ is large enough, the performance of a R-T combiner can achieve the optimum performance without side information.

The worst α for $m = 2, 4$ and 9 are plotted in lower figures of Figs. 3.2, 3.3, and 3.4, respectively. Here we can see why a larger θ provides better performance. First, a large θ forces α_{wc} to be small, which means that the jammer must increase the power at each tone and jam fewer BFSK bands. Secondly, a large θ makes the crossing point $\left(\frac{E_b}{N_J}\right)_{T2}$ high. When $\frac{E_b}{N_J} < \left(\frac{E_b}{N_J}\right)_{T2}$, the BER curve coincides with the lower envelope, which is the optimum performance. So larger the $\left(\frac{E_b}{N_J}\right)_{T2}$, larger the region in which the performance achieves optimum.

However, the conclusion that a larger θ is better is made under the assumption that there is no thermal noise. When noise is considered, too large a θ could cause performance degradation. Thus there should be a finite optimum θ when the effect of thermal noise can not be ignored.

3.2.2 M-ary Case

Under band multitone jamming with $n = 1$, and ignoring the background noise, $F_C(\theta)$ and $F_E(\theta)$ are (see Section 3.6 for details):

$$F_C(\theta) = \begin{cases} 1 & \text{if } \alpha > \theta^2; \\ 1 - \frac{M-1}{M}\mu & \text{otherwise.} \end{cases}$$

$$F_E(\theta) = \begin{cases} \frac{\mu}{M} & \text{if } 0 < \alpha < \frac{1}{\theta^2}; \\ 0 & \text{otherwise.} \end{cases}$$

Here μ is given by [1]:

$$\mu = \frac{\alpha m M}{K E_b / N_J}.$$

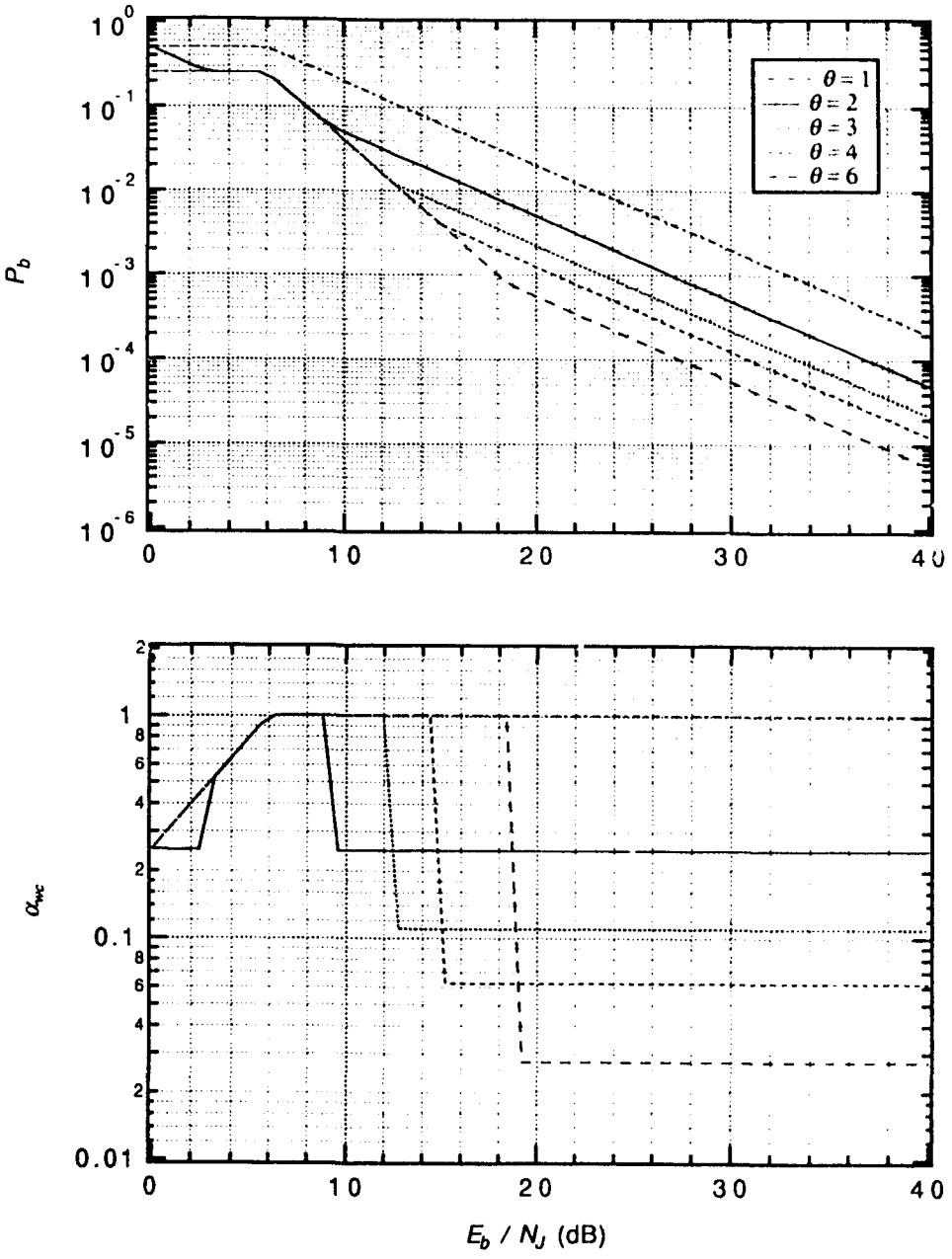

Figure 3.2: Performance of FH/BFSK with diversity $m = 2$ chips/bit and R-T diversity combiner with threshold θ in worst case $n = 1$ band multitone jamming without noise. Upper: BER. Lower: the worst jamming parameter α_{wc}.

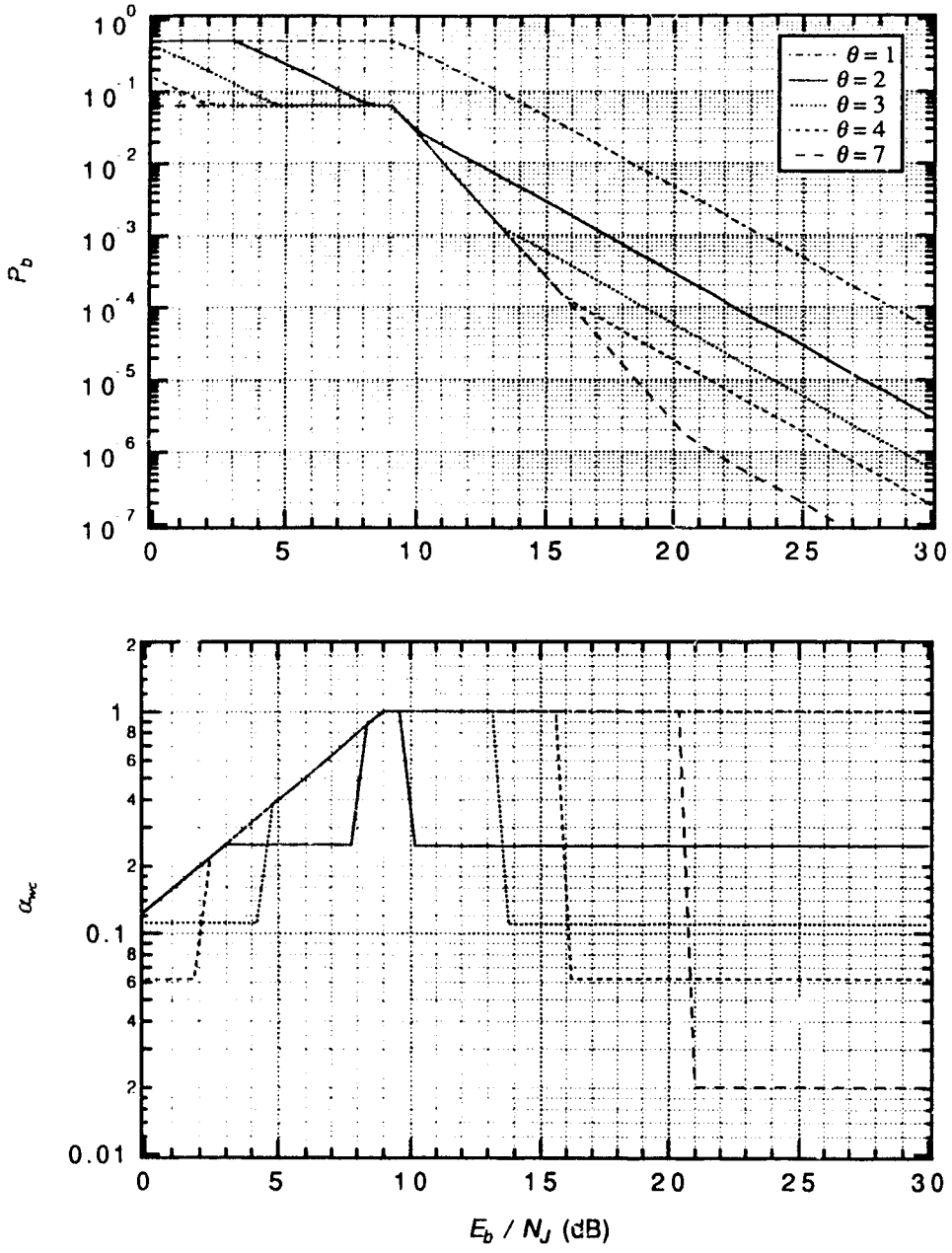

Figure 3.3: Performance of FH/BFSK with diversity $m = 4$ chips/bit and R-T diversity combiner with threshold θ in worst case $n = 1$ band multitone jamming without noise. Upper: BER. Lower: the worst jamming parameter α_{wc}.

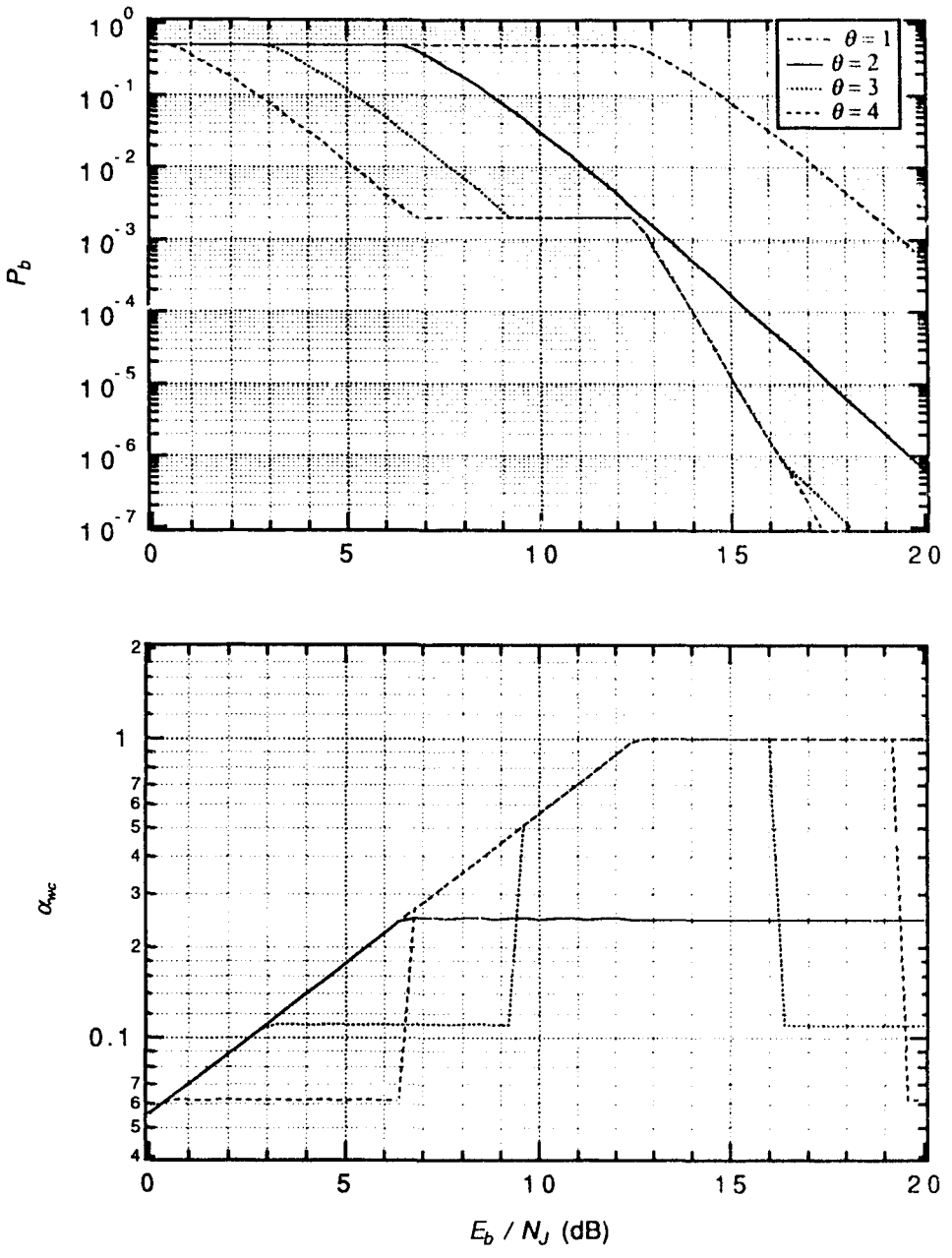

Figure 3.4: Performance of FH/BFSK with diversity $m = 9$ chips/bit and R-T diversity combiner with threshold θ in worst case $n = 1$ band multitone jamming without noise. Upper: BER. Lower: the worst jamming parameter α_{wc}.

F_C and F_E are plotted in Figure 3.5 as functions of α for fixed θ. Then, P_C, P_{CX}, P_{EX}, and P_E can be easily derived,

$$P_C(\theta) = \begin{cases} 1 & \text{if } \alpha > \theta^2; \\ 1 - \frac{M-1}{M}\mu & \text{if } \frac{1}{\theta^2} < \alpha < \theta^2; \\ 1 - \frac{\mu}{2} & \text{otherwise.} \end{cases}$$

$$P_{CX}(\theta) = \begin{cases} \frac{M-1}{M}\mu & \text{if } 1 < \alpha < \theta^2; \\ \left(\frac{1}{2} - \frac{1}{M}\right)\mu & \text{if } \frac{1}{\theta^2} < \alpha < 1; \\ 0 & \text{otherwise.} \end{cases}$$

$$P_{EX}(\theta) = \begin{cases} \frac{\mu}{2} & \text{if } \frac{1}{\theta^2} < \alpha < 1; \\ 0 & \text{otherwise.} \end{cases}$$

$$P_E(\theta) = \begin{cases} \frac{\mu}{2} & \text{if } 0 < \alpha < \frac{1}{\theta^2}; \\ 0 & \text{otherwise.} \end{cases}$$

When θ is fixed, the relation of these transition probabilities with jamming parameter α is also plotted in Figure 3.5.

When $\alpha > 1$, since P_E and P_{EX} are always zero, no erroneous decision can be made at the receiver. Therefore, $P_b = 0$.

When $\frac{1}{\theta^2} < \alpha < 1$, $P_E = 0$. This means good quality decisions are always correct ones. Erroneous decision is possible only when no good quality decision exists, which occurs with probability $(1 - P_C)^m$. So the conditional bit error probability is

$$\begin{aligned} &\Pr(\text{bit error} \mid \text{no good quality decision exists}) \\ &= \sum_{k=\lceil \frac{m}{2} \rceil}^{m} \left[1 - 0.5\delta(k - \frac{m}{2})\right] \binom{m}{k} \left(\frac{P_{EX}}{1 - P_C}\right)^k \left(\frac{P_{CX}}{1 - P_C}\right)^{m-k}. \end{aligned}$$

So the bit error rate is

$$\begin{aligned} P_b &= (1 - P_C)^m \sum_{k=\lceil \frac{m}{2} \rceil}^{m} \left[1 - 0.5\delta(k - \frac{m}{2})\right] \binom{m}{k} \left(\frac{P_{EX}}{1 - P_C}\right)^k \left(\frac{P_{CX}}{1 - P_C}\right)^{m-k} \\ &= \left(\frac{\mu}{2}\right)^m \gamma, \end{aligned}$$

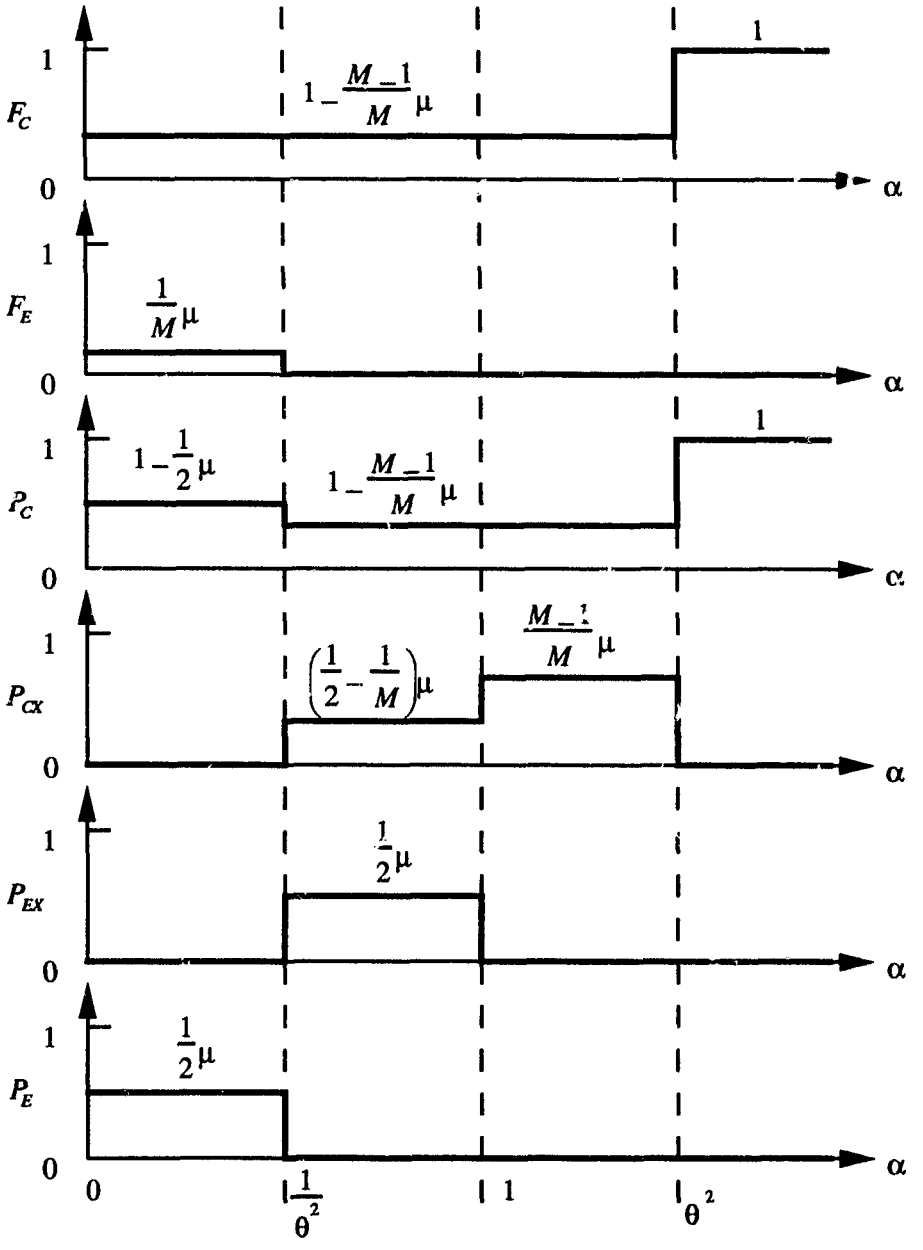

Figure 3.5: Relationship between F_C, F_E, P_C, P_{CX}, P_{EX}, P_E and α for a fixed θ.

where

$$\gamma = \sum_{k=\lceil \frac{m}{2} \rceil}^{m} \left[1 - 0.5\delta(k - \frac{m}{2})\right] \binom{m}{k} \left(\frac{M-2}{M}\right)^{m-k}.$$

Note that γ is a constant when M and m are given.

When $0 < \alpha < \frac{1}{\theta^2}$, $P_{CX} = P_{EX} = 0$. So there is no bad quality decisions. The bit error rate is

$$\begin{aligned} P_b &= \sum_{k=\lceil \frac{m}{2} \rceil}^{m} \left[1 - 0.5\delta(k - \frac{m}{2})\right] \binom{m}{k} P_E^k P_C^{m-k} \\ &= \sum_{k=\lceil \frac{m}{2} \rceil}^{m} \left[1 - 0.5\delta(1 - \frac{m}{2})\right] \binom{m}{k} \left(\frac{\mu}{2}\right)^m \left(1 - \frac{\mu}{2}\right)^{m-k}. \end{aligned}$$

In summary, the bit error rate under band tone jamming with $n = 1$ is:

$$P_b = \begin{cases} 0 & \text{if } \alpha > 1; \\ (\frac{\mu}{2})^m \gamma & \text{if } \frac{1}{\theta^2} < \alpha < 1; \\ \sum_{k=\lceil \frac{m}{2} \rceil}^{m} \left[1 - 0.5\delta(k - \frac{m}{2})\right] \binom{m}{k} & \\ \times \left(\frac{\mu}{2}\right)^k \left(1 - \frac{\mu}{2}\right)^{m-k} & \text{if } 0 < \alpha < \frac{1}{\theta^2}. \end{cases} \tag{3.8}$$

The worst case analysis is almost the same as that in the binary modulation. Again $\mu \leq 1$, so $\alpha \leq \alpha_{max}$, and

$$\alpha_{max} = \frac{K E_b / N_J}{mM}.$$

Following the same way as we did for the binary case, we can find the worst α. Here we just need to change the definition of $h_1(x)$ into

$$h_1(x) = \left(\frac{x}{2}\right)^m \gamma.$$

Because

$$\begin{aligned} h_1(x) &= \left(\frac{x}{2}\right)^r \gamma \\ &= \sum_{\lceil \frac{m}{2} \rceil}^{m} C(m,k) \left(\frac{M-2}{M}\right)^{m-k} \left(\frac{x}{2}\right)^m \\ &= \sum_{\lceil \frac{m}{2} \rceil}^{m} C(m,k) \left(\frac{x}{2}\right)^k \left(\frac{x}{2}\frac{M-2}{M}\right)^{m-k}, \end{aligned}$$

comparing with $h_2(x,\theta)$, it is easy to see that $h_1(x) \le h_2(x,1)$ for $0 \le x \le 1$. Then by using the same approach as in the binary case, we find that

$$\alpha_{wc} = \begin{cases} \alpha_{max} & \text{if} \quad \alpha_{max} < \frac{1}{\theta^2} \ (\text{or } \frac{E_b}{N_J} < \frac{mM}{K\theta^2}); \\ \left(\frac{1}{\theta^2}\right)^- & \text{if} \quad \frac{1}{\theta^2} < \alpha_{max} < 1 \ (\text{or } \frac{mM}{K\theta^2} < \frac{E_b}{N_J} < \frac{mM}{K}) \text{ and } \frac{E_b}{N_J} < \left(\frac{E_b}{N_J}\right)_{T1}; \\ \alpha_{max} & \text{if} \quad \frac{1}{\theta^2} < \alpha_{max} < 1 \ (\text{or } \frac{mM}{K\theta^2} < \frac{E_b}{N_J} < \frac{mM}{K}) \text{ and } \frac{E_b}{N_J} > \left(\frac{E_b}{N_J}\right)_{T1}; \\ \left(\frac{1}{\theta^2}\right)^- & \text{if} \quad \alpha_{max} > 1 \ (\text{or } \frac{E_b}{N_J} > \frac{mM}{K}) \text{ and } \theta^2 < \frac{1}{\mu_0}; \\ 1^- & \text{if} \quad \alpha_{max} > 1 \ (\text{or } \frac{E_b}{N_J} > \frac{mM}{K}) \text{ and } \theta^2 > \frac{1}{\mu_0}, \frac{E_b}{N_J} < \left(\frac{E_b}{N_J}\right)_{T2}; \\ \left(\frac{1}{\theta^2}\right)^- & \text{if} \quad \alpha_{max} > 1 \ (\text{or } \frac{E_b}{N_J} > \frac{mM}{K}) \text{ and } \theta^2 > \frac{1}{\mu_0}, \frac{E_b}{N_J} > \left(\frac{E_b}{N_J}\right)_{T2}; \end{cases} \tag{3.9}$$

where μ_0 is the solution of the following equation:

$$\sum_{k=\lceil \frac{m}{2} \rceil}^{m} C(m,k) \left(\frac{x}{2}\right)^k \left(1-\frac{x}{2}\right)^{m-k} = \gamma 0.5^m;$$

$\left(\frac{E_b}{N_J}\right)_{T1}$ is given by

$$\left(\frac{E_b}{N_J}\right)_{T1} = \frac{Mm}{K\theta^2\mu_0}$$

and the crossing point $\left(\frac{E_b}{N_J}\right)_{T2}$ is the solution of the following equation:

$$\left(\frac{mM}{2KE_b/N_J}\right)^m \gamma = \sum_{k=\lceil \frac{m}{2} \rceil}^{m} \left[1 - 0.5\delta(k-\frac{m}{2})\right]$$

$$\times \begin{pmatrix} m \\ k \end{pmatrix} \left(\frac{mM}{2\theta^2 K E_b/N_J}\right)^k \left(1 - \frac{mM}{2\theta^2 K E_b/N_J}\right)^{m-k}.$$

The corresponding P_b in worst jamming case is

$$P_b = \begin{cases} 0.5 & \text{if } \alpha_{max} < \frac{1}{\theta^2} \text{ (or } \frac{E_b}{N_J} < \frac{mM}{K\theta^2}); \\ 0.5^m \gamma & \text{if } \frac{1}{\theta^2} < \alpha_{max} < 1 \text{ (or } \frac{mM}{K\theta^2} < \frac{E_b}{N_J} < \frac{mM}{K}) \\ & \text{and } \frac{E_b}{N_J} > \left(\frac{E_b}{N_J}\right)_{T1}; \\ \left(\frac{mM}{2KE_b/N_J}\right)^m \gamma & \text{if } \alpha_{max} > 1 \text{ (or } \frac{E_b}{N_J} > \frac{mM}{K}) \\ & \text{and } \theta^2 > \frac{1}{\mu_0}, \frac{E_b}{N_J} < \left(\frac{E_b}{N_J}\right)_{T2}; \\ \sum_{k=\lceil \frac{m}{2} \rceil}^{m} \left[1 - 0.5\delta(k - \frac{m}{2})\right] & \\ \times \begin{pmatrix} m \\ k \end{pmatrix} \left(\frac{mM}{2\theta^2 KE_b/N_J}\right)^k & \\ \times \left(1 - \frac{mM}{2\theta^2 KE_b/N_J}\right)^{m-k} & \text{otherwise.} \end{cases} \tag{3.10}$$

The bit error rate of FFH/4FSK system with R-T combiner under the worst band multitone jamming with $n = 1$ for $m = 2, 4$ and 9 are given in upper figures of Figure 3.6, 3.7 and Figure 3.8, respectively. BER for 8-ary modulation system with same other parameter are plotted in upper figures of Figure 3.9, 3.10 and Figure 3.11. The worst case performances are obtained by using (3.8) with a numerical search for the worst α. The numerical results also verify the analytic results in (3.10). For comparison, the BER of MFSK systems with linear soft combining and perfect side information under the worst case multitone jamming (discussed in [1, pp. 118-121]) are also plotted in these figures.

It can be observed that when m is small ($m = 2$), the lower envelope of BER curves for variant θ is about 2 dB worse than the worst case performance of soft combining with perfect side information. However, when m is large ($m = 9$), the difference between the lower envelope of BER curves of R-T combining and the worst case performance of soft combining with side information is about 3 dB for 4-ary modulation and 4 dB for 8-ary modulation.

In general, the R-T combining scheme can not provide good combining when

both M and m are large, especially under band tone jamming. However, when either M or m is not large, the performance of R-T combining is quite close to that of soft linear combining with side information.

The worst α for 4-ary and 8-ary modulation with $m = 2, 4$ and $m = 9$ are plotted in lower figures of Figure 3.6 - Figure 3.11. The behavior of α_{wc} is similar to the one in the binary case.

3.3 Performance under Band Multitone Jamming with Thermal Noise

We model the thermal noise as additive white Gaussian noise (AWGN). According to the average model discussed in Section 2.3, $F_C(\theta)$ and $F_E(\theta)$ can be computed with (2.20) and (2.21),

$$F_C(\theta) = (1-\mu)F_{C0}(\theta) + \mu F_{C1}(\theta),$$

$$F_E(\theta) = (1-\mu)F_{E0}(\theta) + \mu F_{E1}(\theta),$$

where μ is the probability of an M-ary band being hit by a jamming tone, and the definitions of functions F_{C0}, F_{C1}, F_{E0}, and F_{E1} are given in Section 2.3. Under $n = 1$ band tone jamming, they are given by

$$\begin{aligned}
F_{C0} &= \int_0^\infty p_{s+n}(x)\left[\int_0^{x/\theta} p_n(y)dy\right]^{M-1} dx, \\
F_{C1} &= \frac{1}{M}\int_0^\infty p_{s+j+n}(x)\left[\int_0^{x/\theta} p_n(y)dy\right]^{M-1} dx \\
&\quad + \frac{M-1}{M}\int_0^\infty p_{s+n}(x)\left[\int_0^{x/\theta} p_{j+n}(y)dy\right]\left[\int_0^{x/\theta} p_n(z)dz\right]^{M-2} dx, \\
F_{E0} &= \int_0^\infty p_n(x)\left[\int_0^{x/\theta} p_{s+n}(y)dy\right]\left[\int_0^{x/\theta} p_n(z)dz\right]^{M-2} dx,
\end{aligned}$$

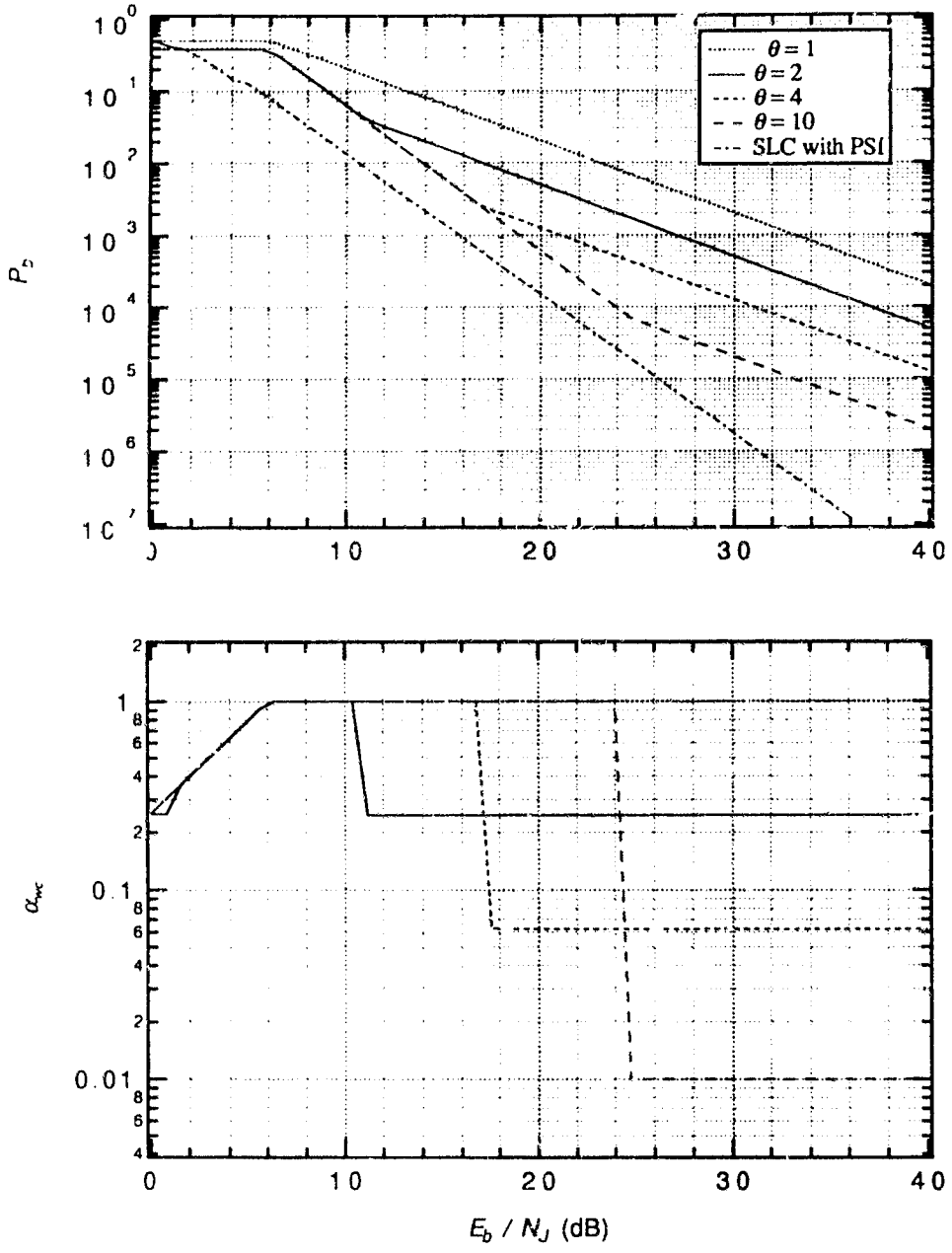

Figure 3.6: Performance of FH/4FSK with diversity $m = 2$ chips/bit and R-T diversity combiner with threshold θ in worst case $n = 1$ band multitone jamming without noise. Upper: BER. Lower: the worst jamming parameter α_{wc}.

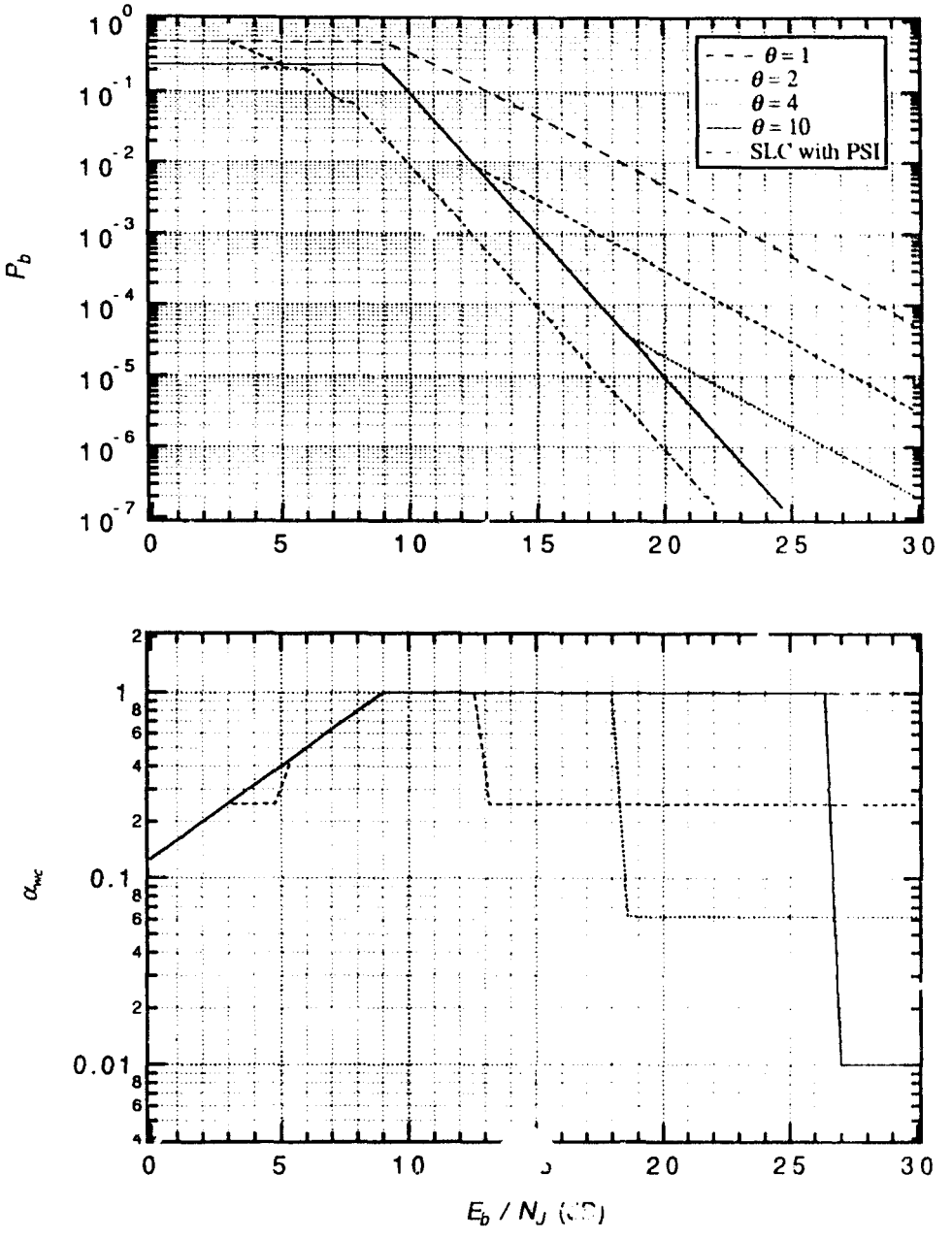

Figure 3.7: Performance of FH/4FSK with diversity $m = 4$ chips/bit and R-T diversity combiner with threshold θ in worst case $n = 1$ band multitone jamming without noise. Upper: BER. Lower: the worst jamming parameter α_{wc}.

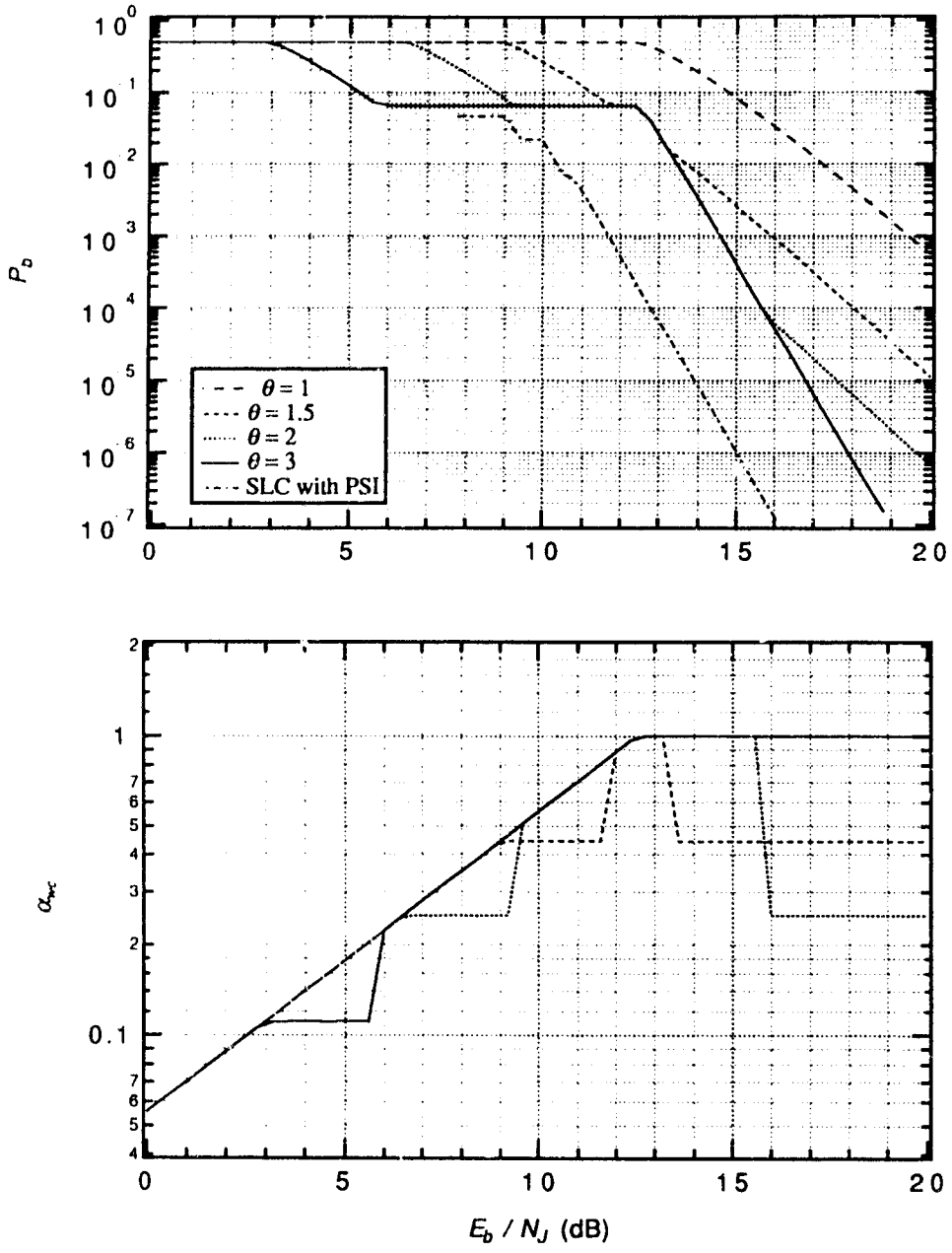

Figure 3.8: Performance of FH/4FSK with diversity $m = 9$ chips/bit and R-T diversity combiner with threshold θ in worst case $n = 1$ band multitone jamming without noise. Upper: BER. Lower: the worst jamming parameter α_{wc}.

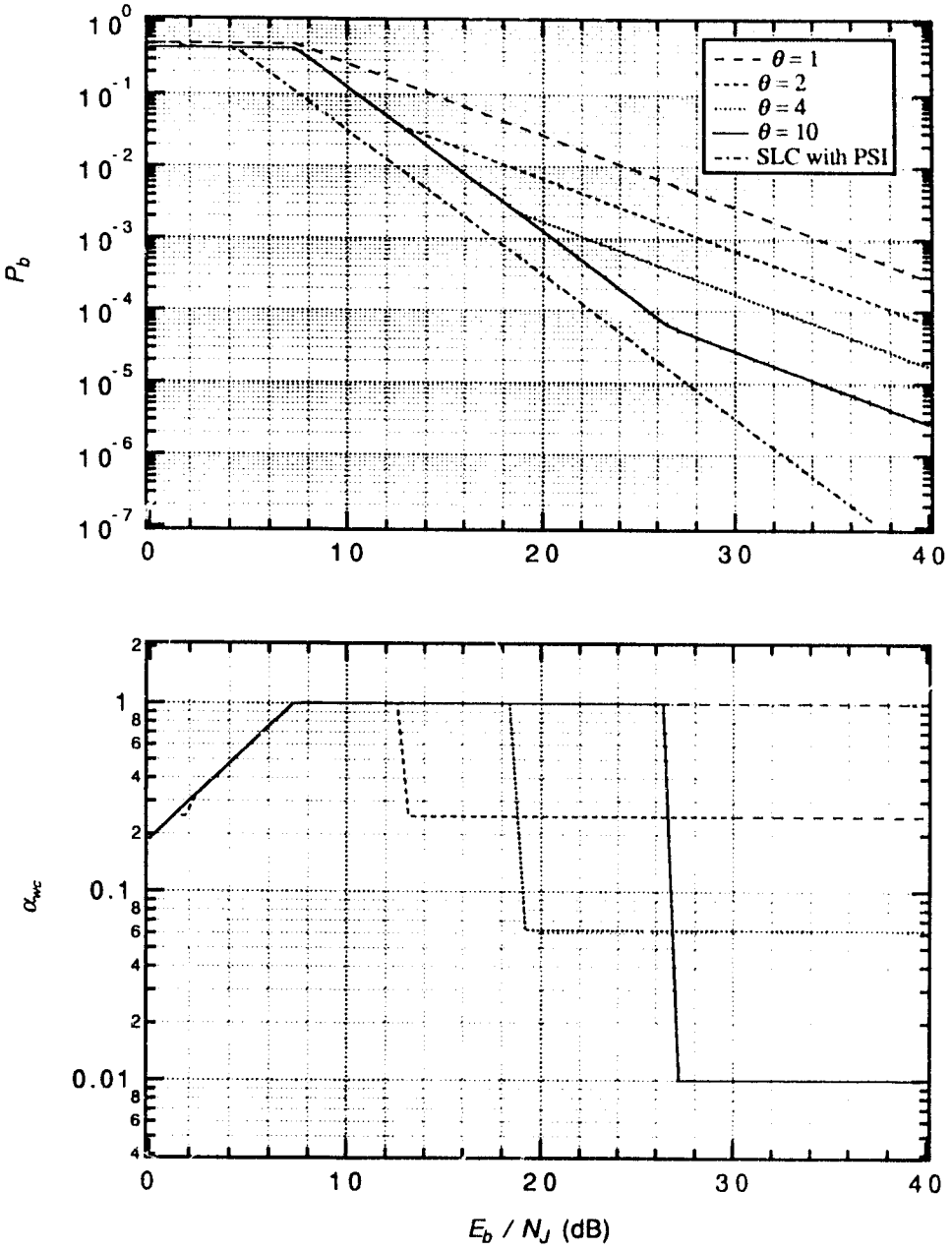

Figure 3.9: Performance of FH/8FSK with diversity $m = 2$ chips/bit and R-T diversity combiner with threshold θ in worst case $n = 1$ band multitone jamming without noise. Upper: BER. Lower: the worst jamming parameter α_{wc}.

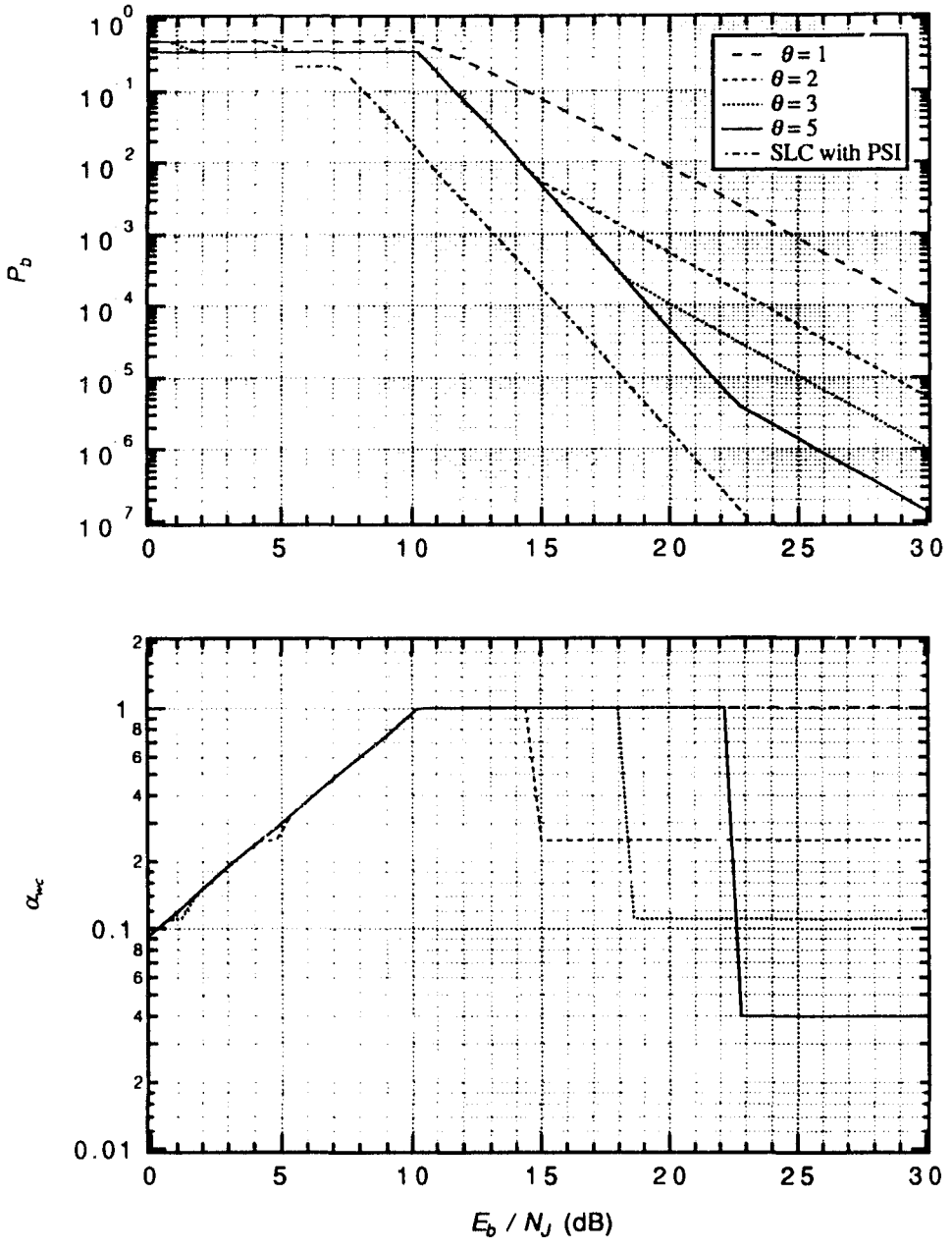

Figure 3.10: Performance of FH/8FSK with diversity $m = 4$ chips/bit and R-T diversity combiner with threshold θ in worst case $n = 1$ band multitone jamming without noise. Upper: BER. Lower: the worst jamming parameter α_{wc}.

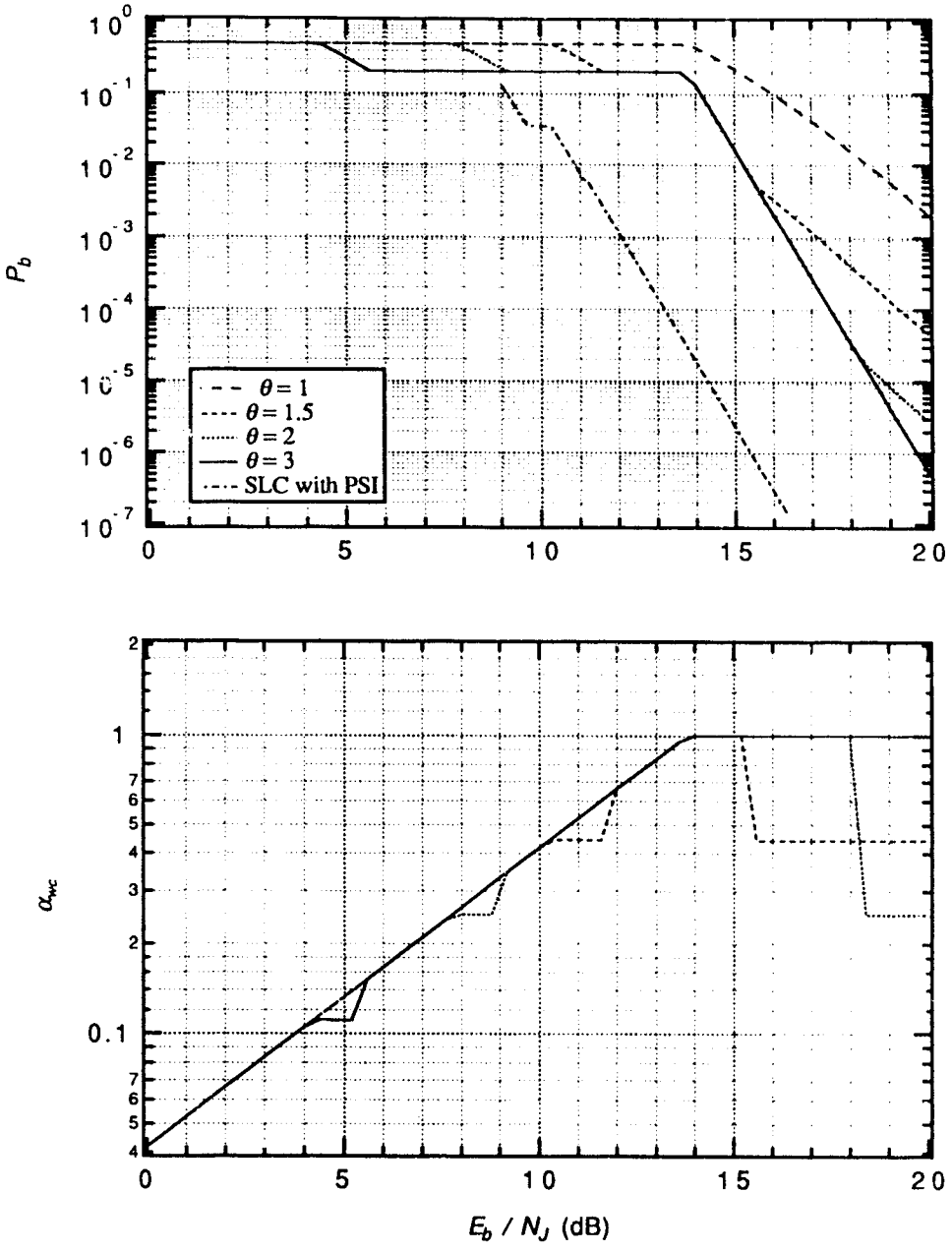

Figure 3.11: Performance of FH/8FSK with diversity $m = 9$ chips/bit and R-T diversity combiner with threshold θ in worst case $n = 1$ band multitone jamming without noise. Upper: BER. Lower: the worst jamming parameter α_{wc}.

$$
\begin{aligned}
F_{E1} &= \frac{1}{M}\int_0^\infty p_n(x)\left[\int_0^{x/\theta} p_{s+j+n}(y)dy\right]\left[\int_0^{x/\theta} p_n(z)dz\right]^{M-2} dx \\
&+\frac{1}{M}\int_0^\infty p_{j+n}(x)\left[\int_0^{x/\theta} p_{s+n}(y)dy\right]\left[\int_0^{x/\theta} p_n(z)dz\right]^{M-2} dx \\
&+\frac{M-2}{M}\int_0^\infty p_n(w)\left[\int_0^{w/\theta} p_{s+n}(x)dx\right]\left[\int_0^{w/\theta} p_{j+n}(y)dy\right] \\
&\times\left[\int_0^{w/\theta} p_n(z)dz\right]^{M-3} dw,
\end{aligned}
$$

where

$$p_n(x) = x\exp\left(-\frac{x^2}{2}\right), \tag{3.11}$$

$$p_{s+n}(x) = x\exp\left(-\frac{x^2+\frac{2KE_b}{mN_0}}{2}\right) I_0\left[x\sqrt{\frac{2KE_b}{mN_0}}\right], \tag{3.12}$$

$$p_{j+n}(x) = x\exp\left(-\frac{x^2+\frac{2KE_b}{\alpha mN_0}}{2}\right) I_0\left[x\sqrt{\frac{2KE_b}{\alpha mN_0}}\right], \tag{3.13}$$

$$p_{s+j+n}(x) = \frac{1}{2\pi}\int_0^{2\pi} x\exp\left(-\frac{x^2+\frac{2\tilde{E}_s(\phi)}{mN_0}}{2}\right) I_0\left[x\sqrt{\frac{2\tilde{E}_s(\phi)}{mN_0}}\right] d\phi, \tag{3.14}$$

and

$$\tilde{E}_s(\phi) = KE_b(1+\frac{2}{\sqrt{\alpha}}\cos\phi+\frac{1}{\alpha}).$$

Carrying out these integrals (see Section 3.7 for detail), we obtain,

$$F_{C0} = \sum_{k=0}^{M-1}(-1)^k\binom{M-1}{k}\frac{\theta^2}{\theta^2+k}\exp\left(-\frac{k}{\theta^2+k}\frac{KE_b}{mN_0}\right). \tag{3.15}$$

$$F_{C1} = \frac{1}{M}g_{c1a}+\frac{M-1}{M}g_{c1b} \tag{3.16}$$

where

$$g_{c1a} = \sum_{k=0}^{M-1}(-1)^k \binom{M-1}{k} \frac{\theta^2}{\theta^2+k} \exp\left[-\frac{k}{\theta^2+k}\left(1+\frac{1}{\alpha}\right)\frac{KE_b}{mN_0}\right] \times I_0\left(\frac{k}{\theta^2+k}\frac{2}{\sqrt{\alpha}}\frac{KE_b}{mN_0}\right),$$

and

$$g_{c1b} = \sum_{k=0}^{M-2}(-1)^k \binom{M-2}{k} \frac{\theta^2}{\theta^2+k} \exp\left(-\frac{k}{\theta^2+k}\frac{KE_b}{mN_0}\right) \times \left\{\frac{\theta^2+k}{\theta^2+k+1}[1-Q(\sqrt{a},\sqrt{b})] + \frac{Q(\sqrt{b},\sqrt{a})}{\theta^2+k+1}\right\},$$

$$a = \frac{\theta^2+k}{\theta^2+k+1}\frac{2KE_b}{\alpha mN_0}$$

$$b = \frac{\theta^2}{(\theta^2+k)(\theta^2+k+1)}\frac{2KE_b}{mN_0}$$

$$F_{E0} = \sum_{k=0}^{M-2}(-1)^k \binom{M-2}{k} \frac{\theta^2}{\theta^2+k}\frac{1}{\theta^2+k+1} \exp\left(-\frac{\theta^2+k}{\theta^2+k+1}\frac{KE_b}{mN_0}\right) \quad (3.17)$$

$$F_{E1} = \frac{1}{M}g_{e1a} + \frac{1}{M}g_{e1b} + \frac{M-2}{M}g_{e1c} \quad (3.18)$$

where

$$g_{e1a} = \sum_{k=0}^{M-2}(-1)^k \binom{M-2}{k} \frac{\theta^2}{\theta^2+k}\frac{1}{\theta^2+k+1} \times \exp\left[-\frac{\theta^2+k}{\theta^2+k+1}\left(1+\frac{1}{\alpha}\right)\frac{KE_b}{mN_0}\right] I_0\left(\frac{\theta^2+k}{\theta^2+k+1}\frac{2}{\sqrt{\alpha}}\frac{KE_b}{mN_0}\right)$$

$$g_{e1b} = \sum_{k=0}^{M-2}(-1)^k \binom{M-2}{k} \frac{\theta^2}{\theta^2+k} \exp\left(-\frac{k}{\theta^2+k}\frac{KE_b}{\alpha mN_0}\right)$$

$$\times \left\{ \frac{\theta^2 + k}{\theta^2 + k + 1}[1 - Q(\sqrt{a}, \sqrt{b})] + \frac{Q(\sqrt{b}, \sqrt{a})}{\theta^2 + k + 1} \right\}$$

$$a = \frac{\theta^2 + k}{\theta^2 + k + 1} \frac{2KE_b}{mN_0}$$

$$b = \frac{\theta^2}{(\theta^2 + k)(\theta^2 + k + 1)} \frac{2KE_b}{\alpha m N_0}$$

and

$$g_{elc} = \sum_{k=0}^{M-3} (-1)^k \binom{M-3}{k} \frac{\theta^2}{(\theta^2 + k)(\theta^2 + k + 1)} \left[f\left(\theta^2, k, \frac{KE_b}{mN_0}, \frac{KE_b}{\alpha m N_0}\right) + f\left(\theta^2, k, \frac{KE_b}{\alpha m N_0}, \frac{KE_b}{mN_0}\right) \right]$$

$$f(w, k, X, Y)$$

$$= \left\{ \frac{w+k+1}{w+k+2} \left[1 - Q\left(\sqrt{\frac{w+k+1}{w+k+2} 2X}, \sqrt{\frac{2Y}{(w+k+1)(w+k+2)}} \right) \right] + \frac{1}{w+k+2} Q\left(\sqrt{\frac{2Y}{(w+k+1)(w+k+2)}}, \sqrt{\frac{w+k+1}{w+k+2} 2X} \right) \right\} \times \exp\left(-\frac{w+k}{w+k+1} Y \right).$$

By using expressions derived above, $F_C(\theta)$ and $F_E(\theta)$ can be evaluated numerically. A method discussed in [16] is used to compute the Marcum Q-function which is used extensively in computations of these $F()$ functions.

The bit error probabilities of the binary system under the worst case band tone jamming versus E_b/N_J for m=4, E_b/N_0=11,13 and 15,17 dB are plotted in Figure 3.12 and 3.13, respectively. The corresponding worst α versus E_b/N_J for $m = 4$, E_b/N_0= 11,13,15,17 dB are plotted in Figure 3.14 - 3.15, respectively. The worst α

is found by searching in the interval $[\alpha_0, \alpha_{max}]$ numerically. α_0, the lower searching bound, should be small enough so that the lowest point of the worst α is higher than it, and is determined by trial and error. α_{max} is such a α that causes μ=1 and it is given by

$$\alpha_{max} = \frac{K}{mM}\frac{E_b}{N_J}$$

for $n = 1$ band tone jamming. The physical meaning of α_{max} is the power ratio of signal tone to one jamming tone when jammer puts one jamming tone in every (frequency hop) M-ary band.

It can be seen that $\theta = 2$ is the best when E_b/N_J is not very low ($\geq$ 8 dB for all cases). When signal to noise ratio E_b/N_0 is high, the worst α versus E_b/N_J approaches to that without noise. Furthermore, the worst α can be greater than 1 when noise exists. This means that the amplitude of the jamming tone does not need to be greater than the amplitude of the signal tone to achieve the maximum interference effect.

In these figures, there is a region of E_b/N_J where α is piecewise linear. In this region, the worst α is α_{max}. Thus in this case, the optimum strategy of the jammer is to put jamming tone in every frequency hop M-ary band.

It can also be seen that when jamming is strong, the jamming may even help the communication due to random cancellation. In other words, lower E_b/N_J may have a lower bit error rate and BER is no longer necessarily a monotonically decreasing function of E_b/N_J as might be expected.

The bit error probabilities of the 8-ary system under worst case band multitone jamming versus E_b/N_J for $m = 4$, and $E_b/N_0 = 10, 12, 14$ dB are plotted in Figure 3.16. The corresponding worst α versus E_b/N_J are plotted in Figure 3.17.

To see the influence of θ and m on the system performance clearly, E_b/N_J required to sustain BER=10^{-5} versus $1/\theta$ with m as a parameter is plotted in Figure 3.18 for the binary system with E_b/N_0=17 dB, and in Figure 3.19 for the

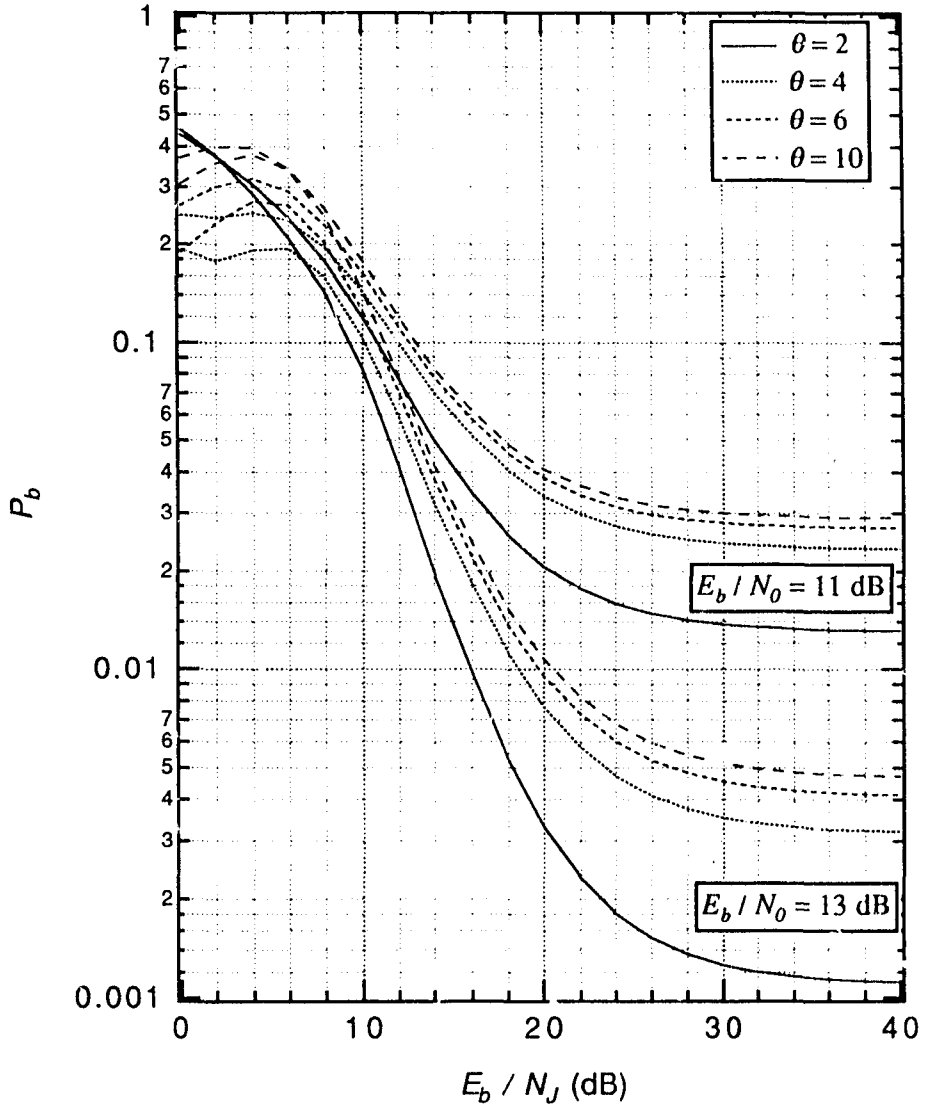

Figure 3.12: The bit error rate of FH/BFSK system with diversity $m = 4$ chips/bit and R-T diversity combiner with threshold θ in the worst band multitone jamming with $n = 1$. E_b/N_0=11,13 dB; θ =2,4,6,10.

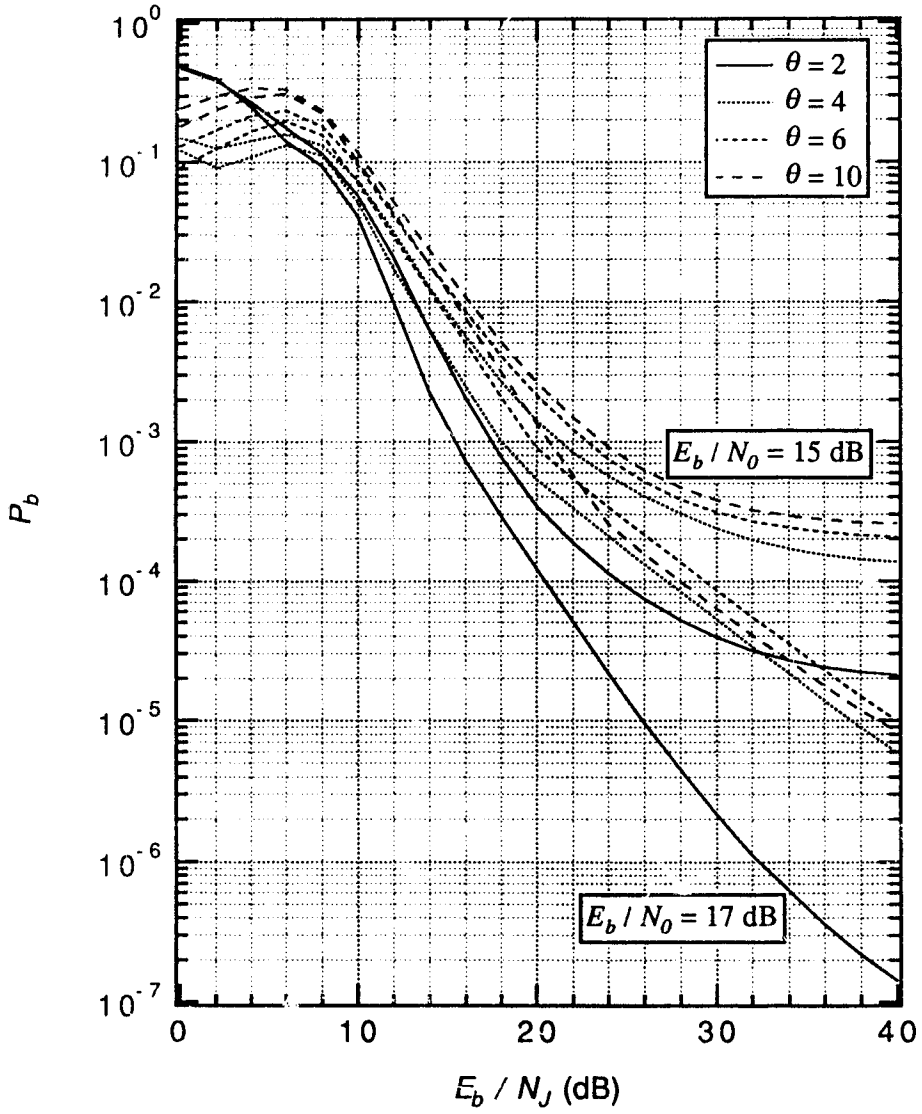

Figure 3.13: The bit error rate of FH/BFSK system with diversity $m = 4$ chips/bit and R-T diversity combiner with threshold θ in the worst band multitone jamming with $n = 1$. E_b/N_0=15,17 dB; θ =2,4,6,10.

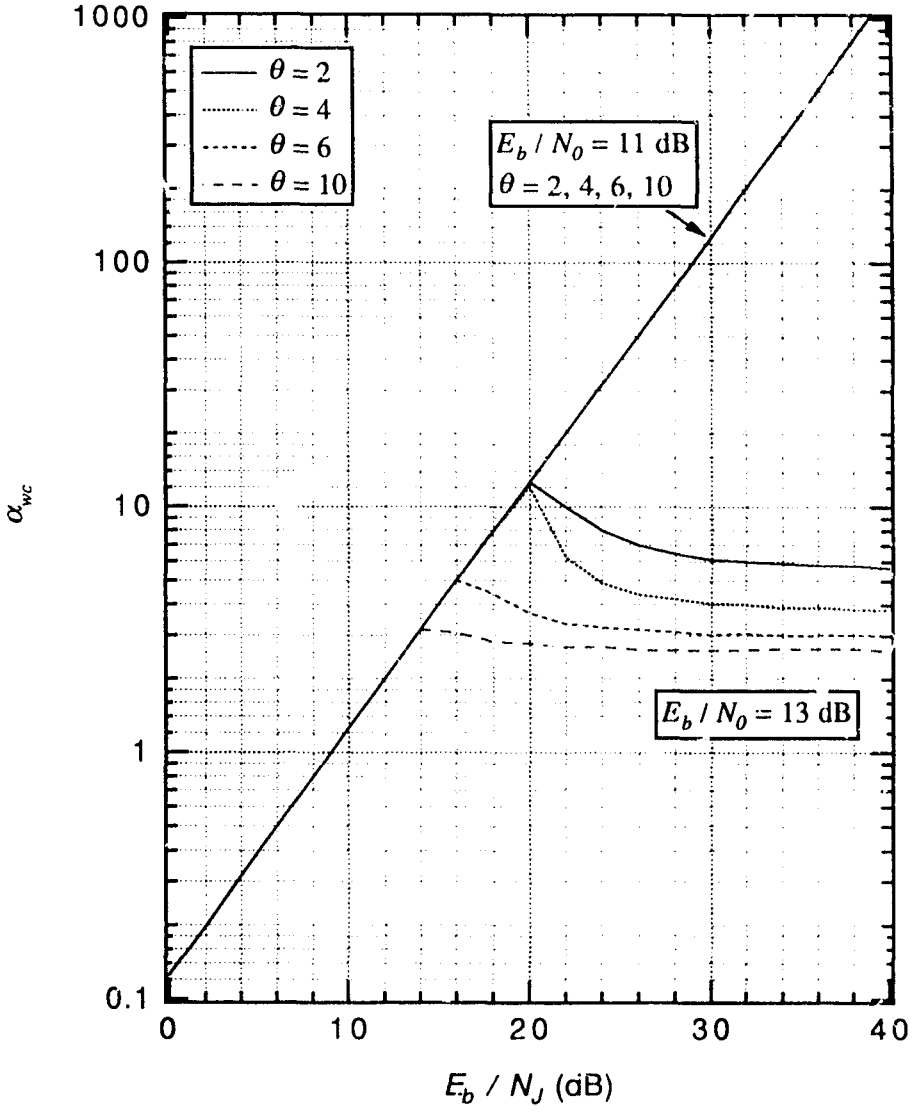

Figure 3.14: The worst α for FH/BFSK system with diversity m = 4 chips/bit and R-T diversity combiner with threshold θ in band multitone jamming with n = 1. E_b/N_0=11,13 dB; θ =2,4,6,10.

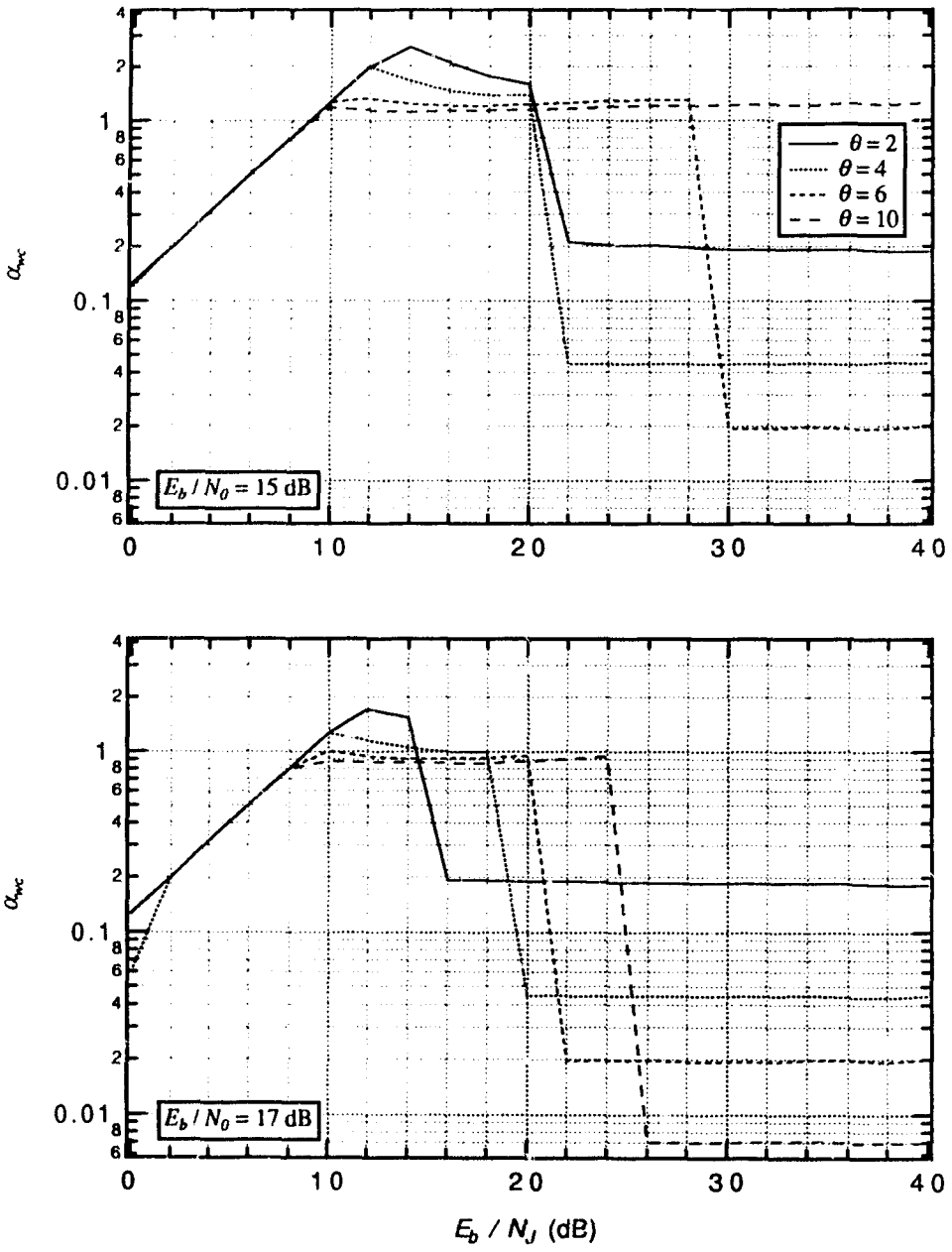

Figure 3.15: The worst α for FH/BFSK system with diversity $m = 4$ chips/bit and R-T diversity combiner with threshold θ in band multitone jamming with $n = 1$. Upper: E_b/N_0=15 dB. Lower: E_b/N_0=17 dB. θ =2,4,6,10.

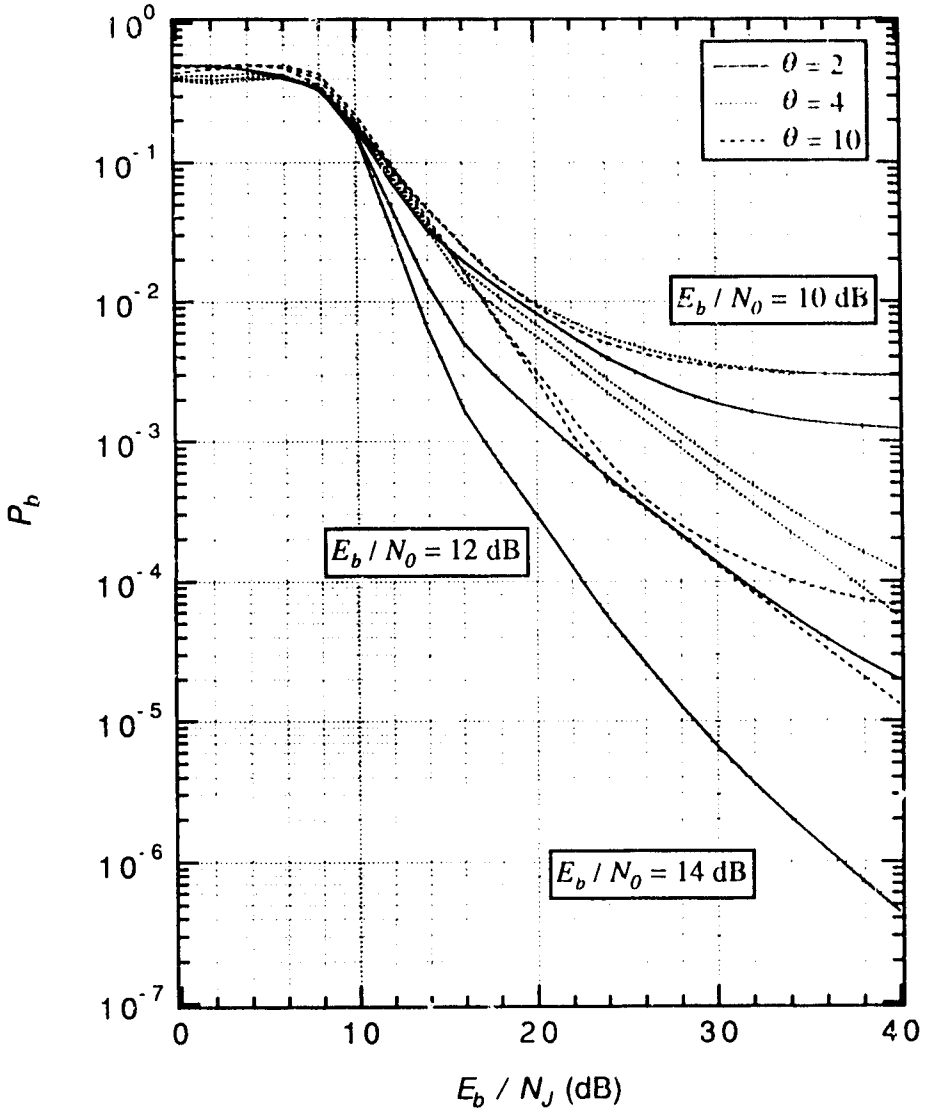

Figure 3.16: The bit error rate of FH/8FSK system with diversity m = 4 chips/bit and R-T diversity combiner with threshold θ in the worst band multitone jamming with $n = 1$. E_b/N_0=10,12,14 dB; θ =2,4,10.

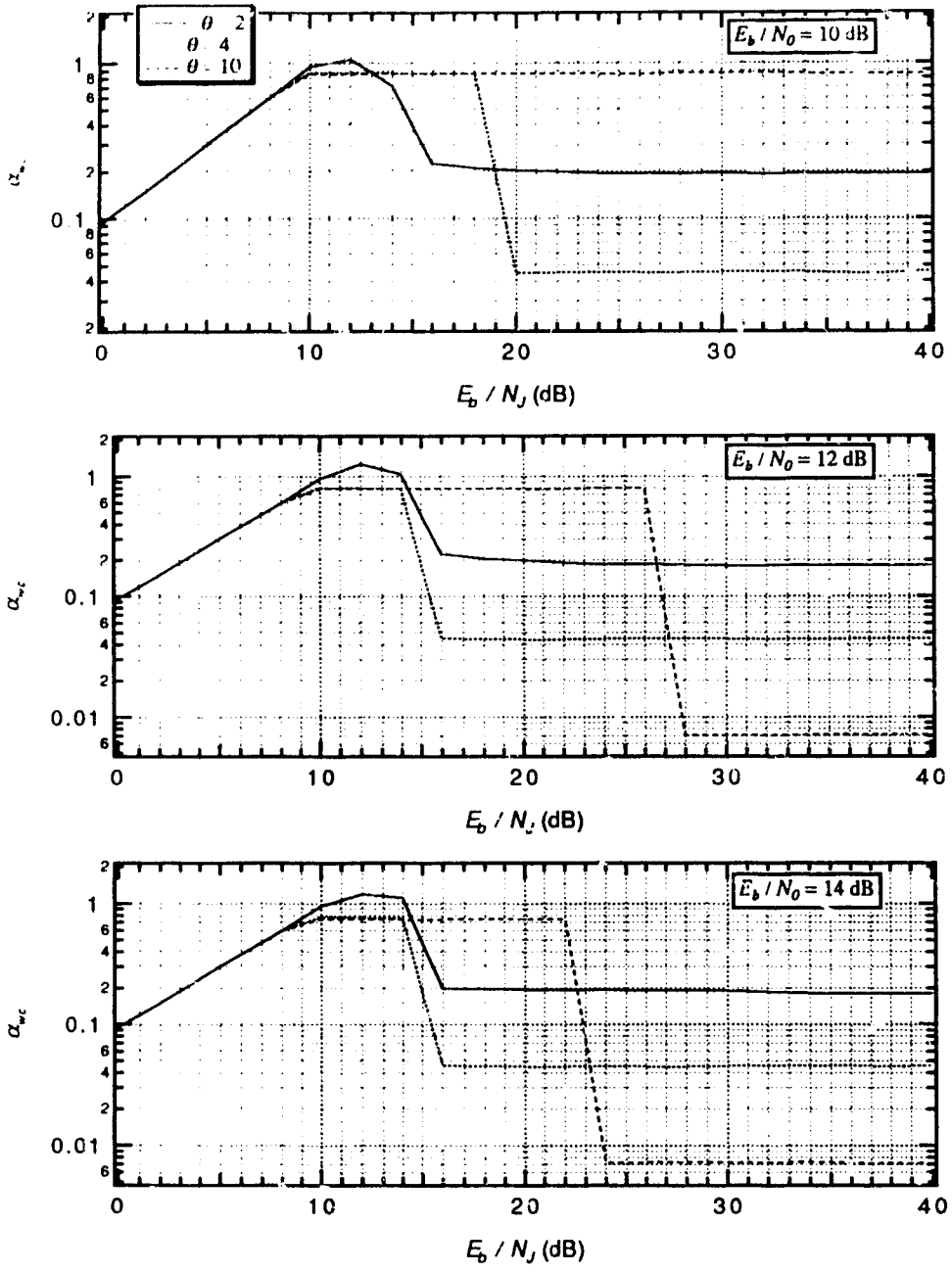

Figure 3.17: The worst α for FH/8FSK system with diversity $m = 4$ chips/bit and R-T diversity combiner with threshold θ in band multitone jamming with $n = 1$. E_b/N_0=10,12,14 dB; θ =2,4,10.

8-ary system with E_b/N_0=14 dB.

From these figures, we can see that $m = 5$ with $\theta = 2$ gives the minimum required E_b/N_J for binary system and $m = 9$ with θ around 1.2 1.4 gives the minimum required E_b/N_J for 8-ary system. It can be seen that the optimum θ is around 2 for binary system, but less than 2 for 8-ary system. In 8-ary system, when m is large ($m \geq 5$), the performance of ratio-threshold diversity combiner is close to that of the hard decision diversity combiner in tone jamming.

The worst case sensitivity

All performances that we have analyzed have been under worst case jamming. In other words, we assume that the jammer has all necessary information to choose certain ρ for partial-band noise jamming or α for band multitone jamming to maximize the jamming effects.

If a communication system makes the jamming effects very sensitive to the jamming parameters, the jammer may have difficulty to choose appropriate jamming parameters since not all necessary information is available to the jammer in practice.

E_b/N_J required for the binary and the 8-ary systems to sustain BER=10^{-5} versus α in multitone jamming with $\theta = 2$, $m = 4$, and $E_b/N_0 = 17$ dB and 12 dB, respectively, are plotted in Figure 3.20 to illustrate the worst case sensitivity.

Comparing two figures, it can be seen that the worst case performance of the binary system is not very sensitive to α. Specifically, α=0.1-1 can result in the performance which is at most 3 dB away from the worst case performance. However, the performance of 8-ary system is more sensitive to α. The corresponding region is about α=0.08-0.4.

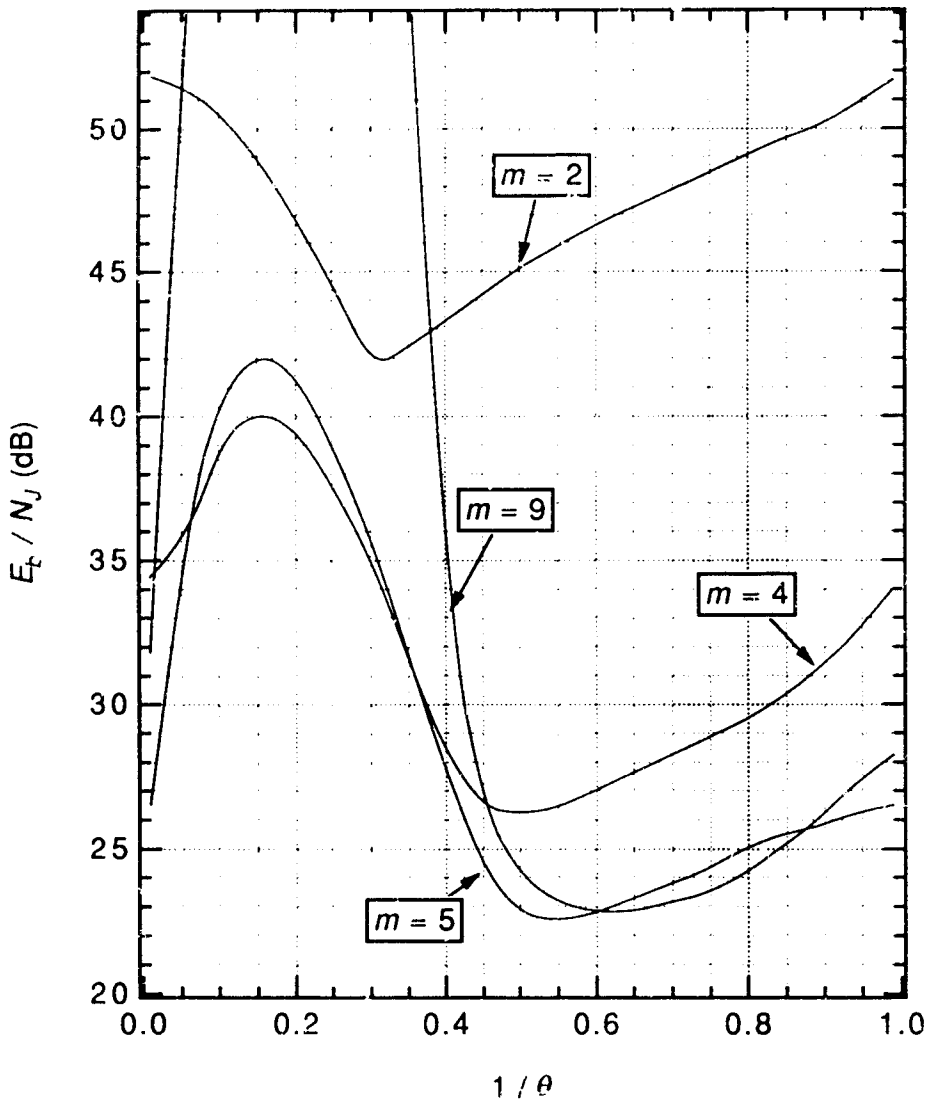

Figure 3.18: E_b/N_J required to achieve BER = 10^{-5} versus $1/\theta$ for the binary system in worst case band tone jamming. E_b/N_0= 17 dB.

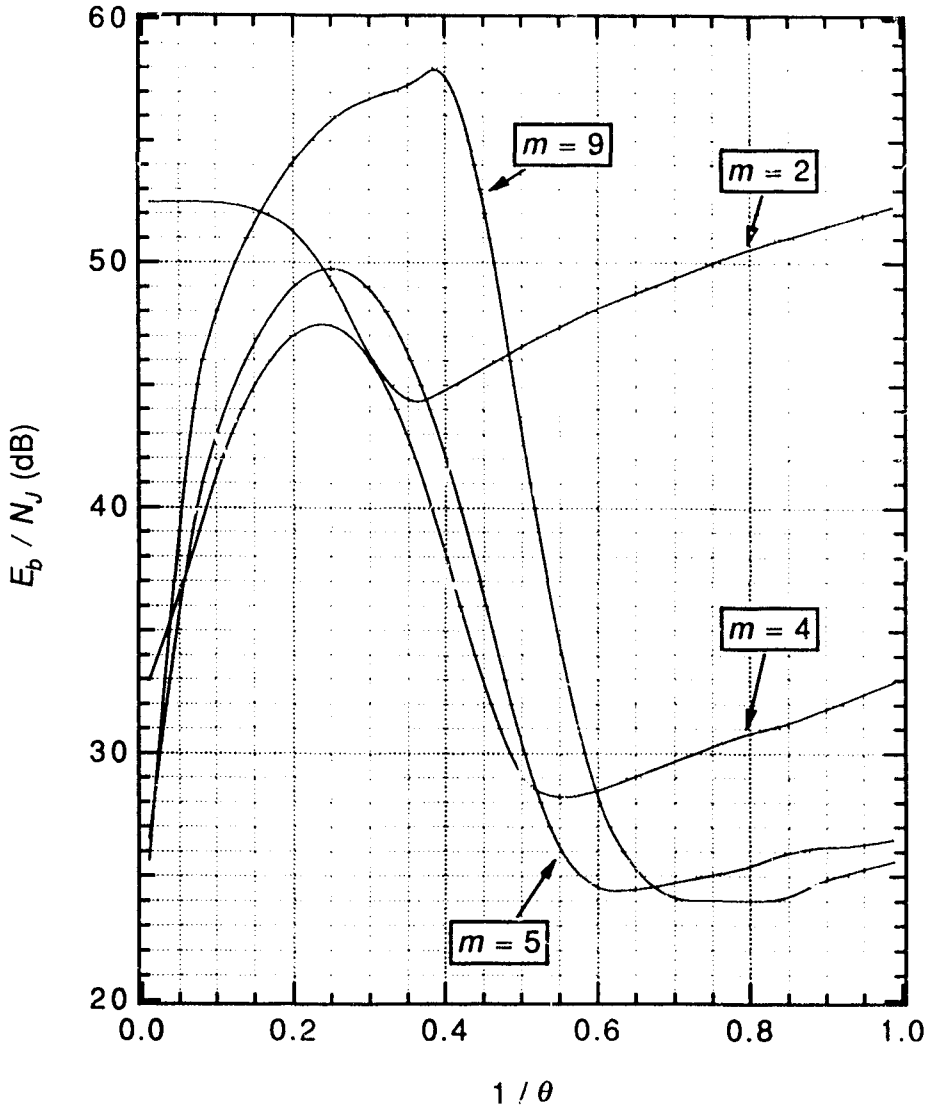

Figure 3.19: E_b/N_J required to achieve BER = 10^{-5} versus $1/\theta$ for the 8-ary system in worst case band tone jamming. E_b/N_0= 14 dB.

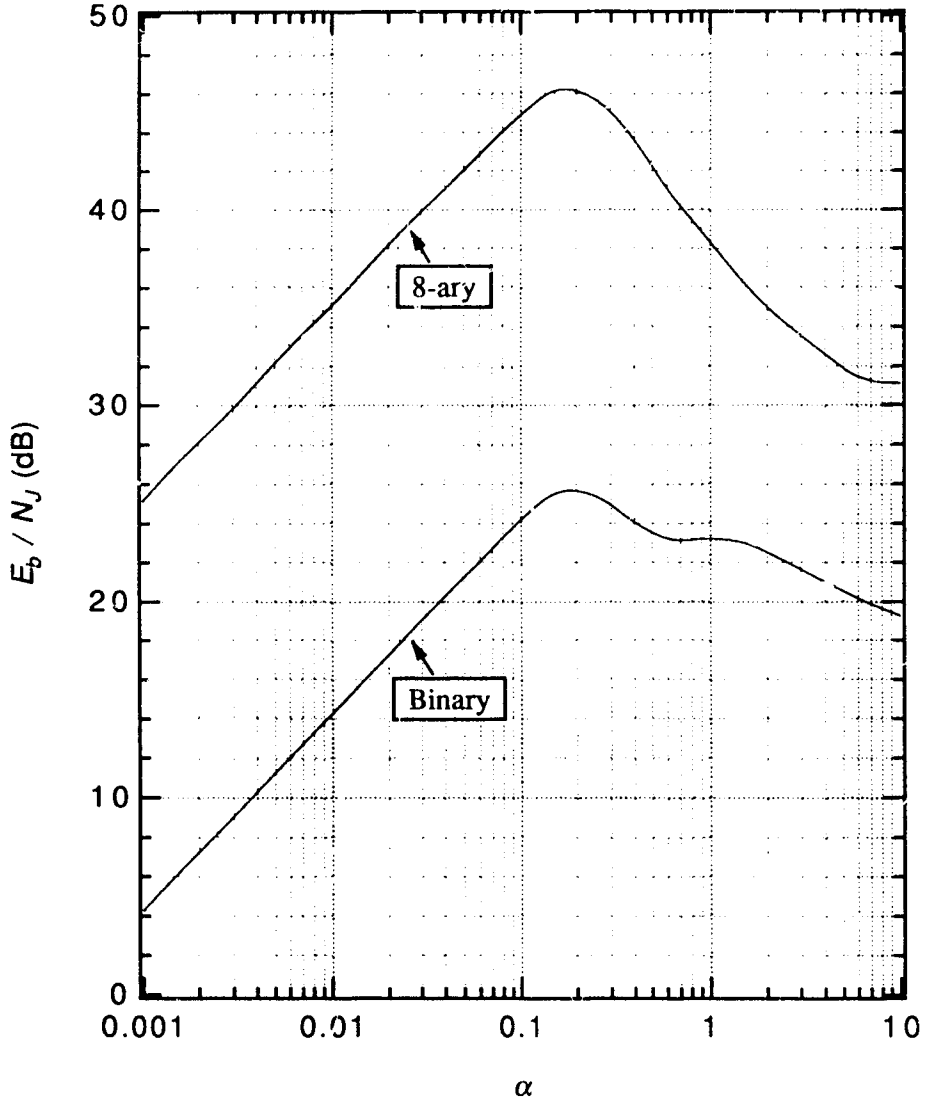

Figure 3.20: The E_b/N_J required to sustain BER=10^{-5} for FH/FSK with diversity $m = 4$ chips/bit and R-T diversity combiner with threshold $\theta = 2$ in $n = 1$ band multitone jamming. Binary system: E_b/N_0=17 dB. 8-ary system: E_b/N_0=12 dB.

3.4 Comparison of Performances in Partial-Band Noise Jamming and Multitone Jamming

In order to see which type of jamming is more effective for the ratio-threshold diversity combiner, the performance of the binary and 8-ary systems under worst case partial-band noise and multitone jamming with E_b/N_0=17 dB and 14 dB are with θ as parameter are plotted in Figure 3.21 and Figure 3.22, respectively. It is interesting to see that the effects of two types of jamming are almost the same as in the binary system. However in the 8-ary system, the tone jamming is more effective than partial-band jamming. Specifically, it requires about 10 dB more in E_b/N_J to achieve BER = 10^{-5} under tone jamming in the 8-ary system with $\theta = 2$.

For comparison, the minimum E_b/N_J required to sustain BER = 10^{-5} under partial-band noise jamming for the binary and the 8-ary system are depicted in Figs. 2.24 and 2.26, respectively. Then we can compare Figs. 3.18 and 3.19 with Figs. 2.24 and 2.26 respectively. In the binary system, the curves of required E_b/N_J versus $1/\theta$ are quite similar for partial-band noise and tone jammings. This confirms the results in Figure 3.21. In partial-band noise jamming (Figure 2.24), the minimum required E_b/N_J to sustain BER = 10^{-5} is about 23 dB for m=5 and 9 and θ=1.4-2. In tone jamming (Figure 3.18), the minimum required E_b/N_J is about 23-24 dB for for m=5 and 9 and θ=1.4-2.

However, in the 8-ary system, the curves of required E_b/N_J versus $1/\theta$ are quite different for partial-band noise and tone jammings. It appears that the performance is much more sensitive to θ under tone jamming. In Figure 2.26, the variation for m=5, which is the smallest one on the figure, is within 5 dB. While in Figure 3.19, the variation for m=5, which also is the smallest one on the figure, is more than 20 dB. Furthermore, in partial-band noise jamming, the minimum required E_b/N_J to sustain BER=10^{-5} is about 18 dB for $m = 5$ and θ around 1.6. And in tone jamming, the minimum required E_b/N_J is about 24 dB for $m = 9$ and

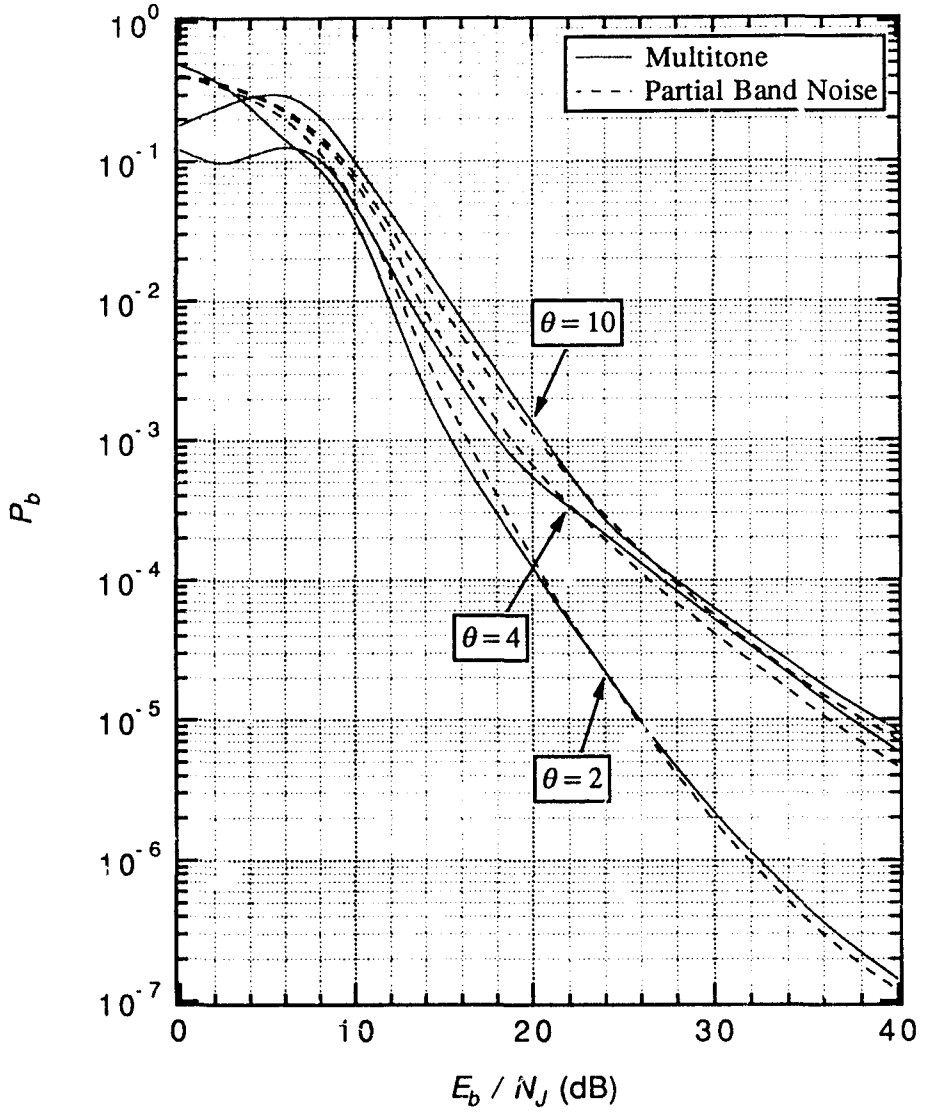

Figure 3.21: The bit error probability of FH/BFSK system with diversity $m = 4$ chips/bit and R-T diversity combiner with threshold θ in the worst partial band noise and $n = 1$ band multitone jamming. E_b/N_0=17 dB; θ =2,4,10.

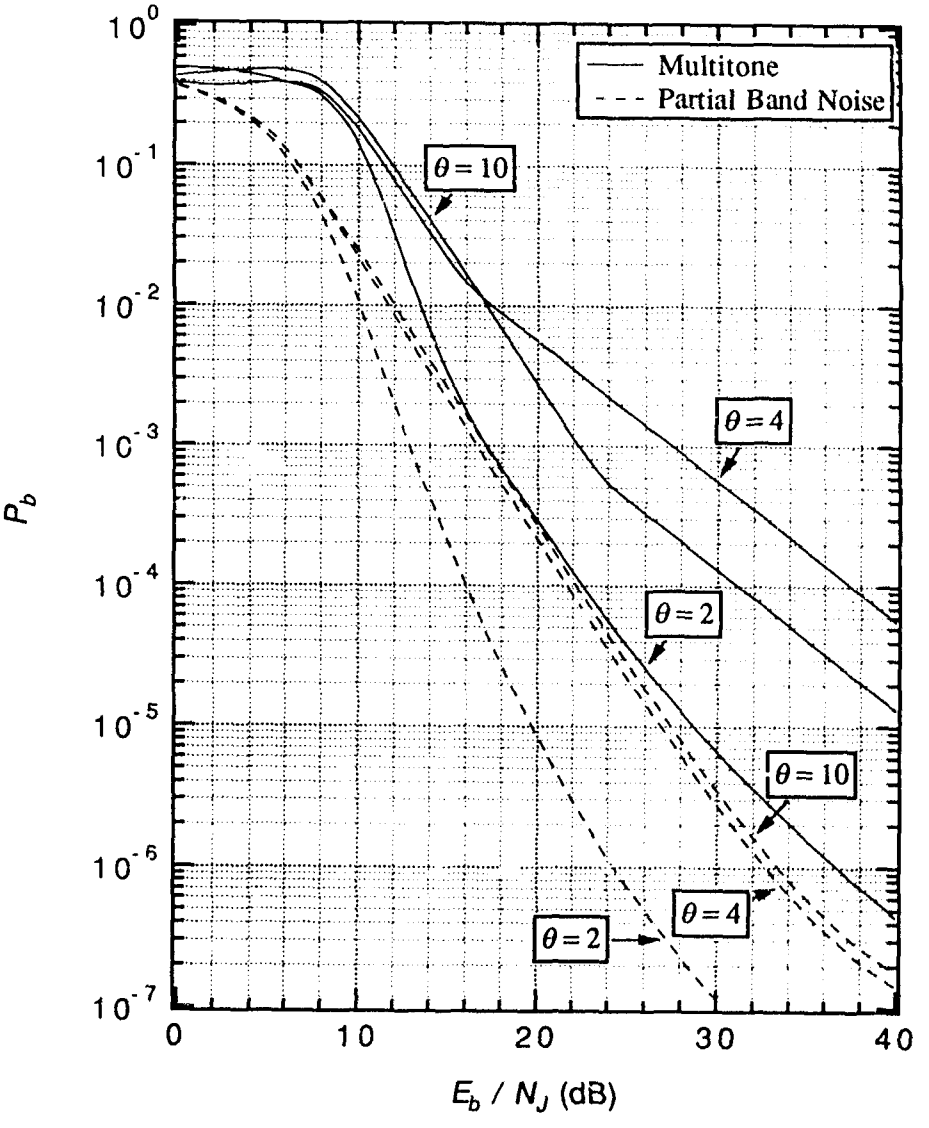

Figure 3.22: The bit error probability of FH/8FSK system with diversity $m = 4$ chips/bit and R-T diversity combiner with threshold θ in the worst partial band noise and $n = 1$ band multitone jamming. E_b/N_0=14 dB; θ =2,4,10.

θ=1.2-1.4. There is a 6 dB difference in the best performances on the two figures.

3.5 Conclusion

The performance of FFH/FSK spread spectrum system with ratio-threshold diversity combining has been analyzed. The exact bit error probabilities in worst case $n = 1$ band tone jamming with additive white Gaussian noise are computed.

Under $n = 1$ band tone jamming, for a given M, the optimum BER performance with an optimum ratio-threshold θ is almost the same for diversity order $m = 4$ - 9. However the performance is quite sensitive to the choice of θ. For 8-ary modulation, the optimum performance is close to the one of hard decision combining, especially when m is large.

The performances of ratio-threshold combining under partial-band noise and band tone jamming is almost the same for the binary system, but not for the 8-ary system. In general, tone jamming is more effective to the system with the ratio-threshold combining than partial-band jamming. Furthermore, in contrast to the binary FSK systems, the bit error probability is much more sensitive to θ under tone jamming in the 8-ary systems than under partial-band noise jamming. For optimum performance with the optimum θ under tone jamming, there is a 6 dB difference in the required E_b/N_J to achieve BER = 10^{-5} between the two types of jamming against 8-ary FSK systems.

3.6 Derivation of $F_C(\theta)$ and $F_E(\theta)$ under Band Multitone Jamming

Because $n = 1$, there is at most one jamming tone in an M-ary orthogonal band. An erroneous decision can possibly be made only when the jamming tone falls in an empty frequency bin that does not contain a signal tone, and in this case, the ratio of the output of the signal tone envelope matched filter X_S and the output

of the jammed tone envelope matched filter X_J is (see [1] for detail)

$$\frac{X_S}{X_J} = \sqrt{\alpha}$$

So, when $\sqrt{\alpha} > \theta$, $F_C(\theta) = 1$. Otherwise, $\frac{X_S}{X_{NS}} \geq \theta$ only happens when either the M-ary band is not hit by the jamming or the jamming tone hits the signal tone (where X_{NS} is the output of a matched filter corresponding to an empty frequency bin), so we have

$$F_C(\theta) = 1 - \mu + \frac{\mu}{M} = 1 - \frac{M-1}{M}\mu.$$

Only when an M-ary band is hit by the jamming and the jamming tone falls in an empty bin, the ratio of the output of the matched filter corresponding to the empty frequency bin to the output of the matched filter corresponding to the signal tone is possibly greater than threshold θ. In this case, the ratio is

$$\frac{X_J}{X_S} = \frac{1}{\sqrt{\alpha}}$$

If $\frac{1}{\sqrt{\alpha}} < \theta$, $\frac{X_J}{X_S}$ is always less than θ. So $F_E(\theta) = 0$. However, the probability that the jamming tone falls in an empty frequency bin is μ/M, so $F_E(\theta) = \frac{\mu}{M}$ when $\sqrt{\alpha} < \frac{1}{\theta}$. In summary, we get

$$F_C(\theta) = \begin{cases} 1 & \text{if } \alpha > \theta^2; \\ 1 - \frac{M-1}{M}\mu & \text{otherwise.} \end{cases}$$

$$F_E(\theta) = \begin{cases} \frac{\mu}{M} & \text{if } 0 < \alpha < \frac{1}{\theta^2}; \\ 0 & \text{otherwise.} \end{cases}$$

In binary case, $M = 2$, then we have

$$F_C(\theta) = \begin{cases} 1 & \text{if } \alpha > \theta^2; \\ 1 - \frac{\mu}{2} & \text{otherwise.} \end{cases}$$

$$F_E(\theta) = \begin{cases} \frac{\mu}{2} & \text{if } 0 < \alpha < \frac{1}{\theta^2}; \\ 0 & \text{otherwise.} \end{cases}$$

3.7 Derivation of F Functions

We are concerned with following functions.

$$F_{C0} = \int_0^\infty p_{s+n}(x)\left[\int_0^{x/\theta} p_n(y)dy\right]^{M-1} dx$$

$$F_{C1} = \frac{1}{M}\int_0^\infty p_{s+j+n}(x)\left[\int_0^{x/\theta} p_n(y)dy\right]^{M-1} dx$$

$$+\frac{M-1}{M}\int_0^\infty p_{s+n}(x)\left[\int_0^{x/\theta} p_{j+n}(y)dy\right]\left[\int_0^{x/\theta} p_n(z)dz\right]^{M-2} dx$$

$$F_{E0} = \int_0^\infty p_n(x)\left[\int_0^{x/\theta} p_{s+n}(y)dy\right]\left[\int_0^{x/\theta} p_n(z)dz\right]^{M-2} dx$$

$$F_{E1} = \frac{1}{M}\int_0^\infty p_n(x)\left[\int_0^{x/\theta} p_{s+j+n}(y)dy\right]\left[\int_0^{x/\theta} p_n(z)dz\right]^{M-2} dx$$

$$+\frac{1}{M}\int_0^\infty p_{j+n}(x)\left[\int_0^{x/\theta} p_{s+n}(y)dy\right]\left[\int_0^{x/\theta} p_n(z)dz\right]^{M-2} dx$$

$$+\frac{M-2}{M}\int_0^\infty p_n(x)\left[\int_0^{x/\theta} P_{s+n}(y)dy\right]\left[\int_0^{x/\theta} p_{j+n}(z)dz\right]$$

$$\times\left[\int_0^{x/\theta} p_n(w)dw\right]^{M-3} dx$$

and p_n, p_{s+n},p_{j+n}, and p_{s+j+n} are given in (3.11) - (3.14).

3.7.1 Computation of F_{C0}

$$F_{C0} = \int_0^\infty p_{s+n}(x)\left[\int_0^{x/\theta} p_n(y)dy\right]^{M-1} dx$$

Since

$$\int_0^{x/\theta} p_n(y)dy = \int_0^{x/\theta} y\exp\left(-\frac{y^2}{2}\right)dy = 1-\exp\left(-\frac{x^2}{2\theta^2}\right)$$

so

$$\begin{aligned} F_{C0} &= \int_0^\infty x \exp\left(-\frac{x^2}{2} - \frac{KE_b}{mN_0}\right) I_0\left(x\sqrt{\frac{2KE_b}{mN_0}}\right)\left[1-\exp\left(-\frac{x^2}{2\theta^2}\right)\right]^{M-1} dx \\ &= \sum_{k=0}^{M-1}(-1)^k \binom{M-1}{k} \int_0^\infty x \exp\left[-\left(1+\frac{k}{\theta^2}\right)\frac{x^2}{2} - \frac{KE_b}{mN_0}\right] \\ &\quad \times I_0\left(x\sqrt{\frac{2KE_b}{mN_0}}\right) dx. \end{aligned}$$

Changing variable x into y by substituting

$$x = \frac{\theta}{\sqrt{\theta^2+k}} y$$

into above equation. Then there is

$$\begin{aligned} F_{C0} &= \sum_{k=0}^{M-1}(-1)^k \binom{M-1}{k} \frac{\theta^2}{\theta^2+k} \int_0^\infty y \exp\left(-\frac{y^2}{2} - \frac{KE_b}{mN_0}\right) \\ &\quad \times I_0\left(y\sqrt{\frac{\theta^2}{\theta^2+k}\frac{2KE_b}{mN_0}}\right) dy \\ &= \sum_{k=0}^{M-1}(-1)^k \binom{M-1}{k} \frac{\theta^2}{\theta^2+k} \exp\left(-\frac{k}{\theta^2+k}\frac{KE_b}{mN_0}\right) \\ &\quad \times \underbrace{\int_0^\infty y \exp\left(-\frac{y^2}{2} - \frac{\theta^2}{\theta^2+k}\frac{KE_b}{mN_0}\right) I_0\left(y\sqrt{\frac{\theta^2}{\theta^2+k}\frac{2KE_b}{mN_0}}\right) dy}_{=1} \\ &= \sum_{k=0}^{M-1}(-1)^k \binom{M-1}{k} \left(\frac{\theta^2}{\theta^2+k}\right) \exp\left(-\frac{k}{\theta^2+k}\frac{KE_b}{mN_0}\right) \end{aligned}$$

3.7.2 Computation of F_{C1}

$$F_{C1} = \frac{1}{M} g_{c1a} + \frac{M-1}{M} g_{c1b}$$

g_{c1a} and g_{c1b} can be computed as following.

$$\begin{aligned}
g_{c1a} &= \int_0^\infty p_{s+j+n}(x)\left[\int_0^{x/\theta} p_n(y)dy\right]^{M-1} dx \\
&= \int_0^{2\pi} \frac{1}{2\pi}\sum_{k=0}^{M-1}(-1)^k\binom{M-1}{k}\left(\frac{\theta^2}{\theta^2+k}\right)\exp\left[-\frac{k}{\theta^2+k}\frac{K\tilde{E}_s(\phi)}{mN_0}\right]d\phi \\
&= \frac{1}{2\pi}\sum_{k=0}^{M-1}(-1)^k\binom{M-1}{k}\frac{\theta^2}{\theta^2+k}\exp\left[-\frac{k}{\theta^2+k}\left(1+\frac{1}{\alpha}\right)\frac{KE_b}{mN_0}\right] \\
&\quad \times\int_0^{2\pi}\exp\left(-\frac{k}{\theta^2+k}\frac{KE_b}{mN_0}\frac{2}{\sqrt{\alpha}}\cos\phi\right)d\phi \\
&= \sum_{k=0}^{M-1}(-1)^k\binom{M-1}{k}\frac{\theta^2}{\theta^2+k}\exp\left[-\frac{k}{\theta^2+k}\left(1+\frac{1}{\alpha}\right)\frac{KE_b}{mN_0}\right] \\
&\quad \times I_0\left(\frac{k}{\theta^2+k}\frac{KE_b}{mN_0}\frac{2}{\sqrt{\alpha}}\right)
\end{aligned}$$

In the last step, we have used the following relationship

$$I_0(x) = \frac{1}{2\pi}\int_0^{2\pi}\exp(x\cos\phi)d\phi$$

$$\begin{aligned}
g_{c1b} &= \int_0^\infty p_{s+n}(x)\left[\int_0^{x/\theta} p_{j+n}(y)dy\right]\left[\int_0^{x/\theta} p_n(z)dz\right]^{M-2} dx \\
&= \int_0^\infty x\exp\left(-\frac{x^2}{2}-\frac{KE_b}{mN_0}\right)I_0\left(x\sqrt{\frac{2KE_b}{mN_0}}\right)\left[1-Q\left(\sqrt{\frac{2KE_b}{\alpha mN_0}},\frac{x}{\theta}\right)\right] \\
&\quad \times\left[1-\exp\left(-\frac{x^2}{2\theta^2}\right)\right]^{M-2} dx \\
&= \sum_{k=0}^{M-2}(-1)^k\binom{M-2}{k}\int_0^\infty x\exp\left[-\left(1+\frac{k}{\theta^2}\right)\frac{x^2}{2}-\frac{KE_b}{mN_0}\right] \\
&\quad \times I_0\left(x\sqrt{\frac{2KE_b}{mN_0}}\right)\left[1-Q\left(\sqrt{\frac{2KE_b}{mN_0}},\frac{x}{\theta}\right)\right]dx
\end{aligned}$$

$$= X - Y$$

where

$$X = \sum_{k=0}^{M-2}(-1)^k \binom{M-2}{k} \int_0^\infty x \exp\left[-\left(1+\frac{k}{\theta^2}\right)\frac{x^2}{2} - \frac{KE_b}{mN_0}\right] \times I_0\left(x\sqrt{\frac{2KE_b}{mN_0}}\right) dx.$$

Changing variable x into y by substituting

$$x = \frac{\theta}{\sqrt{\theta^2+k}} y$$

into above equation. Then there is

$$\begin{aligned} X &= \sum_{k=0}^{M-2}(-1)^k \binom{M-2}{k} \frac{\theta^2}{\theta^2+k} \int_0^\infty y \exp\left(-\frac{y^2}{2} - \frac{KE_b}{mN_0}\right) \times I_0\left(y\sqrt{\frac{\theta^2}{\theta^2+k}\frac{2KE_b}{mN_0}}\right) dy \\ &= \sum_{k=0}^{M-2}(-1)^k \binom{M-2}{k} \frac{\theta^2}{\theta^2+k} \exp\left(-\frac{k}{\theta^2+k}\frac{KE_b}{mN_0}\right) \\ &\quad \times \underbrace{\int_0^\infty y \exp\left(-\frac{y^2}{2} - \frac{\theta^2}{\theta^2+k}\frac{KE_b}{mN_0}\right) I_0\left(y\sqrt{\frac{\theta^2}{\theta^2+k}\frac{2KE_b}{mN_0}}\right) dy}_{=1} \\ &= \sum_{k=0}^{M-2}(-1)^k \binom{M-2}{k} \frac{\theta^2}{\theta^2+k} \exp\left(-\frac{k}{\theta^2+k}\frac{KE_b}{mN_0}\right) \end{aligned}$$

and

$$Y = \sum_{k=0}^{M-2}(-1)^k \binom{M-2}{k} \int_0^\infty x \exp\left[-\left(1+\frac{k}{\theta^2}\right)\frac{x^2}{2} - \frac{KE_b}{mN_0}\right] \times I_0\left(x\sqrt{\frac{2KE_b}{mN_0}}\right) Q\left(\sqrt{\frac{2KE_b}{\alpha mN_0}}, \frac{x}{\theta}\right) dx.$$

Changing variable x into y by substituting

$$x = \frac{\theta}{\sqrt{\theta^2 + k}} y$$

into above equation. Then there is

$$\begin{aligned} Y &= \sum_{k=0}^{M-2} (-1)^k \binom{M-2}{k} \frac{\theta^2}{\theta^2 + k} \exp\left(-\frac{k}{\theta^2 + k} \frac{KE_b}{mN_0}\right) \\ &\quad \times \int_0^\infty Q\left(\sqrt{\frac{2KE_b}{\alpha mN_0}}, \frac{y}{\sqrt{\theta^2 + k}}\right) y \exp\left(-\frac{y^2}{2} - \frac{\theta^2}{\theta^2 + k} \frac{KE_b}{mN_0}\right) \\ &\quad \times I_0\left(y \sqrt{\frac{\theta^2}{\theta^2 + k} \frac{2KE_b}{mN_0}}\right) dy \end{aligned}$$

By using an integral discussed in [17],

$$\begin{aligned} &\int_0^\infty Q\left(\frac{a_2}{\sigma_2}, \frac{x}{\sigma_2}\right) \frac{x}{\sigma_1^2} \exp\left(-\frac{x^2 + a_1^2}{2\sigma_1^2}\right) I_0\left(\frac{a_1 x}{\sigma_1^2}\right) dx \\ &= \frac{\sigma_1^2}{\sigma_1^2 + \sigma_2^2} \left[1 - Q(\sqrt{t}, \sqrt{s})\right] + \frac{\sigma_2^2}{\sigma_1^2 + \sigma_2^2} Q(\sqrt{s}, \sqrt{t}) \end{aligned} \tag{3.19}$$

where

$$s = \frac{a_2^2}{\sigma_1^2 + \sigma_2^2}; \qquad t = \frac{a_1^2}{\sigma_1^2 + \sigma_2^2}$$

we obtain

$$\begin{aligned} Y &= \sum_{k=0}^{M-2} (-1)^k \binom{M-2}{k} \frac{\theta^2}{\theta^2 + k} \exp\left(-\frac{k}{\theta^2 + k} \frac{KE_b}{mN_0}\right) \\ &\quad \times \left\{ \frac{1}{\theta^2 + k + 1} \left[1 - Q\left(\sqrt{b}, \sqrt{a}\right)\right] + \frac{\theta^2 + k}{\theta^2 + k + 1} Q(\sqrt{a}, \sqrt{b}) \right\} \end{aligned}$$

where

$$a = \frac{\theta^2 + k}{\theta^2 + k + 1} \frac{2KE_b}{\alpha mN_0}; \qquad b = \frac{\theta^2}{(\theta^2 + k)(\theta^2 + k + 1)} \frac{2KE_b}{mN_0}.$$

Then

$$\begin{aligned} g_{c1b} &= X - Y \\ &= \sum_{k=0}^{M-2}(-1)^k \binom{M-2}{k} \frac{\theta^2}{\theta^2+k} \exp\left(-\frac{k}{\theta^2+k}\frac{KE_b}{mN_0}\right) \\ &\quad \times \left\{\frac{\theta^2+k}{\theta^2+k+1}\left[1 - Q(\sqrt{a},\sqrt{b})\right] + \frac{1}{\theta^2+k+1}Q(\sqrt{b},\sqrt{a})\right\} \end{aligned}$$

3.7.3 Computation of F_{E0}

$$\begin{aligned} F_{E0} &= \int_0^\infty p_n(x)\left[\int_0^{x/\theta} p_{s+n}(y)dy\right]\left[\int_0^{x/\theta} p_n(z)dz\right]^{M-2} dx \\ &= \sum_{k=0}^{M-2}(-1)^k \binom{M-2}{k} \int_0^\infty x \exp\left[-\left(1+\frac{k}{\theta^2}\right)\frac{x^2}{2}\right] \\ &\quad \times \left[1 - Q\left(\sqrt{\frac{2KE_b}{mN_0}}, \frac{x}{\theta}\right)\right] dx \\ &= U - V \end{aligned}$$

where

$$\begin{aligned} U &= \sum_{k=0}^{M-2}(-1)^k \binom{M-2}{k} \int_0^\infty x \exp\left[-\left(1+\frac{k}{\theta^2}\right)\frac{x^2}{2}\right] dx \\ &= \sum_{k=0}^{M-2}(-1)^k \binom{M-2}{k} \frac{\theta^2}{\theta^2+k} \end{aligned}$$

and

$$V = \sum_{k=0}^{M-2}(-1)^k \binom{M-2}{k} \int_0^\infty x \exp\left[-\left(1+\frac{k}{\theta^2}\right)\frac{x^2}{2}\right] Q\left(\sqrt{\frac{2KE_b}{mN_0}}, \frac{x}{\theta}\right) dx.$$

Changing variable x into y by substituting

$$x = \frac{\theta}{\sqrt{\theta^2+k}}y$$

into above equation. Then there is

$$V = \sum_{k=0}^{M-2}(-1)^k \binom{M-2}{k} \frac{\theta^2}{\theta^2+k} \int_0^\infty y \exp(-\frac{y^2}{2}) Q\left(\sqrt{\frac{2KE_b}{mN_0}}, \frac{y}{\sqrt{\theta^2+k}}\right) dy$$

By using Eq. (3.19) once more, we have

$$\begin{aligned} V &= \sum_{k=0}^{M-2}(-1)^k \binom{M-2}{k} \frac{\theta^2}{\theta^2+k} \\ &\quad \times \left\{ \frac{1}{\theta^2+k+1} \left[1 - Q\left(0, \sqrt{\frac{\theta^2+k}{\theta^2+k+1}\frac{2KE_b}{mN_0}}\right)\right] \right. \\ &\quad \left. + \frac{\theta^2+k}{\theta^2+k+1} Q\left(\sqrt{\frac{\theta^2+k}{\theta^2+k+1}\frac{2KE_b}{mN_0}}, 0\right) \right\} \\ &= \sum_{k=0}^{M-2}(-1)^k \binom{M-2}{k} \frac{\theta^2}{\theta^2+k} \left[1 - \frac{1}{\theta^2+k+1} \exp\left(-\frac{\theta^2+k}{\theta^2+k+1}\frac{KE_b}{mN_0}\right)\right] \end{aligned}$$

In the last step, the following Marcum Q function properties have been used:

$$Q(0,x) = \exp\left(-\frac{x^2}{2}\right); \qquad Q(x,0) = 1.$$

Therefore,

$$\begin{aligned} F_{E0} &= U - V \\ &= \sum_{k=0}^{M-2}(-1)^k \binom{M-2}{k} \frac{\theta^2}{(\theta^2+k)(\theta^2+k+1)} \exp\left(-\frac{\theta^2+k}{\theta^2+k+1}\frac{KE_b}{mN_0}\right) \end{aligned}$$

3.7.4 Computation of F_{E1}

$$F_{E1} = \frac{1}{M} g_{e1a} + \frac{1}{M} g_{e1b} + \frac{M-2}{M} g_{e1c}$$

g_{e1a}, g_{e1b}, and g_{e1c} are computed as follows.

Note the similarity between g_{e1a} and F_{E0}.

$$
\begin{aligned}
g_{e1a} &= \int_0^\infty p_n(x)\left[\int_0^{x/\theta} p_{s+j+n}(y)dy\right]\left[\int_0^{x/\theta} p_n(z)dz\right]^{M-2} dx \\
&= \frac{1}{2\pi}\int_0^{2\pi}\sum_{k=0}^{M-2}(-1)^k\binom{M-2}{k}\frac{\theta^2}{(\theta^2+k)(\theta^2+k+1)} \\
&\quad \times \exp\left[-\frac{\theta^2+k}{\theta^2+k+1}\frac{K\tilde{E}_b(\phi)}{mN_0}\right]d\phi \\
&= \sum_{k=0}^{M-2}(-1)^k\binom{M-2}{k}\frac{\theta^2}{(\theta^2+k)(\theta^2+k+1)} \\
&\quad \times \exp\left[-\frac{\theta^2+k}{\theta^2+k+1}\left(1+\frac{1}{\alpha}\right)\frac{KE_b}{mN_0}\right] \\
&\quad \times \frac{1}{2\pi}\int_0^{2\pi}\exp\left(-\frac{\theta^2+k}{\theta^2+k+1}\frac{2}{\sqrt{\alpha}}\frac{KE_b}{mN_0}\cos\phi\right)d\phi \\
&= \sum_{k=0}^{M-2}(-1)^k\binom{M-2}{k}\frac{\theta^2}{(\theta^2+k)(\theta^2+k+1)} \\
&\quad \times \exp\left[-\frac{\theta^2+k}{\theta^2+k+1}\left(1+\frac{1}{\alpha}\right)\frac{KE_b}{mN_0}\right] I_0\left(\frac{\theta^2+k}{\theta^2+k+1}\frac{2}{\sqrt{\alpha}}\frac{KE_b}{mN_0}\right)
\end{aligned}
$$

$$
g_{e1b} = \int_0^\infty p_{n+j}(x)\left[\int_0^{x/\theta} p_{s+n}(y)dy\right]\left[\int_0^{x/\theta} p_n(z)dz\right]^{M-2} dx
$$

It can be seen that the integral in above equation is the same as the one in g_{c1b} with exchange positions of p_{s+n} and p_{j+n}. So, g_{e1b} can be obtained by exchanging the positions of E_b and E_b/α in g_{c1b}, i.e.,

$$
\begin{aligned}
g_{e1b} &= \sum_{k=0}^{M-2}(-1)^k\binom{M-2}{k}\frac{\theta^2}{\theta^2+k}\exp\left(-\frac{k}{\theta^2+k}\frac{KE_b}{\alpha mN_0}\right) \\
&\quad \times\left\{\frac{\theta^2+k}{\theta^2+k+1}\left[1-Q(\sqrt{c},\sqrt{d})\right]+\frac{1}{\theta^2+k+1}Q(\sqrt{d},\sqrt{c})\right\}
\end{aligned}
$$

where

$$c = \frac{\theta^2 + k}{\theta^2 + k + 1}\frac{2KE_b}{mN_0}; \qquad d = \frac{\theta^2}{(\theta^2 + k)(\theta^2 + k + 1)}\frac{2KE_b}{\alpha mN_0}.$$

$$\begin{aligned} g_{\text{rlc}} &= \int_0^\infty p_n(w)\left[\int_0^{w/\theta} p_{s+n}(x)dx\right]\left[\int_0^{w/\theta} p_{j+n}(y)dy\right]\left[\int_0^{w/\theta} p_n(z)dz\right]^{M-3} dw \\ &= \int_0^\infty p_{j+n}(w)\left\{\int_{\theta w}^\infty p_n(x)\left[\int_0^{x/\theta} p_{s+n}(y)dy\right]\left[\int_0^{x/\theta} p_n(z)dz\right]^{M-3} dx\right\} dw \\ &= \int_0^\infty p_{j+n}(w)h(w)dw \end{aligned}$$

where $h(w)$ is

$$\begin{aligned} h(w) &= \int_{\theta w}^\infty p_n(x)\left[\int_0^{x/\theta} p_{s+n}(y)dy\right]\left[\int_0^{x/\theta} p_n(z)dz\right]^{M-3} dx \\ &= \int_{\theta w}^\infty x\exp(-\frac{x^2}{2})\left[1 - Q\left(\sqrt{\frac{2KE_b}{mN_0}}, \frac{x}{\theta}\right)\right] \\ &\quad \times \sum_{k=0}^{M-3}(-1)^k \binom{M-3}{k} \exp(-\frac{k}{\theta^2}\frac{x^2}{2})dx \\ &= \sum_{k=0}^{M-3}(-1)^k \binom{M-3}{k}(J - K) \end{aligned}$$

$$J = \int_{\theta w}^\infty x\exp\left[-\left(1 + \frac{k}{\theta^2}\right)\frac{x^2}{2}\right]dx = \frac{\theta^2}{\theta^2 + k}\exp\left[-\left(\theta^2 + k\right)\frac{w^2}{2}\right]$$

$$\begin{aligned} K &= \int_{\theta w}^\infty x\exp\left[-\left(1 + \frac{k}{\theta^2}\right)\frac{x^2}{2}\right] Q\left(\sqrt{\frac{2KE_b}{mN_0}}, \frac{x}{\theta}\right) dx \\ &\overset{x=\theta y}{=} \theta^2 \int_w^\infty y\exp\left[-\left(\theta^2 + k\right)\frac{y^2}{2}\right] Q\left(\sqrt{\frac{2KE_b}{mN_0}}, y\right) dy \end{aligned}$$

$$
\begin{aligned}
&= -\frac{\theta^2}{\theta^2+k} Q\left(\sqrt{\frac{2KE_b}{mN_0}}, y\right) \exp\left[-\left(\theta^2+k\right)\frac{y^2}{2}\right]\Big|_w^\infty \\
&\quad + \frac{\theta^2}{\theta^2+k}\int_w^\infty \exp\left[-\left(\theta^2+k\right)\frac{y^2}{2}\right]\frac{d}{dy}Q\left(\sqrt{\frac{2KE_b}{mN_0}}, y\right) dy \\
&= \frac{\theta^2}{\theta^2+k} Q\left(\sqrt{\frac{2KE_b}{mN_0}}, w\right) \exp\left[-\left(\theta^2+k\right)\frac{w^2}{2}\right] + \tilde{K}
\end{aligned}
$$

$$
\tilde{K} = \frac{\theta^2}{\theta^2+k}\int_w^\infty \exp\left[-\left(\theta^2+k\right)\frac{y^2}{2}\right]\frac{d}{dy}Q\left(\sqrt{\frac{2KE_b}{mN_0}}, y\right) dy
$$

Since

$$
Q\left(\sqrt{\frac{2KE_b}{mN_0}}, y\right) = \int_y^\infty t \exp\left(-\frac{t^2}{2} - \frac{KE_b}{mN_0}\right) I_0\left(t\sqrt{\frac{2KE_b}{mN_0}}\right) dt
$$

so

$$
\frac{d}{dy}Q\left(\sqrt{\frac{2KE_b}{mN_0}}, y\right) = -y \exp\left(-\frac{y^2}{2} - \frac{KE_b}{mN_0}\right) I_0\left(y\sqrt{\frac{2KE_b}{mN_0}}\right)
$$

then

$$
\tilde{K} = -\frac{\theta^2}{\theta^2+k}\int_w^\infty y \exp\left[-\left(\theta^2+k+1\right)\frac{y^2}{2} - \frac{KE_b}{mN_0}\right] I_0\left(y\sqrt{\frac{2KE_b}{mN_0}}\right) dy.
$$

Changing variable y into z by substituting

$$
y = \frac{z}{\sqrt{\theta^2+k+1}}
$$

into above equation, then

$$
\begin{aligned}
\tilde{K} &= -\frac{\theta^2}{(\theta^2+k)(\theta^2+k+1)}\int_{w\sqrt{\theta^2+k+1}}^\infty z \exp\left(-\frac{z^2}{2} - \frac{KE_b}{mN_0}\right) \\
&\quad \times I_0\left(z\sqrt{\frac{1}{\theta^2+k+1}\frac{2KE_b}{mN_0}}\right) dz
\end{aligned}
$$

$$= -\frac{\theta^2}{(\theta^2+k)(\theta^2+k+1)}\exp\left(-\frac{\theta^2+k}{\theta^2+k+1}\frac{KE_b}{mN_0}\right)$$
$$\times Q\left(\sqrt{\frac{1}{\theta^2+k+1}\frac{2KE_b}{mN_0}}, w\sqrt{\theta^2+k+1}\right)$$

then

$$K = \frac{\theta^2}{\theta^2+k}Q\left(\sqrt{\frac{2KE_b}{mN_0}}, w\right)\exp\left[-\left(\theta^2+k\right)\frac{w^2}{2}\right] - \frac{\theta^2}{(\theta^2+k)(\theta^2+k+1)}$$
$$\times \exp\left(-\frac{\theta^2+k}{\theta^2+k+1}\frac{KE_b}{mN_0}\right) Q\left(\sqrt{\frac{1}{\theta^2+k+1}\frac{2KE_b}{mN_0}}, w\sqrt{\theta^2+k+1}\right)$$

Therefore

$$h(w) = \sum_{k=0}^{M-3}(-1)^k\binom{M-3}{k}\frac{\theta^2}{\theta^2+k}$$
$$\times\left\{\exp\left[-\left(\theta^2+k\right)\frac{w^2}{2}\right] - Q\left(\sqrt{\frac{2KE_b}{mN_0}}, w\right)\right.$$
$$\times\exp\left[-\left(\theta^2+k\right)\frac{w^2}{2}\right] + \frac{1}{\theta^2+k+1}\exp\left(-\frac{\theta^2+k}{\theta^2+k+1}\frac{KE_b}{mN_0}\right)$$
$$\left.\times Q\left(\sqrt{\frac{1}{\theta^2+k+1}\frac{2KE_b}{mN_0}}, w\sqrt{\theta^2+k+1}\right)\right\}$$

Then we have

$$g_{\text{elc}} = \int_0^\infty p_{j+n}(w)h(w)dw$$
$$= \int_0^\infty w\exp\left(-\frac{w^2}{2} - \frac{KE_b}{\alpha mN_0}\right) I_0\left(w\sqrt{\frac{2KE_b}{\alpha mN_0}}\right) h(w)dw$$
$$= \sum_{k=0}^{M-3}(-1)^k\binom{M-3}{k}\frac{\theta^2}{\theta^2+k}(R-S+T)$$

where

$$R = \int_0^\infty w \exp\left(-\frac{w^2}{2} - \frac{KE_b}{\alpha m N_0}\right) I_0\left(w\sqrt{\frac{2KE_b}{\alpha m N_0}}\right) \exp\left[-\left(\theta^2 + k\right)\frac{w^2}{2}\right] dw.$$

Substituting

$$w = \frac{x}{\sqrt{\theta^2 + k + 1}}$$

into above equation, then

$$\begin{aligned} R &= \frac{1}{\theta^2 + k + 1} \int_0^\infty x \exp\left(-\frac{x^2}{2} - \frac{KE_b}{\alpha m N_0}\right) I_0\left(x\sqrt{\frac{1}{\theta^2 + k + 1}\frac{2KE_b}{\alpha m N_0}}\right) dx \\ &= \frac{1}{\theta^2 + k + 1} \exp\left(-\frac{\theta^2 + k}{\theta^2 + k + 1}\frac{KE_b}{\alpha m N_0}\right) \\ &\quad \times \underbrace{\int_0^\infty x \exp\left(-\frac{x^2}{2} - \frac{1}{\theta^2 + k + 1}\frac{KE_b}{\alpha m N_0}\right) I_0\left(x\sqrt{\frac{1}{\theta^2 + k + 1}\frac{2KE_b}{\alpha m N_0}}\right) dx}_{=1} \\ &= \frac{1}{\theta^2 + k + 1} \exp\left(-\frac{\theta^2 + k}{\theta^2 + k + 1}\frac{KE_b}{\alpha m N_0}\right) \end{aligned}$$

$$\begin{aligned} S &= \int_0^\infty w \exp\left(-\frac{w^2}{2} - \frac{KE_b}{\alpha m N_0}\right) I_0\left(w\sqrt{\frac{2KE_b}{\alpha m N_0}}\right) \exp\left[-\left(\theta^2 + k\right)\frac{w^2}{2}\right] \\ &\quad \times Q\left(\sqrt{\frac{2KE_b}{m N_0}}, w\right) dw \end{aligned}$$

Do the same variable change as we did in the computation of R, then

$$\begin{aligned} S &= \frac{1}{\theta^2 + k + 1} \int_0^\infty x \exp\left(-\frac{x^2}{2} - \frac{KE_b}{\alpha m N_0}\right) I_0\left(x\sqrt{\frac{1}{\theta^2 + k + 1}\frac{2KE_b}{\alpha m N_0}}\right) \\ &\quad \times Q\left(\sqrt{\frac{2KE_b}{m N_0}}, \frac{x}{\sqrt{\theta^2 + k + 1}}\right) dx \end{aligned}$$

$$= \frac{1}{\theta^2+k+1}\exp\left(-\frac{\theta^2+k}{\theta^2+k+1}\frac{KE_b}{\alpha m N_0}\right)$$
$$\times\int_0^\infty x\exp\left(-\frac{x^2}{2}-\frac{1}{\theta^2+k+1}\frac{KE_b}{\alpha m N_0}\right)I_0\left(x\sqrt{\frac{1}{\theta^2+k+1}\frac{2KE_b}{\alpha m N_0}}\right)$$
$$\times Q\left(\sqrt{\frac{2KE_b}{mN_0}},\frac{x}{\sqrt{\theta^2+k+1}}\right)dx$$

Using (3.19), we have

$$S = \frac{1}{\theta^2+k+1}\exp\left(-\frac{\theta^2+k}{\theta^2+k+1}\frac{KE_b}{\alpha m N_0}\right)$$
$$\times\left\{\frac{1}{\theta^2+k+2}\left[1-Q(\sqrt{\delta},\sqrt{\gamma})\right]+\frac{\theta^2+k+1}{\theta^2+k+2}Q(\sqrt{\gamma},\sqrt{\delta})\right\}$$

where

$$\gamma=\frac{\theta^2+k+1}{\theta^2+k+2}\frac{2KE_b}{mN_0};\qquad \delta=\frac{1}{(\theta^2+k+1)(\theta^2+k+2)}\frac{2KE_b}{\alpha m N_0}.$$

$$T = \frac{1}{\theta^2+k+1}\int_0^\infty w\exp\left(-\frac{w^2}{2}-\frac{KE_b}{\alpha m N_0}\right)$$
$$\times I_0\left(w\sqrt{\frac{2KE_b}{\alpha m N_0}}\right)\exp\left(-\frac{\theta^2+k}{\theta^2+k+1}\frac{KE_b}{mN_0}\right)$$
$$\times Q\left(\sqrt{\frac{1}{\theta^2+k+1}\frac{2KE_b}{mN_0}},w\sqrt{\theta^2+k+1}\right)dw$$
$$= \frac{1}{\theta^2+k+1}\exp\left(-\frac{\theta^2+k}{\theta^2+k+1}\frac{KE_b}{mN_0}\right)$$
$$\times\int_0^\infty w\exp\left(-\frac{w^2}{2}-\frac{KE_b}{\alpha m N_0}\right)I_0\left(w\sqrt{\frac{2KE_b}{\alpha m N_0}}\right)$$
$$\times Q\left(\sqrt{\frac{1}{\theta^2+k+1}\frac{2KE_b}{mN_0}},w\sqrt{\theta^2+k+1}\right)dw$$

Using (3.19), we have

$$\begin{aligned} T &= \frac{1}{\theta^2+k+1}\exp\left(-\frac{\theta^2+k}{\theta^2+k+1}\frac{KE_b}{mN_0}\right) \\ &\quad \times\left\{\frac{\theta^2+k+1}{\theta^2+k+2}\left[1-Q(\sqrt{\eta},\sqrt{\zeta})\right]+\frac{1}{\theta^2+k+2}Q(\sqrt{\zeta},\sqrt{\eta})\right\} \end{aligned}$$

where

$$\zeta=\frac{1}{(\theta^2+k+1)(\theta^2+k+2)}\frac{2KE_b}{mN_0};\qquad \eta=\frac{\theta^2+k+1}{\theta^2+k+2}\frac{2KE_b}{\alpha mN_0}.$$

Comparing $R-S$ with T, we found that $R-S+T$ can be written as

$$R-S+T=\frac{1}{\theta^2+k+1}\left[f\left(\theta^2,k,\frac{KE_b}{mN_0},\frac{KE_b}{\alpha mN_0}\right)+f\left(\theta^2,k,\frac{KE_b}{\alpha mN_0},\frac{KE_b}{mN_0}\right)\right]$$

where

$$\begin{aligned} &f(w,k,X,Y) \\ &= \left\{\frac{w+k+1}{w+k+2}\left[1-Q\left(\sqrt{\frac{w+k+1}{w+k+2}2X},\sqrt{\frac{2Y}{(w+k+1)(w+k+2)}}\right)\right]\right. \\ &\quad \left.+\frac{1}{w+k+2}Q\left(\sqrt{\frac{2Y}{(w+k+1)(w+k+2)}},\sqrt{\frac{w+k+1}{w+k+2}2X}\right)\right\} \\ &\quad \times\exp\left(-\frac{w+k}{w+k+1}Y\right) \end{aligned}$$

Then finally, we have

$$\begin{aligned} g_{e1c} &= \sum_{k=0}^{M-3}(-1)^k\binom{M-3}{k}\frac{\theta^2}{\theta^2+k}\frac{1}{\theta^2+k+1} \\ &\quad \times\left[f\left(\theta^2,k,\frac{KE_b}{mN_0},\frac{KE_b}{\alpha mN_0}\right)+f\left(\theta^2,k,\frac{KE_b}{\alpha mN_0},\frac{KE_b}{mN_0}\right)\right] \end{aligned}$$

Chapter 4

Maximum-Likelihood Diversity Combining in Partial-Band Noise

4.1 Introduction

There have been several diversity combining methods proposed in the last decade for fast frequency hopped FSK spread spectrum systems working in a channel with partial-band noise interference [3, 5, 6, 9]. Their performances in various conditions (with or without channel information, with or without background thermal noise, etc.) have been analyzed and compared.

Although much profound work has been done in this area, there is still lack of a general theoretic framework in this subject, which may provide some theoretical, if not practical, insight and guidance. For example, the structure of the optimum diversity combining on a channel with both PBN interference and background noise modeled as additive white Gaussian noise is unknown. How far away the performances of those proposed combining schemes are from the optimal performance is also unknown. It is also not clear on what type of channel information is required to implement certain optimum diversity combining on the PBN channel with AWGN.

In this chapter, we consider maximum-likelihood diversity combining in a partial-band noise. In Section 4.2, the assumptions, on which our analysis is based, are

presented. In Section 4.3, the structure of optimum diversity combining is discussed and performance of the optimum diversity combiner is illustrated. In Section 4.4, some sub-optimum combining schemes are analyzed. The performance of the optimum combining scheme is compared with that of some well-known diversity combining schemes in Section 4.5. Summary is given in Section 4.6.

4.2 Assumptions

We consider an FFH M-ary FSK receiver, as shown in Figure 4.1. Suppose the diversity order is m chips/symbol. The samples of the envelope detection output of all hops corresponding to one symbol are combined together in the diversity combiner. The background thermal noise is assumed to be additive white Gaussian noise (AWGN) with two-sided spectral density $N_0/2$.

The channel model is the PBN interference channel with parameter ρ and the equivalent two-sided spectral density $N_J/2$. For this channel, the total interference power is distributed uniformly over a fraction ρ of the total spread spectrum system bandwidth.

With above assumptions, the decision of which M-ary symbol was transmitted after dehopping can be formulated as the following hypothesis:

$$H_{i(0\le i\le M-1)}: \qquad r(t) = s_i(t) + n(t) \qquad 0 \le t \le T_s$$

where T_s is the duration of a symbol, $r(t)$ is the received signal contaminated with interference and noise, $s_i(t)$ is dehopped FH/MFSK modulated signal and $n(t)$ is the sum of interference and AWGN. $s_i(t)$ and $n(t)$ are given by

$$\begin{aligned} s_i(t) &= \sum_{k=1}^{m} s_{ik}(t) g_k(t) \\ &= \sum_{k=1}^{m} A_k \cos(2\pi f_i t + \theta_{ik}] g_k(t) \end{aligned}$$

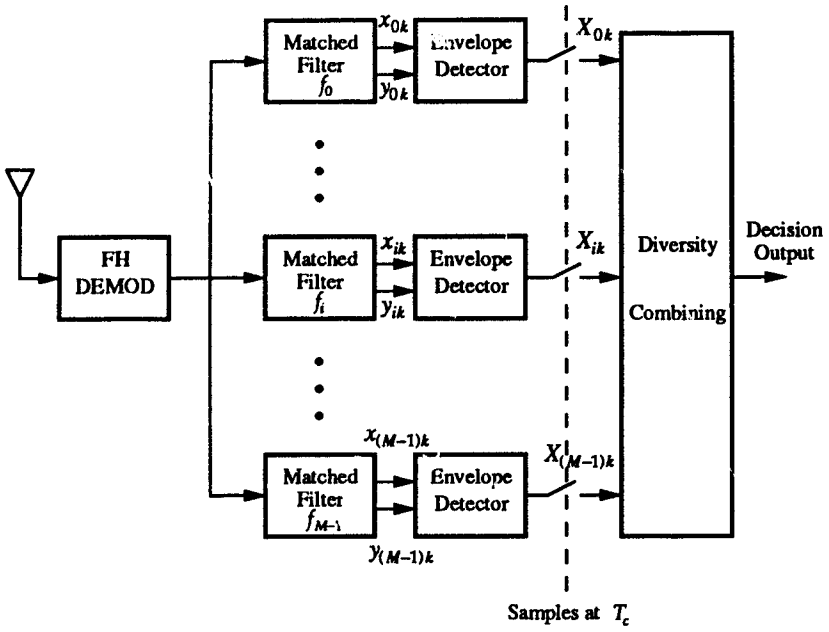

Figure 4.1: The FFH noncoherent MFSK spread spectrum receiver

$$n(t) = \sum_{k=1}^{m} n_k(t) g_k(t)$$

and

$$g_k(t) = \begin{cases} 1 & (k-1)T_c \le t \le kT_c; \\ 0 & \text{otherwise.} \end{cases}$$

In the definition of $g_k(t)$, T_c is the chip interval, and $T_s = mT_c$. We assume the signal amplitude does not change for the different hops corresponding to one M-ary symbol, so

$$A_k = A = \sqrt{\frac{2E_s}{T_s}} = \sqrt{\frac{2E_c}{T_c}} \quad 1 \le k \le m,$$

where E_s is the M-ary symbol energy and $E_c = E_s/m$ is the chip energy. f_i is the M-ary FSK modulation tone. θ_{ik} is the phase of the signal in the kth hop and is assumed uniformly distributed in $[0, 2\pi)$. The phases in each hop are mutually statistically independent. $n_k(t)$ is additive white Gaussian noise (AWGN) with

spectral density $N_k/2$. N_k is given by

$$N_k = \begin{cases} N_0 & \text{if the } k\text{th hop has no interference;} \\ N_1 = N_0 + \frac{N_J}{\rho} & \text{if the } k\text{th hop has interference.} \end{cases}$$

$n_k(t)$ are mutually independent. It can be shown that the outputs of the integrators x_{ik} and y_{ik} are random variable with distributions $N(\sqrt{E_c}\cos\theta_{ik}, N_k/2)$ and $N(\sqrt{E_c}\sin\theta_{ik}, N_k/2)$, respectively, if the ith symbol is sent. Otherwise, both x_{ik} and y_{ik} have distribution $N(0, N_k/2)$ [18, pages 300 - 305].

4.3 Maximum-Likelihood Diversity Combining

The observation space is the outputs of M noncoherent matched filters. A noncoherent matched filter consists of a matched filter followed by an envelope detector. Let the output of the filter matched to the ith symbol in kth hop be X_{ik},

$$X_{ik} = \sqrt{x_{ik}^2 + y_{ik}^2}$$

where $i = 0, 1, 2, \cdots, M-1$ and $k = 1, 2, \cdots, m$. Let X be the matrix representing all samples:

$$X = \begin{bmatrix} X_{01} & X_{02} & \cdots & X_{0m} \\ X_{11} & X_{12} & \cdots & X_{1m} \\ \vdots & \ddots & & \vdots \\ X_{(M-1)1} & X_{(M-1)2} & \cdots & X_{(M-1)m} \end{bmatrix} \tag{4.1}$$

The conditional probability density function (PDF) of X_{ik} conditional on the ith symbol being sent and the kth hop being without interference is given by

$$\begin{aligned} P_{ik}^{(0)}(x) &= P_{X_{ik}}(x|i\text{th symbol sent, no interference in } k\text{th hop}) \\ &= \frac{2x}{N_0}\exp\left[-\frac{x^2+E_c}{N_0}\right] I_0\left(\frac{2x\sqrt{E_c}}{N_0}\right). \end{aligned} \tag{4.2}$$

The conditional PDF of X_{ik} conditional on the ith symbol being sent and the kth hop having interference is

$$\begin{aligned} P_{ik}^{(1)}(x) &= P_{X_{ik}}(x|i\text{th symbol sent, interference in } k\text{th hop}) \\ &= \frac{2x}{N_1}\exp\left[-\frac{x^2+E_c}{N_1}\right] I_0\left(\frac{2x\sqrt{E_c}}{N_1}\right). \end{aligned} \tag{4.3}$$

The conditional PDF of X_{ik} conditional on the ith symbol not being sent and the kth hop having no interference is

$$\begin{aligned} Q_{ik}^{(0)}(x) &= P_{X_{ik}}(x|i\text{th symbol not sent, no interference in } k\text{th hop}) \\ &= \frac{2x}{N_0}\exp\left(-\frac{x^2}{N_0}\right), \end{aligned} \tag{4.4}$$

and the conditional PDF of X_{ik} conditional on the ith symbol not being sent and the kth hop having interference is

$$\begin{aligned} Q_{ik}^{(1)}(x) &= P_{X_{ik}}(x|i\text{th symbol not sent, interference in } k\text{th hop}) \\ &= \frac{2x}{N_1}\exp\left(-\frac{x^2}{N_1}\right). \end{aligned} \tag{4.5}$$

Suppose PBN interference are present in j out of m hops, where $0 \leq j \leq m$. Without loss of generality, it is assumed that first j hops of total m hops suffer PBN interference. Then, the joint PDF of the samples X conditional on Kth symbol being sent is

$$\begin{aligned} P(X|K) &= \Pr(X|K\text{th symbol sent}) \\ &= \left[\prod_{k=1}^{j} P_{Kk}^{(1)} \prod_{i=0,i\neq K}^{M-1} Q_{ik}^{(1)}\right]\left[\prod_{k=j+1}^{m} P_{Kk}^{(0)} \prod_{i=0,i\neq K}^{M-1} Q_{ik}^{(0)}\right]. \end{aligned}$$

Comparing $P(X|K)$ and $P(X|J)$, where $J \neq K$, is equivalent to compare:

$$\left[\prod_{k=1}^{j} P_{Kk}^{(1)} \prod_{i=0,i\neq K}^{M-1} Q_{ik}^{(1)}\right]\left[\prod_{k=j+1}^{m} P_{Kk}^{(0)} \prod_{i=0,i\neq K}^{M-1} Q_{ik}^{(0)}\right]$$

and

$$\left[\prod_{k=1}^{j} P_{Jk}^{(1)} \prod_{i=0,i\neq J}^{M-1} Q_{ik}^{(1)}\right]\left[\prod_{k=j+1}^{m} P_{Jk}^{(0)} \prod_{i=0,i\neq J}^{M-1} Q_{ik}^{(0)}\right].$$

Removing the common factors from both expressions, the comparison becomes

$$\prod_{k=1}^{j} P_{Kk}^{(1)} Q_{Jk}^{(1)} \prod_{k=j+1}^{m} P_{Kk}^{(0)} Q_{Jk}^{(0)} \sim \prod_{k=1}^{j} P_{Jk}^{(1)} Q_{Kk}^{(1)} \prod_{k=j+1}^{m} P_{Jk}^{(0)} Q_{Kk}^{(0)},$$

where $\sim$ means versus. The above comparison is equivalent to

$$\frac{\prod_{k=1}^{j} P_{Kk}^{(1)} \prod_{k=j+1}^{m} P_{Kk}^{(0)}}{\prod_{k=1}^{j} Q_{Kk}^{(1)} \prod_{k=j+1}^{m} Q_{Kk}^{(0)}} \sim \frac{\prod_{k=1}^{j} P_{Jk}^{(1)} \prod_{k=j+1}^{m} P_{Jk}^{(0)}}{\prod_{k=1}^{j} Q_{Jk}^{(1)} \prod_{k=j+1}^{m} Q_{Jk}^{(0)}}$$

Substitute Eqs. (4.2)-(4.5) into the above expression, it can be shown that the comparison becomes

$$\prod_{k=1}^{j} I_0\left(\frac{2X_{Kk}\sqrt{E_c}}{N_1}\right) \prod_{k=j+1}^{m} I_0\left(\frac{2X_{Kk}\sqrt{E_c}}{N_0}\right) \sim \prod_{k=1}^{j} I_0\left(\frac{2X_{Jk}\sqrt{E_c}}{N_1}\right) \prod_{k=j+1}^{m} I_0\left(\frac{2X_{Jk}\sqrt{E_c}}{N_0}\right)$$

Therefore, the maximum-likelihood diversity combining is to compute

$$\lambda_i = \sum_{k=1}^{j} \ln I_0\left(\frac{2X_{ik}\sqrt{E_c}}{N_1}\right) + \sum_{k=j+1}^{m} \ln I_0\left(\frac{2X_{ik}\sqrt{E_c}}{N_0}\right) \tag{4.6}$$

for $i = 0, 1, \cdots, M-1$, and choose the index of the largest λ_i as the decision. Note that it requires the knowledge of E_c, N_0, N_J, ρ and side information to compute λ_i. It is easy to see that knowledge of N_J, ρ and side information is used to determine N_1. So equivalently, Eq. (4.6) can be rewritten as:

$$\lambda_i = \sum_{k=1}^{m} \ln I_0\left(\frac{2X_{ik}\sqrt{E_c}}{N_k}\right) = \sum_{k=1}^{m} \ln I_0\left(\sqrt{\frac{2E_c}{N_k}}\frac{X_{ik}}{\sqrt{N_k/2}}\right) \tag{4.7}$$

where $N_k/2$ is the noise variance (power) at each hop. Thus the required information to compute λ_i is equivalent to the information on signal-to-noise ratio and noise variance at each hop.

4.3.1 Performance of the Optimum Diversity Combining

The worst case bit error rate for optimum diversity combining versus E_b/N_J is obtained by Monte Carlo simulation. Figure 4.2 shows the BER of a binary FSK/FFH spread spectrum system with diversity order m =2, 3, 4, and 7. The E_b/N_0 is 13.35 dB, which is the signal-to-thermal noise ratio required to maintain a BER of 10^{-5} for the same system without diversity and interference. Also shown in the figure are the BER of the same system without diversity under full-band noise interference ($\rho = 1$), and the BER of the same system without diversity under worst case PBN interference, which is given by [19, page 574]

$$P_b = \max_{0<\rho\leq 1} \{\rho P_{fsk}(E_b/N_1) + (1-\rho)P_{fsk}(E_b/N_0)\}$$

where

$$P_{fsk}(x) = \frac{M/2}{M-1} \sum_{k=1}^{M-1} \frac{(-1)^{k+1}}{k+1} \binom{M-1}{k} \exp\left(-\frac{k}{k+1} x \log_2 M\right).$$

The BER for full-band interference represents the damage a jammer with fixed average power can do to the system, when all other jamming strategies fail to provide better effects. In other words, this is the least effect that a fixed average power interference can have on the system.

It can be observed in the figure that at low E_b/N_J and high E_b/N_J regions, the optimum diversity order is 2, and for E_b/N_J between 15 dB and 28 dB, the optimum diversity order is 3. For a BER around 0.1, or for E_b/N_J less than 8 dB, in fact, there is no need to employ diversity reception, as the no diversity case gives the best results. This phenomenon is due to the noncoherent combination loss in AWGN. When E_b/N_J is small, the interference or jamming is so strong that the worst case interference is full-band interference, which is seen by the system as AWGN. So in this case, there is no advantage using diversity reception. Actually there is a disadvantage due to the noncoherent combination loss in AWGN. Thus,

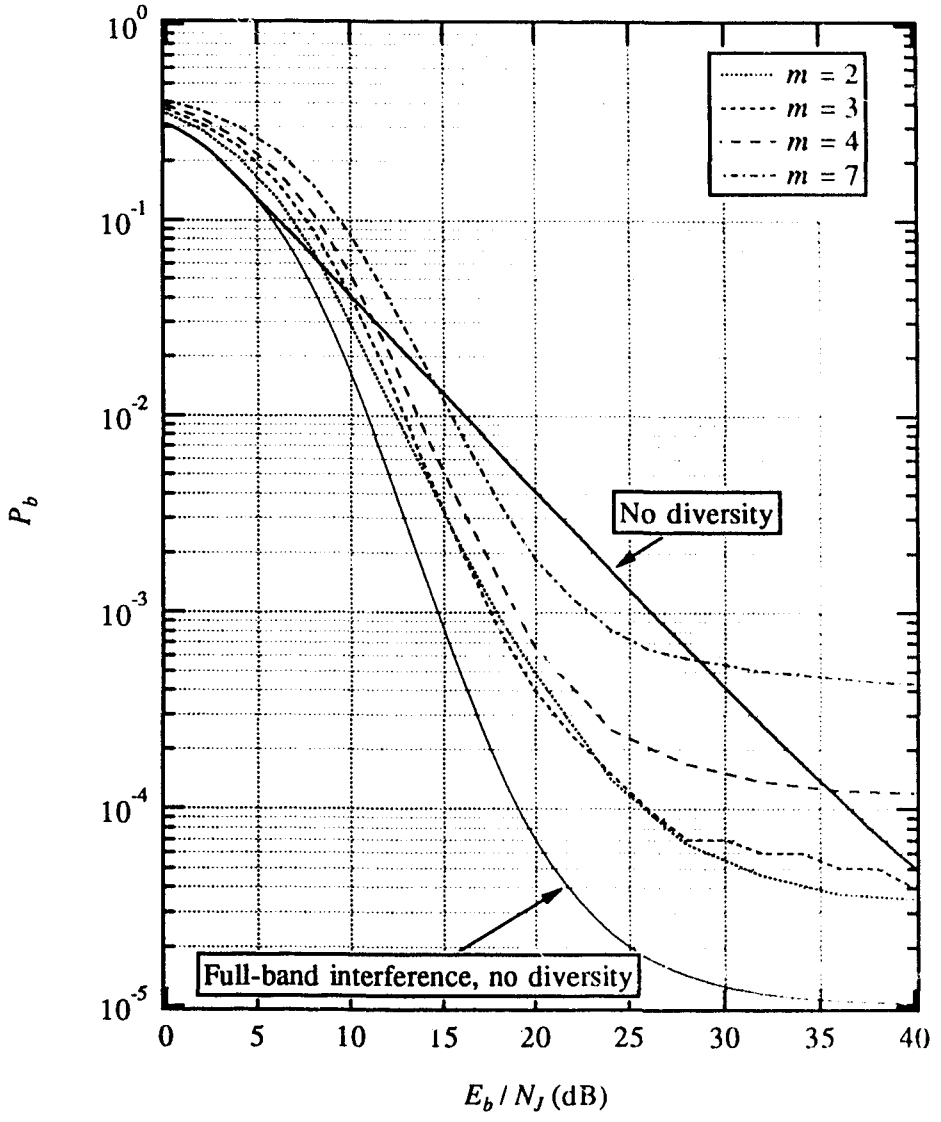

Figure 4.2: BER of FH/BFSK maximum-likelihood diversity receiver with different diversity order in worst case partial band noise interference. $E_b/N_0 = 13.35$ dB.

the effects of using diversity reception in full-band interference is negative with regard to the system performance. When E_b/N_J is high, the interference is very weak, and the most effective interference strategy is to concentrate the limited average power in a small portion of the transmission band. Diversity reception is an effective way to combat this type of interference, but due to the existence of background thermal noise, a high order of diversity is not desirable because of noncoherent combination loss. Thus, for $E_b/N_0 = 13.35$ dB, the highest optimum diversity order is 3. For higher E_b/N_0, more curves corresponding to different diversity orders may crossover each other, and the highest optimum diversity order can be higher.

The performance of the optimum diversity reception under the worst case PBN interference is not as good as that of the system without diversity under full-band interference. The difference is about 3 dB at a BER of 10^{-3}. This means that an intentional interference source, or jammer, can still use PBN to increase its interference effects. Therefore, other measures have to be taken to force the jammer to go back to full-band jamming. Error correction coding is a very efficient way to achieve this. From the error correction coding theory point of view, the diversity transmission used here, is just a repetition code, and a repetition code is a very simple error correction code. Therefore, if further improvement of the system's anti-jam capability is required, a sophisticated form of error correction coding must be employed.

It can be seen that the requirement of signal-to-thermal noise E_b/N_0 in diversity transmission system is higher than a system without diversity. For example, we can see from Figure 4.2 that it is not possible for the system with diversity to achieve a BER of 10^{-5} when E_b/N_0 is 13.35 dB, no matter how weak the interference is. The solution to this problem is either increasing E_b/N_0 or using a concatenation of diversity and error correction coding.

Now consider an 8-ary FSK/FFH system as an example for M-ary system. The BER of the 8-ary FSK/FFH spread spectrum system under worst case PBN

is shown in Figure 4.3. The E_b/N_0 is 9.09 dB, which is the signal-to-thermal noise ratio required to maintain a BER of 10^{-5} for the same system without diversity and interference. The performance is similar to that in binary case. The optimum diversity order is $m = 2$ except in the region of E_b/N_J from 10 dB to 20 dB, where $m = 3$ is the optimum diversity order.

4.4 Some Sub-optimum Combining Schemes

It has been shown that in maximum-likelihood combining, the decision variable is a sum of the nonlinear function $\ln I_0(x)$s. It is well-known that when x is small, the following approximation can be used [20, pages 243-244] [21, page 339]:

$$I_0(x) \approx 1 + \frac{1}{4}x^2$$

and

$$\ln I_0(x) \approx \ln(1 + \frac{1}{4}x^2) \approx \frac{1}{4}x^2,$$

and when x is large,

$$\ln I_0(x) \approx x - \frac{1}{2}\ln(2\pi x) \approx x.$$

Figure 4.4 shows three functions $\ln I_0(x)$, $\frac{1}{4}x^2$, and x. It can be seen that x^2 is a good approximation of $\ln I_0(x)$ for $x < 1$. The relative difference between x and $\ln I_0(x)$ becomes small when x become large. Nevertheless, x and $\ln I_0(x)$ can be viewed as parallel. In our application, that all elements in the summation shift a constant does not influence the final results. Therefore, for small x, the square sum of x should used, and for large x, a linear sum of x should be used. Considering both ends, we can use the following piecewise function to approximate $\ln I_0(x)$:

$$f(x) = \begin{cases} \frac{1}{4}x^2 & \text{if } 0 \le x < 4; \\ x & \text{if } x \ge 4. \end{cases}$$

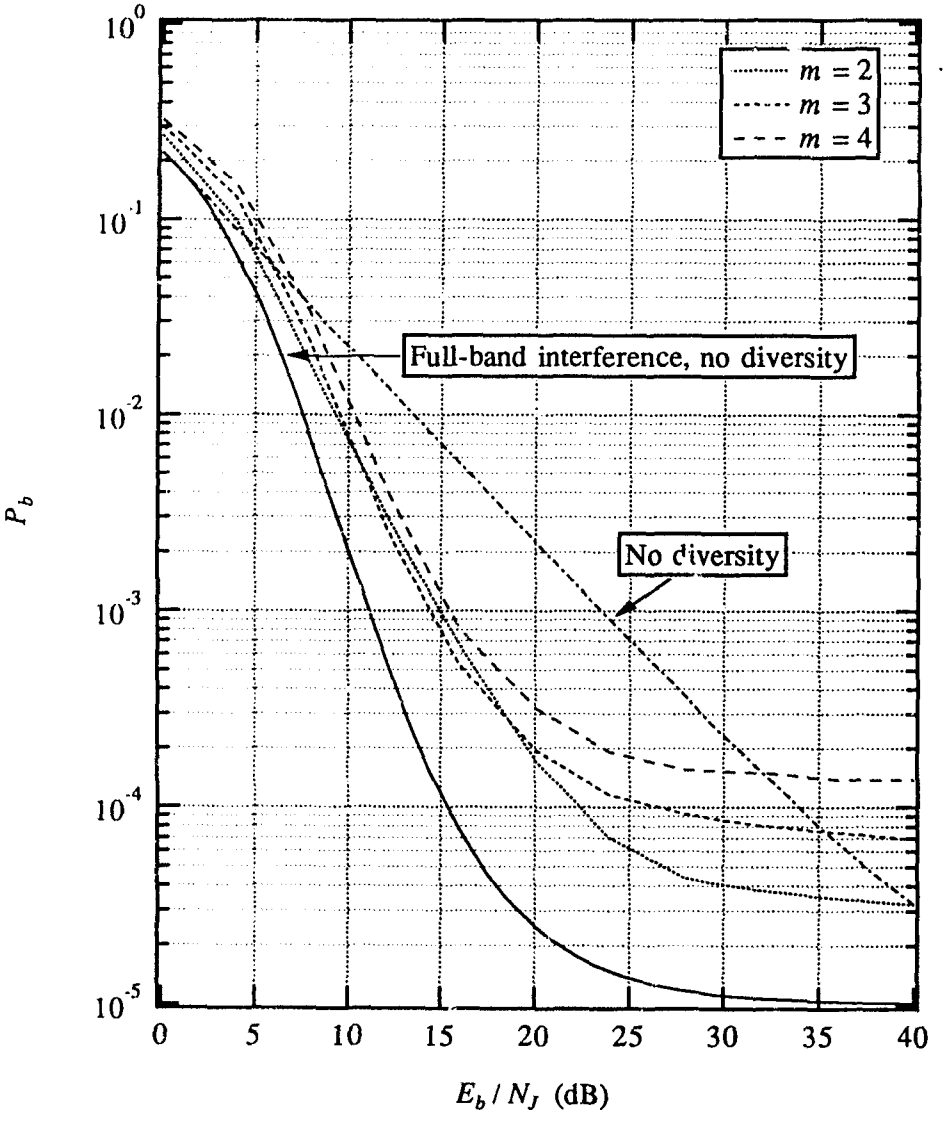

Figure 4.3: BER of FH/8FSK maximum-likelihood diversity receiver with different diversity order in worst case partial band noise interference. $E_b/N_0 = 9.09$ dB.

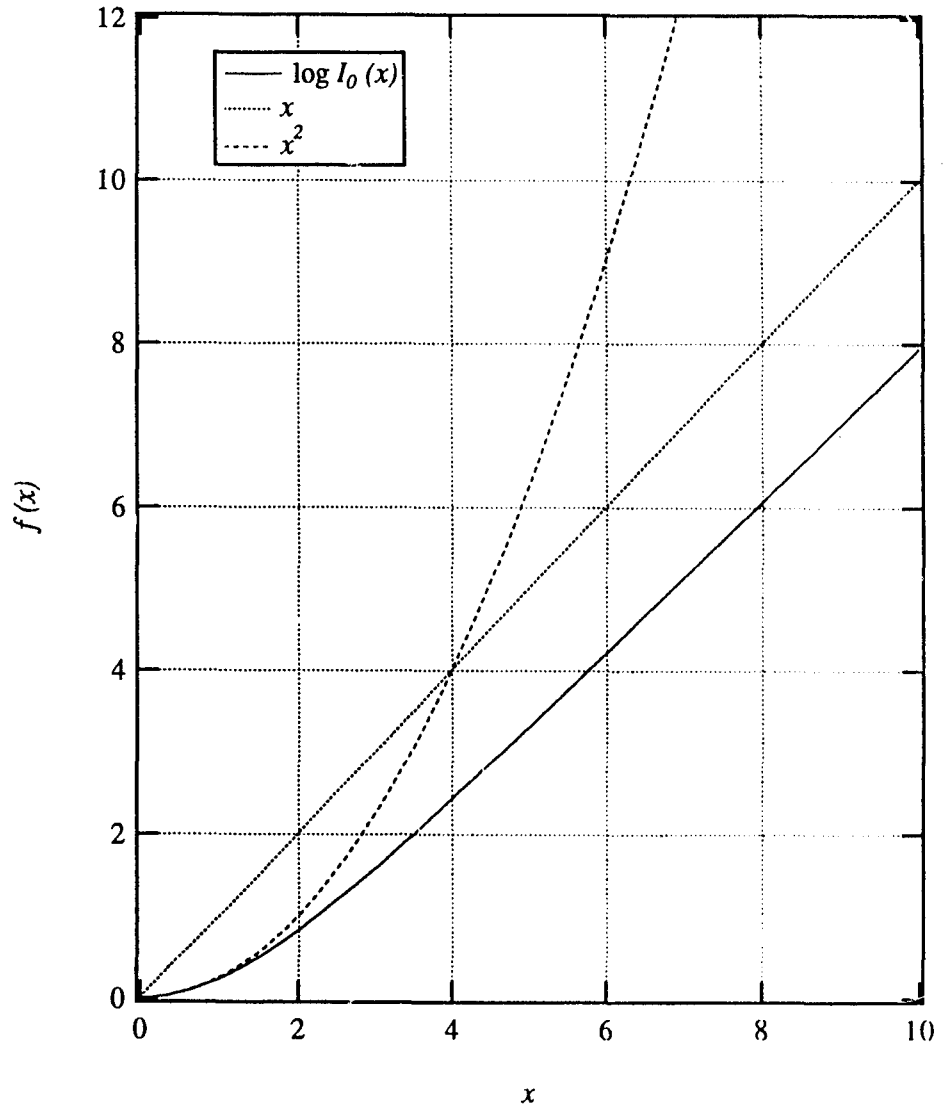

Figure 4.4: Comparison of functions $\ln I_0(x)$, x and $x^2/4$.

The BER of a system using $\ln I_0(x)$ and a system using $f(x)$ under worst case interference are shown in Figure 4.5. It can be seen that the difference of performance of two system is almost indistinguishable for both $m = 4$ and $m = 2$ cases.

If we can afford some performance loss in high signal-to-noise ratio region, then we can just use the square sum as the approximation. Therefore λ_i can be computed by

$$\begin{aligned}\lambda_i &= \frac{E_c}{N_1^2}\sum_{k=1}^{j} X_{ik}^2 + \frac{E_c}{N_0^2}\sum_{k=j+1}^{m} X_{ik}^2 \\ &= \frac{1}{2}\left(\frac{E_c}{N_1}\sum_{k=1}^{j}\frac{X_{ik}^2}{N_1/2} + \frac{E_c}{N_0}\sum_{k=j+1}^{m}\frac{X_{ik}^2}{N_0/2}\right)\end{aligned}$$

So λ_i is simply the sum of normalized samples of matched filters outputs squared with signal-to-noise ratio as weights.

It is easy to see that λ_i can be computed equivalently by

$$\lambda_i = \frac{1}{N_1^2}\sum_{k=1}^{j} X_{ik}^2 + \frac{1}{N_0^2}\sum_{k=j+1}^{m} X_{ik}^2. \tag{4.8}$$

Thus, the information required to implement optimum diversity combining is the noise variance (power) at each hop.

When N_0 is very small, or $N_0 \to 0$, the weight for a hop free of interference can be much larger than the jammed hop. If all hops corresponding to one symbol contain interference, then λ_i is simply the square sum of X_{ik}'s. This leads to the well-known soft linear combining with perfect side information (PSI).

Soft Linear Combining with PSI[22]:linearly combining the energy detector outputs of all hops free of jamming corresponding to one symbol. If all hops corresponding to one symbol have interference, linearly combining the energy detector output from these hops.

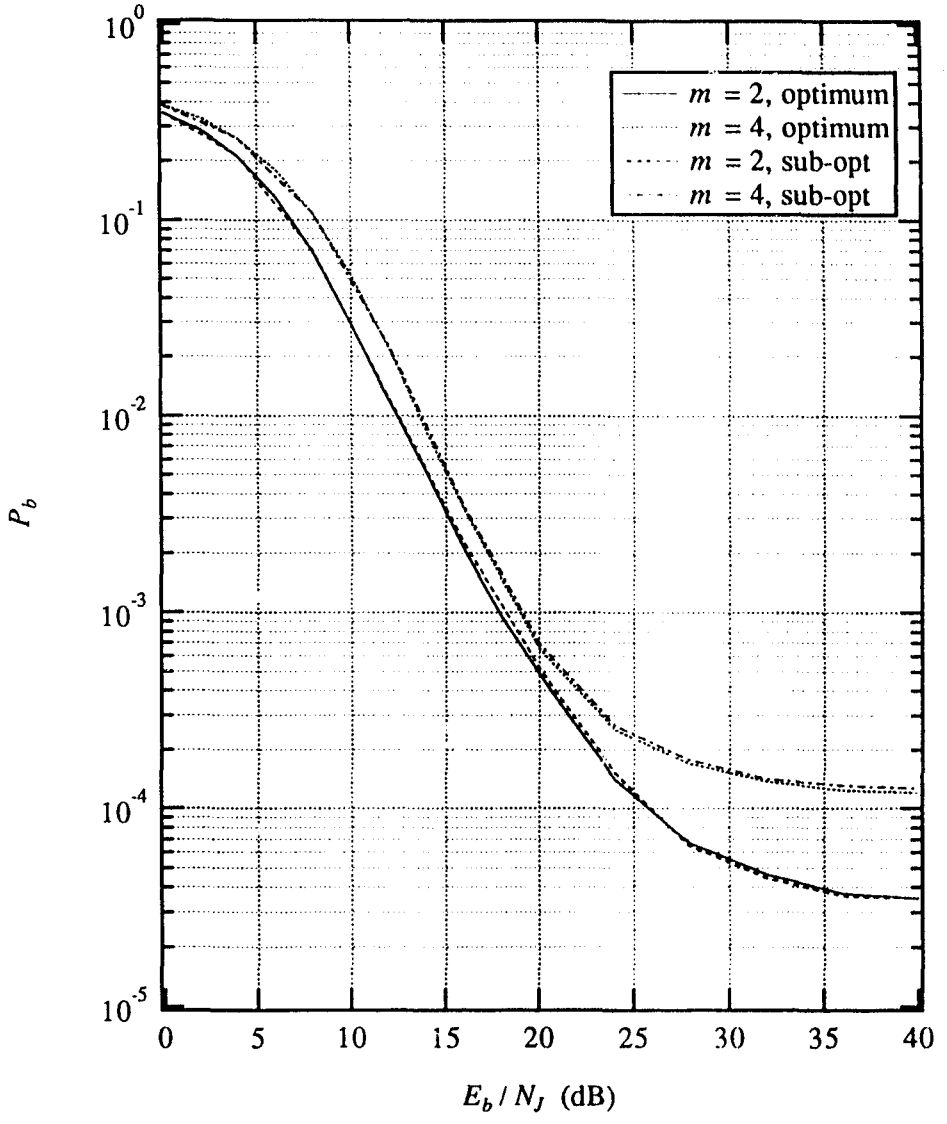

Figure 4.5: BER of FH/BFSK maximum-likelihood diversity receiver and sub-optimum diversity receiver in worst case partial band noise interference. E_b/N_0 = 13.35 dB. m = 2 and 4.

Therefore, if the background noise is negligible, the performance of Soft Linear Combining with PSI is very close to the optimum performance. Otherwise the performance is poor. This has been confirmed by our simulation results, presented in the following section, and from results given in [23]. The reason for this is that only the outputs of hops without interference are used, and some portion of the signal energy is not used, resulting in a lower effective signal-to-thermal noise ratio. For example, if L out of m hops are used, then it is equivalent to having a signal-to-thermal noise ratio of $\frac{L}{m}E_b/N_0$. If half of m hops are used, then signal-to-noise ratio is reduced by 3 dB.

Note that the weights of two summations in Eq. (4.8) are $1/N_0^2$ and $1/N_1^2$. It is quite interesting to find by simulation that the BER of a system with λ_i computed by Eq. (4.8) is almost the same as that of a system with λ_i computed by

$$\lambda_i = \frac{1}{N_1}\sum_{k=1}^{j} X_{ik}^2 + \frac{1}{N_0}\sum_{k=j+1}^{m} X_{ik}^2. \tag{4.9}$$

Note that Eq. (4.9) is just Adaptive Gain Control (AGC) combining analyzed in [8].

AGC Combining: Linear sum of the energy detector outputs which are normalized by the noise variance of each hop.

The BER of three binary FSK/FFH spread spectrum systems with λ_i computed with Eqs. (4.6), (4.8) and (4.9), respectively, are shown in Figure 4.6. It can be seen that results for λ_i from (4.8) and (4.9) are the same, and they are almost the same as the optimum performance when E_b/N_J <20 dB. Therefore, AGC combining can be viewed as the optimum diversity combining under PBN when the interference is not very weak.

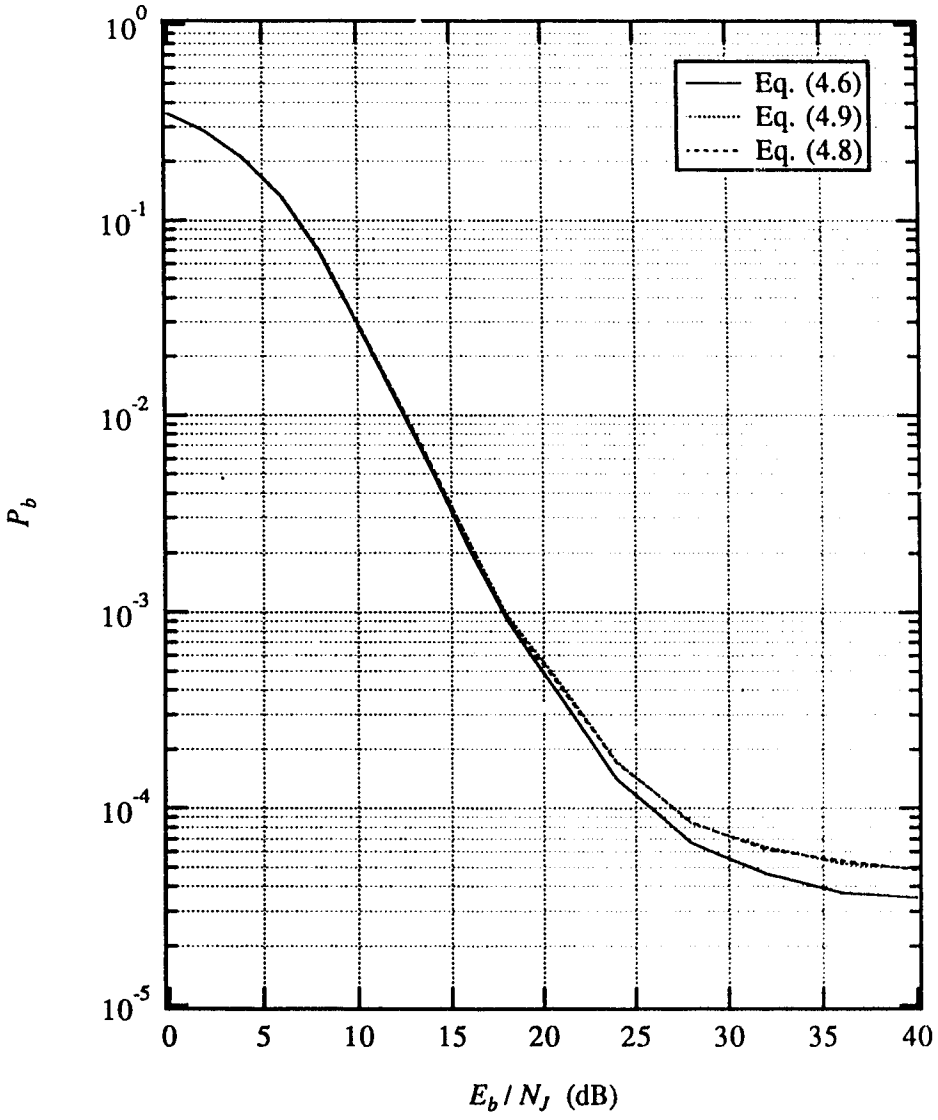

Figure 4.6: Comparison of BER of FH/BFSK with different diversity receivers in worst case partial band noise interference. $m = 2$ chips/bit. $E_b/N_0 = 13.35$ dB.

4.5 Comparison of Several Diversity Combining Schemes

In this section, performance of several diversity combining schemes are compared. Note that the BER for maximum-likelihood diversity combining can serve as the lower bound, or the best achievable performance for other schemes, which require less information to operate.

In Figure 4.7, the BER of the maximum-likelihood diversity receiver and that of the ratio-threshold, the AGC, and the self-normalizing [3] diversity combining under worst case PBN interference are plotted. The system parameters are: binary FSK, diversity order = 4 chips/bit, $E_b/N_0 = 13.35$ dB. It can be seen that at BER=10^{-3}, the optimum performance is about 3 dB better than the performance of self-normalizing combining, and 5 dB better than that of ratio-threshold combining. The performance of the equal weight square sum combining receiver (Soft Linear Energy Combining) with perfect side information is also depicted in Figure 4.7. It can be seen that when E_b/N_s is small, the performance of the equal weight square sum combining is optimum. However, when E_b/N_J is high, the performance is very poor.

Note that the noise floors for all diversity combining schemes are more than one order higher than that without diversity. This is due to the noncoherent combination loss when the jamming is weak. It can be seen that the noise floor for the linear square sum scheme is the highest, and of course, the noise floor for the optimum combining is the lowest.

In Figure 4.8, the BERs for the same group of systems with $m = 2$ are plotted. The difference between optimum diversity combining and sub-optimum diversity combining becomes large. This is because $m = 2$ chips/symbol is the optimum diversity order for optimum diversity combining while the performance of sub-optimum diversity combining for $m = 2$ is worse than that for $m = 4$ (Compare Figure 4.8 and Figure 4.7). Also note for all of the schemes noise floors are lower

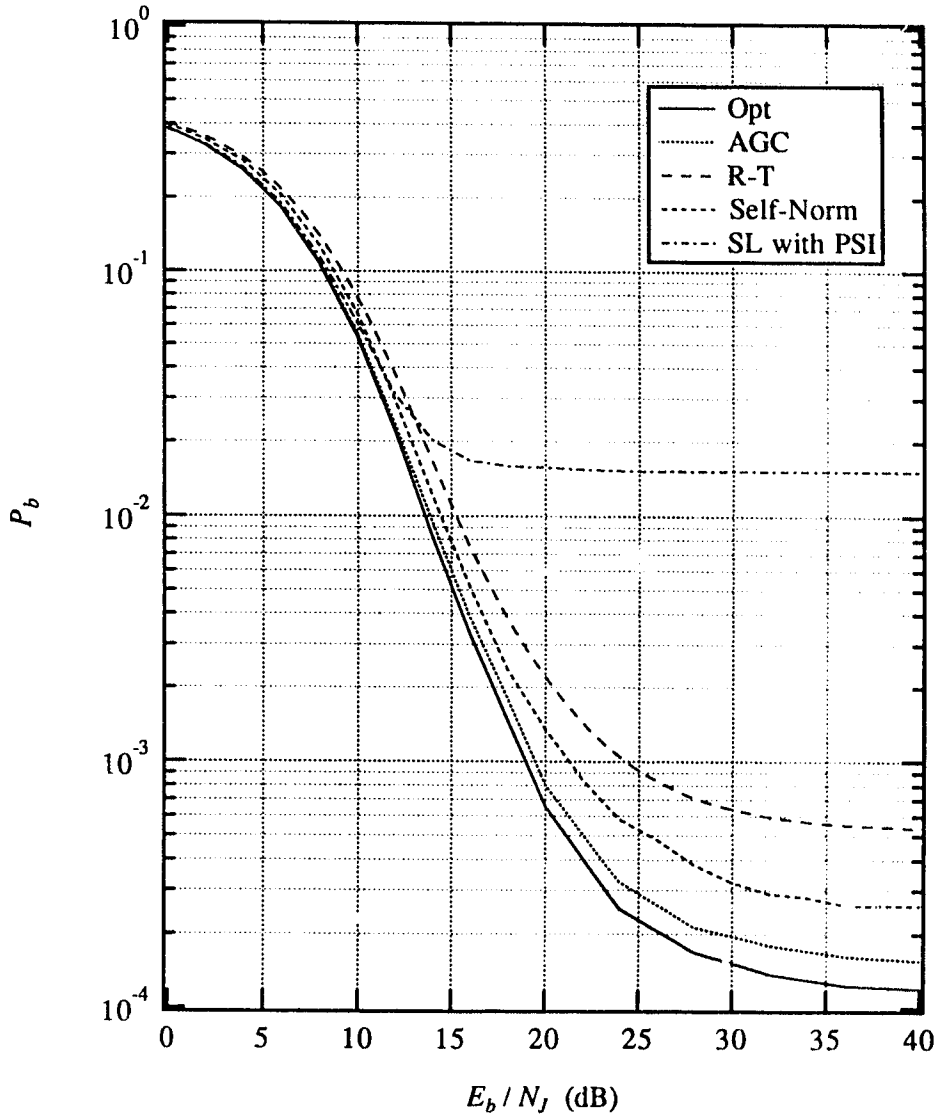

Figure 4.7: BER of FH/BFSK maximum-likelihood diversity receivers and self-normalizing diversity receiver in worst case partial band noise interference. $m = 4$ chips/bit. $E_b/N_0 = 13.35$ dB.

than that for $m = 4$. Since the largest difference between the optimum combining and the self-normalizing combining, which does not require any noise variance information, is about 7 dB, there is still some room left for possible improvement, especially for low diversity order, with a new diversity combining scheme that does not rely on channel parameters, such as N_1 and N_0.

4.6 Summary

Maximum likelihood diversity combining in PBN channel is investigated. The corresponding performance is evaluated by Monte Carlo simulation. It is shown that AGC combining can be viewed as maximum-likelihood diversity combining in PBN channel with AWGN. The performance of AGC combining can be computed numerically and is known, as shown in [8]. Therefore, the performance of AGC can be used as the optimum performance of diversity reception in PBN channel. It also has been shown that to implement maximum-likelihood diversity combining, information on noise variance at each hop is required. It is illustrated that for optimum diversity reception, the worst case PBN interference is not full-band interference for the value of E_b/N_J in the region of interest. Thus the use of diversity only is not adequate to defeat the interference completely. To restore full-band interference as the worst case interference, error correction coding must be used.

Since the knowledge of the noise variance for each hop is used to normalize the data in the optimum diversity combining, some diversity combining schemes without requirement of knowing noise variance have certain automatic normalization function. For example, the self-normalizing diversity combining uses the noncoherent matched filter outputs in one hop to estimate the noise variance and then using this estimate to normalize the corresponding data. Consider clipped linear combining and product combining schemes as other examples. The clipper function and the logarithm function are soft limit functions and the effect of the soft

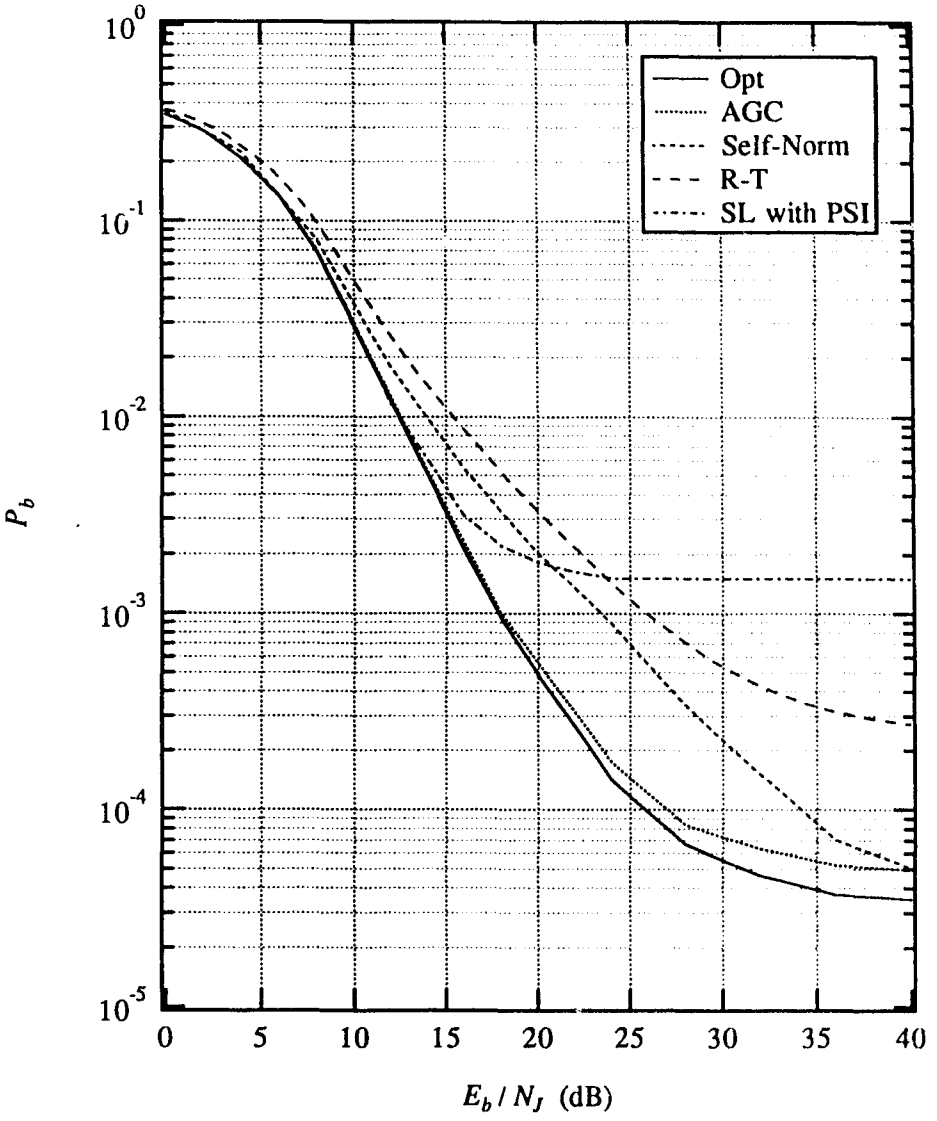

Figure 4.8: BER of FH/BFSK maximum-likelihood diversity receivers and self-normalizing diversity receiver in worst case partial band noise interference. $m = 2$ chips/bit. $E_b/N_0 = 13.35$ dB.

limit function is actually imperfect normalization. The ratio-threshold combining analyzed in the previous two chapters, however, does not belong to this category. It is in fact a scheme which implements hard decision combining with estimated side information.

Chapter 5

Repeated Convolutional Codes for High-Error-Rate Channels

5.1 Introduction

In this chapter, we consider error-correction schemes that can correct errors at the output of a high-error-rate channel. Such a large channel error rate may result from the presense of strong interference or jamming. Conventional error-correction schemes, such as the widely used constraint-length-7, rate-1/2 binary convolutional code due to Odenwalder[24], which is an international standard[25], may fail in such situations. It is clear that a low-rate code must be used for such a channel by considering the channel capacity or cutoff rate.

Kasami, *et al* have considered a cascaded coding scheme for a binary symmetric channel (BSC) with a large error probability p_e [26]. Their scheme consists of two linear block codes. The inner code (closer to the channel) is a binary code and the outer code is a Reed-Solomon (RS) code. The parameters of the inner and outer codes have to be properly chosen to match each other in order to obtain good performance. It turns out that for a large p_e whether a coding scheme works or not is very sensitive to p_e. For example, in [26], a scheme that consists of a (63,31) RS outer code and a (32, 6) biorthogonal inner code works well at $p_e = 0.2$ but will not work at $p_e = 0.3$. The sensitivity to the values of p_e and the somewhat rigid

structure of the cascaded scheme implies that we should know p_e before designing a coding scheme. Also, two encoder/decoder systems are needed for a cascaded scheme. In a jamming environment, however, it is hardly possible to predict p_e. Thus, a system that can easily adapt to the actual p_e would be desirable.

In 1977, Shaft searched low-rate convolutional codes and considered their use to combat burst interference[27]. Use of repeated convolutional codes seemed to be favored. In 1985, Chase proposed the scheme again for the BSC with well-made arguments[28]. To show that repeated binary convolutional codes are near optimum, both Shaft and Chase compared their free distances with Heller's bound for binary convolutional codes[29]. Chase also made a comparison of code rates with the channel capacity of the BSC.

Nevertheless, there are still some practical problems that need to be addressed. For instance, for the BSC, if each code symbol is repeated m times, maximum likelihood decoding requires $m + 1$ levels of quantization. Since m can be very large for a high channel error rate and practical convolutional decoders have a finite, and likely a smaller number of quantization levels, what is the corresponding performance degradation? Further, can we use a repeated binary convolutional code for an M-ary symmetric channel (MSC), and what is the best way to generate a binary decoding metric for use in the binary decoder? This question is motivated by the fact that there are commercially available high speed binary codecs, and considerable efforts are being made to further improve the speed and reduce the cost of such codecs.

In this chapter, we consider repeated convolutional codes for an MSC (with the BSC as a special case) with a large error probability p_e. The value of p_e can be near, but smaller than, $1 - 1/M$ for which the channel capacity is zero. In Section 5.2, we focus on the BSC and begin with a conventional analysis based on the union bound for the BSC. For large m, the central limit theorem is applied to provide another analytical tool. In Section 5.3, Monte Carlo simulation results for the BSC are provided and compared with theoretical analyses. The quantization

effect is shown. Based on these results, we compare the code rates of repeated convolutional code with the channel cutoff rate. In Section 5.4 we consider the use of a binary code over an MSC. The emphasis is placed on the methods to generate binary decoding metrics and on their performances.

5.2 Theoretical Analysis for the BSC

We are particularly interested in the above mentioned Odenwalder rate-1/2, constraint-length-7 convolutional code. The single-chip encoder/Viterbi decoder is commercially available at a low price from several sources. The decoder normally has up to eight levels of quantization. We consider Viterbi decoding, which is maximum likelihood decoding when infinite quantization is assumed. Each M-ary channel symbol is repeated m times. We call m the repetition order.

For the BSC case, each encoded symbol is repeated m times over a BSC. The BSC is assumed to have a large error probability (transition probability) p_e which is in the neighborhood of 0.1 or higher, but of course, smaller than 0.5. The BSC is a good channel model for some anti-jam communication systems with complex demultiplexing between the demodulator and the decoder. In such a situation, the decoder has to cope with a hard-decision channel, and explicit and/or implicit interleaving/deinterleaving makes the errors random. One example of possible implicit interleaving/deinterleaving is a multiplexed multi-user system where each user has a decoder after demultiplexing.

It is clear that for two trellis paths at Hamming distance d, the repetition of order m increases the distance to $d \times m$. It is well known that the decoder output bit error rate (BER) P_b can be upperbounded by an exponentially tight union bound. Specifically, suppose P_d is the pairwise error probability of two trellis paths with Hamming distance d, then

$$P_b < \sum_{d=d_{free}}^{\infty} C_d P_{dm} \tag{5.1}$$

where d_{free} is the free distance of the convolutional code and C_d is the total number of information bit errors when pairwise errors between paths with Hamming distance d occur. For the Odenwalder code, C_d is nonzero only for even d and $d \geq 10$, since $d_{free} = 10$. Over the BSC, for an even d,

$$P_d = \frac{1}{2}\binom{d}{d/2} p_e^{d/2}(1-p_e)^{d/2} + \sum_{i=d/2+1}^{d} \binom{d}{i} p_e^i (1-p_e)^{d-i}. \qquad (5.2)$$

C_d can be found by expanding the transfer function of the convolutional code or using computer search through the trellis of the code. For the Odenwalder code, the first nine terms are[1, page 148]: $C_{10} = 36$, $C_{12} = 211$, $C_{14} = 1,404$, $C_{16} = 11,633$, $C_{18} = 77,433$, $C_{20} = 502,690$, $C_{22} = 3,322,763$, $C_{24} = 21,292,910$, and $C_{26} = 134,365,911$.

Using Equations (5.1) and (5.2) for $m = 3$, 7, and 15, respectively, P_b is plotted versus p_e for the Odenwalder code in Figure 5.1 using the first term, the first four terms, and the first nine terms of C_d, respectively. It can be seen from the figure that nine terms of the transfer function provide a sufficiently accurate bound, especially at a low P_b. The results using the first nine terms are used in the rest of the paper. In fact, it has been known that the union bound provides an accurate approximation for a low P_b provided enough quantization levels are available to facilitate the maximum likelihood decoding (MLD). For MLD it is well known that the decoding metric should be

$$mt_k = \sum_{i=1}^{m} r_{ki} \qquad (5.3)$$

where r_{ki} is the received i-th repeated symbol (0 or 1) over the BSC for the k-th convolutional encoded symbol. Here $mt_k = 0$ means that the k-th encoded symbol is most likely a 0 and $mt_k = m$ means that the k-th encoded symbol is most likely a 1. For eight levels of quantization from 0 to 7 (where 0 represents the most reliable logic 0 and 7 represents the most reliable logic 1), uniform quantization is

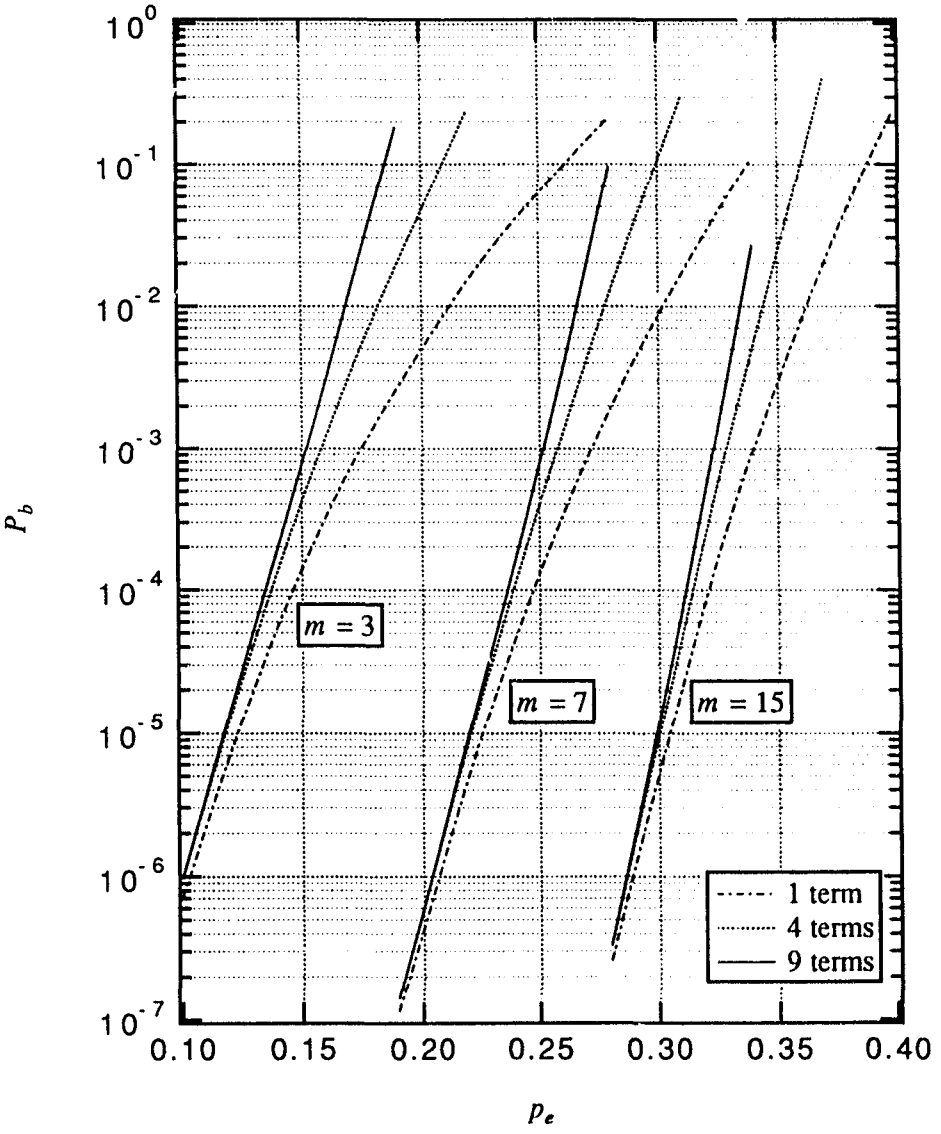

Figure 5.1: Union bounds for the repeated Odenwalder code over the BSC using the first term, the first four terms, and the first nine terms of the transfer function, respectively, for $m = 3$, 7, and 15.

natural and reasonable. Then, the above metric is modified as

$$mt_k = \lfloor \frac{\sum_{i=1}^{i=m} r_{ki}}{m} \times 7 + 0.5 \rfloor \tag{5.4}$$

where $\lfloor x \rfloor$ is the largest integer not exceeding x.

As mentioned earlier, the repetition order m must be large in order to correct the errors with a large probability p_e. For a large m we may apply the central limit theorem or the Gaussian approximation of the binomial probability distribution. Consider the following metric which is equivalent to Equation (5.3)

$$\alpha_k = \frac{\sum_{i=1}^{i=m}(-1)^{r_{ki}}}{m}. \tag{5.5}$$

Note that $(-1)^{r_{ki}}$ has a mean of $E = 1 - 2p_e$ $(= (1 - p_e) \times 1 + p_e \times (-1))$ if the k-th encoded symbol is a 0, and a mean of $E = -(1 - 2p_e)$ if the k-th encoded symbol is a 1. The variance is

$$\sigma^2 = [1 - (1 - 2p_e)]^2(1 - p_e) + [-1 - (1 - 2p_e)]^2 p_e = 4p_e(1 - p_e). \tag{5.6}$$

By use of the central limit theorem (see, e.g. [19, page 667]), we know that

$$\beta_k = \frac{\sum_{i=1}^{i=m}[(-1)^{r_{ki}} - E]}{\sqrt{m}} \tag{5.7}$$

is a zero-mean Gaussian random variable with variance σ^2 when $m \to \infty$ (or m is very large). Since

$$\alpha_k = \frac{1}{\sqrt{m}}[\frac{\sum_{i=1}^{i=m}(-1)^{r_{ki}}}{\sqrt{m}}] = \frac{1}{\sqrt{m}}[\frac{[\sum_{i=1}^{i=m}[(-1)^{r_{ki}} - E)] + mE}{\sqrt{m}}] = \frac{\beta_k}{\sqrt{m}} + E \tag{5.8}$$

then, for a large m, α_k is also a Gaussian random variable with a mean of E and a variance of

$$\sigma_\alpha^2 = \frac{4p_e(1 - p_e)}{m}. \tag{5.9}$$

Thus, for a sufficiently large m, the variance can be reduced to an arbitrarily small number. Compared with coherently demodulated BPSK in AWGN with noise spectral density N_0[30], the asymptotical Gaussian distribution of α_k implies an effective symbol energy (half of the bit energy for the rate-1/2 code) of $E_s' = (1-2p_e)^2$ and an effective noise spectral density of $N_0'/2 = \sigma_\alpha^2$, i.e.,

$$E_s'/N_0' = \frac{(1-2p_e)^2}{8p_e(1-p_e)}m. \tag{5.10}$$

Note that the effective signal-to-noise ratio is proportional to the diversity order m. Since the simulated or measured BER curve for the Odenwalder code is well known (see, e.g. [31]), for a large m and a given p_e, we can use Equation (5.10) to determine the required E_s'/N_0', and thus the m required to sustain a required P_b. Even for a small m, the Gaussian approximation can be used to estimate the required m, and then it can be adjusted from there.

Since the simulated or measured BER curves for the Odenwalder code take into account the finite levels of quantization and other practical constraints such as a finite trellis length, these factors are also included in the BER curves of the repeated convolutional code if the Gaussian approximation is used. In other words, for a large m performance degradations due to finite quantization, etc., will be about the same as what we have known for convolutional-coded coherent BPSK in AWGN.

In Figure 5.2, P_b, obtained from the Gaussian approximation, versus p_e is given for $m = 3$, 7, 15, and 31, respectively. For $m > 7$, eight levels of quantization and trellis length 84 are assumed. This trellis length is considered instead of five or six times the constraint length because 84 or so has been used in commercial realizations in order to accommodate the punctured rate 3/4 code[25]. For $m \leq 7$, MLD decoding is assumed since it can be implemented with eight levels of quantization. In this case, the interest is to see the approximation error of the Gaussian approximation. For comparison, the results based on the union bound are also given in Figure 5.2.

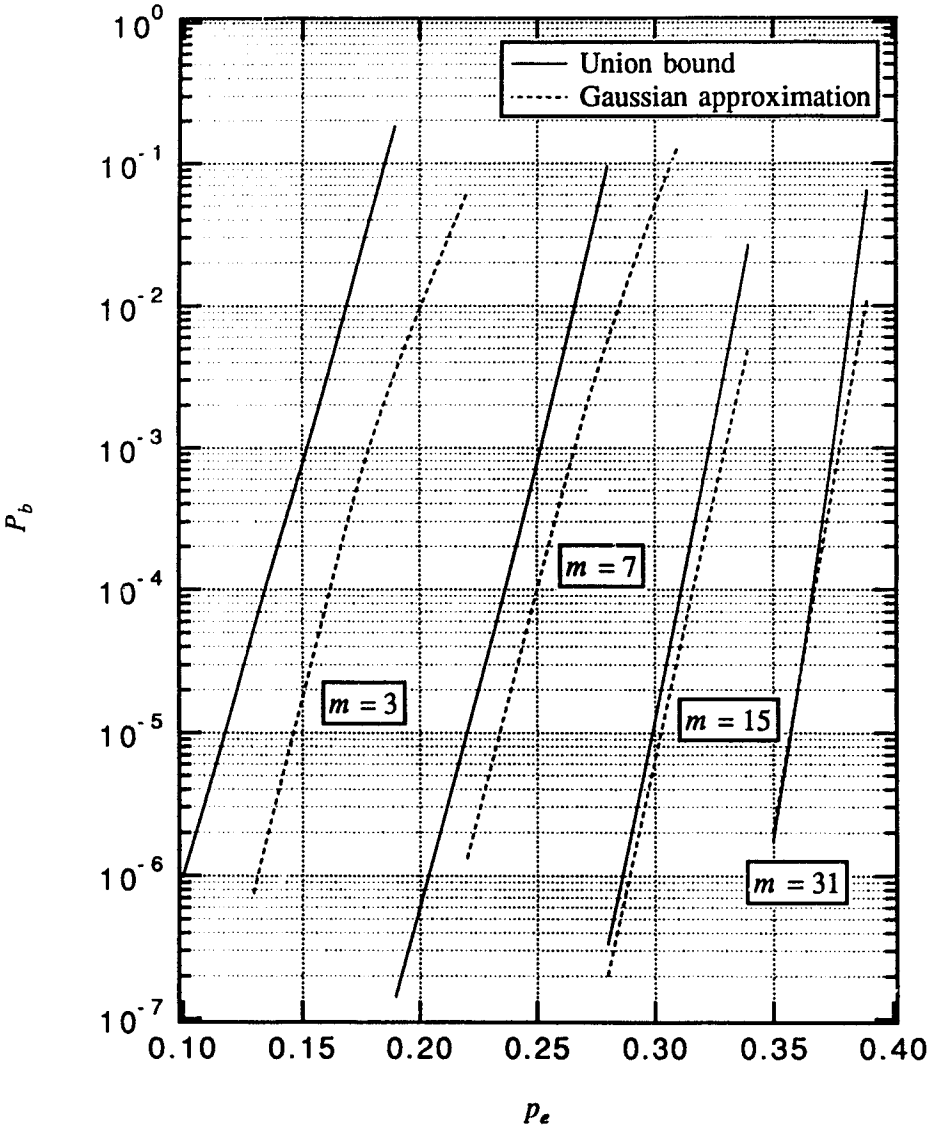

Figure 5.2: BER based on the Gaussian approximation and the union bound for the repeated Odenwalder code over the BSC. $m = 3$, 7, 15, and 31.

It can be seen from the figure that for a small m the Gaussian approximation results in a lower BER. For a reasonably large m (e.g., $m \geq 15$) the Gaussian approximation seems to be fairly accurate, which needs to be verified by simulation. It is also noted that for $m = 31$, the BER obtained from the Gaussian approximation is slightly higher than the union bound. The basic reason for this difference is that for the union bound, ideal maximum likelihood decoding is assumed, i.e., no quantization and infinite trellis length, while for the Gaussian approximation curve, practical constraints have been taken into account.

5.3 Computational Results for the BSC

In order to verify the BER performance, Monte Carlo simulations have been performed. A trellis length of 84 and eight levels of quantization are assumed and Equation (5.4) is used to generate the metrics for various value of m. Figure 5.3 shows the simulated P_b versus p_e performances for $m = 3$, 5, 7, 15, and 31, respectively. Union bounds and the Gaussian approximation are also shown for comparison.

It can be seen from the figure that for $m < 8$ the union bound, which assumes the MLD, is almost exact. Note that for $m = 3$, we have metrics of 0, 2, 5, and 7, which means that we are not doing exactly MLD. This applies to the $m = 5$ case as well. But the performance degradation is insignificant. For a large m, the Gaussian approximation is fairly close to the simulation results. Note that finite quantization results in a higher BER that is not upperbounded by the union bound, and in fact, the Gaussian approximation is more accurate than the union bound at a high BER.

For $m = 5$, the overall code rate is 0.1, which is slightly higher than the rate, 0.092, of the coding scheme considered in [26] with comparable BER performance. In consideration of its simplicity, the repeated Odenwalder code is favored.

Figure 5.4 shows the cutoff rate R_0 for the BSC[19, pages 632 - 633] and the

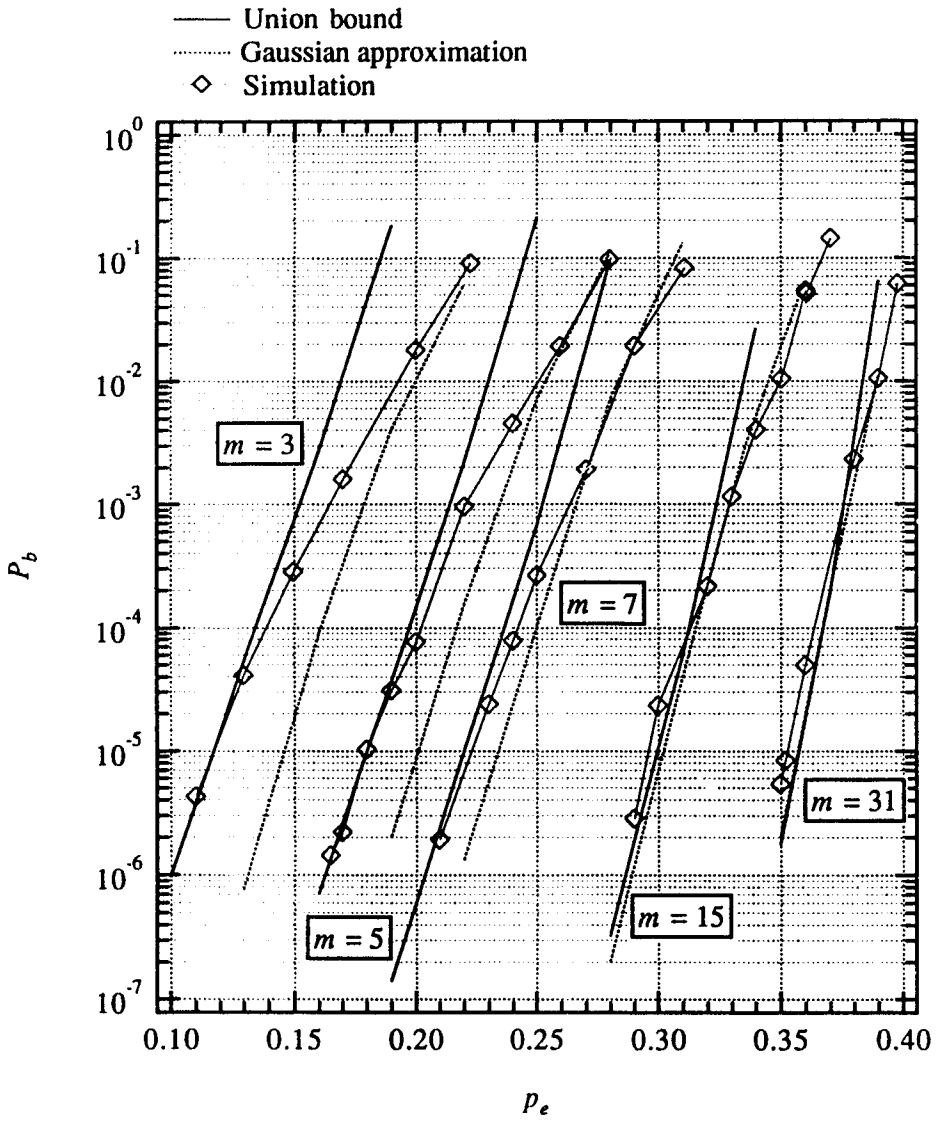

Figure 5.3: BER based on simulation, the union bound, and the Gaussian approximation for the repeated Odenwalder code over the BSC. m = 3, 5, 7, 15, and 31.

overall code rate $r = \frac{1}{2m}$ to sustain $P_b = 10^{-4}$ (based on the simulated BER), which was also used in [28]. From this figure, it seems that r moves closer to R_0 as p_e increases. But from the r/R_0 versus p_e curve shown in Figure 5.5, r decreases faster than R_0 as p_e increases. Nevertheless, it is interesting to note that the deviation between r and R_0 is bounded: as p_e approaches 0.5, r approaches $0.6R_0$. If compared to the channel capacity, r is near 30 percent of channel capacity. In conclusion, the repeated Odenwalder code can achieve more than one half of what is promised by the cutoff rate even for very large p_e, say, 0.3 to 0.5.

5.4 M-ary Symmetric Channel

In this section, we consider the M-ary symmetric channel (MSC) with high symbol error probability, which is illustrated in Figure 5.6. Here p_e is the symbol error probability, which is near $1 - \frac{1}{M}$, but smaller than it. Again, the coding scheme consists of an outer convolutional code and an inner repetition code where each M-ary channel symbol is repeated m times. This MSC model directly reflects a hard-decision demodulated fast frequency hopped M-ary FSK (FFH/MFSK) system where the repetition is inherent in the system. Here we are especially interested in $M = 4$ and 8. Previous work has shown that under certain conditions this type of a system represents a good compromise in order to combat both partial-band noise jamming and multitone jamming [1]. As mentioned earlier, the hard decisions may be due to complex demultiplexing between the demodulator and decoder. We first consider a Trumpis code[32] as the outer code, since it is optimum for an M-ary orthogonal channel. The 4-ary and 8-ary $R = 1$ bit/channel symbol Trumpis codes with constraint length 7 are considered. These codes have the same implementation complexity as the Odenwalder code because they have the same constraint length. In view of commercially available binary codecs, we then consider the possible use of the constraint length $K = 7$, rate $R = \frac{1}{2}$ Odenwalder code for the MSC. The emphasis is placed on how to generate binary decoding metrics.

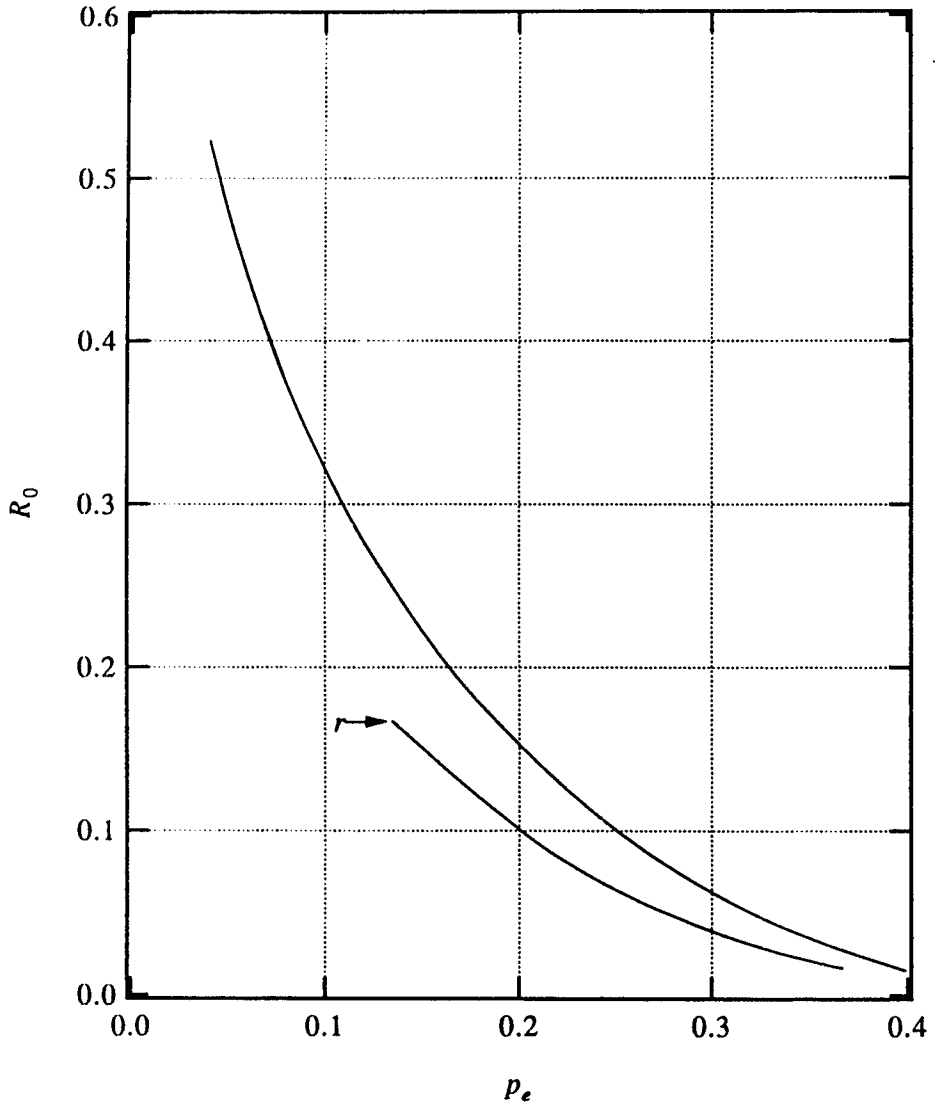

Figure 5.4: Comparison of the cutoff rate R_0 of the BSC and the overall code rate r of the repeated Odenwalder code over the BSC to sustain $P_b = 10^{-4}$.

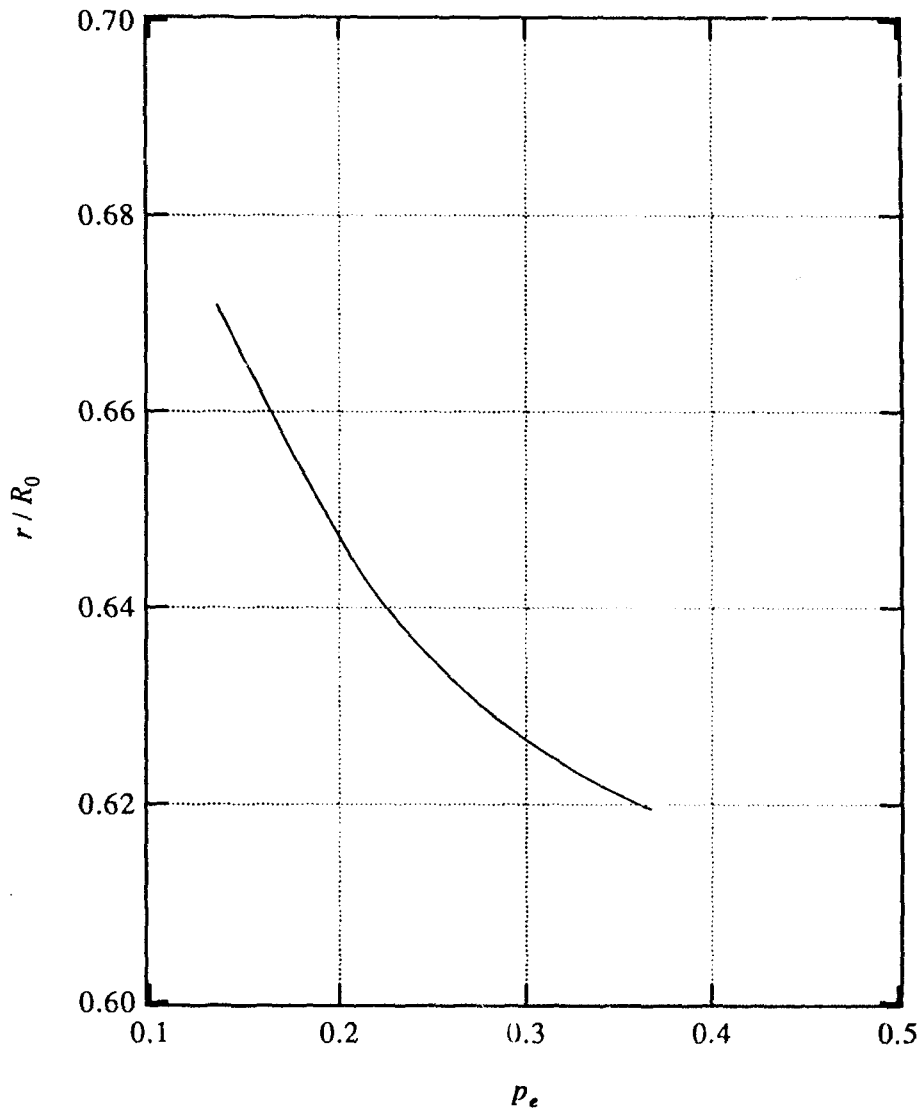

Figure 5.5: Ratio of the overall code rate r of the repeated Odenwalder code over the BSC to sustain $P_b = 10^{-4}$ to the cutoff rate R_0 of the BSC.

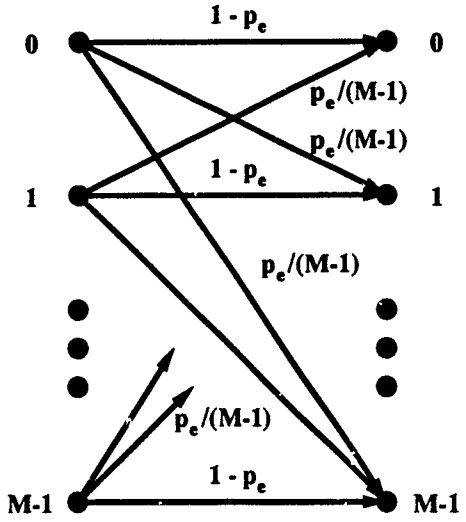

Figure 5.6: Model of M-ary Symmetric Channel

5.4.1 M-ary Metric

For the Trumpis codes, it is known that the union bound of the decoder output BER, P_b, is [32]

$$P_b \leq 7P_{7m}+39P_{8m}+104P_{9m}+352P_{10,m}+1187P_{11m}+\cdots \text{ for 4-ary channels} \quad (5.11)$$

and

$$P_b \leq P_{7m}+4P_{8m}+8P_{9m}+49P_{10m}+92P_{11m}+\cdots \text{ for 8-ary channels} \quad (5.12)$$

where P_d is the pairwise error probability between two trellis paths with Hamming distance d.

To consider the use of the Odenwalder code over a 4-ary symmetric channel (4SC), the most natural way is as follows. Recall that the encoder of the rate 1/2 code generates a pair of encoded bits at the encoder output for each incoming information bit. This pair of encoded bits can be considered as a 4-ary symbol and transmitted m times over the 4SC. In decoding, ideally, two encoded bits corresponding to one trellis branch are assigned a 4-ary metric. This assumes that the decoder can accommodate 4-ary metrics. Using a trellis search algorithm, we

found the union bound of the decoder output BER, P_b, as

$$\begin{aligned} P_b \leq\ & P_{6m} + 10P_{7m} + 38P_{8m} + 92P_{9m} + 355P_{10m} + 1440P_{11m} \\ & + 4684P_{12m} + 16043P_{13m} + 52240P_{14m} + 170679P_{15m} + \cdots \end{aligned} \quad (5.13)$$

Note that the Trumpis codes are optimum over the MSC in the sense that they have the largest M-ary free Hamming distance (7 for the 4-ary code) and fewest number of information bit errors due to path errors at the free distance. The Odenwalder code is not optimum for the 4SC. Its free 4-ary Hamming distance is 6, which is one less than the optimum Trumpis code. But the number of information bit errors due to an incorrect trellis path at the free distance is only one. Thus, we may expect that the Odenwalder code will have near-optimum BER performance.

The use of the Odenwalder code over 8-ary symmetric channels (8SC) is similar. The encoder of the rate-1/2 code generates three pairs of encoded bits for every three incoming information bits. Then, the first pair of encoded bits and one bit of the second pair of encoded bits are considered as an 8-ary symbol. The other bit of the second pair and the third pair are considered as another 8-ary symbol. Each of these 8-ary symbols is transmitted over the 8SC m times. At the decoder, an 8-ary metric is assigned to the three encoded bits corresponding to one and a half trellis branches. Of course, it is assumed that the decoder can accommodate an 8-ary metrics. We found the union bound of this kind of decoder output BER as

$$\begin{aligned} P_b \leq\ & 3P_{5m} + 28P_{6m} + 83P_{7m} + 649P_{8m} + 2419P_{9m} + 10295P_{10m} \\ & + 45175P_{11m} + 193378P_{12m} + \cdots \end{aligned} \quad (5.14)$$

By comparing with (5.12), we find the Odenwalder code is not bad over the 8SC. The 8-ary free Hamming distance is 7 for the rate-1/3 Trumpis code and 5 for the rate-1/2 Odenwalder code.

For the MSC with a repeated M-ary code, the maximum likelihood decoding metric for each M-ary symbol is the Hamming distance between the sequence of

m repeated symbols and the corresponding received symbol sequence of length m. Here it is implied that for an M-ary symbol, a smaller metric is more favorable in that the M-ary symbol is more likely to be transmitted. This MLD metric is an M-ary metric in the sense that there are a total of M metrics for all M M-ary symbols.

For the MLD, we can find the pairwise error probability between two paths with Hamming distance d, P_d. Recall that P_d is the probability of a specific trellis path at Hamming distance d having a more favorable path metric than the correct path, given a correct transmitted trellis path. Consider one symbol period where there is a symbol difference in the two paths. The correct symbol is called c, and the symbol from the incorrect path is called e. Because $M > 2$, the MSC output can be neither c nor e. In fact, the probability of the channel output being c or e, denoted as p_{ce}, is given by

$$p_{ce} = 1 - p_e + \frac{p_e}{M-1}.$$

Then, over d symbol periods where two paths have different symbols, there can be j $(0 \leq j \leq d)$ periods where the channel output is neither c nor e and hence no contribution can be made to the metrics for either c or e. We can calculate a conditional pairwise error probability $P'_d(j)$ over the remaining $d-j$ symbols where the channel output must be either c or e with probabilities (which are conditional probabilities under the condition that the channel output must be either c or e) of $\frac{1-p_e}{p_{ce}}$ and $\frac{p_e}{p_{ce}(M-1)}$, respectively. Specifically, we have

$$P'_d(j) = \sum_{i=\lceil \frac{d-j}{2} \rceil}^{d-j} (1 - 0.5\delta(i - \frac{d-j}{2})) \binom{d-j}{i} \left(\frac{p_e}{(M-1)p_{ce}}\right)^i \left(\frac{1-p_e}{p_{ce}}\right)^{d-j-i} \tag{5.15}$$

where $\lceil x \rceil$ is the smallest integer greater than or equal to x, and

$$\delta(x) = \begin{cases} 1 & \text{if } x = 0; \\ 0 & \text{otherwise.} \end{cases}$$

In fact, the δ function is equal to 1 (so that $1 - 0.5\delta = 0.5$) only if $d - j$ is even and $i = \frac{d-j}{2}$. Otherwise the δ function is 0 and $1 - 0.5\delta = 1$. The probability that j of d channel output symbols are neither c nor e is

$$P(j,d) = \binom{d}{j} p_{ce}^{d-j}(1-p_{ce})^j. \tag{5.16}$$

Therefore, the pairwise error probability is

$$\begin{aligned} P_d &= \sum_{j=0}^{d} P(j,d)P'_d(j) \\ &= \sum_{j=0}^{d} \binom{d}{j} p_{ce}^{d-j}(1-p_{ce})^j \times \\ &\quad \times \sum_{i=\lceil \frac{d-j}{2} \rceil}^{d-j} (1 - 0.5\delta(i - \frac{d-j}{2})) \binom{d-j}{i} \left(\frac{p_e}{p_{ce}(M-1)}\right)^i \left(\frac{1-p_e}{p_{ce}}\right)^{d-j-i}. \end{aligned}$$

There is a factor p_{ce}^{d-j} in the inner summation and it can be canceled with the one outside. So finally we get

$$\begin{aligned} P_d &= \sum_{j=0}^{d} \binom{d}{j} \left(\frac{M-2}{M-1} p_e\right)^j \\ &\quad \times \sum_{i=\lceil \frac{d-j}{2} \rceil}^{d-j} (1 - 0.5\delta(i - \frac{d-j}{2})) \binom{d-j}{i} \left(\frac{p_e}{M-1}\right)^i (1-p_e)^{d-j-i}. \end{aligned} \tag{5.17}$$

Using Equations (5.11), (5.13) and (5.17) for m = 3,7,15, and 31, the bound of P_b versus p_e is plotted for the Trumpis and Odenwalder codes with M-ary MLD metric and a 4-ary channel in Figure 5.7. From this figure, we can see that the Trumpis code is indeed better. However, it is interesting to note that the performance of the Odenwalder code is only slightly inferior to that of the Trumpis code. This is the basis for considering the use of the Odenwalder code over the 4-ary channel.

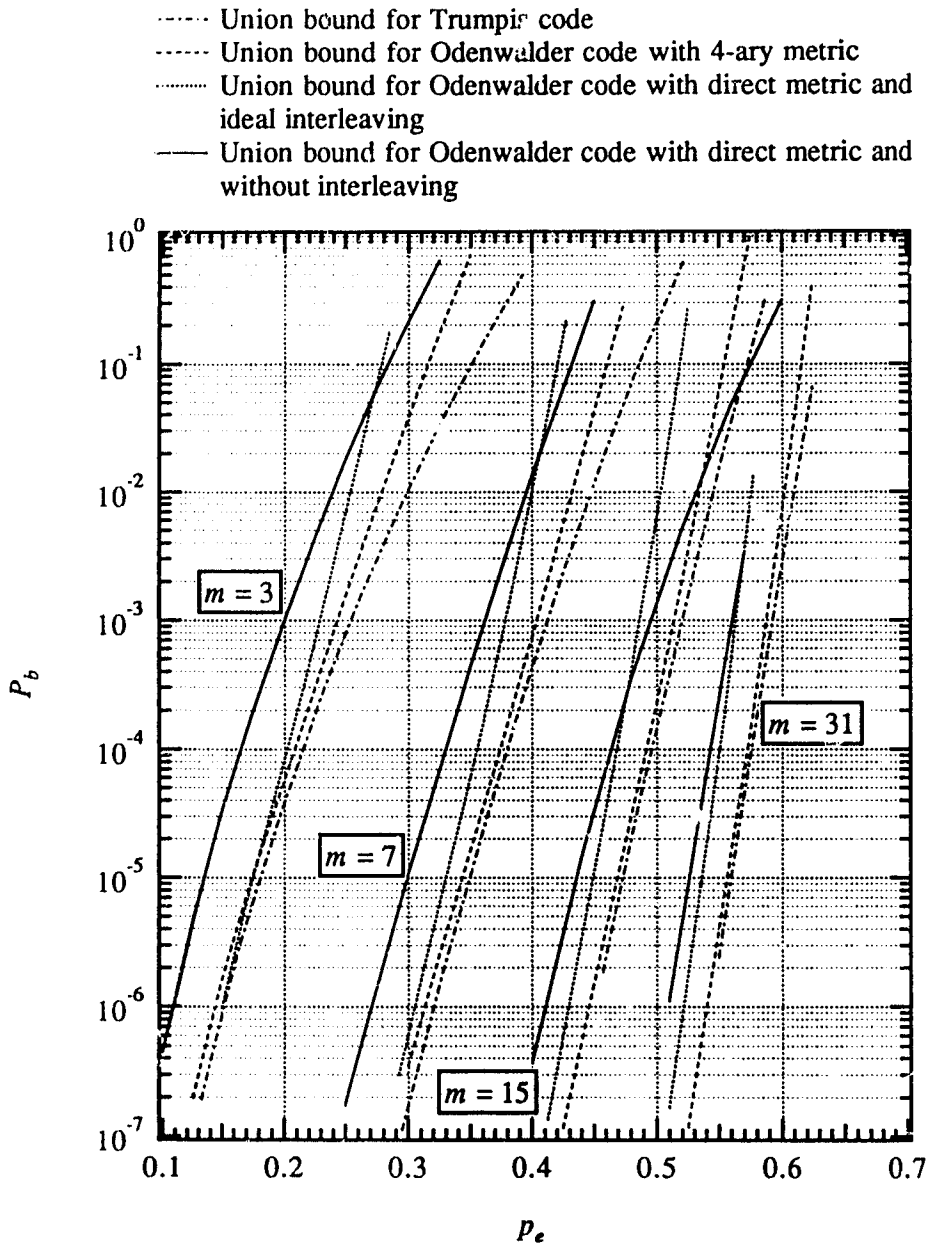

Figure 5.7: Union bounds for the repeated Trumpis and Odenwalder codes with three kinds of metrics over 4-ary symmetric channels. m=3,7,15, and 31.

Using Equations (5.12), (5.14) and (5.17) for m = 3,7,15, and 31, the bound of P_b for an 8-ary channel is plotted in Figure 5.8. It appears that the performance of the Trumpis code is much better than that of the Odenwalder code in the 8-ary case. But recall that the 8-ary Trumpis code is a rate-1/3 code. So the code rate of this Trumpis code is only two thirds of the code rate of the Odenwalder code. So the direct comparison in Figure 5.8 is not fair.

Since the total code rates of the repeated Trumpis and Odenwalder codes are $\frac{1}{3m}$ and $\frac{1}{2m}$, respectively, if the repetition order for the Odenwalder code is chosen to be 50 percent larger than that for the Trumpis code, the code rates for both repeated codes are the same. Then comparison can be made. So the union bounds of P_b for the Odenwalder code with m = 5, 11, 23, and 47 and with m = 4, 10, 22, and 46 are plotted in Figure 5.9. The bounds of P_b for the Trumpis code with m = 3,7,15, and 31 are also plotted in Figure 5.9. The corresponding code rates of the three groups are almost the same, but code rates of the Odenwalder code with m = 5,11,23, and 47 are a little bit lower than that of the Trumpis code, and code rates of the Odenwalder code with m=4,10, 22 and 46 are a little bit higher.

From Figure 5.9, we can see that for a BER less than 10^{-4}, the curve for the Trumpis code is between the two curves for the Odenwalder code. Considering the two curves corresponding to the Odenwalder code with a higher and a lower code rate, respectively, we can see that the repeated Odenwalder code has almost the same performance as the repeated Trumpis code at the same overall code rate. Therefore, the same conclusion as in 4-ary channel can be drawn that the performance of the Odenwalder code is only slightly inferior to that of the Trumpis code. Because the comparison is based on the union bounds, which are quite loose at high BERs, and the number of terms used in computing those union bounds are different, our comparisons are only made at low BERs.

Note that the union bound for the Odenwalder code is based on the assumption that the decoder can accommodate M-ary metrics for the MLD. This is generally not the case if we want to use commercially available decoding chips directly. In

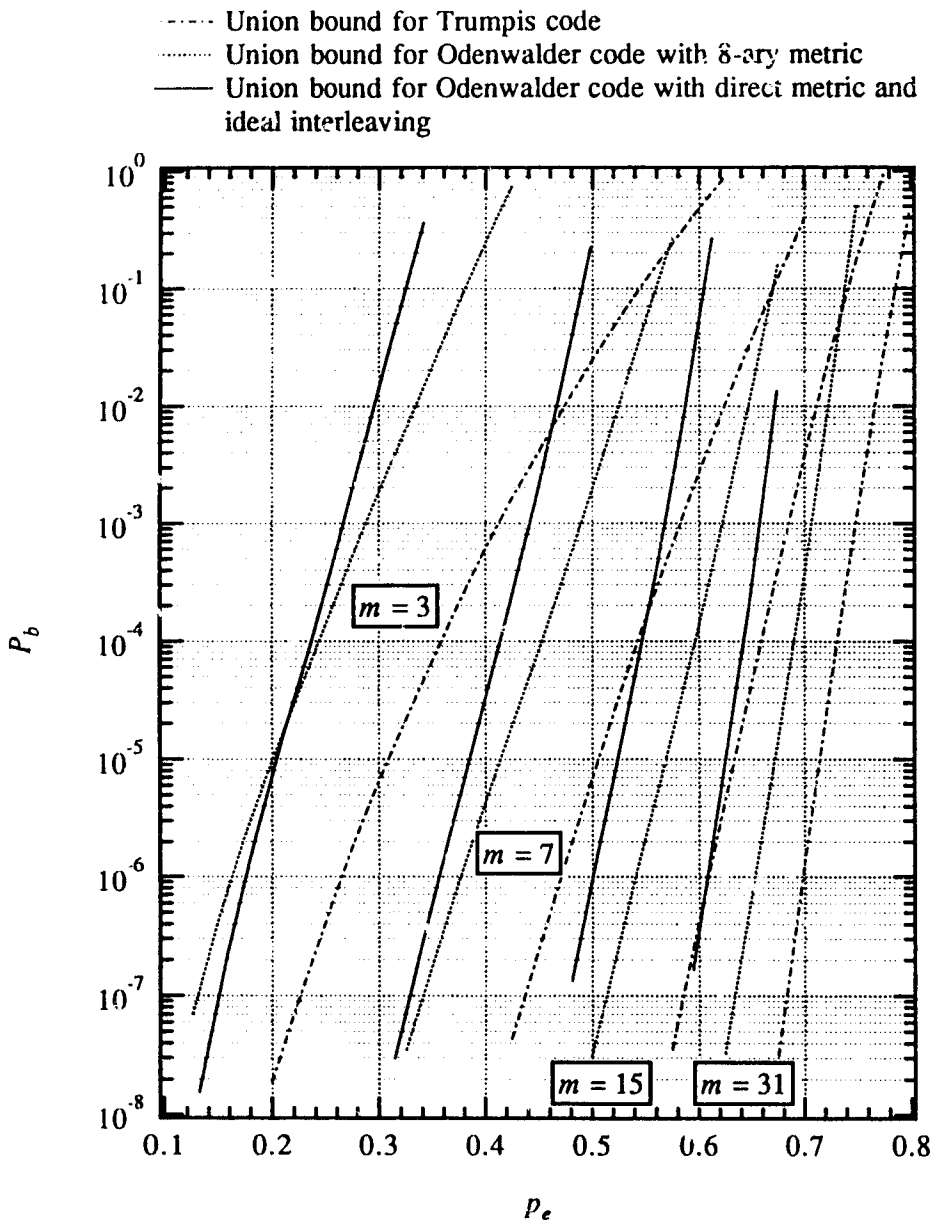

Figure 5.8: Union bounds for the repeated Trumpis and Odenwalder codes with two kinds of metrics over 8-ary symmetric channels. m=3,7,15, and 31.

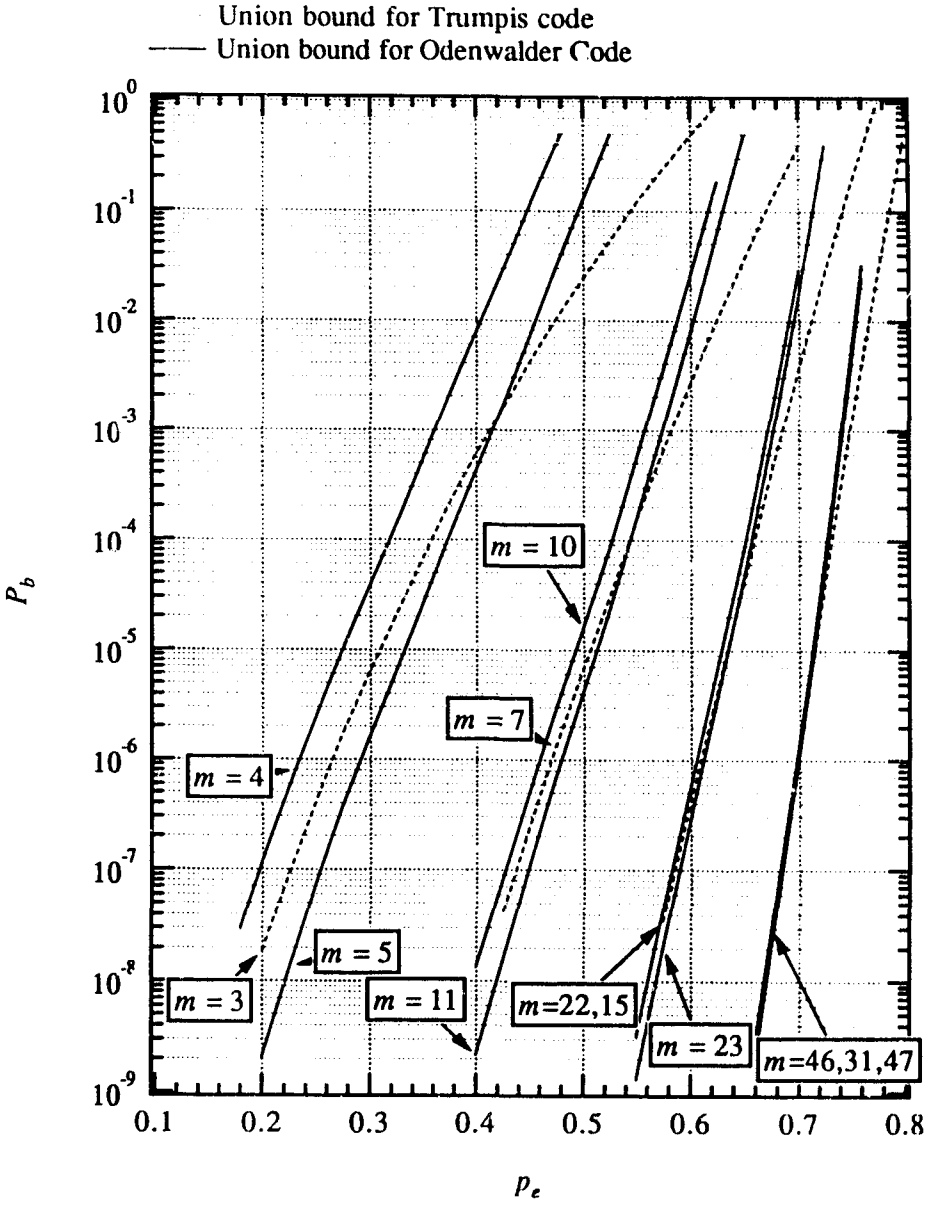

Figure 5.9: Union bounds for the repeated Trumpis and Odenwalder codes with 8-ary metrics over 8-ary symmetric channels. m=3,7,15, and 31 for the Trumpis code; m=4,10,22, and 46 and m=5,11,23, and 47 for the Odenwalder code.

this case, the decoder is designed to only accommodate binary metrics. With this constraint, the above union bound should be understood as an upper bound on the BER performance of the decoder using binary metrics. But the free M-ary Hamming distance of the binary code shown in the union bound of Equations (5.13) and (5.14) and the corresponding error coefficient provide a basic indicator on how well the binary code can work over the M-ary channel.

Since the performance degradation of the Odenwalder code is small relative to the optimum Trumpis code using M-ary metrics, the code is a good candidate for the M-ary system from a practical point of view. The practicality is that we can use commercially available codec chips provided we can properly generate binary decoding metrics. Further performance degradation will be introduced by using binary metrics because a binary metric is not a MLD decoding metric in an M-ary channel. How much the degradation will be depends on how the binary metrics are generated. In the following sections, we consider several possible methods of generating binary decoding metrics and their performances.

Binary Metric Approximation of the M-ary Metrics

Since the use of a binary decoder requires binary metrics, M-ary metrics can not be used directly in a binary decoder. The most natural attempt would be to approximate M-ary metrics with $\log_2 M$ binary metrics. This method avoids interleaving.

Since the trellis decoding is based on comparing the metrics of different trellis paths, adding a number to all M metrics in one symbol period does not affect the decoding performance. Therefore, we only need to be concerned about differences between metrics for different M-ary symbols. There are $M-1$ M-ary metric differences.

Let m_{00}, m_{01}, m_{10}, and m_{11} be the 4-ary metrics, respectively. The maximum likelihood decision decoding requires that the branch metric for symbol ij is m_{ij} and that the survivor has the smallest path metric. Thus, MLD can be imple-

mented by considering three differences between four m_{ij}s. Unfortunately, they cannot be exactly represented by two binary metrics.

Assume the metric range is [0,7]. Without loss of generality, we assume m_{00} to be the smallest. Suppose the branch metric is $B_{00} = a + b$ corresponds to two binary metrics (a and b) for symbol 00. Then for symbol 01, the branch metric is $B_{01} = a + 7 - b$. And we have

$$B_{00} - B_{01} = 2b - 7.$$

Because $m_{00} \leq m_{01}$, it is natural to require $B_{00} - B_{01} \leq 0$, i.e., $b \leq 3.5$. If we require

$$B_{00} - B_{01} = m_{00} - m_{01}$$

then

$$2b - 7 = m_{00} - m_{01}$$

hence

$$b = \frac{7 - (m_{01} - m_{00})}{2}.$$

For symbol 10, the branch metric $B_{10} = 7 - a + b$. Similarly, because $m_{00} \leq m_{10}$, $a \leq 3.5$. And if we let

$$B_{00} - B_{10} = m_{00} - m_{10}$$

then

$$a = \frac{7 - (m_{10} - m_{00})}{2}.$$

For symbol 11, the branch metric B_{11} is

$$B_{11} = 7 - a + 7 - b.$$

Because $a \leq 3.5$ and $b \leq 3.5$,

$$B_{11} - B_{01} = 7 - 2a \geq 0$$

and

$$B_{11} - B_{10} = 7 - 2b \geq 0.$$

This means that no matter what $m_{11} - m_{00}$ is, the term B_{11} always gives the least favorable metric. This problem is inevitable as long as there are only two binary metrics used. This is simply because if 00 is the most favorable symbol, 11, which is the farthest symbol to 00 in binary Hamming distance, should be the least favorable in binary metric representation. Thus, the 4-ary metric m_{11} is not always preserved depending on its value, but the metrics m_{10} and m_{01} are genuinely preserved.

In summary, the proposed method to generate binary metrics to approximate 4-ary metrics is as follows:

1. Find $m_{ij} = \min(m_{00}, m_{01}, m_{10}, m_{11})$, where $i, j \in (0, 1)$. Denote the 1's complement of i as $\bar{i}$ and j as $\bar{j}$.

2. Then compute

$$a = \frac{7 - (m_{\bar{i}j} - m_{ij})}{2},$$

$$b = \frac{7 - (m_{i\bar{j}} - m_{ij})}{2}.$$

3. The actual two binary metrics sent to the decoder, b_1 and b_2 are

$$b_1 = a(1 - i) + (7 - a)i,$$

$$b_2 = b(1 - j) + (7 - b)j.$$

For a larger M, for example, $M = 8$, there are seven 8-ary metric differences but only three binary metrics. The method given above can only accurately represent three out of seven differences. Thus it does not appear to be proper to extend the method to a larger M. In the following sections, we consider more general methods. The basic principle of these methods is to generate "sensible " binary metrics directly from M-ary metrics without attempting to approximate them.

5.4.2 Binary Metric Generation

When a binary code is used over an M-ary channel, the $\log_2 M$ encoded bits at the output of encoder are mapped into M-ary symbols through a one-to-one mapping. At the receiver, the received M-ary symbol is mapped back to the group of binary bits, and the corresponding metric for each binary bit is generated accordingly. The optimum binary metric generation method is the one that has the BER performance closest to that of the Odenwalder code with M-ary metrics. Here we propose a binary metric generation method called the direct binary metric generation.

The Direct Binary Metric Generation Method

At the receiver, after receiving m M-ary symbols, we can generate the binary metric in the following way:

1. Map the m received M-ary symbols back to m binary bit groups, respectively.
2. For each of the $\log_2 M$ bits, accumulate over m repetitions the number of 0 or 1 bits received and form a binary metric like the one discussed in Section 5.2 for the BSC.
3. Feed these binary metrics to the decoder in a certain order.

For example, for 4-ary symbols 0,1,2, and 3, we can map them to four groups of two binary bits, say, 00, 01,10, and 11, respectively. If $m = 3$ and the three received symbols are 0, 1, and 3, the corresponding two binary metrics are 1 and 2.

"Certain order" in step 3 depends on whether interleaving is used or not. Here we analyze two extreme cases: ideal interleaving and no interleaving at all.

The Direct Binary Metric Generation with Ideal Interleaving

Obviously, the binary metrics generated using this direct method bear some dependence. Ideal interleaving makes the decoder input metrics statistically independent of each other over one decoder trellis length. This requires a block interleaver with an interleaving depth of $\log_2 M$ and a span of at least 5 to 6 times the constraint length. In this case, the M-ary symmetric channel can be simplified to the BSC model with the BSC transition probability of

$$p_e^{(B)} = \frac{M}{2(M-1)} p_e. \tag{5.18}$$

Then analysis can be carried out easily in the same way as for the BSC model. Specifically, the analytical results for the binary channel given in Equations (5.1) and (5.2) can be applied directly by substituting the transition probability p_e with $\frac{M}{2(M-1)}p_e$. The bounds of P_b versus p_e are plotted for the Odenwalder code, with the direct binary metrics with ideal interleaving for the 4-ary channel in Figure 5.7 and for the 8-ary channel in Figure 5.8, respectively.

The Direct Binary Metric Generation without Interleaving

No interleaving means that $\log_2 M$ consecutive binary decoding metrics are generated from one M-ary symbol. Here we consider the 4-ary case. Generalization for a larger M involves a higher level of sophistication but no more ingenuity.

For the 4SC, the probability of receiving one of three wrong 4-ary symbols is $p_e/3$. However, two of the three wrong symbols result in only one binary bit error, and the other one leads to two binary bit errors.

Consider two trellis paths that differ in d bit positions. One path is considered as the correct path, while the other one is considered as the incorrect path. Assume there are d bits different positions in Z branches in the incorrect path. Among the Z branches, there are two kinds of branches. One kind of branch only has one

bit different from the corresponding branch in the correct path. The other kind has both bits different from the branch in the correct path. We call the first kind one-bit-error branches and the second kind two-bit-error branches. For a received symbol, the metrics are different for these two kinds of branches.

Suppose the branch in the correct path is 00. Then, the one-bit-error branch is either 01 or 10 and the two-bit-error branch is 11. We consider 01 as an example of the one-bit-error branch. With the binary Hamming distance used as the metric, we have:

symbol received	probability	metric for correct branch (00)	metric for error branch (01)
00	$1\text{-}p_e$	0	1
01	$p_e/3$	1	0
10	$p_e/3$	1	2
11	$p_e/3$	2	1

For a two-bit-error branch, similarly, we have:

symbol received	probability	metric for correct branch (00)	metric for error branch (11)
00	$1\text{-}p_e$	0	2
01	$p_e/3$	1	1
10	$p_e/3$	1	1
11	$p_e/3$	2	0

Here we can see that the metrics are different for the two kinds of error branches, and therefore, for different combinations of the two kinds of branches the pairwise error probabilities are different even for the same d, the total number of different bits.

To compute the union bound on the BER at the output of a decoder, we need to know the number of one-bit-error and two-bit-error branches exist for each d and the corresponding contributions of each combination to information bit errors.

Suppose there are X one-bit-error branches, Y two-bit-error branches, and

d	X	Y	$C_d(X,Y)$
10	2	4	1
	4	3	10
	6	2	25
12	4	4	13
	6	3	61
	8	2	137
14	4	5	29
	6	4	176
	8	3	792
	10	2	407
16	2	7	2
	4	6	42
	6	5	597
	8	4	3019
	10	3	5177
	12	2	2796

Table 5.1: $C_d(X,Y)$ for the constraint-length-7 Odenwalder code.

$X+Y=Z$. Then the union bound on the BER at the output of the decoder is

$$P_b \leq \sum_{d=d_{free}}^{\infty} \sum_{X,Y \in \Gamma_d} C_d(X,Y) P_d(X,Y) \tag{5.19}$$

where Γ_d is the set of all possible X and Y combinations, which are determined by the code. $C_d(X,Y)$ is the information bit error contribution for a trellis path with X one-bit-error branches, Y two-bit-error branches, and total of d bits different from the correct path. $P_d(X,Y)$ is the pairwise probability of having two trellis paths with the binary Hamming distance d, X one-bit-error branches, and Y two-bit-error branches.

$C_d(X,Y)$ can be obtained by computer search. We found $C_d(X,Y)$ for the Odenwalder code, and the values for small d's are given in Table 5.1.

Now we compute the pairwise error probability $P_d(X,Y)$. Suppose that the correct path is the all-zero path. If during $Z=X+Y$ transmissions, symbol 00

is received k_0 times, symbol 01 k_1 times, symbol 10 k_2 times, and symbol 11 k_3 times, then the metric for the correct path corresponding the Z branches is

$$m_c = k_1 + k_2 + 2k_3. \tag{5.20}$$

To compute the metric of the error path, we have to consider how received symbols match the branches in the error path.

Let k_{0x} be the number of 00 symbols received corresponding one-bit-error branches in the incorrect path, and k_{0y} be the number of 00 symbols received corresponding two-bit-error branches in the incorrect path, and so on. Obviously,

$$\begin{aligned} k_0 &= k_{0x} + k_{0y} \\ k_1 &= k_{1x} + k_{1y} \\ k_2 &= k_{2x} + k_{2y} \\ k_3 &= k_{3x} + k_{3y} \end{aligned}$$

and

$$\begin{aligned} k_{0x} + k_{1x} + k_{2x} + k_{3x} &= X \\ k_{0y} + k_{1y} + k_{2y} + k_{3y} &= Y. \end{aligned}$$

As discussed in Section 5.6, we can assume, without loss of generality, that all one-bit-error branches are 01. Then the metric for the incorrect path corresponding to the Z branches is

$$m_e = k_{0x} + 2k_{2x} + k_{3x} + 2k_{0y} + k_{1y} + k_{2y}. \tag{5.21}$$

The pairwise error probability is

$$\begin{aligned} P_d(X,Y) &= \sum_{\Omega} u(m_c - m_e) \frac{X!}{k_{0x}!k_{1x}!k_{2x}!k_{3x}!} \frac{Y!}{k_{0y}!k_{1y}!k_{2y}!k_{3y}!} \\ &\quad \times \left(\frac{p_e}{3}\right)^{k_1+k_2+k_3} (1-p_e)^{k_0} \end{aligned} \tag{5.22}$$

where

$$\Omega = \{k_{ix}, k_{iy}, i = 0,1,2,3 \mid \quad 0 \le k_{ix}, 0 \le k_{iy}, i = 0,1,2,3, \sum_{i=0}^{3} k_{ix} = X, \sum_{i=0}^{3} k_{iy} = Y\}$$

and

$$u(x) = \begin{cases} 0 & x < 0; \\ 0.5 & x = 0; \\ 1 & x > 0. \end{cases}$$

The union bound of (5.19) is plotted in Figure 5.7 for the Odenwalder code on a 4-ary channel with direct metric generation without interleaving.

Binary Metric Generation Based on M-ary Metrics without Interleaving

In order to generate binary metrics, Gong proposed a conversion scheme which converts M-ary metrics into binary metrics [4]. For the i-th bit in $\log_2 M$ bits corresponding to an M-ary symbol, the binary metric is given by

$$\begin{aligned} b_i \;=\; & \max\{M\text{-ary metrics for symbols with } i\text{-th bit equal to ``1''}\} \\ & - \max\{M\text{-ary metrics for symbols with } i\text{-th bit equal to ``0''}\} \\ & i = 1,2,\ldots,\log_2 M. \end{aligned}$$

Here we use Gong's conversion scheme in the following way: first we find M-ary MLD metrics; then binary metrics are generated using the above equation. Since interleaving can cause a substantial delay in addition to its implementation cost, which sometimes is not desirable or tolerable, it is always interesting to know the trade-off between interleaving and the BER performance. Thus, we consider both Gong's conversion scheme and our direct metric generation scheme without interleaving. It is interesting to compare the performances of these two schemes. Further, we note that the use of Trumpis codes does not require interleaving. Thus, comparison based on no interleaving is fair to all cases.

5.4.3 Simulation Results

A Monte Carlo simulation is carried out to obtain the bit error rate at the decoder output for the Odenwalder code on a 4-ary symmetric channel with three metrics, our approximation of M-ary metrics, directly generated metrics and Gong's conversion metrics, and for the Odenwalder code on an 8-ary symmetric channel with two metrics, our directly generated metrics and Gong's conversion metrics, both without interleaving. The results are plotted in Figure 5.10 for the 4-ary case and in Figure 5.11 for the 8-ary case. For comparison, the union bound for the Odenwalder code with the M-ary metrics and with the directly generated binary metrics with ideal interleaving are also depicted in Figure 5.10 and Figure 5.11. The union bounds for the Odenwalder code on a 4-ary channel with the direct-generation metrics without interleaving are also plotted in Figure 5.10.

From the simulation results on a 4-ary channel (Figure 5.10), we can see that the directly generated metric gives the best performance among three metrics. For small m ($m \leq 7$), the approximation metric and the conversion metric have almost the same performance. But for large m, the conversion metric has a better performance. In Figure 5.11, the simulation results on an 8-ary channel are similar. The direct-generation metric has better performance. All three metrics work without interleaving. Therefore, the direct binary metric generation method is recommended when no interleaving is preferred.

It is also noted that the union bound for the direct-generation metrics without interleaving is quite tight for BERs less than 10^{-3}. Comparing the union bounds and simulation results with ideal interleaving and those for the direct-generation metric without interleaving, we can see that the difference between the two cases gets smaller when m becomes larger. So when m is large ($m \geq 15$), interleaving may not improve the performance significantly, and therefore may not be necessary.

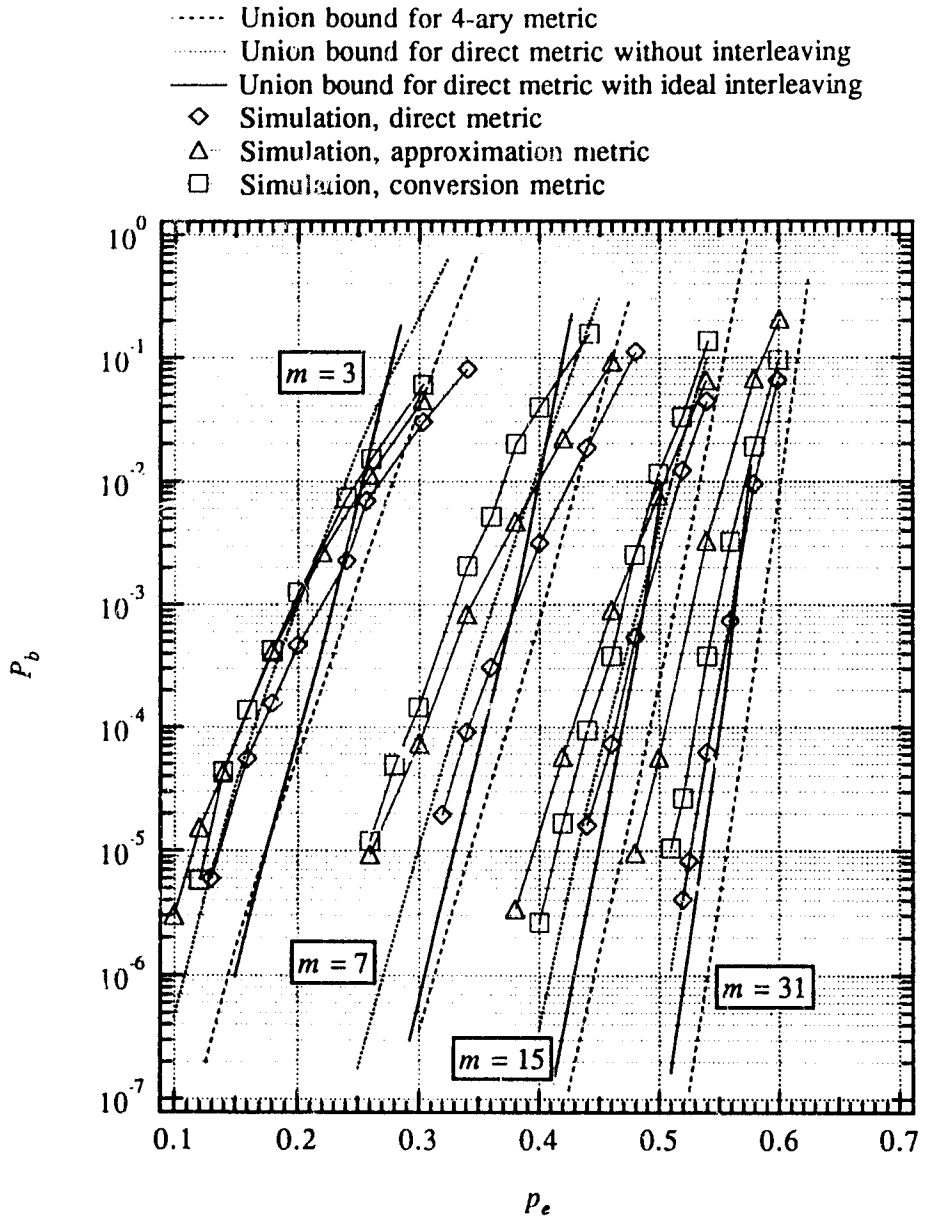

Figure 5.10: Monte Carlo simulation BER performance for a 4-ary symmetric channel using a repeated Odenwalder code without interleaving and direct-generation, approximation, and conversion metrics.

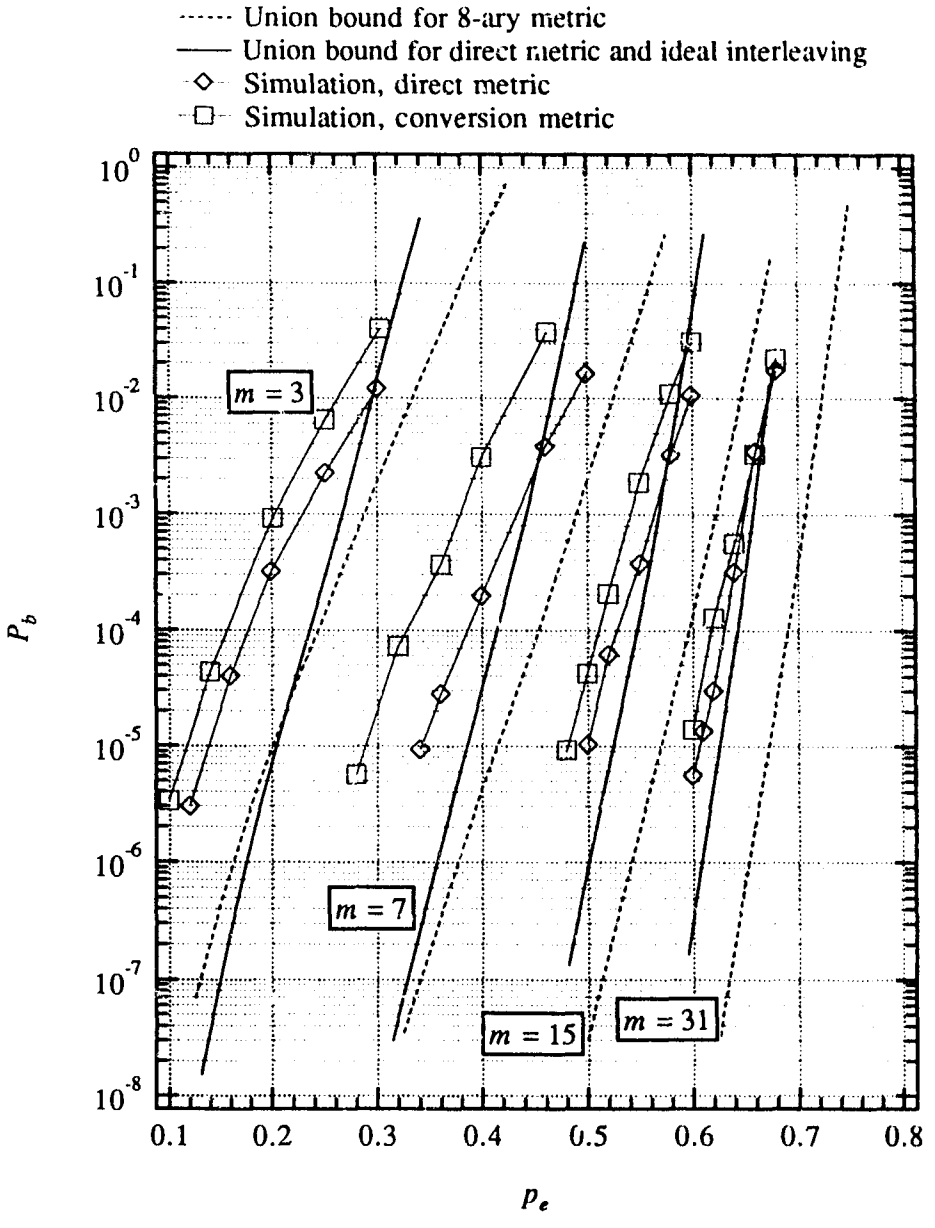

Figure 5.11: Monte Carlo simulation BER performance for an 8-ary symmetric channel using a repeated Odenwalder code without interleaving and direct-generation and conversion metrics.

5.5 Concluding Remarks

We have considered a repeated convolutional coding scheme for the MSC with a large p_e in this chapter. BER performance has been analyzed and simulated. We first considered a BSC. A BER approximation method is proposed for a large m based on the central limit theorem. The overall code rate r is considered relative to the channel cutoff rate, R_0. It is shown that r is larger than $0.6R_0$. In comparison with a cascaded coding scheme proposed in [26], the repeated coding scheme has some clear advantages. One of them is that we can vary m to match the unknown p_e without changing the decoding procedure.

We then extended the repeated convolutional coding scheme to the M-ary symmetric channel. We have investigated the influence of various decoding metrics for the MSC model. If ideal interleaving is available, and m is not very large, then the repeated Odenwalder code with binary metrics is almost as good as the one with M-ary metrics. Further, the performance of the Odenwalder code over 4-ary and 8-ary channels is quite close to that of the optimum Trumpis codes. When interleaving is not available, three methods of generating binary metrics from the M-ary channel are proposed. The first is based on an approximation of the differences of M-ary metrics with binary metrics. In the second, binary metrics are generated directly from M-ary metrics. The third method is a conversion method. Simulation results indicate that the direct binary generation method is the best for our coding scheme among these binary metric generation methods. Therefore, the direct binary metric generation method is recommended if no interleaving is preferred. Union bound and simulation results also indicate that there is not much improvement from interleaving when m is large.

5.6 Further Analysis of One-bit-error Branch

In this section, we will show that no matter what one-bit-error branches actually are (all 01 or all 10 or combinations of 01 and 10), the pairwise probability can be

obtained by assuming a convenient form, e.g. they are all 01.

Suppose the incorrect trellis path is A and that there are X_1 01 branches and X_2 10 branches in path A. Suppose that there are k_{0x_1} 00 symbols, k_{1x_1} 01 symbols, k_{2x_1} 10 symbols, and k_{3x_1} 11 symbols received corresponding to 01 branches, and k_{0x_2} 00 symbols, k_{1x_2} 01 symbols, k_{2x_2} 10 symbols, and k_{3x_2} 11 symbols received corresponding to 10 branches, respectively. Obviously,

$$k_{ix_1} + k_{ix_2} = k_{ix} \qquad \text{for } i = 0, 1, 2, 3$$

and

$$\sum_{i=0}^{3} k_{ix_1} = X_1,$$

$$\sum_{i=0}^{3} k_{ix_2} = X_2.$$

Then the metric for path A is

$$m_e(k_{2x_1} + k_{1x_2}) = 2(k_{2x_1} + k_{1x_2}) + C \tag{5.23}$$

where $C = k_{0x} + k_{3x} + 2k_{0y} + k_{1y} + k_{2y}$. The pairwise error probability is

$$\begin{aligned} P_d^{(A)}(X, Y) &= \sum_{\Omega_A} u(m_c - m_e(k_{2x_1} + k_{1x_2})) \\ &\quad \times \frac{X_1!}{k_{0x_1}!k_{1x_1}!k_{2x_1}!k_{3x_1}!} \frac{X_2!}{k_{0x_2}!k_{1x_2}!k_{2x_2}!k_{3x_2}!} \\ &\quad \times \frac{Y!}{k_{0y}!k_{1y}!k_{2y}!k_{3y}!} \left(\frac{p_e}{3}\right)^{k_1+k_2+k_3} (1 - p_e)^{k_0} \end{aligned} \tag{5.24}$$

where

$$\begin{aligned} \Omega_A = \{k_{ix_1}, k_{ix_2}, k_{iy}, i = 0, 1, 2, 3 \mid \quad & 0 \le k_{ix_1}, 0 \le k_{ix_2}, \\ & 0 \le k_{iy}, i = 0, 1, 2, 3, \\ & \sum_{i=0}^{3} k_{ix_1} = X_1, \sum_{i=0}^{3} k_{ix_2} = X_2, \sum_{i=0}^{3} k_{iy} = Y\}. \end{aligned}$$

Note that in the above equation, the summation constraint on k_{1x_2} and k_{2x_2} is identical. In other words, k_{1x_2} can assume the same range of values as k_{2x_2}. Thus, we can exchange these two variables in (5.24) without affecting the value of $P_d^{(A)}(X,Y)$. The only change the equation is that the argument of m_e becomes $k_{2x_1} + k_{2x_2} = k_{2x}$. By definition of multinomial coefficients, it is not difficult to see that $P_d^{(A)}(X,Y)$ is equal to the right-hand side of $P_d(X,Y)$ in (5.22), which is based on the assumption that all one-bit-error branches have 01. It is worth mentioning that the advantage of using Equation (5.22) is that the summation involves many fewer terms, thus much less computing time, than that in Equation (5.24).

Chapter 6

Conclusions

A brief summary of the results described in previous chapters is given in Section 6.1. Suggestions for future research are addressed in Section 6.2.

6.1 Summary of the Thesis

In Chapter 2, a method for computation of exact bit error probability of the ratio-threshold diversity combining system under jamming is proposed. The amount of numerical computation required can be dramatically reduced by using an average computation model. Next, the exact bit error probability of FFH/FSK spread spectrum system with ratio-threshold diversity combining in an environment with worst case partial-band noise jamming and AWGN are computed. The results from exact bit error probability analysis, rather than results from an analysis of bounds on error probability, are especially useful in comparing performance of diversity combining schemes. It is found that there is an optimum diversity order. With this diversity order, the system performance is optimum in the sense of requiring the least amount of signal energy to achieve certain bit error probability, and the performance is not sensitive to the choice of ratio threshold. The performance of ratio-threshold combining is about 2 dB worse than that of soft linear combining with perfect side information without AWGN for the diversity order of 4 in 4-ary, 8-ary and 16-ary systems.

The performance of ratio-threshold diversity combining under $n = 1$ band tone jamming is analyzed in Chapter 3. The analysis under tone jamming is usually more difficult than the analysis under partial-band noise jamming, especially when AWGN is included, because of the complexity of probability distribution functions involved. Nevertheless, the exact bit error probability under the worst case band tone jamming including the influence of AWGN is computed by the method we developed in Chapter 2. The anti-jam capability of the ratio-threshold diversity combining under tone jamming is well demonstrated by our results. By comparing results obtained in Chapter 2, we found that the performance of ratio-threshold combining under partial-band noise and band tone jamming is almost the same in a binary system. But in an 8-ary system, tone jamming is much more effective.

In Chapter 4, the maximum-likelihood diversity combining in partial-band noise channel is addressed. Performance of the maximum-likelihood diversity reception can be used as a standard in performance comparison. It is shown that AGC combining is actually the optimum when interference is not very weak. But to implement the optimum combining, the noise variance in a hop has to be known. The performance difference between the maximum-likelihood combining and the self-normalizing combining, which does not require hop noise variance and is more practical, can be more than 6 dB. Thus there might be better practical diversity combining methods which we need to find. Since the worst case interference for optimum combining is not full-band noise interference, the utilization of diversity alone is not enough to defeat the interference completely.

A repeated convolutional coding scheme for the MSC with a high error probability was considered in Chapter 5. For the BSC, a special case of the MSC, an analysis method based on the central limit theorem is proposed. The advantages of the repeated coding scheme are illustrated. One advantage is the flexibility to adjust coding rate to adapt to channel error rate without the need to change coding structure. For the MSC, when the repetition coding rate is not very low, interleaving is necessary. If ideal interleaving is available, the optimum binary con-

volutional code can be used in the MSC with a resulting performance close to that of the optimum M-ary convolutional codes. The direct binary metric generation method developed in Chapter 5 is recommended when a binary convolutional code is used in an M-ary channel without interleaving. Results show that there is not much improvement with the addition of interleaving when the repetition coding rate is low.

6.2 Future Research

Since some multiple-access interference can be modeled as partial-band interference, it would be interesting to extend the analysis conducted in Chapter 2 to the performance analysis of ratio-threshold diversity combining (and other diversity reception schemes) in a multiple-access system. In the multiple-access system, the interference is usually not hostile, so the communication system is not forced to operate in the worst case interference environment often. The worst case only happens with small probability. The system performance is characterized by the average of performance under all possible duty factors of partial-band noise interference. However, the worst case performance still might be useful for the following two reasons. The first reason is that the worst case performance contributes to the average performance, thus the system average performance may not be good if worst case performance is poor. The second reason is that a poor worst case performance may indicate the system's instantaneous performance varies too much, or performance is not stable.

Another type of multitone interference is independent multitone interference [1, page 80]. Since some multiple-access interference can be modeled as independent multitone interference, it is meaningful to analyze the performance of diversity combining schemes under this kind of interference. Previous analysis of diversity combining schemes concentrated mainly on partial-band noise interference. As a result, the performance of some diversity combining schemes which work well in a

partial-band noise channel are unknown under multitone interference. Thus it is necessary to investigate the performance of both optimum and sub-optimum (or practical) diversity combining in multitone interference.

A natural extension of the work on repeated convolutional codes is to consider using a block code as the outer code. It is interesting to search the method to generate soft decision metrics from the decoder of inner repetition code and evaluate the performance of this error correction coding scheme.

Appendix A

List of Symbols

E_b	energy per information bit
E_c	energy per chip (energy per hop in FFH)
E_s	energy per channel symbol
N_0	AWGN power spectral density
N_J	jamming power spectral density
m	diversity order (repetition order in Chapter 5)
M	size of channel alphabet
p_e	error probability in MSC
P_b	bit error rate
P_C	transition probability in binary-input-quaternary-output channel
P_{CX}	transition probability in binary-input-quaternary-output channel
P_E	transition probability in binary-input-quaternary-output channel
P_{EX}	transition probability in binary-input-quaternary-output channel
P_d	pairwise error probability between two trellis paths with Hamming distance d
R_0	cutoff rate
T_c	chip interval
T_s	channel symbol interval
W_{ss}	spread spectrum bandwidth
X_{ik}	output of non-coherent matched filter corresponding to the ith symbol in the kth hop
α	ratio of signal power to one jamming tone power
α_{max}	upper limit of α
α_{wc}	worst case α
θ	threshold in ratio-threshold test
λ_i	decision variable for the ith symbol in diversity combining
μ	probability of an M-ary band hit by a jamming tone
ρ	duty factor of PBN jamming

ρ_{wc} worst case ρ

Appendix B

List of Abbreviations

AGC	adaptive gain control
AWGN	additive white Gaussian noise
BER	bit error rate
BSC	binary symmetric channel
FH	frequency-hop
FFH	fast frequency-hop
MFSK	M-ary frequency shift keying
MLD	maximum-likelihood decoding
MSC	M-ary symmetric channel
PBN	partial band noise
PN	pseudonoise
PSI	perfect side information
R-T	ratio-threshold
SFH	slow frequency-hop

Bibliography

[1] M. K. Simon, J. K. Omura, R. A. Scholtz, and B. Levitt, *Spread Spectrum Communications*, vol. II. Rockville: Computer Science Press, 1985.

[2] J. S. Bird and E. B. Felstead, "Antijam performance of fast frequency-hopped M-ary NCFSK - An overview," *IEEE Journal on Selected Areas on Communications*, vol. SAC-4, pp. 216–233, Mar. 1986.

[3] L. E. Miller, J. S. Lee, and A. P. Kadrichu, "Probability of error analyses of a BFSK frequency-hopping system with diversity under partial-band jamming interference — Part III: Performance of a square-law self-normalizing soft decision receiver," *IEEE Transactions on Communications*, vol. COM-34, pp. 669–675, July 1986.

[4] K. S. Gong, "Performance of diversity combining technique for FH/MFSK in worst case partial band noise and multi-tone jamming," in *Proceedings of 1983 IEEE Millitary Communications Conference*, pp. 17–21, 1983.

[5] C. M. Keller and M. B. Pursley, "Cilpped diversity combining for channels with partial-band interference—Part I: Clipped-linear combining," *IEEE Transactions on Communications*, vol. COM-35, pp. 1320–1328, Dec. 1987.

[6] R. Viswanathan and K. Taghizadeh, "Diversity combining in FH/BFSK systems to combat partial band jamming," *IEEE Transactions on Communications*, vol. COM-36, pp. 1062–1069, Sept. 1988.

[7] J. S. Lee, R. H. French, and L. E. Miller, "Probability of error analysis of a BFSK frequency-hopping system with diversity under partial-band jamming interference —Part I: Performance of square-law linear combining soft decision receiver," *IEEE Transactions on Communications*, vol. COM-32, pp. 645–653, June 1984.

[8] J. S. Lee, L. E. Miller, and Y. K. Kim, "Probability of error analyses of a BFSK frequency-hopping system with diversity under partial-band jamming interference — Part II: Performance of square-law nonlinear combining soft decision receivers," *IEEE Transactions on Communications*, vol. COM-32, pp. 1243–1250, Dec. 1984.

[9] A. Viterbi, "A robust ratio-threshold technique to mitigate tone and partial band jamming in coded MFSK systems," in *Proceedings of 1982 IEEE Military Communications Conference*, pp. 22.4–1 – 22.4–5, 1982.

[10] A. Viterbi, "Robust decoding of jammed frequency hopped modulation," in *Recent Advances in Communication and Control Theory*, New York: Optimization Software, 1987.

[11] L. F. Chang, *An information-theoretic study of ratio-threshold antijam techniques.* Ph.D. Dissertation, University of Illinois at Urbana-Champaign, 1985.

[12] K. M. Clifford and T. Schonhoff, "Performance evaluation of ratio threshold for frequency hopped mfsk communication in partial-band tone jamming plus background noise," in *Proceedings of 1986 IEEE Military Communications Conference*, pp. 12.3.1–12.3.5, 1986.

[13] C. M. Keller, *Diversity combining for frequency-hop spread spectrum communications with partial-band interference and fading.* Ph.D. Dissertation, University of Illinois at Urbana-Champaign, 1985.

[14] S. Laufer and A. Reichman, "Analysis of frequency-hopping systems with combined convolutional and diversity encoding and non-idea linterleaving in worst case partial band jamming," in *Proceedings of 1988 IEEE Military Communications Conference*, pp. 43.2.1–43.2.5, 1988.

[15] A. M. Michelson and A. H. Levesque, *Error-Control Techniques for Digital Communication.* New York: John Wiley & Sons, 1985.

[16] D. Shnidman, "The calculation of the probability of detection and the generalized Marcum Q-function," *IEEE Transactions on Information Theory*, vol. IT-35, pp. 389–400, Mar. 1989.

[17] S. Stein, "Unified analysis of certain coherent and noncoherent binary communications systems," *IEEE Transactions on Information Theory*, vol. IT-10, pp. 43–51, Jan. 1964.

[18] S. Haykin, *Digital Communications.* New York: John Wiley & Sons, 1988.

[19] R. E. Ziemer and R. I. Peterson, *Digital Communications and Spread Spectrum Systems.* New York: MacMillan, 1985.

[20] A. D. Whalen, *Detection of Signals in Noise.* New York: Academic Press, 1971.

[21] H. L. Van Trees, *Detection, Estimation, and Modulation Theory, Part I.* New York: John Wiley & Sons, 1968.

[22] M. K. Simon, J. K. Omura, R. A. Scholtz, and B. Levitt, *Spread Spectrum Communications*, vol. I. Rockville: Computer Science Press, 1985.

[23] J. S. Lee and L. E. Miller, "On the use of side information in diversity combining in frequency-hopping communication in parial-band jamming," in *Proceedings of 1991 IEEE International Symposium on Information Theory*, p. 323, 1991.

[24] J. P. Odenwalder, *Optimal Decoding of Convolutional Codes.* Ph.D. Dissertation, University of California, Los Angeles, 1970.

[25] Q. Wang, R. D. Nicholson, and L. Y. Onotera, "Some practical issues in the design and application of a VLSI FEC chip," *International Journal of Satellite Communications*, vol. 7, pp. 129–142, July 1989.

[26] T. Kasami, T. Fujiwara, T. Takata, and S. Lin, "A cascaded coding scheme for error control and its performance analysis," *IEEE Transactions on Information Theory*, vol. IT-34, pp. 448–462, May 1988.

[27] P. D. Shaft, "Low-rate convolutional code applications in spread-spectrum communications," *IEEE Transactions on Communications*, vol. COM-25, pp. 815–821, Aug. 1977.

[28] D. Chase, "Code combining — a maximum-likelihood decoding approach for combining an arbitrary number of noisy packets," *IEEE Transactions on Communications*, vol. COM-33, pp. 385–393, May 1985.

[29] J. A. Heller, "Sequential decoding: short constraint length convolutional codes," in *JPL Space Programs Summary 37-54*, vol. III, pp. 171–177, Oct. 1968.

[30] G. C. Clark Jr. and J. B. Cain, *Error-Correction Coding for Digital Communications.* New York: Plenum Press, 1981.

[31] V. K. Bhargava, D. Haccoun, R. Matyas, and P. P. Nuspl, *Digital Communications by Satellite.* New York: John Wiley & Sons, 1981.

[32] B. D. Trumpis, *Convolutional Coding for M-ary Channels.* Ph.D. Dissertation, University of California, Los Angeles, 1975.